

Sheet Piling Handbook

Design



ThyssenKrupp GfT Bautechnik

A company of ThyssenKrupp Services



ThyssenKrupp

Sheet Piling Handbook

Design

Sheet Piling Handbook

Design

ThyssenKrupp GfT Bautechnik GmbH
HSP HOESCH Spundwand und Profil GmbH

All the details contained in this handbook are non-binding.

We reserve the right to make changes. Reproduction, even of extracts, is permitted only with our consent.

Preface

This edition follows in the footsteps of the well-known and universally acclaimed book **Spundwand-Handbuch Berechnungen** by Klaus Lupnitz dating from 1977. The preface to that book contained the following words: “This edition of the Sheet Piling Handbook is intended to provide an outline of the fundamentals and analysis options for the design of sheet piling structures. The theory is mentioned only where this is essential for understanding.”

A revision has now become necessary because the state of the art has moved on considerably over the past 30 years. Changes have been brought about by the latest recommendations of the Committee for Waterfront Structures (EAU 2004), the new edition of DIN 1054 with the latest modifications from 2005, and the recently published recommendations of the Committee for Excavations (EAB 2006). Common to all of these is the new safety philosophy based on the partial safety factors concept.

In particular, the sample calculations enable users to become quickly familiar with the new standards and recommendations. The Sheet Piling Handbook should continue to serve as a standard work of reference for engineering students and practising engineers.

I should like to thank Jan Dührkop, Hans Hügel, Steffen Kinzler, Florian König and Klaus-Peter Mahutka for their assistance. This book was produced in close cooperation with the staff of ThyssenKrupp GfT Bautechnik, and I should like to thank Messrs. Drees, Stüber, Kubani, Potchen, Haase, Lütkenhaus, Schletz and Schmidt of ThyssenKrupp GfT Bautechnik plus Messrs. Petry and Billecke of HSP.

Philip Thrift from Hannover produced the English translation.

Hamburg, July 2008

Jürgen Grabe

Contents

1	Introduction	1
2	Sheet pile walls	5
2.1	Sections and interlocks	5
2.2	Properties of steel	8
2.2.1	Stress-strain behaviour	8
2.2.2	Designation of steel grades	8
2.2.3	Suitability for welding	9
2.2.4	Corrosion and service life	10
2.3	Driving sheet pile walls	13
2.3.1	Threading piles into precut trenches	13
2.3.2	Pressing	14
2.3.3	Impact driving	15
2.3.4	Vibratory driving	16
2.3.5	Vibrations and settlement	17
3	Subsoil	23
3.1	Field tests	24
3.1.1	Boreholes	24
3.1.2	Penetrometer tests	24
3.1.3	Geophysical measurements	26
3.1.4	Assessment of penetration resistance	26
3.2	Laboratory tests	27
3.2.1	Granulometric composition	27
3.2.2	Determining unit weight and in situ density	27
3.2.3	Consistency	28
3.2.4	Unconfined compression	29
3.2.5	Shear parameters	30
3.3	Soil parameters	33

4	Groundwater	39
4.1	The basics of hydrostatic and hydrodynamic pressure	39
4.1.1	Hydraulic head	39
4.1.2	Permeability law after DARCY	40
4.2	Excess hydrostatic pressure	41
4.2.1	Calculating the excess hydrostatic pressure	41
4.2.2	Critical water levels	42
4.3	Taking account of groundwater flows	42
4.3.1	The effect of groundwater flows on hydrostatic and earth pressures . . .	42
4.3.2	Flow net	45
4.3.3	Approximate method assuming modified unit weights	47
4.3.4	Flow around a sheet pile wall in stratified subsoil	48
4.4	Hydraulic ground failure	49
5	Earth pressure	53
5.1	General	53
5.2	Limit and intermediate values of earth pressure	55
5.2.1	Active earth pressure after COULOMB	55
5.2.2	Passive earth pressure after COULOMB	57
5.2.3	Steady-state earth pressure	58
5.2.4	Intermediate earth pressure values	58
5.2.5	Further methods for determining the resultant earth pressure	59
5.3	Earth pressure distribution	60
5.4	Calculating the earth pressure due to self-weight	62
5.4.1	Wall friction angle	62
5.4.2	Active and passive earth pressure coefficients for soil self-weight . . .	63
5.4.3	Slip plane angle	65
5.5	Calculating the earth pressure in cohesive soils	65
5.5.1	Cohesion on the active earth pressure side	66
5.5.2	Cohesion on the passive earth pressure side	67
5.6	Earth pressure due to unconfined surcharges	69
5.7	Considering special boundary conditions	70
5.7.1	Stratified soils	70
5.7.2	Confined surcharges	71
5.7.3	Stepped ground surface	72
5.7.4	Earth pressure relief	72
5.7.5	Earth pressure due to compaction	74
5.7.6	Groundwater	74

5.7.7	Three-dimensional earth pressure	76
5.8	Earth pressure redistribution	76
5.9	Examples of earth pressure calculations	79
6	Design of sheet pile walls	83
6.1	General	83
6.2	Safety concept	83
6.2.1	Geotechnical categories	83
6.2.2	Limit states	84
6.2.3	Loading cases	84
6.2.4	Partial safety factors	85
6.2.5	Analysis format	86
6.2.6	Further factors	87
6.3	Actions and action effects	87
6.3.1	Earth pressure	87
6.3.2	Action effects due to earth pressure	88
6.3.3	Hydrostatic pressure	88
6.4	Resistances	88
6.4.1	Passive earth pressure	88
6.4.2	Component resistances	88
6.5	Structural systems	89
6.6	Structural calculations	94
6.6.1	Fully fixed wall without anchors	94
6.6.2	Simply supported wall with one row of anchors	101
6.6.3	Fully fixed wall with one row of anchors	108
6.6.4	Partially fixed wall with one row of anchors	115
6.6.5	Walls with different support conditions at the base and more than one row of anchors	118
6.7	Analyses for the ultimate limit state	118
6.7.1	Failure of earth resistance	118
6.7.2	Subsidence of components	125
6.7.3	Material failure of components	127
6.8	Analysis for the serviceability limit state	128
6.9	Overall stability	129
7	Ground anchors	133
7.1	Types of ground anchors	133
7.1.1	Round steel tie rods	133
7.1.2	Grouted anchors	134

7.1.3	Driven anchor piles	134
7.1.4	Driven pile with grouted skin	134
7.1.5	Vibratory-driven grouted pile	134
7.1.6	Micropiles (diameter ≤ 300 mm)	135
7.1.7	Jet-grouted piles	136
7.1.8	Retractable raking piles	136
7.2	Loadbearing capacity	136
7.3	Design	136
7.3.1	Design against material failure	137
7.3.2	Pull-out resistance	140
7.3.3	Design against uplift	141
7.3.4	Design against failure of the anchoring soil	141
7.3.5	Verification of stability at the lower slip plane	143
7.3.6	Design for serviceability	149
7.4	Testing	150
7.5	Construction details	150
8	Using FEM for the design of sheet piling structures	155
8.1	Possibilities and limitations	155
8.2	Recommendations regarding the use of FEM in geotechnics	155
8.2.1	Advice on the use of FEM for retaining walls	156
8.3	Example of application	158
8.3.1	Initial problem	158
8.3.2	Modelling	160
8.3.3	Results	164
9	Dolphins	169
9.1	General	169
9.2	Loads	169
9.3	Determining the passive earth pressure	170
9.4	Spring constants	172
10	Choosing pile sections	175
	Literature	177
A	Section tables for preliminary design	181
B	Round steel tie rods	189

Nomenclature

Greek symbols

α	Reduction coefficient; factor for adapting embedment depth; angle of wall
β	Slope of ground
Δe	Change in earth pressure ordinate
Δh	Difference in hydraulic head
Δt	Driving allowance
Δw	Hydrostatic pressure difference
δ	Angle of wall friction
δ_{ij}	Deformation at point i due to action j
η	Adjustment factor
γ	Unit weight
$\bar{\gamma}$	Averaged unit weight
γ'	Submerged unit weight of soil
γ_r	Saturated unit weight of soil
γ_w	Unit weight of water
γ_φ	Partial safety factor for coefficient of friction $\tan \varphi$
γ_A	Partial safety factor for resistance of grout
γ_B	Partial safety factor for pull-out resistance of flexible reinforcing elements
γ_{cu}	Partial safety factor for cohesion of undrained soil
γ_c	Partial safety factor for cohesion

γ_{E0g}	Partial safety factor for permanent actions due to steady-state earth pressure
γ_{Ep}	Partial safety factor for passive earth pressure
$\gamma_{G,dst}$	Partial safety factor for unfavourable permanent loads at limit state LS 1A
$\gamma_{G,stab}$	Partial safety factor for favourable permanent loads at limit state LS 1A
γ_{Gl}	Partial safety factor for resistance to sliding
γ_{Gr}	Partial safety factor for resistance to ground failure
γ_G	Partial safety factor for general permanent actions
γ_H	Partial safety factor for actions due to flow
γ_M	Partial safety factor for material strength
γ_N	Partial safety factor for the pull-out resistance of the steel tension member of a grouted anchor
γ_{Pc}	Partial safety factor for pile compression resistance during pile loading test
γ_{Pt}	Partial safety factor for pile tension resistance during pile loading test
γ_P	Partial safety factor for pile resistance to tension and compression based on empirical values
$\gamma_{Q,dst}$	Partial safety factor for unfavourable variable actions at limit state LS 1A
γ_Q	Partial safety factor for unfavourable variable actions
γ_Z	Partial safety factor for tension piles
λ	Wavelength
λ_r	Wavelength of surface wave
μ	Degree of utilisation
ν	Compressibility coefficient
Ω	Exciting frequency
ω	Compressibility exponent
ρ_d	Oven-dry density
ρ_S	Particle density
σ	Stress
σ_z	Vertical stress in soil

σ'_z	Effective vertical stress in soil
τ	Shear stress
τ_{1-0}	Degree of fixity
ε	Compression
ε	Angle of end tangent
ε_u	Minimum elongation at failure
φ	Angle of friction
φ_u	Undrained angle of friction
ϑ	Angle of slip plane
ξ	Length component

Latin symbols

a	Length
a_A	Anchor spacing
A_b	Bearing area
$A_{k,exist}$	Energy absorption capacity of a dolphin
A_{poss}	Possible anchor force when verifying lower slip plane
A_s	Cross-sectional area
B	Resultant reaction
C	Cohesion force; factor for method of driving; BLUM equivalent force
c	Cohesion; ground wave propagation velocity; change in load below point of zero loading; spring constant for design of elastic dolphins
C_C	Compression coefficient
c_{fu}	Undrained shear strength in vane shear test
c_{fv}	Maximum shear resistance in vane shear test
C_h	Horizontal component of BLUM equivalent force
c_{rv}	Residual shear resistance in vane shear test

c_u	Undrained cohesion
D	In situ density
D	Degree of damping
d	Thickness of stratum
d_{60}, d_{10}	Particle diameter for 60% or 10% passing through sieve
E	Elastic modulus
E	Resultant earth pressure force
e	Earth pressure ordinate
e_{min}	Minimum earth pressure ordinate
e	Void ratio
E_d	Design value for general action effect
E_S	Modulus of compressibility
$E_{ph, mob}^r$	Mobilised three-dimensional passive earth pressure
E_{ph}^r	Three-dimensional passive earth pressure
e_{ph}^r	Ordinate of three-dimensional earth pressure
f	Frequency
f	Horizontal deflection of dolphin at the level of the point of force application
$\max f$	Maximum dolphin deformation
F_d	Dynamic force
F_{st}	Static force
f_s	Skin friction in cone penetrometer test
f_s	Hydrodynamic pressure
F_S	Force of ship impact
$f_{t,0.1}$	Stress in steel tension member at 0.1% permanent strain
f_u	Tensile strength
f_y	Yield strength
G	Weight

g	Acceleration due to gravity
h	Hydraulic head
H	Height
h	Depth ordinate when determining embedment length of dolphins
h	Vertical seepage path
h_Z	Cantilever length of dolphin
h_{sum}	Total length of dolphin
I	Second moment of area
i	Hydraulic gradient
I_C	Consistency index
I_D	Relative in situ density
I_P	Plasticity index
K	Coefficient of active earth pressure
\bar{K}	Averaged coefficient of active earth pressure
k	Coefficient of permeability
l	Length
l_r	Minimum anchoring length
M	Bending moment
m	Mass; factor after BLUM
N	Normal force
n	Porosity; number of potential lines; factor after BLUM
N_{10}	Number of blows per 10 cm penetration
P	Force; power
p	Variable ground surcharge
Q	Shear force; reaction due to friction
q_c	Toe resistance for cone penetrometer test
q_u	Unconfined compressive strength

q_s	Skin friction
R	Distance to source of vibration
R_d	Design value for general resistance
R_f	Friction ratio
R_M	Material resistance
R_b	Toe resistance
r_u	Distance between centre of gravity of eccentric mass and centre of rotation
S	Hydrodynamic force
T	Shear force
t	Embedment depth; time
U	Perimeter of cross-section; uniformity coefficient; force due to hydrostatic pressure
u	Point of zero load
v	Flow velocity
\bar{v}	Amplitude of oscillation velocity
V	General vertical force
w	Water content; energy of a source of vibration; hydrostatic pressure
w'	Rotation
w_L	Water content at liquid limit
w_P	Water content at plastic limit
w_u	Excess hydrostatic pressure
W_y	Moment of resistance
x	Variable after BLUM
Z	Tensile strength of anchor
z	Depth
z_g	Geodesic head
z_p	Hydraulic head
z_v	Velocity head

Indices

0	steady-state pressure
a	active
c	due to cohesion
d	design value
h	horizontal component
g	due to permanent loads
k	characteristic value
p	due to variable loads
p	passive
H	due to horizontal line load
V	due to vertical line load
v	vertical component

Chapter 1

Introduction

The history of sheet piling goes back to the beginning of the last century. The book *Ein Produkt erobert die Welt – 100 Jahre Stahlspundwand aus Dortmund* (A product conquers the world – 100 years of sheet pile walls from Dortmund) describes the success story of sheet piling. The story is closely linked with Tryggve Larssen, government building surveyor in Bremen, who invented the *sheet pile wall made from rolled sections with a channel-shaped cross-section*. In 1902 the so-called LARSEN sheet piles – known as such from this date onwards – were used as a waterfront structure at Hohentorshafen in Bremen – and are still doing their job to this day! Since then, LARSEN sheet piles have been manufactured in the rolling mill of HOESCH Spundwand und Profil GmbH.

Over the years, ongoing developments in steel grades, section shapes and driving techniques have led to a wide range of applications for sheet piling. The applications include securing excavations, waterfront structures, foundations, bridge abutments, noise abatement walls, highway structures, cuttings, landfill and contaminated ground enclosures, and flood protection schemes.

The main engineering advantages of sheet pile walls over other types of wall are:

- the extremely favourable ratio of steel cross-section to moment of resistance,
- their suitability for almost all soil types,
- their suitability for use in water,
- the fast progress on site,
- the ability to carry loads immediately,
- the option of extracting and reusing the sections,
- their easy combination with other rolled sections,
- the option of staggered embedment depths,
- the low water permeability, if necessary using sealed interlocks, and
- there is no need for excavations.

Thanks to the aforementioned engineering advantages, plus their functionality, variability and economy, sheet pile walls have become widely acknowledged and frequently used components in civil and structural engineering projects worldwide.

Chapter 2 provides an overview of the most common sections and interlocks. Detailed information about the HSP sections available can be found in the *Sheet Piling Handbook* published by ThyssenKrupp GfT Bautechnik. This chapter also includes information on the relevant steel properties, the stress-strain behaviour, steel grade designations, suitability for welding and corrosion. The main driving techniques with their advantages and disadvantages are outlined, and publications containing further information are mentioned.

Chapter 3 describes briefly the field and laboratory investigations required when considering the use of sheet piling and includes the characteristic soil parameters from EAU 2004 as a guide. Of course, the publications referred to plus the valid standards and directives must be taken into account.

Geotechnics must always take account of the effects of water. Chapter 4 therefore explains the basics of water flows, hydrostatic and hydrodynamic pressures, and hydraulic ground failure.

Chapter 5 deals with earth pressure. Reference is made to the classic earth pressure theory of Coulomb, the calculation of earth pressures according to current recommendations and standards, the consideration of special boundary conditions and earth pressure redistribution. Earth pressure calculations are explained by means of examples.

Chapter 6 first outlines the safety concept according to DIN 1054:2005-01 and EAU 2004, which is based on the partial safety factor concept of Eurocode 7. The special feature in the calculation of sheet pile walls is that the earth pressure can act as both action and resistance. First of all, the engineer chooses the structural system for the sheet pile wall, e.g. sheet pile wall with one row of anchors, fixed in the ground. The required length of the sheet piles, the anchor forces and the actions on the cross-section necessary for the design are then determined from the equilibrium and support conditions. The calculation and design procedure are explained by means of simple examples.

Chapter 7 provides an overview of current types of anchors, e.g. anchor piles, grouted anchors, tie rods and retractable raking piles. The most important methods of analysis are explained using two examples.

DIN 1054:2005-01 also requires a serviceability analysis (limit state LS 2). The principal options here are the method using the modulus of subgrade reaction (please refer to the Recommendations of the Committee for Excavations, EAB 2006), and the Finite Element Method (FEM). The latter has in the meantime become firmly established in practice thanks to the availability of ever-better computer programs. The experiences gained with FEM and recommendations for its use in the design of retaining wall structures can be found in chapter 8. An example explains the principal steps entailed in the modelling work and the interpretation of the results.

Chapter 9 deals with dolphins.

The choice of section depends not only on the design, but also on the transport and the method of driving the section into the subsoil, the corrosion requirements and, possibly, multiple use considerations. Chapter 10 provides helpful information in this respect.

All that remains to be said at this point is that this sheet piling manual can offer only a brief,

incomplete insight into the current state of the art regarding the engineering, design and construction of sheet pile walls. No claim is made with respect to correctness and completeness; ThyssenKrupp GfT Bautechnik will be pleased to receive notification of any omissions and corrections.

Chapter 2

Sheet pile walls

2.1 Sections and interlocks

Fig. 2.1 shows a steel sheet pile wall made from LARSEN U-sections and a wall made from Z-sections with off-centre interlocks.

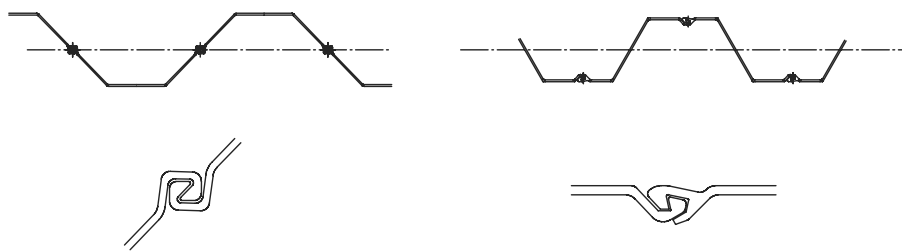


Figure 2.1: Steel sheet pile walls made from U-sections (left) and Z-sections (right) plus details of their interlocks

Straight-web sections (Fig. 2.2) have a high interlock strength for accommodating tensile forces. Applications include, for example, cellular cofferdams.

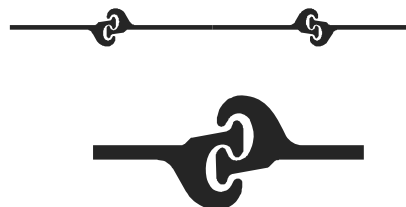


Figure 2.2: Steel sheet pile wall made from straight-web sections plus detail of interlock

The **interlocks** of a sheet pile join together the individual piles to form a complete wall. As the interlocks of U-sections lie on the neutral axis and hence coincide with the maximum shear stresses, the full moment of resistance may only be used in the case of welded or crimped interlocks. When using welded/crimped interlocks, the maximum permissible bending moment is two to three times that of a single sheet pile.

The driving work calls for a certain amount of play in the interlocks and so these joints between the sheet piles are not watertight. Owing to their convoluted form, however, water seeping through the joint does have to negotiate a relatively long path. Ultra-fine particles in the soil accumulate in the interlocks over time, which results in a “self-sealing” effect, which is augmented by corrosion. According to EAU 2004 section 8.1.20.3 (R 117), in walls standing in water this natural sealing process can be assisted by installing environmentally compatible synthetic seals. If a sheet pile wall is required to be especially watertight, the interlocks can be filled with a permanently plastic compound or fitted with a preformed polyurethane **interlock seal**. The materials used exhibit high ageing and weathering resistance plus good resistance to water, seawater and, if necessary, acids and alkalis. Polyurethane interlock seals are factory-fitted to the interlocks of multiple piles and the joints threaded on site are sealed with further preformed polyurethane seals.

Interlocks can be sealed with bituminous materials to achieve a watertight joint. Such materials can be applied in the works or on site. The watertightness is achieved according to the displacement principle: excess sealant is forced out of the interlock when threading the next pile.

Driving the sheet piles with an impact hammer places less load on the seals because the movement takes place in one direction only. The load on polyurethane seals in piles driven by vibration is greater because of the friction and the associated temperature rise. The permeability of a sheet pile wall joint can be estimated using DIN EN 12063 appendix E.

Welding the interlocks achieves a completely watertight sheet pile wall. In the case of multiple piles, the interlocks are factory-welded, which means that only the remaining interlocks between groups of sheet piles have to be welded on site. Such joints must be cleaned and dried before welding.

Sheet pile walls can also be sealed by hammering in wooden wedges, which then swell when in water. Rubber or plastic cords together with a caulking compound with swelling and setting properties can also be used.

When a sheet pile no longer interlocks properly with its neighbour, this is known as declutching. Interlock damage cannot be ruled out completely even with careful driving. EAU 2004 section 8.1.13.2 (R 105) recommends checking for declutching to increase the reliability of sheet pile walls. Visual inspections can be carried out for the part of the sheet pile wall still visible after driving, but signal transmitters must be used for those parts of the wall that are buried or below the waterline, and especially in those cases where a high watertightness is critical, e.g. enclosures to landfill or contaminated land.

Fig. 2.3 shows various combination sheet steel pile walls made from single or double PSp pile sections with intermediate panels.

In such structures the sheet pile walls transfer the loads due to earth and water pressure to the piles, and this enables heavily loaded retaining walls, e.g. quay walls, to be built.

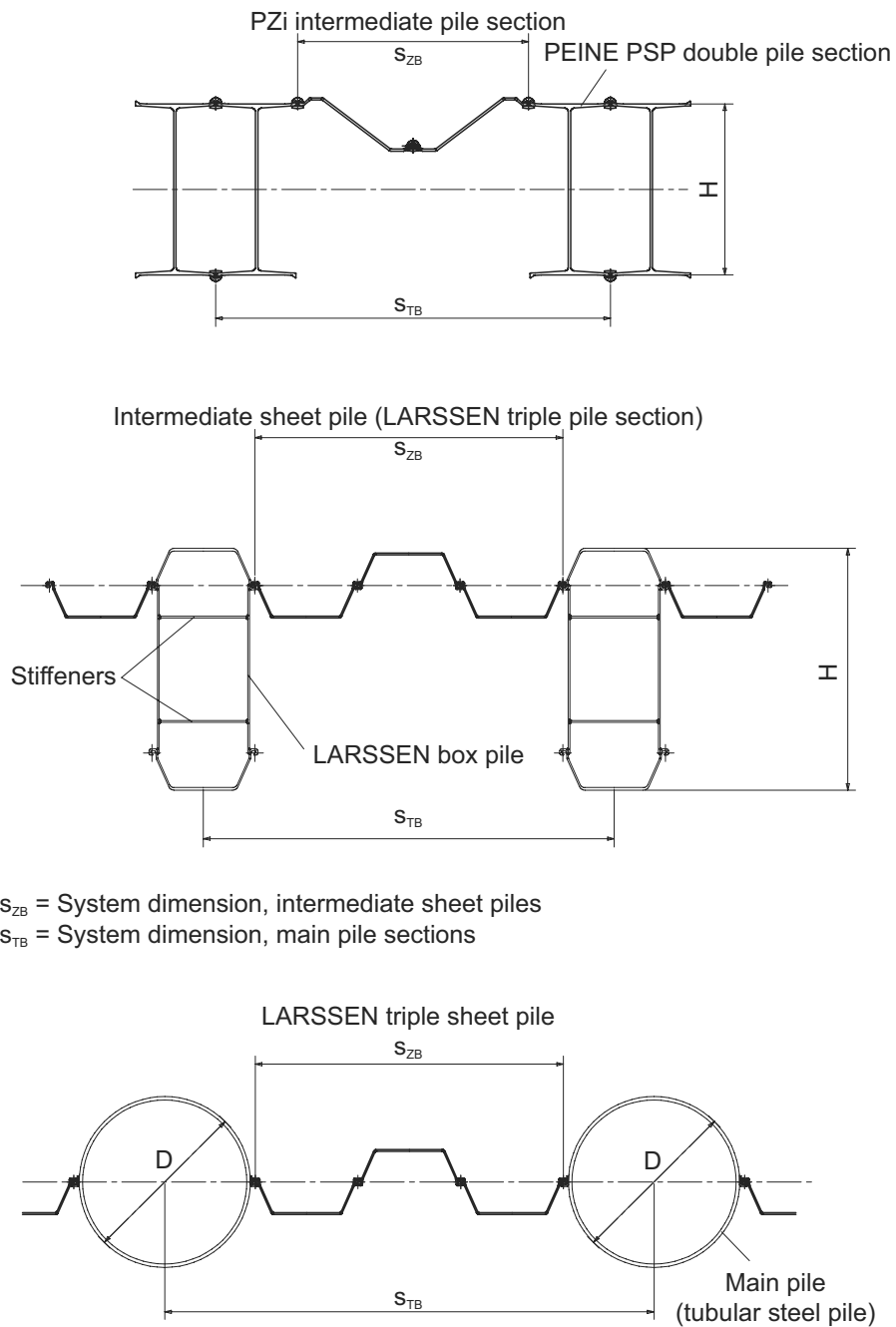


Figure 2.3: Examples of combination steel sheet pile walls

2.2 Properties of steel

Steel is a homogeneous building material whose load-deformation behaviour is characterised by an elastic portion and considerable plastic reserves. In addition, there is its favourable strength-to-weight ratio. The tensile strength of steel ranges from 300 N/mm² for simple mild steels up to 2000 N/mm² for prestressing steels.

2.2.1 Stress-strain behaviour

Fig. 2.4 shows a representative stress-strain diagram for steel. The elastic range depends on the grade of steel. The elastic modulus is the same for all types of steel: $E_{steel} = 210\,000$ N/mm². The **yield strength** f_y is the value at which the stress remains constant or drops or exhibits a permanent strain of 0.2% after removing the load. If the load is increased further, a maximum stress is reached, which is designated the **tensile strength** f_u . Generally speaking, an increase in the strength involves a decrease in the deformation capacity of the steel.

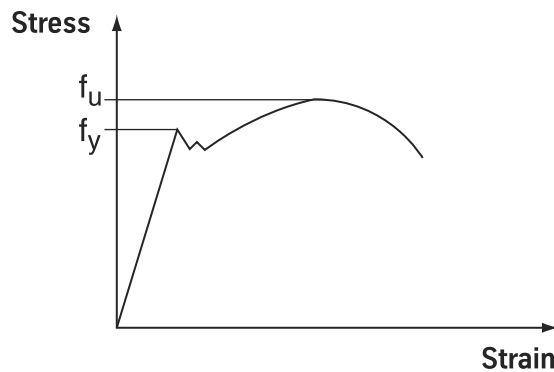


Figure 2.4: Representative stress-strain diagram for steel

The resistance of a sheet pile wall has to be verified according to DIN EN 1993-5. The method of analysis is based on the partial safety factor concept. The design value of the internal forces S_d must be compared with the design value of the section's resistance R_d :

$$S_d \leq R_d \quad (2.1)$$

The design value of the internal forces depends on DIN 1054 or DIN EN 1997-1 (see also chapter 6). When determining the design value of the section's resistance R_d , the yield strength f_y must be reduced by the partial safety factor $\gamma_M = 1.1$ according to DIN EN 1993-5.

2.2.2 Designation of steel grades

Hot-rolled steel sheet piles must comply with DIN EN 10248. Table 2.1 lists various hot-rolled **steel grades** for sheet piles; steel grades S 270 GP and S 355 GP are generally used. The choice of steel grade depends on structural aspects, the method of driving selected, the embedment depth and the ground conditions.

Table 2.1: Steel grades for hot-rolled steel sheet piles and their characteristic mechanical properties to DIN EN 10248-1

Steel grade	Min. tensile strength f_u [N/mm ²]	Min. yield strength f_y [N/mm ²]	Min. elongation at failure ϵ_u [%]
S 240 GP	340	240	26
S 270 GP	410	270	24
S 320 GP	440	320	23
S 355 GP	480	355	22
S 390 GP	490	390	20
S 430 GP	510	430	19

The characteristic mechanical properties of **cold-worked steel sheet piles** according to DIN EN 10249-1 are shown in table 2.2. These sheet piles are used, for example, when a lightweight section is required or for trench sheeting.

Table 2.2: Steel grades for cold-worked steel sheet piles and their characteristic mechanical properties to DIN EN 10249-1

Steel grade	Min. tensile strength f_u [N/mm ²]	Min. yield strength f_{yb} [N/mm ²]	Min. elongation at failure ϵ_u [%]
S 235 JR	340	235	26
S 275 JR	410	275	22
S 355 JOC	490	355	22

2.2.3 Suitability for welding

Welding involves fusing together two identical or very similar steels to form one homogenous component, and this is done by melting them together at their interface through liquefaction or plastic deformation. This can be carried out with or without the addition of another material. Arc welding is a very common method (manual metal-arc welding, shielded metal-arc welding). In this method an electric arc is generated between an electrode, which supplies the welding material, and the component. The suitability for welding depends not only on the material, but also on its shape, the dimensions and the fabrication conditions. Killed steels should generally be preferred.

According to EAU 2004 section 8.1.6.4 (R 67), and taking into account general welding specifications, arc welding can be used for all the grades of steel used for sheet piles. The building authority approvals must be adhered to for high-strength steel grades S 390 GP and S 430 GP. In addition, the carbon equivalent CEV should not exceed the value for steel grade S 355 to DIN EN 10025 table 4 if welding is to be employed.

Furthermore, EAU 2004 section 8.1.6.4 (R 67) recommends using fully killed steels of the

J2 G3 or K2 G3 groups to DIN EN 10025 in special cases, e.g. where plastic deformation due to heavy driving is expected, at low temperatures, in three-dimensional stress conditions and when the loads are principally dynamic, because of the better resistance to embrittlement and ageing required. Welding electrodes conforming to DIN EN 499, DIN EN 756 and DIN EN 440 or the specification of the supplier should be selected. According to EAU 2004 section 8.1.18.2 (R 99), basic electrodes or filler materials with a high basicity should generally be used.

Table 2.3 provides general information about the selection of suitable electrodes according to DIN EN 499.

Table 2.3: Welding electrodes for manual metal-arc welding to DIN EN 499 for steel grades S 240 GP to S 355 GP

Applications	Welding electrode/ standard designation	Properties
Site welding: e.g. welding of interlocks in non-ideal position	E 42 0 RC 11	Rutile/cellulose-coated electrode. For most applications. Particularly suitable for tack welds; good gap-filling ability; welding positions: w,h,s,q,ü,f
Factory and site welding: butt and fillet welds	E 38 0 RA 12	Rutile/acid-coated electrode with fine-drop-type material transition. Particularly suitable for fillet welds, acute angles and rusty workpieces; high current-carrying performance; welding positions: w,h,s,q,ü
Factory and site welding: heavily loaded welds in structures with risk of cracking; butt and fillet welds	E 42 5 BA32 H5	Basic-covered electrode with high demands on toughness and crack prevention; good welding properties in non-ideal positions; welding positions: w,h,s,q,ü

2.2.4 Corrosion and service life

The service life of a sheet piling structure is to a large extent dependent on the natural process of **corrosion**. Corrosion is the reaction of the steel to oxygen and the associated formation of iron oxide. Therefore, a continuous weakening of the sheet piling cross-section necessary for the stability of the wall takes place over several years. This weakening must be taken into account when analysing the serviceability and the ultimate load capacity. For corrosion in the atmosphere, i.e. without the effects of water or splashing water, a corrosion rate of approx. 0.01 mm/a is low. Also very low is the corrosion rate (on both sides) of sheet pile walls embedded in natural soils, which is also approx. 0.01 mm/a (EAU 2004 section 8.1.8.3, R 35).

The reason for this is the exclusion of oxygen. The same corrosion rate can be expected on sheet pile walls backfilled with sand. However, in this case it must be ensured that the troughs of the sections are filled completely with sand. A coating with a high protective effect forms in calcareous water and soils with a calcium carbonate content. Aggressive soils, e.g. humus, or aggressive groundwater should not be allowed to come into contact with the surface of a sheet pile wall. Furthermore, corrosion of the sheet piling can be promoted by bacteria in the soil.

Considerably more severe corrosion can be expected in hydraulic structures, which is, however, not evenly distributed over the full height of the structure. Fig. 2.5, in accordance with EAU 2004 section 8.1.8 (R 35), illustrates the **corrosion zones** using the North Sea and Baltic Sea as examples. The greatest weakening of the wall thickness and hence the resistance of the component takes place in the low water zone. When designing a sheet pile wall, care should be taken to ensure that the maximum bending moments do not occur at the same level as the main corrosion zones.

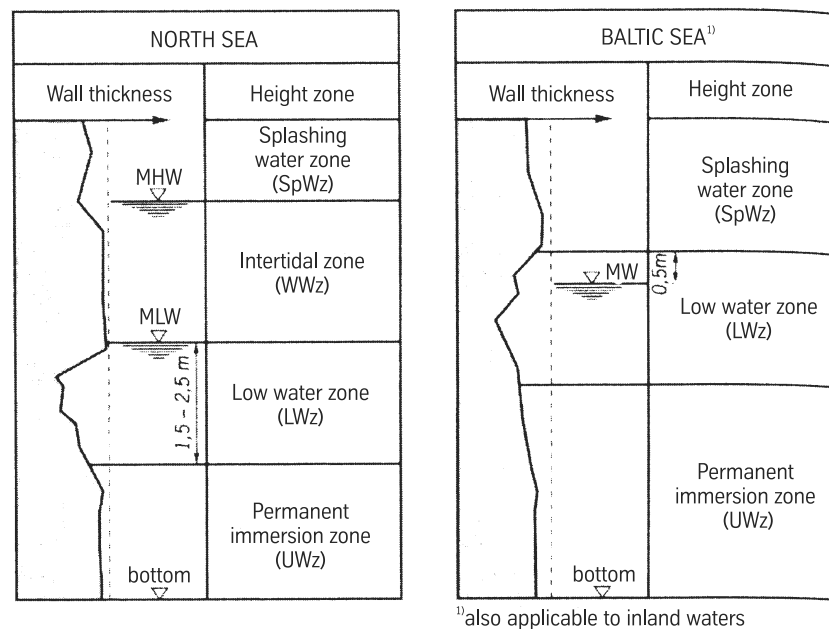


Figure 2.5: Qualitative diagram of the corrosion zones for steel sheet piling using the North Sea and Baltic Sea as examples (EAU 2004)

EAU 2004 includes diagrams in section 8.1.8.3 (R 35) with which the weakening of the wall thickness due to corrosion can be calculated (Fig. 2.6). Using these diagrams, sheet pile walls can be designed for the mean and maximum losses in wall thickness if no wall thickness measurements are available from neighbouring structures. The areas shaded grey in the diagrams represent the scatter for structures investigated hitherto. To avoid uneconomic forms of construction, EAU 2004 recommends using the measurements above the regression curves only when local experience renders this necessary. For structures located in briny water, i.e. in areas in which freshwater mixes with seawater, the reduction in wall thickness can be interpolated from the diagrams for seawater and freshwater.

According to current knowledge, adding a coating to the sheet piles can delay the onset of

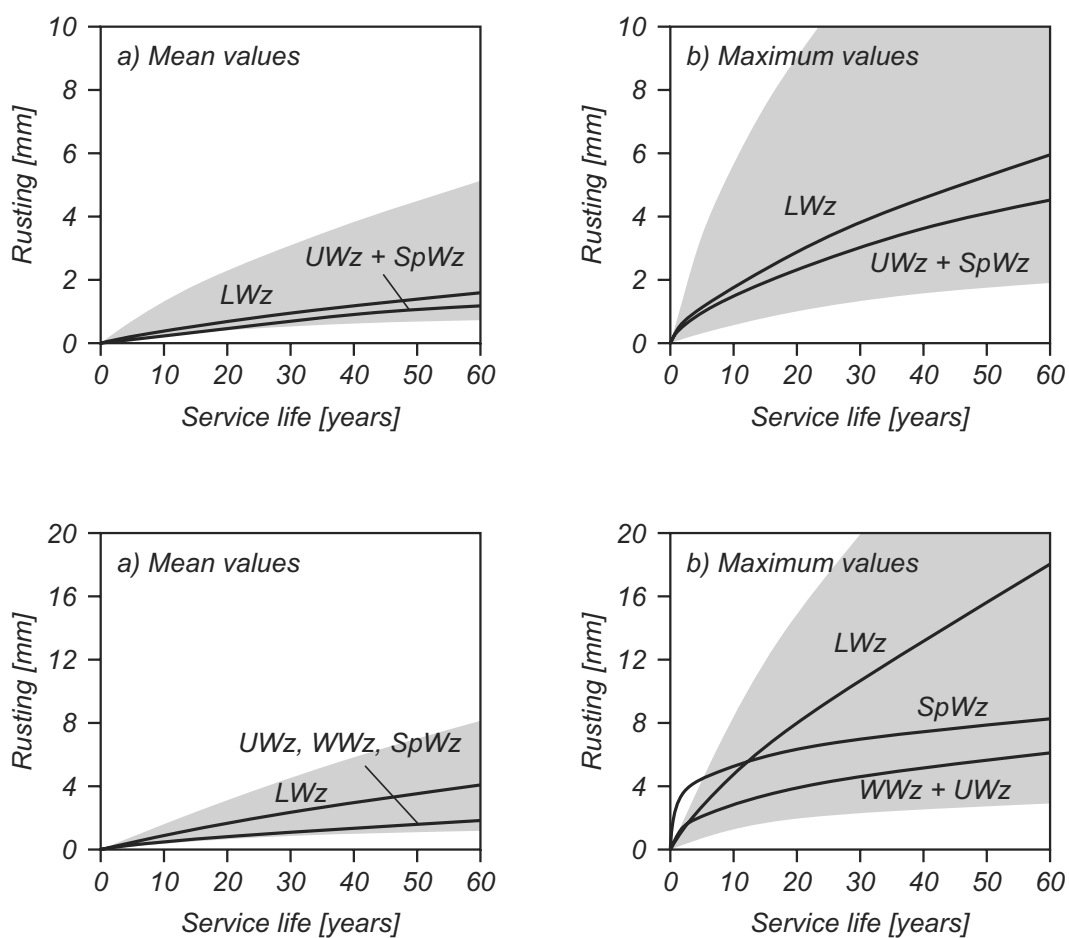


Figure 2.6: Decrease in thickness of sheet pile walls in freshwater (top) and seawater (bottom) due to corrosion (EAU 2004)

corrosion by more than 20 years. One way of virtually eliminating corrosion below the waterline is to employ an electrolytic method in the form of a sacrificial anode. Another way of achieving protection against corrosion is to overdesign the sections, but in this case an economic analysis must be carried out first.

2.3 Driving sheet pile walls

Sheet pile walls can be threaded into precut trenches, or pressed, impact-driven or vibrated into position. Threading and pressing do not involve any knocks or shocks, which is a complete contrast to impact driving and vibration methods. In difficult soils, the driving can be eased by pre-drilling, water-jetting, pre-blasting or even by replacing the soil.

When driving sheet pile walls, it is possible for the sheet piles to start leaning forwards or backwards with respect to the direction of driving (Fig. 2.7). **Forward lean** is caused by friction in the interlocks and by compaction of the soil while driving the previous sheet pile. The driving force is transferred to the pile concentrically, but the reaction forces are distributed unevenly across the sheet pile. **Backward lean** can occur in dense soils if the previous sheet pile has loosened the soil. To prevent leaning of sheet piles, they should be held in a guide frame or trestle. Vertical alignment during driving can be impaired by obstacles in the soil or hard strata at unfavourable angles.

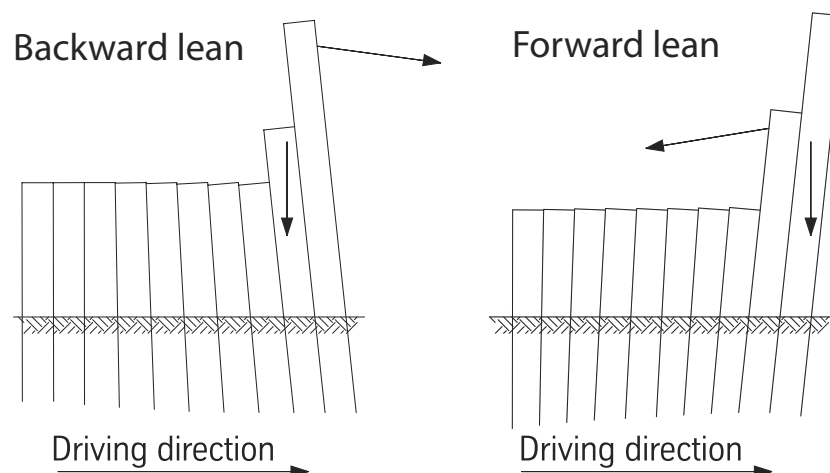


Figure 2.7: Sheet pile sections exhibiting backward lean (left) and forward lean (right)

2.3.1 Threading piles into precut trenches

This method can be used in almost any soil. To do this, a trench must be excavated or holes drilled in the ground first, which are then filled with a suspension. If necessary, the sheet piles can be subsequently driven to their full depth.

2.3.2 Pressing

Pressing is used primarily when there are severe restrictions placed on noise and vibration. This is mostly the case in residential districts, very close to existing buildings and on embankments. In contrast to driving using impact hammers and vibration techniques, the sheet piles are simply forced into the ground using hydraulic pressure. Noise and vibration are therefore kept to a minimum. We distinguish between pressing plant supported from a crane, plant guided by a leader and plant supported on the heads of piles already driven.

In the first method, a crane lifts the pressing plant onto a group of piles which are then pressed into the ground by means of hydraulic cylinders (Fig. 2.8). To do this, the hydraulic cylinders are clamped to each individual sheet pile. At first, the self-weight of the pressing plant and the sheet piles themselves act as the reaction to the pressing force. As the sheet piles are driven further into the ground, it is increasingly the skin friction that provides the reaction. Both U- and Z-sections can be pressed, and the method can also be used to extract sheet piles.

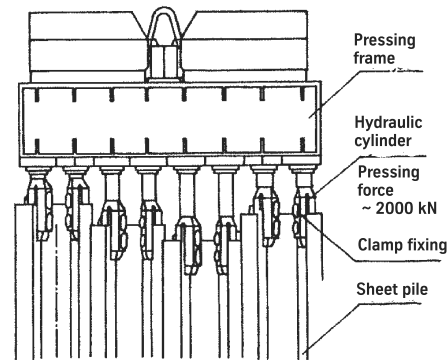


Figure 2.8: Pile-pressing using crane-supported pressing plant (BUJA, 2001)

The leader-guided method (Fig. 2.9) works similarly to the crane-supported method. However, the setup is lighter. Owing to the relatively low pressing forces, the leader-guided method is primarily used for lightweight sections and in loose to medium-dense soils.

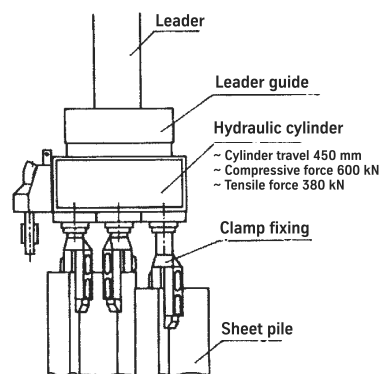


Figure 2.9: Pile-pressing using the leader-guided method (BUJA, 2001)

Fig. 2.10 shows the principle of pile-pressing with plant supported on the sheet piles already driven. In this method, only a single sheet pile is pressed into the ground in each pressing operation. The self-weight and the sheet piles already driven provide the reaction. The pressing plant moves forward on the wall itself to each next pressing position as the wall progresses.

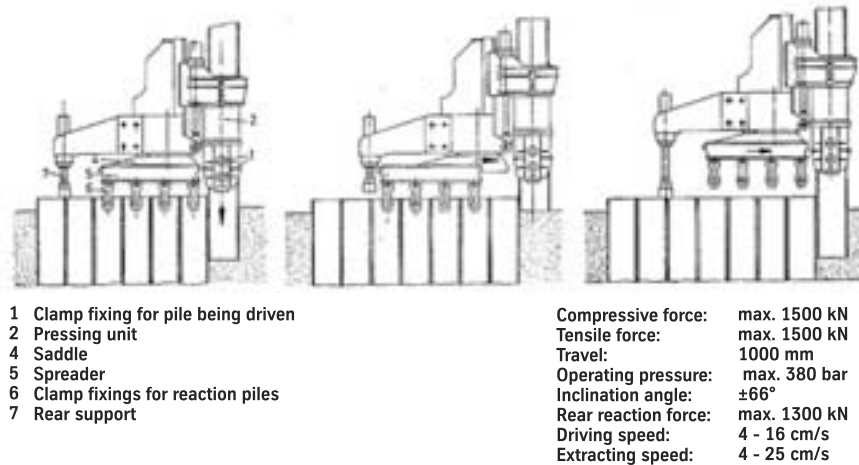


Figure 2.10: Pile-supported pressing system *Silent Piler*

2.3.3 Impact driving

Impact driving involves driving the sheet piles into the ground with a succession of hammer-blows (Fig. 2.11). A timber driving cap is usually placed between the hammer and the sheet pile. We distinguish between slow- and rapid-action systems. Slow-action plant such as drop hammers and diesel hammers is primarily used in cohesive soils so that the ensuing pore water pressure has time to dissipate between the individual blows. In a drop hammer, a weight is lifted mechanically and then allowed to fall from a height h . Modern drop hammers operate hydraulically. The number of blows can be set as required between 24 and 32 blows per minute. The drop height of a diesel hammer is determined by the explosion of a diesel fuel/air mixture in a cylinder. Depending on the type of hammer, the weight is either allowed to drop freely onto the driving cap or instead the weight can be braked on its upward travel by an air buffer and then accelerated on its downward travel by a spring. Using this latter technique, 60–100 blows per minute are possible, whereas with the non-accelerated hammer the figure is only 36–60 blows per minute. Rapid-action hammers are characterised by their high number of blows per minute: between 100 and 400. However, the driving weight is correspondingly lighter. Rapid-action hammers are driven by compressed air and the weight is accelerated as it falls.

The head of the sheet pile can be overstressed during impact driving if the hammer is too small or the resistance of the ground is too great. Possible remedies are to strengthen the head or use a larger hammer. In the case of a high ground resistance, excessive driving force or an incorrectly attached driving cap, the pile can buckle below the point of impact. To avoid this, use thicker sections or loosen the ground beforehand.

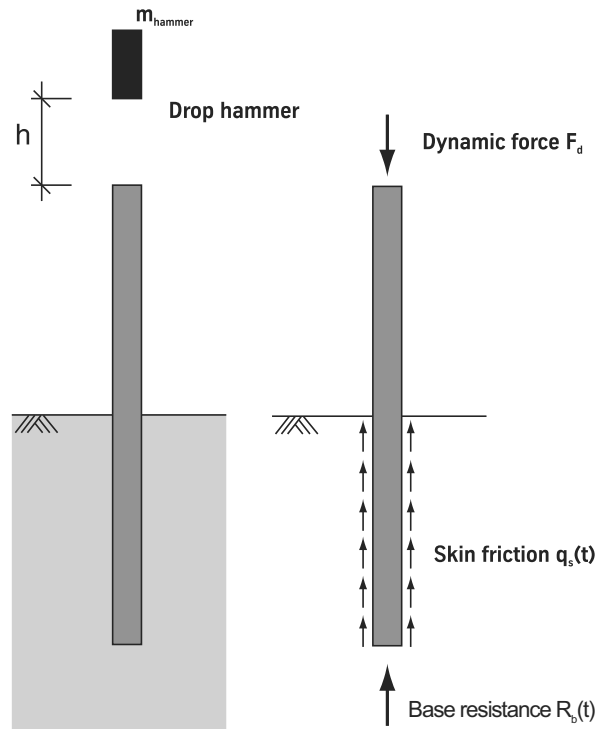


Figure 2.11: Principle of impact driving

2.3.4 Vibratory driving

Vibratory driving is based on the harmonic excitation of the sheet pile. This causes a redistribution of the soil and reduces the friction between soil and sheet pile, also the toe resistance. Local liquefaction of the soil may also take place at the boundary layer between sheet pile and soil, and this also leads to a decrease in the driving resistance. One advantage of vibration is that the same plant can be used for driving and also for extracting sheet piles.

The harmonic excitation is generated by eccentric weights in the vibrator (Fig. 2.12). The isolator prevents the oscillations being transmitted to the pile-driving plant as the eccentric weights rotate. The sheet pile is loaded by a static force due to the self-weight of the vibrator and, if necessary, by an additional leader-guided prestressing force. The maximum centrifugal force F_d is

$$F_d = m_u r_u \Omega^2 \quad (2.2)$$

In this equation, m_u is the mass of the eccentric weights, r_u is the distance of the centre of gravity of the eccentric weights to the point of rotation, and Ω is the exciter frequency. The product of m_u and r_u is also known as a static moment.

Vibrators can be mounted on the head of the sheet pile, suspended from an excavator or crane or also guided by leaders. Vibrators are driven hydraulically and with modern vibrators it is possible, for a constant centrifugal force, to adjust the frequency, and hence the static moment, to suit the soil properties in order to achieve optimum driving progress.

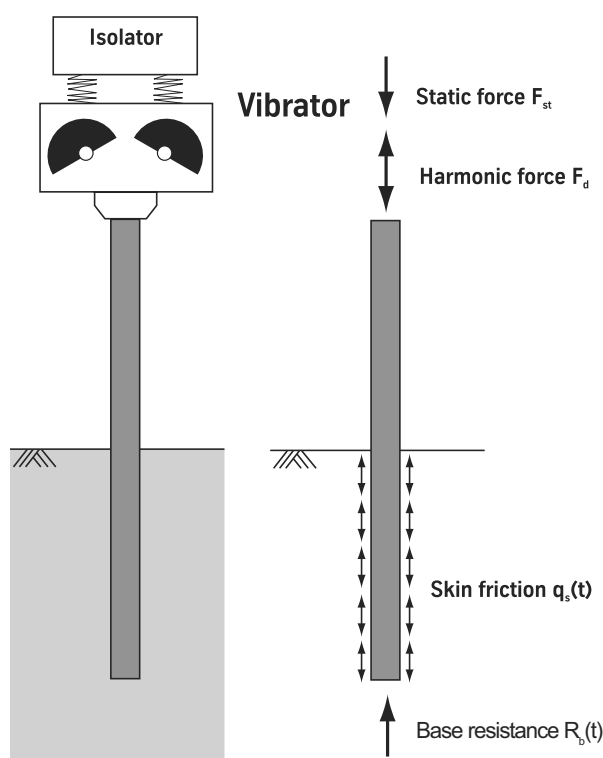


Figure 2.12: Principle of vibratory driving

The acceleration and braking of the eccentric weights is critical in vibratory driving because in doing so they pass through the low frequencies and thus excite the natural frequencies of buildings (approx. 1–5 Hz) and suspended floors (approx. 8–15 Hz). These days, vibrators are therefore in the position of being able to accept the maximum r.p.m. initially and then generate a variable (from zero to maximum) imbalance moment by rotating the eccentric weights. Furthermore, there are systems that permit online monitoring of the oscillation velocities at measuring points close by. The vibrator operator, in conjunction with variable imbalance, is therefore in the position of being able to react to unacceptably high oscillation velocities by changing the imbalance amplitude or frequency.

2.3.5 Vibrations and settlement

The use of impact driving and vibratory driving causes **ground vibrations** that propagate in the subsoil. Besides possibly causing damage to neighbouring buildings through **vibrations**, there may be a risk of compacting the soil at some distance from the sheet pile, which can lead to **settlement**. This risk is particularly problematic in the case of long-term, repetitive vibration effects on buildings founded on loosely packed, uniform sands and silts. Liquefaction of the soil is another risk: the build-up of pore water pressure due to dynamic actions causes the soil to lose its shear strength briefly and hence its bearing capacity. Impact driving causes vibrations in the ground which, however, quickly dissipate after each blow.

Vibrations in the ground propagate in the form of different types of waves. Fig. 2.13 shows

the wave types recognised in elastodynamics. We distinguish between **body waves** (compression and shear waves) and **surface waves** (Rayleigh waves). In stratified soils, additional shear waves, called Love waves after A.E.H. Love, occur at the boundaries between the strata.

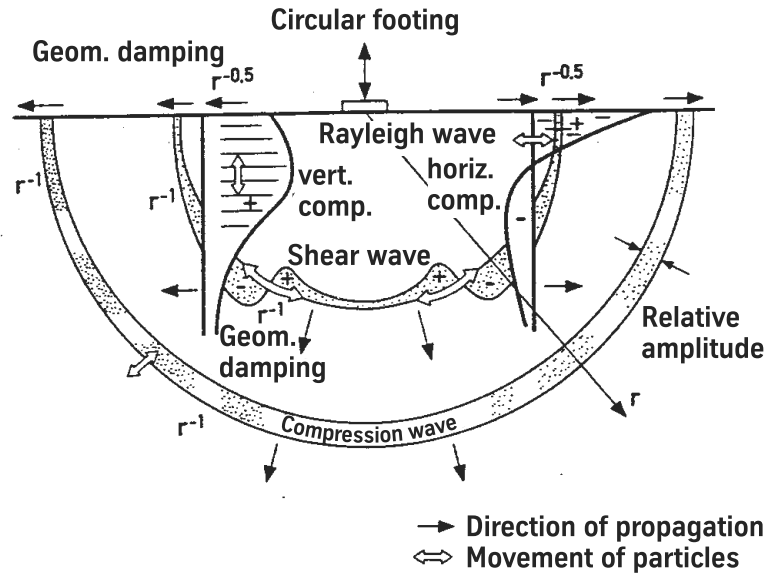


Figure 2.13: Propagation of vibrations in an elastic half space (WOODS, 1968)

Excessive vibrations can damage buildings. If the source of the vibrations is near ground level, the propagation of the vibrations in the ground is primarily by way of Rayleigh waves. According to DIN 4150-1, the decrease in the oscillation velocity amplitude \bar{v} [mm/s] in the far-field can be estimated using the following equation:

$$\bar{v} = \bar{v}_1 \left[\frac{R}{R_1} \right]^{-n} \exp[-\alpha(R - R_1)] \quad (2.3)$$

where

\bar{v}_1 = amplitude of oscillation velocity in mm/s at distance R_1

R_1 = reference distance in m

R = distance from source

n = an exponent that depends on type of wave, source geometry and type of vibration

α = decay coefficient in m^{-1} , $\alpha \approx 2\pi D/\lambda$

D = degree of damping

λ = critical wavelength in m, $\lambda = c/f$

c = wave propagation velocity in m/s

f = frequency in Hz

Table 2.4: Guide values for oscillation velocity which can be used to assess the effects of transient vibrations on structures according to DIN 4150-3

Line	Type of building	Guide values for maximum oscillation velocity v_i in mm/s			
		Foundation frequencies			Topmost floor level, horizontal
		1–10 Hz	10–50 Hz	50–100 Hz*)	all frequencies
1	Commercial, industrial and similarly constructed buildings	20	20 to 40	40 to 50	40
2	Residential buildings and other buildings with similar construction and/or uses	5	5 to 15	15 to 20	15
3	Buildings that owing to their particular sensitivity to vibration cannot be classed under those buildings of lines 1 and 2 and are particularly worthy of conservation (e.g. protected by preservation orders)	3	3 to 8	8 to 10	8

*) The guide values for 100 Hz may be used as a minimum for frequencies > 100 Hz.

The reference distance R_1 is the distance of the transition of the unrestricted wave propagation (far-field) from the complex processes in the immediate vicinity of the source of vibration (near-field). It is defined by:

$$R_1 = \frac{a}{2} + \lambda_r \quad (2.4)$$

where a = dimension of vibration source parallel to direction of propagation, and λ_r = wavelength of surface wave.

Table 2.4 contains guide values for maximum oscillation velocity amplitudes which can be used to assess the effects of transient vibrations on structures according to DIN 4150-3.

DIN ENV 1993-5 includes an equation for predicting the maximum oscillation velocity ampli-

tude of a particle during impact and vibratory driving:

$$v = C \frac{\sqrt{w}}{r} \quad (2.5)$$

where

C = a factor to allow for the method of driving and the ground conditions according to table C.1, DIN ENV 1993-5 (these values based on measurements are also listed in table 2.5)

r = radial distance from source in m, where $r \geq 5$ m

w = source energy in Joule

In the case of impact driving, the energy per blow can be taken from data sheets, or in the case of drop hammers it can be calculated using $w = mgh$. When using vibratory driving, the energy per revolution can be estimated from the power P of the vibrator in W and the frequency f in Hz using the following equation:

$$w = \frac{P}{f} \quad (2.6)$$

Table 2.5: Typical values for factor C to DIN ENV 1993-5

Driving method	Ground conditions	Factor C in eq. 2.5
Impact driving	Very stiff cohesive soils, dense grainy soils, rock; backfilling with large boulders.	1.0
	Stiff cohesive soils, medium-dense grainy soils, compacted backfilling.	0.75
	Soft cohesive soils, loose grainy soils, loosely fill, soils with organic constituents.	0.5
Vibratory driving	for all ground conditions	0.7

In order to avoid causing settlement of neighbouring buildings, DIN 4150-3 includes advice on the clearances to be maintained when using vibratory techniques to drive sheet piles into homogeneous non-cohesive soils. Fig. 2.14 shows the clearance to be maintained between sheet pile walls and existing buildings as recommended by DIN 4150-3. Accordingly, an angle of at least 30° , in groundwater 45° , from the vertical should be maintained between base of sheet piling and building foundation.

The driving method parameters and variables linked with the ground conditions are not included in this. Studies by GRABE & MAHUTKA (2005) reveal that settlement depends on the exciting frequency and the soil strata. As the process of dynamically induced settlement has not been fully researched, DIN 4150-3 recommends consulting a geotechnical engineer.

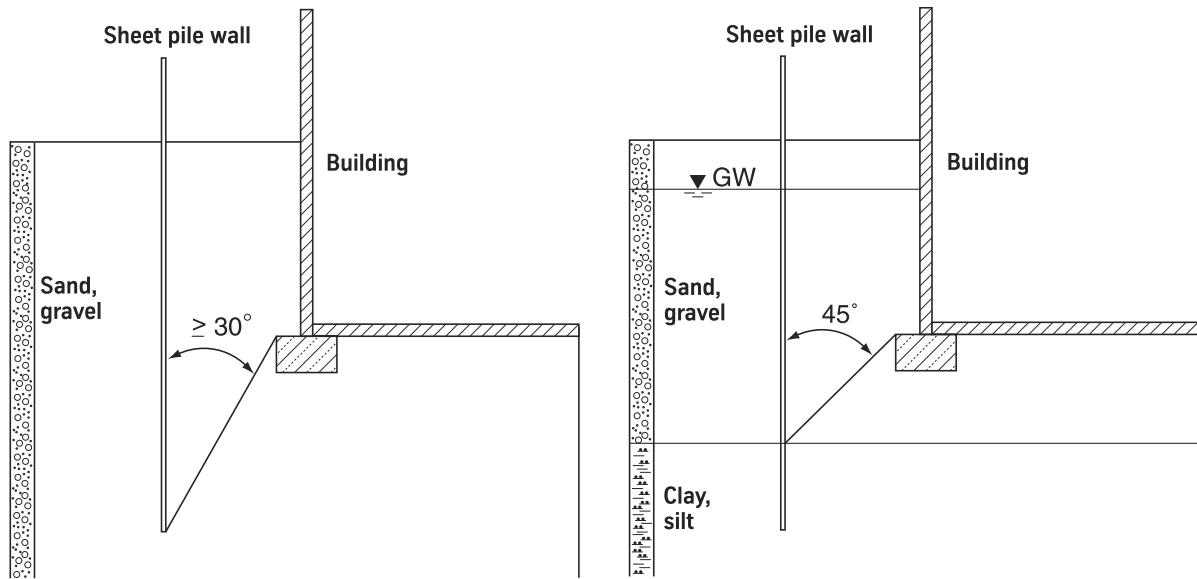


Figure 2.14: Schematic diagram of clearances between sheet piling and buildings according to DIN 4150-3, without groundwater (left) and with groundwater (right)

Chapter 3

Subsoil

In order to guarantee the safe and economic execution of a construction project, soil investigations are necessary. The nature and scope of the **soil investigations** depend on the geotechnical categories according to DIN EN 1997-1:2005-10, and DIN 4020:2003-09 provides information on the scope of the explorations. Soil investigations are divided into field (in situ) and laboratory tests.

The following is intended to provide an overview of field and laboratory tests that serve as the basis for the design and installation of sheet pile walls and combined walls. Table 3.1 provides an overview of the various target variables of investigation measures. It also shows which variables can be determined with which tests.

Table 3.1: Target variables of investigation measures

Target variable/ soil parameter	Method	
	Field test	Lab. test
Sequence of strata	3.1.1	3.2.1
Groundwater	x	-
Soil type	-	3.2.1+3.2.3
Obstacles	3.1.3	-
In situ density I_D, D	3.1.2	3.2.2
Consistency I_C	-	3.2.3
Water content w	-	x
Shear parameters $\varphi, c, \varphi_u, c_u$	3.1.2	3.2.5
Deformation behaviour $E_S, C_C, C_S, c_V, c_\alpha$	3.1.2	3.2.4
Unit weight γ	-	3.2.2
Overconsolidation ratio OCR	-	3.2.4

When using material laws of better quality (see chapter 8), it is necessary to specify not only the laboratory test results assessed by the specialist in the soil investigation report, but also to include complete test curves.

3.1 Field tests

3.1.1 Boreholes

Boreholes are used to obtain soil samples from greater depths. The boring method is chosen to suit the subsoil. When the sides of the borehole are unstable or exhibit little stability (e.g. in saturated sands), methods with casings are used, but in stable strata (e.g. cohesive, stiff soils), casings may be unnecessary. In the normal case, class 2 samples and in favourable conditions class 1 samples to DIN 4021:1990-10 can be obtained from the ground. In heavily stratified soils, it is advisable to carry out the boring and acquisition of samples in fixed casings to DIN 4020:2003-09, as so-called liner or core samples. If the sequence of strata is known and the strata are relatively thick, obtaining special samples in steel tubes about 25 cm long represents an economic alternative to core samples. The tubes are pressed or driven into the base of the borehole and subsequently withdrawn. This also results in class 1 and 2 samples, which, for example, are necessary for determining the shear parameters in laboratory tests (see section 3.2.5). Like with all soil samples, the soil should be taken from a representative area of the stratum; sampling at the boundaries between strata should be avoided. If the soil samples are used for determining shear parameters or the coefficient of compressibility, a tube or liner with a diameter of at least 100 mm is advisable. Samples should generally be protected against drying out.

The presence of any groundwater should be recorded as the boring work proceeds. Every borehole can be widened for measuring the groundwater level.

3.1.2 Penetrometer tests

Penetrometer tests are indirect methods of exploration which are used in addition to boreholes as part of more extensive soil investigations. Penetrometer tests are carried out at least down to the depth of the principal boreholes. For calibration purposes, a penetrometer test should be carried out in the direct proximity of a principal borehole.

Cone penetration tests

Cone penetration tests should be carried out according to DIN 4094-1:2002-06. The toe resistance q_c , the local skin friction f_s and, if applicable, the pore water pressure u are measured using a cone, which is pressed vertically into the subsoil. The friction ratio is defined as $R_f = f_s/q_c$. The angle of friction φ' , the undrained cohesion c_u and the in situ density D or I_D can be derived with the help of empirical methods according to DIN 4094-1:2002-06. A modulus of compressibility E_S irrespective of the stress can be estimated by using the OHDE method.

$$E_S = \nu \cdot \rho_a [(\sigma_{\bar{u}} + 0.5 \cdot \Delta\sigma_z) / \rho_a]^\omega \quad (3.1)$$

where ν : compressibility coefficient

$$\nu = 176 \lg q_c + 113 \quad (\text{soil group SE) for } 5 \leq q_c \leq 30$$

$$\nu = 463 \lg q_c - 13 \quad (\text{soil group SW) for } 5 \leq q_c \leq 30$$

$$\nu = 15.2 \lg q_c + 50 \quad (\text{soil groups TL, TM) for } 0.6 \leq q_c \leq 3.5$$

ω : compressibility exponent $\omega = 0.5$ for non-cohesive soils
 $\omega = 0.6$ for cohesive soils

ρ_a : atmospheric pressure

$\sigma_{\ddot{u}}$: overburden stress at depth z

$\Delta\sigma_z$: increase in vertical stress at depth z due to construction measures

The driving guidelines of HSP HOESCH Spundwand und Profil GmbH specify a relationship between toe resistance q_c and in situ density D or relative density I_D which is based on experience.

Table 3.2: Estimation of in situ density of non-cohesive soils from cone or dynamic penetration tests (extract from RAMMFIBEL FÜR STAHLSPUNDBOHLLEN)

In situ density	Cone penetration test (CPT) q_c in MN/m ²	Dynamic penetration test (DPH) N_{10}
very loose	2.5	-
loose	2.5-7.5	3
medium dense	7.5-15	3-15
dense	15-25	15-30
very dense	> 25	> 30

Fig. 3.1 shows a typical result of a cone penetration test and the associated soil exploration.

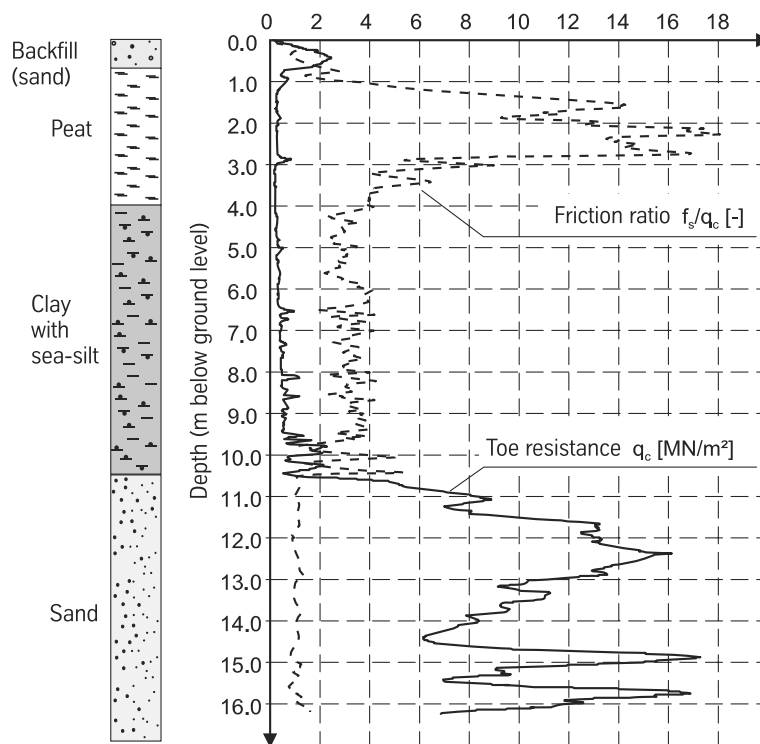


Figure 3.1: Example of a CPT

Dynamic penetration tests

In the **dynamic penetration test**, a cone with defined dimensions is driven into the subsoil with a constant driving energy and the number of blows N_{10} required for 10 cm penetration are recorded. Various methods (DPL, DPM, DPH, DPG), hammer weights and drop heights are described in DIN 4094-3:2002-01.

Vane shear tests

The **vane shear test** to DIN 4094-4:2002-01 is suitable for soft, cohesive and non-stony soils. The vane is pressed into a soft stratum, either directly or at the base of a borehole, and subsequently rotated with a defined speed between $0.1^\circ/\text{s}$ and $0.5^\circ/\text{s}$. The maximum torque M_{max} is measured while doing this. Afterwards, at least 10 shearing processes are carried out at a speed of $10^\circ/\text{s}$ and the residual torque determined from this. The maximum shear resistance c_{fv} , the residual shear resistance c_{rv} and the undrained shear strength c_{fu} can be determined from these measurements.

Pressuremeter tests

In the pressuremeter test, the borehole is widened over a small area and the force required and the resulting deformation are determined (DIN 4094-5:2001-06). The modulus of compressibility E_S of the soil can be derived from this measurement.

3.1.3 Geophysical measurements

The use of geophysical exploration methods can be helpful in some projects. These include seismic and thermal techniques, radiometry, gravimetry, geoelectrics, georadar, geomagnetics and electromagnetics.

3.1.4 Assessment of penetration resistance

Easy driving can be expected with loosely layered sands and gravels, also soft, cohesive soils. Heavy driving frequently occurs in densely layered sands or gravels, also stiff, cohesive soils and rock. Generally speaking, the penetration resistance is higher with dry soils than with damp or saturated soils.

Sands and gravels with rounded grains and soft, cohesive soils are suitable for vibratory driving; non-plastic soils with angular grains or cohesive soils with a stiff consistency are less suitable. Non-cohesive soils with a uniform, fine granular structure can be compacted to such an extent during vibratory driving that penetration becomes impossible. In such cases driving aids should be employed.

3.2 Laboratory tests

3.2.1 Granulometric composition

The **granulometric composition** specifies the relative proportions by weight of various particle sizes in the soil. A sieve analysis is carried out for particle diameters > 0.06 mm, a sedimentation or hydrometer analysis for particle sizes smaller than approx. 0.1 mm. A soil can be classified as a clay, silt, sand or gravel according to the grading curve. Mixed-particle soils are designated according to their principal soil type. Soils that are essentially influenced by their physical properties are known as non-plastic or granular. Soils are termed cohesive when their soil mechanics properties are essentially dependent on the electrochemical forces between the particles, and clay minerals are particularly prevalent here. The average gradient of the grading curve indicates whether the soil has a uniform or non-uniform composition. The uniformity coefficient U is defined as

$$U = \frac{d_{60}}{d_{10}} \quad (3.2)$$

where d_{60} designates the particle diameter for 60% passing through the sieve, d_{10} the corresponding designation for 10%. Soils with $U < 5$ are uniform, $5 < U < 15$ non-uniform, and $U > 15$ extremely non-uniform.

3.2.2 Determining unit weight and in situ density

It is necessary to know the unit weight for the earth pressure analyses. The unit weight describes the ratio of the soil self-weight to the volume and is determined using the methods given in DIN 18125. The void ratio e and the porosity n for a soil can be calculated from the unit weight and the water content:

$$e = \frac{\rho_s}{\rho_d} - 1 \text{ or } n = 1 - \frac{\rho_d}{\rho_s} \quad (3.3)$$

In non-cohesive soils, these variables can be used to determine the **in situ density** D or the relative density I_D of the soil in its natural state. To do this, the determination of the in situ density for the loosest and densest states is carried out on samples in the laboratory according to DIN 18126:1996-11, which results in the following:

$$D = \frac{n_{max} - n}{n_{max} - n_{min}} \quad (3.4)$$

where n_{max} : Porosity for loosest state
 n_{min} : Porosity for densest state
 n : Porosity in natural state

$$I_D = \frac{e_{max} - e}{e_{max} - e_{min}} \quad (3.5)$$

where e_{max} : Void ratio for loosest state
 e_{min} : Void ratio for densest state
 e : Void ratio in natural state

The designation of the in situ density can be taken from table 3.3.

Table 3.3: Designation of in situ densities

Designation	D	I_D
very loose	0-0.15	-
loose	0.15-0.3	0-0.33
medium dense	0.3-0.5	0.33-0.66
dense	0.5-0.7	0.66-1.0
very dense	0.7-1.0	-

The in situ density can also be derived from dynamic and cone penetration tests (see section 3.1.2). Typical values for attainable and necessary in situ densities of non-cohesive soils are given in EAU 2004 sections 1.5 (R 71), 1.6 (R 175) and 1.7 (R 178).

3.2.3 Consistency

The **consistency** (deformability) of cohesive soils essentially depends on the water content. As the water content falls, so the consistency of the soil is described as fluid, very soft, soft, stiff, semi-firm, firm. The water contents at the transitions between fluid to plastic (liquid limit w_L), plastic to stiff (plastic limit w_P) and semi-firm to firm (shrinkage limit w_S) were defined by ATTERBERG in tests.

The plasticity index I_P describes the sensitivity of a soil to changes in its water content:

$$I_P = w_L - w_P \quad (3.6)$$

The larger the I_P value, the greater is the plastic range of the soil and the less the consistency varies for changes in the water content. The consistency index I_C includes the natural water content of the soil. The consistency of a soil is defined by this (see table 3.4):

$$I_C = \frac{w_L - w}{w_L - w_P} \quad (3.7)$$

The consistency limits w_L and w_P plus the plasticity index I_P are characteristic for cohesive

Table 3.4: Designation of cohesive soils in relation to their consistency

Designation	I_C
very soft	$I_C < 0.5$
soft	$0.5 < I_C < 0.75$
stiff	$0.75 < I_C < 1.0$
firm	$I_C > 1.0$

soils and are helpful for classifying such soils (see Fig. 3.2).

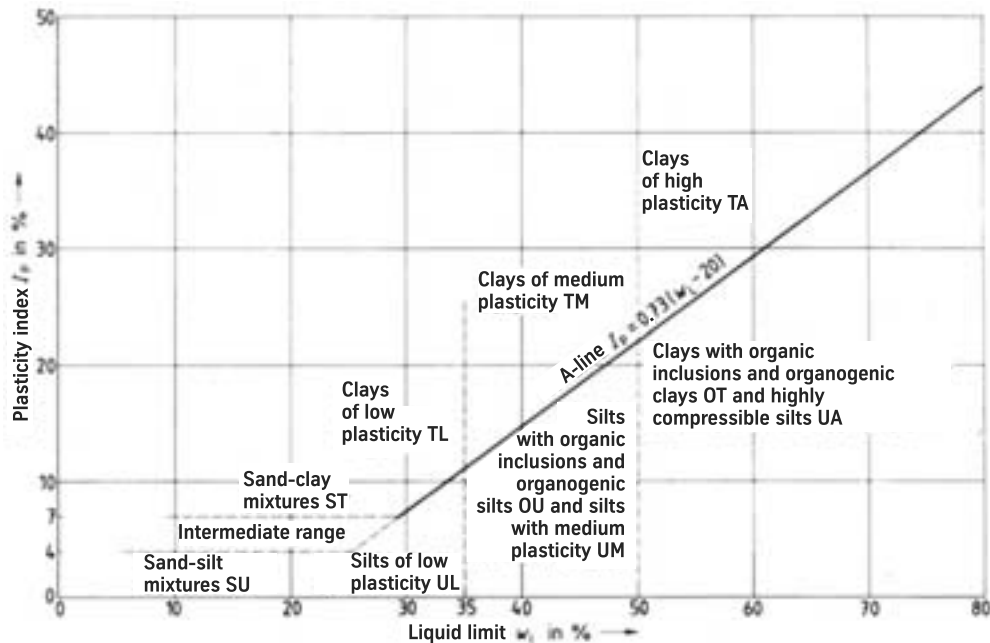


Figure 3.2: Plasticity diagram to DIN 18196:2006-06

3.2.4 Unconfined compression

The unconfined **compression test** imitates the load-deformation behaviour of a soil. It is the most important parameter and supplies the **modulus of compressibility** E_S or the coefficient of compressibility C_c of a soil. In the unconfined compression test, the undisturbed or prepared soil sample is placed in a ring (normally 70 mm dia.) which prevents radial deformation of the sample. The sample is subsequently compressed in the axial direction in several loading steps and the axial deformation measured. In doing so, at least the primary consolidation should be waited for per loading step. The values measured are plotted on a stress-compression graph (see Fig. 3.3) or stress-void ratio graph. As the stress-compression ratio of a soil, in contrast to steel, is non-linear, it must be ensured that the modulus of compressibility is determined for a stress range to which the soil is actually subjected in the field.

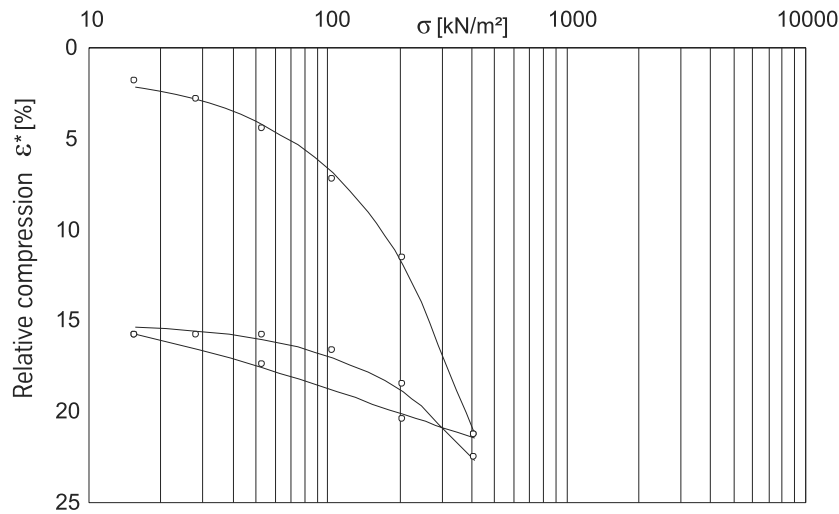


Figure 3.3: Stress–compression graph for an unconfined compression test

3.2.5 Shear parameters

The determination of the **shear parameters** is carried out in the laboratory with the direct shear test (also called the shear box test) or the triaxial test according to DIN 18137. Both tests require at least 3 to 5 individual tests to be carried out with different consolidation stresses so that a shear line after COULOMB can be drawn.

$$\tau = c + \sigma \tan \varphi \quad (\text{COULOMB boundary condition}) \quad (3.8)$$

We distinguish between the shear parameters of the dry soil (φ, c) and those of the saturated soil. In saturated soils, the pore water pressure u reduces the total stresses $\sigma' = \sigma - u$. Here, σ' is the effective stress and the shear parameters of the saturated soil are called the effective shear parameters φ', c' .

In the **direct shear test**, the undisturbed or prepared sample is placed in a square or circular box and subsequently consolidated under a vertical stress σ_V . The shear box is divided horizontally: one part of the cell is fixed, the other slid horizontally (see Fig. 3.4). This shears the sample along a given shear plane. The force required to do this is measured and via the shear surface converted directly into a shear stress τ . The deformations in the horizontal direction, but also in the vertical direction, are recorded in order to assess the expansion or contraction behaviour of the sample. The results are plotted on a σ – τ diagram as a straight line. The gradient of the straight line corresponds to the angle of friction φ or the effective angle of friction φ' , the point of intersection with the axis indicates the cohesion c or the effective cohesion c' .

Samples of cohesive test material should be of class 1 quality to DIN 4021:1990-10. A minimum sample diameter of 70 mm is generally necessary.

The **triaxial compression test** is carried out on a cylindrical sample with a sample height-to-diameter ratio of 2 to 2.5. In the apparatus, the sample is subjected to an axially symmetrical stress state. Therefore, only axial stress σ_1 and radial stress $\sigma_2 = \sigma_3$ are distinguished. Fig. 3.5 shows the principle of the test setup. The test is divided into three phases:

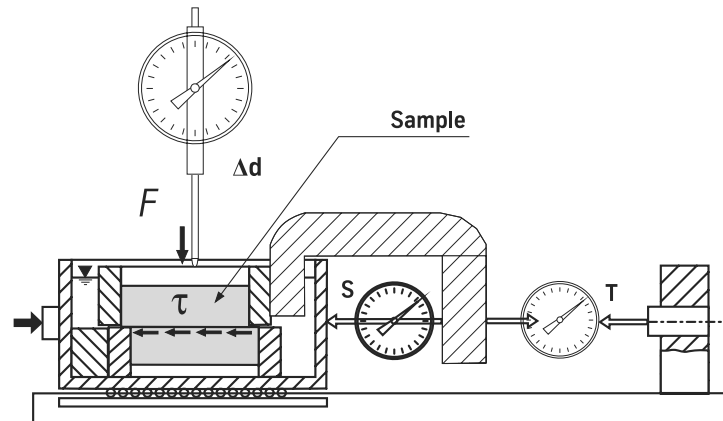


Figure 3.4: Shear box test

- **Saturation:** The sample is generally fully saturated. Water can flow through the sample in an axial direction for this. A saturation pressure of at least 3 bar guarantees that the air in the pores dissolves in the water.
- **Consolidation:** The sample is consolidated by increasing the pressure around the sample. This can transfer the sample to the stress state to which it was subjected when in the ground. The change in volume of the sample can be determined from the quantity of pore water forced out.
- **Shearing off:** After completing the consolidation, the sample is sheared off by slowly increasing the axial stress σ_1 . The limit state is reached when the axial stress reaches a maximum value. If a peak does not form, the value is read off at a vertical compression of $\varepsilon_1 = 20\%$. The shearing process can be carried out on the drained or undrained sample. In the undrained test, the pore water pressure u is measured and the effective stresses $\sigma'_1 = \sigma_1 - u$ and $\sigma'_3 = \sigma_3 - u$ used for the evaluation.

The test is carried out with at least three different cell pressures $\sigma_2 = \sigma_3$ and the shear parameters φ' and c' are determined from the maximum stresses obtained for σ'_1 according to the MOHR-COULOMB boundary condition. The triaxial compression test also requires class 1 samples. The cross-sectional area of samples from fine-grained soils should be at least 10 cm^2 , and coarse-grained soils require a minimum sample diameter of 10 cm.

We distinguish shear tests according to the method and the parameters that can be derived from them:

- **Consolidated, drained test (D test):** The sample can absorb or release water without hindrance during the entire duration of the test. A very slow shearing speed must therefore be selected. The test supplies the effective shear parameters φ' and c' at a limit state with unhindered volume changes.
- **Consolidated, undrained test (CU test):** The shearing process is carried out with self-contained drainage. The test supplies the shear parameters φ' and c' at a limit state with hindered volume changes.

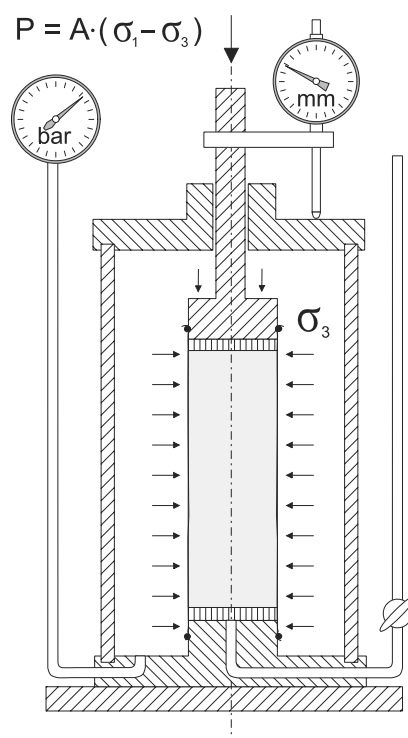


Figure 3.5: Principle of test setup for triaxial compression test

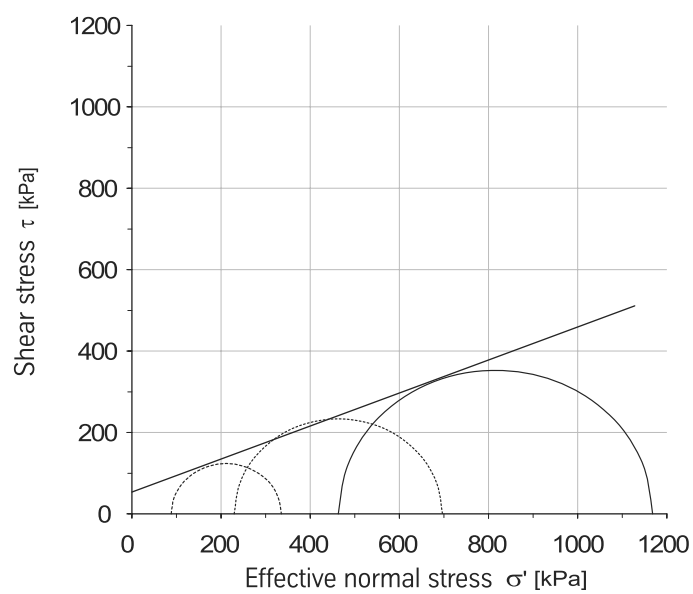


Figure 3.6: Result of a CU test: MOHR's circles of stress

- **Unconsolidated, undrained test (UU test):** The sample is not consolidated and is sheared off with a self-contained drainage line. The test supplies the shear parameters φ_u and c_u at a limit state with constant water content. These values are primarily important for the initial stability.
- **Uniaxial compression test:** In the uniaxial compression test to DIN 18136:2003-11, a cylindrical sample is sheared off under an axial stress σ_1 . The radial stresses are $\sigma_2 = \sigma_3 = 0$. The test supplies the uniaxial compressive strength q_u , from which the undrained cohesion $c_u = q_u/2$ can be derived.

Non-cohesive soil is cohesionless in the fully saturated or dry condition. Partially saturated soils, however, exhibit an apparent cohesion due to capillary action, which increases the shear strength of the soil. According to EAB 2006 section 2.2 (R 2), this capillary cohesion may be taken into account if it is guaranteed that this cannot be lost through drying out or complete flooding, e.g. due to a rise in the groundwater level. Empirical values for capillary cohesion $c_{c,k}$ are given in EAB 2006 appendix A3.

3.3 Soil parameters

The characteristic values of resistances and actions are required for the analyses to DIN 1054:2005-01. According to EAB 2006 section 2.2 (R 2), they should be defined on the safe side of the average value of the results of field or laboratory tests. The difference from the average value can be low here (representative samples) but may also be large (flawed database or inconsistent subsoil). DIN 4020:2003-09 should always be used for defining the characteristic variables. If a variation coefficient $V_G > 0.1$ results during the statistical evaluation of the field and laboratory tests, upper and lower values for the soil parameters must be specified. The following boundary conditions result for the individual **soil parameters**:

- γ The unit weight may be defined as an average value if the loadbearing structure shows little sensitivity to changes in the permanent actions. If it is sensitive, especially with respect to buoyancy, uplift and hydraulic ground failure, upper and lower values are required for the unit weight. Any vertical flow through the soil strata must be taken into account.
- φ' The shear strength is specified by means of the lower characteristic values. Possible clefs, hairline cracks, inclusions, distortions or inclined boundaries between strata should be taken into account. According to EAU 2004 section 1.1 (R 9), the angle of friction for dense soils may be increased by up to 10% with respect to the triaxial compression test in the case of long waterfront structures.
- c' The cohesion of cohesive soils may only be taken into account when the consistency is soft at least.
- c_u, φ_u If no investigations are carried out into the dissipation behaviour of the pore water pressure in the case of cohesive soil strata, calculations should be carried out with c_u and φ_u for the initial state, and c' and φ' for the final state.

E_S The modulus of compressibility E_S , as a three-dimensional variable, should be defined as a cautious estimate of the average value.

Table 3.5 contains empirical values for soil parameters according to EAU 2004 section 1.1 (R 9), which are on the safe side and may be used as characteristic values in the meaning of DIN 1054:2005-01. Without an analysis, the low strength values should be assumed for natural sands and the soft consistency values for cohesive soils.

Table 3.5: Characteristic values of soil parameters (empirical values) to EAU 2004

No.	1	2	3	4	5		6		7	8	9	10
1	Soil type	Soil group to DIN 18196 ¹⁾	Penetration resistance	Strength or consistency in initial state	Unit weight		Compressibility ²⁾ Initial loading ³⁾ $E_S = \nu_e \sigma_{at} (\sigma / \sigma_{at})^{\omega_e}$		Shear parameters of drained soil	Shear parameter of undrained soil	Permeability factor	
2			q_c		γ	γ'	ν_e	ω_e	φ'_k	c'_k	$c_{u,k}$	k_k
3	Gravel, uniform	GE U ⁴⁾ < 6	< 7.5 7.5-15 > 15	low medium high	16.0 17.0 18.0	8.5 9.5 10.5	400 900	0.6 0.4	30.0-32.5 32.5-37.5 35.0-40.0			$2 \cdot 10^{-1}$ to $1 \cdot 10^{-2}$
4	Gravel, non-uniform or gap grading	GW, GI $6 \leq U^4)$ ≤ 15	< 7.5 7.5-15 > 15	low medium high	16.5 18.0 19.5	9.0 10.5 12.0	400 1100	0.7 0.5	30.0-32.5 32.5-37.5 35.0-40.0			$1 \cdot 10^{-2}$ to $1 \cdot 10^{-6}$
5	Gravel, non-uniform or gap grading	GW, GI U ⁴⁾ > 15	< 7.5 7.5-15 > 15	low medium high	17.0 19.0 21.0	9.5 11.5 13.5	400 1200	0.7 0.5	30.0-32.5 32.5-37.5 35.0-40.0			$1 \cdot 10^{-2}$ to $1 \cdot 10^{-6}$
6	Sandy gravel with $d < 0.06 \text{ mm} < 15\%$	GU, GT	< 7.5 7.5-15 > 15	low medium high	17.0 19.0 21.0	9.5 11.5 13.5	400 800 1200	0.7 0.6 0.5	30.0-32.5 32.5-37.5 35.0-40.0			$1 \cdot 10^{-5}$ to $1 \cdot 10^{-6}$
7	Gravel-sand-fine grain mixture with $d < 0.06 \text{ mm} > 15\%$	GU, GT	< 7.5 7.5-15 > 15	low medium high	16.5 18.0 19.5	9.0 10.5 12.0	150 275 400	0.9 0.8 0.7	30.0-32.5 32.5-37.5 35.0-40.0			$1 \cdot 10^{-7}$ to $1 \cdot 10^{-11}$
8	Sand, uniform grading Coarse sand	SE U ⁴⁾ < 6	< 7.5 7.5-15 > 15	low medium high	16.0 17.0 18.0	8.5 9.5 10.5	250 475 700	0.75 0.60 0.55	30.0-32.5 32.5-37.5 35.0-40.0			$5 \cdot 10^{-3}$ to $1 \cdot 10^{-4}$
9	Sand, uniform grading Fine sand	SE U ⁴⁾ < 6	< 7.5 7.5-15 > 15	low medium high	16.0 17.0 18.0	8.5 9.5 10.5	150 225 300	0.75 0.65 0.60	30.0-32.5 32.5-37.5 35.0-40.0			$1 \cdot 10^{-4}$ to $2 \cdot 10^{-5}$
10	Sand, non-uniform or gap grading	SW,SI $6 \leq U^4)$ ≤ 15	< 7.5 7.5-15 > 15	low medium high	16.5 18.0 19.5	9.0 10.5 12.0	200 400 600	0.70 0.60 0.55	30.0-32.5 32.5-37.5 35.0-40.0			$5 \cdot 10^{-4}$ to $2 \cdot 10^{-5}$

No.	1	2	3	4	5		6		7	8	9	10
11	Sand, non-uniform or gap grading	SW, SI U ⁴) > 15	< 7.5 7.5-15 > 15	low medium high	17.0 19.0 21.0	9.5 11.5 13.5	200 400 600	0.70 0.60 0.55	30.0-32.5 32.5-37.5 35.0-40.0			1 · 10 ⁻⁴ to 1 · 10 ⁻⁵
12	Sand, <i>d</i> < 0.06 mm < 15%	SU, ST	< 7.5 7.5-15 > 15	low medium high	16.0 17.0 18.0	8.5 9.5 10.5	150 350 500	0.80 0.70 0.65	30.0-32.5 32.5-37.5 35.0-40.0			2 · 10 ⁻⁵ to 5 · 10 ⁻⁷
13	Sand, <i>d</i> < 0.06mm > 15%	SU, ST	< 7.5 7.5-15 > 15	low medium high	16.5 18.0 19.5	9.0 10.5 12.0	50 250	0.90 0.75	30.0-32.5 32.5-37.5 35.0-40.0			2 · 10 ⁻⁶ to 1 · 10 ⁻⁹
14	Inorganic cohesive soils with low plasticity (<i>w_L</i> < 35%)	UL		soft stiff semi-firm	17.5 18.5 19.5	9.0 10.0 11.0	40 110	0.80 0.60	27.5-32.5	0 2-5 5-10	5-60 20-150 50-300	1 · 10 ⁻⁵ to 1 · 10 ⁻⁷
15	Inorganic cohesive soils with medium plasticity (50% > <i>w_L</i> > 35%)	UM		soft stiff semi-firm	16.5 18.0 19.5	8.5 9.5 10.5	30 70	0.90 0.70	25.0-30.0	0 5-10 10-15	5-60 20-150 50-300	2 · 10 ⁻⁶ to 1 · 10 ⁻⁹
16	Inorganic cohesive soils with low plasticity (<i>w_L</i> < 35%)	TL		soft stiff semi-firm	19.0 20.0 21.0	9.0 10.0 11.0	20 50	1.0 0.90	25.0-30.0	0 5-10 10-15	5-60 20-150 50-300	1 · 10 ⁻⁷ to 2 · 10 ⁻⁹
17	Inorganic cohesive soils with medium plasticity (50% > <i>w_L</i> > 35%)	TM		soft stiff semi-firm	18.5 19.5 20.5	8.5 9.5 10.5	10 30	1.0 0.95	22.5-27.5	5-10 10-15 15-20	5-60 20-150 50-300	5 · 10 ⁻⁸ to 1 · 10 ⁻¹⁰

Nr.	1	2	3	4	5		6		7	8	9	10
18	Inorganic cohesive soils with high plasticity ($w_L > 50\%$)	TA		soft stiff semi-firm	17.5 18.5 19.5	7.5 8.5 9.5	6 20	1.0 1.0	20.0-25.0	5-15 10-20 15-25	5-60 20-150 50-300	$1 \cdot 10^{-9}$ to $1 \cdot 10^{-11}$
19	Organic silt, organic clay	OU and OT		very soft soft stiff	14.0 15.5 17.0	4.0 5.5 7.0	5 20	1.00 0.85	17.5-22.5	0 2-5 5-10	2-<15 5-60 20-150	$1 \cdot 10^{-9}$ to $1 \cdot 10^{-11}$
20	Peat ⁵⁾	HN, HZ		very soft soft stiff semi-firm	10.5 11.0 12.0 13.0	0.5 1.0 2.0 3.0	5) 5)	5) 5)	5)	5)	5)	$1 \cdot 10^{-5}$ to $1 \cdot 10^{-8}$
21	Mud ⁶⁾ Digested sludge	F		very soft soft	12.5 16.0	2.5 6.0	4 15	1.0 0.9	6)	0 0	< 6 6-60	$1 \cdot 10^{-7}$ $1 \cdot 10^{-9}$

Notes:

1) Code letters for primary and secondary components:

G gravel U silt O organic inclusions F mud S sand T clay H peat (humus)

Code letters for characteristic physical soil parameters:

Particle size distribution:

W well-graded particle size distribution

E uniform particle size distribution

I gap-graded particle size distribution

Plastic properties:

L low plasticity

M medium plasticity

A high plasticity

Degree of decomposition for peat:

N not or hardly decomposed

Z decomposed

2) ν_e : stiffness factor, empirical parameter

σ : load in kN/m²

ω_e : empirical parameter

σ_{at} : atmospheric pressure (= 100 kN/m²)

3) ν_e values for repeated load up to 10 times higher, ω_e tends towards 1

4) U uniformity coefficient

5) The scatters of the values for compressibility and the shear parameters for peat are so extreme that it is not possible to specify empirical values.

6) The effective angle of friction of fully consolidated mud can attain very high values, but the value corresponding to the true degree of consolidation always governs, which can be determined reliably by means of laboratory tests.

Chapter 4

Groundwater

If a sheet pile structure is located in open water or in groundwater, then a **hydrostatic pressure** acts on the sheet piling from both sides. If the water levels on either side of the sheet piling can be at different levels, then an excess hydrostatic pressure caused by the difference in the hydrostatic pressures on both sides of the wall must be taken into account. The magnitude of the excess hydrostatic pressure depends on the water level fluctuations on both sides of the sheet piling, the flow conditions and possibly the existence of any drainage systems.

4.1 The basics of hydrostatic and hydrodynamic pressure

4.1.1 Hydraulic head

Water always flows from places with high hydraulic energy to places with lower hydraulic energy. The hydraulic energy is generally expressed as a **hydraulic head** h . It is calculated according to BERNOULLI from the geodesic head z_g with respect to a defined reference head chosen at random, the pressure head $z_p = w/\gamma_w$ and the velocity head $z_v = v^2/(2g)$ as follows:

$$h = z_g + \frac{w}{\gamma_w} + \frac{v^2}{2g} \quad (4.1)$$

The flow velocity v is generally low, which means that the velocity head can be neglected.

The pressure head z_p is the quotient of the hydrostatic pressure w and the unit weight of water γ_w . The hydrostatic pressure can be illustrated by the water level that becomes established in a standpipe z_p (Fig. 4.1), irrespective of whether open water or groundwater is involved. In the latter case, the hydrostatic pressure w is also called the **pore water pressure**.

In stationary, unconfined groundwater, the pore water pressure at depth z below the water level is $w = z \cdot \gamma_w$ (hydrostatic pressure distribution). In this case the pressure head z_p is equal to the depth below the water level. Confined groundwater is present when the pore water pressure is greater than $z \cdot \gamma_w$, i.e. when the pressure head is greater than the depth below the water level.

In flowing groundwater, the distribution of the pore water pressure is calculated by determining the hydraulic gradient or by constructing a flow net.

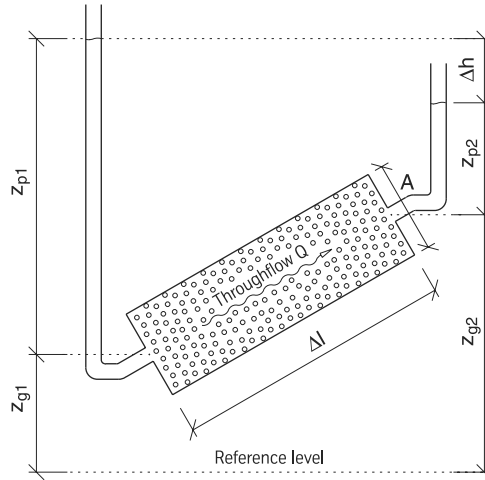


Figure 4.2: Water flowing through a soil sample

4.2 Excess hydrostatic pressure

4.2.1 Calculating the excess hydrostatic pressure

In sheet pile walls with different water levels on either side, the **excess hydrostatic pressure** is included in the sheet piling calculation as a characteristic action. The excess hydrostatic pressure w_u at depth z of the sheet pile wall is calculated from the difference in the hydrostatic pressures on the two sides (Fig. 4.3).

$$w_u(z) = w_r(z) - w_l(z) = h_r(z) \cdot \gamma_w - h_l(z) \cdot \gamma_w \quad (4.4)$$

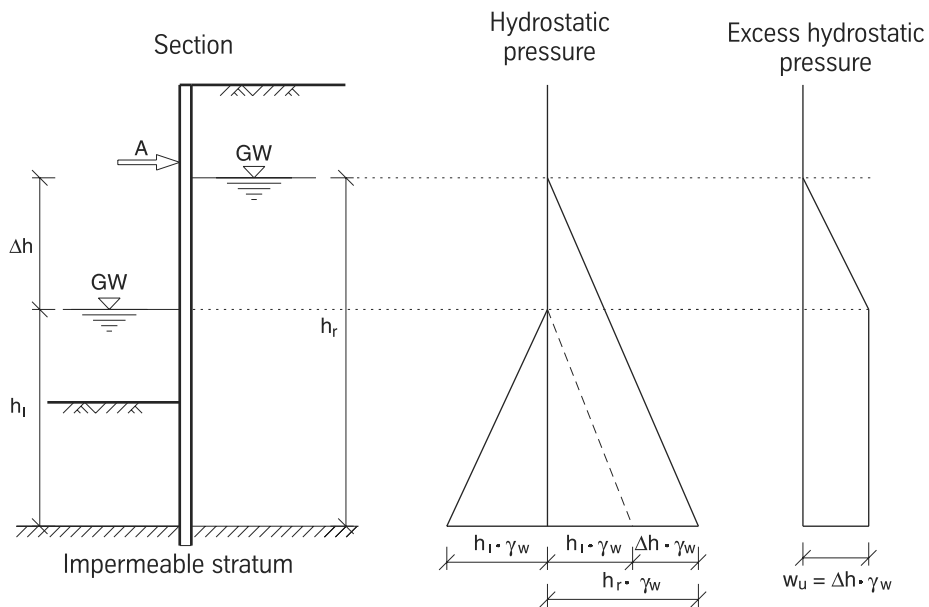


Figure 4.3: Excess hydrostatic pressure assumptions for a wall in stationary water

If we neglect the flow around the sheet pile wall, e.g. if the sheet pile wall is embedded in an impermeable stratum, the result is an excess hydrostatic pressure with a triangular distribution in the region of the one-sided hydrostatic load and a constant load in the lower region down to the base of the sheet piling.

4.2.2 Critical water levels

The calculation of the critical external water and groundwater levels requires a long-term analysis of the geological and hydrological conditions. The groundwater level behind the sheet pile wall is mainly characterised by the soil strata and the construction of the wall. In tidal regions, there is a relationship between the groundwater level and the tides where permeable soils are present.

If there is a considerable flow of groundwater behind the sheet pile wall, a build-up can occur at the sheet pile wall. The length of the planned sheet piling structure should also be considered in this case because a long structure hinders the flow of the groundwater around the ends of the structure, which leads to a steep rise in the groundwater level behind the sheet pile wall.

For calculating the water levels, EAU 2004 section 4.2 specifies typical values for certain boundary conditions such as water level fluctuations and drainage options (Figs. 4.4 and 4.5). The critical loading case should be determined according to EAU 2004 section 5.4 (E18), or DIN 1054:2005 section 6.3.3.

4.3 Taking account of groundwater flows

4.3.1 The effect of groundwater flows on hydrostatic and earth pressures

If the base of the sheet pile wall is not embedded in an impermeable stratum, groundwater can flow under the sheet piling structure. Proper planning and design of sheet pile walls located in groundwater flows calls for a knowledge of the effects of the flowing groundwater.

As the groundwater flows from regions of high hydraulic head to regions with a lower head, the hydrodynamic pressure is directed downwards on the excess hydrostatic pressure side and upwards on the opposite side. This means that the hydrostatic pressure on the excess hydrostatic pressure side is lower and that on the opposite side higher than the hydrostatic pressure.

The hydrodynamic pressure also acts on the granular structure of the soil: it increases the effective particle-to-particle stresses on the excess hydrostatic pressure side and decreases them on the opposite side. This means that the active earth pressure on the excess hydrostatic pressure side is increased, and the passive earth pressure on the opposite side is decreased (see section 5.7.6).

Taking into account the **groundwater flows** has a beneficial effect on the excess hydrostatic pressure and a detrimental effect on the passive earth pressure. Whether on the whole a more favourable or less favourable influence prevails, must be investigated in each individual case.

Generally, there are three ways of considering the hydrostatic pressure on a wall in flowing groundwater:

Non-tidal area				
Situation	Figure	Loading cases according to R 18		
		1	2	3
<p>1</p> <p>Minor water level fluctuations ($h < 0.50$ m) with weepholes or permeable soil and structure</p>		$\Delta h = 0.50$ m	$\Delta h = 0.50$ m	
<p>2a</p> <p>Major water level fluctuations ($h > 0.50$ m) with weepholes or highly permeable soil and structure</p>		$\Delta h = 0.50$ m at common level	$\Delta h = 1.00$ m at unfavourable level	$\Delta h \geq 1.00$ m max. drop in outer water level over 24 h and at unfavourable level
<p>2b</p> <p>Major water level fluctuations without weepholes</p>		$\Delta h = a + 0.30$ m	$\Delta h = a + 0.30$ m	-

Figure 4.4: Excess hydrostatic pressure at waterfront structures for permeable soils in non-tidal areas according to EAU 2004 section 4.2

Tidal area				
Situation	Figure	Loading cases according to R 18		
		1	2	3
<p>3a</p> <p>Major water level fluctuations without drainage – normal case</p>		$\Delta h = a + 0.30 \text{ m} + d$ $a = \frac{\text{MHW} - \text{MLW}}{2}$ $d = \text{MLW} - \text{MLWS}$	-	-
<p>3b</p> <p>Major water level fluctuations without drainage – limiting case with extremely low water level</p>		-	-	$\Delta h = a + 2b + d$ $a = \frac{\text{MHW} - \text{MLW}}{2}$ $b = \frac{\text{MLWS} - \text{LLW}}{2}$ $d = \text{MLW} - \text{MLWS}$
<p>3c</p> <p>Major water level fluctuations without drainage – limiting case with falling high water</p>		-	-	$\Delta h = 0.30 \text{ m} + 2a$
<p>3d</p> <p>Major water level fluctuations with drainage</p>		$\Delta h = 1.00 \text{ m}$ <p>for outer water level at MLWS</p>	$\Delta h = 0.30 \text{ m} + b + d$	-

Figure 4.5: Excess hydrostatic pressure at waterfront structures for permeable soils in tidal areas according to EAU 2004 section 4.2

1. Ignore the flow and assume the excess hydrostatic pressure according to section 4.2.
2. Perform calculations with the help of a flow net.
3. Perform calculations with the help of an approximation method assuming modified unit weights.

In the majority of cases it is sufficient to ignore the groundwater flow and assume the excess hydrostatic pressure according to section 4.2. If high excess hydrostatic pressures are present, then more accurate flow net calculations are advisable in the case of stratified soils with different permeabilities. In addition, an accurate investigation of the flow conditions is necessary for verifying resistance to hydraulic ground failure (section 4.4), especially in the case of large water level differences and strata with low permeability near the surface on the passive earth pressure side.

4.3.2 Flow net

The drop in the pore water pressure from regions with high hydraulic energy to regions with lower hydraulic energy is expressed by the potential equation:

$$\frac{\partial^2 h}{\partial x^2} + \frac{\partial^2 h}{\partial y^2} + \frac{\partial^2 h}{\partial z^2} = 0 \quad (4.5)$$

The solution of this differential equation, i.e. the function $h(x, y, z)$, supplies the distribution of the pore water pressure. The differential equation can be solved numerically, e.g. with the finite element method or the finite differences method. In the special case of a laminar flow and homogeneous soil, a graphical method is suitable, which is often sufficient for practical engineering purposes.

In this method, the solution is presented in two sets of curves that intersect at right-angles and whose mesh sizes exhibit a constant ratio and form a so-called **flow net** (Fig. 4.6). One set of curves constitutes the flow lines representing the paths of the individual water molecules. Perpendicular to these are the **equipotential lines**. The water level in a standpipe is the same at each point on the same equipotential line.

The construction of a flow net and the calculation of the hydrostatic pressures can be seen in the example shown in Fig. 4.6.

When constructing a flow net, the system boundaries must be defined first. Impermeable boundaries and curved unconfined water levels (seepage paths) form the perimeter flow lines. Horizontal groundwater levels and watercourse beds form the boundary equipotential lines with constant standpipe level.

The flow net is constructed according to the following criteria:

- Flow lines and potential lines are always at right-angles to each other.
- The flow lines pass through the cross-sectional area available; at constrictions they are closer together, at widenings further apart.

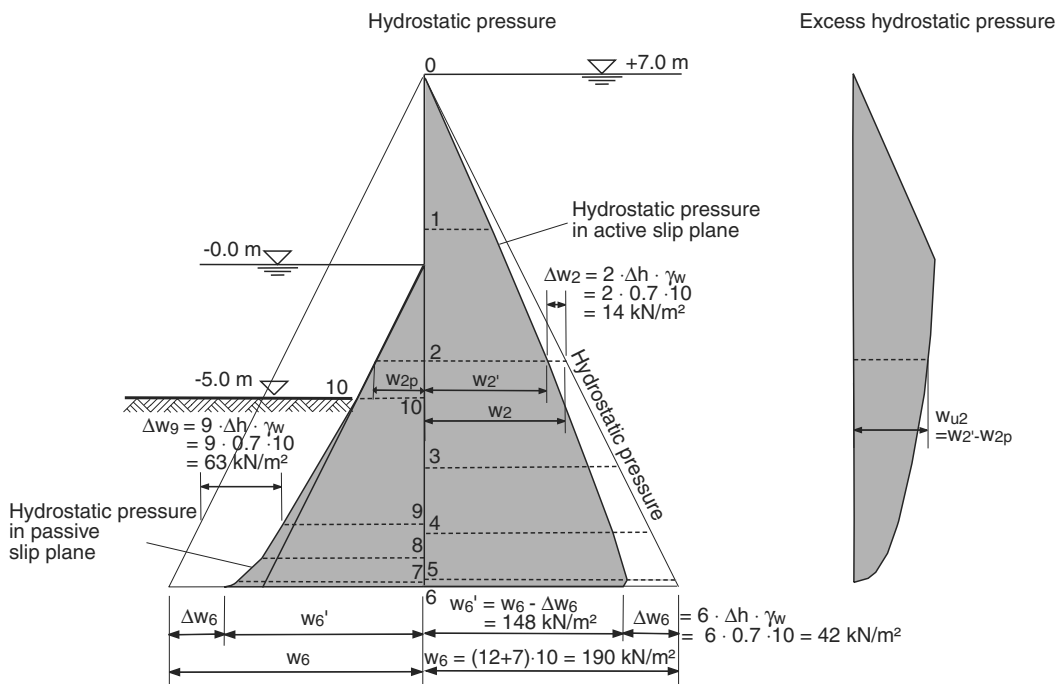
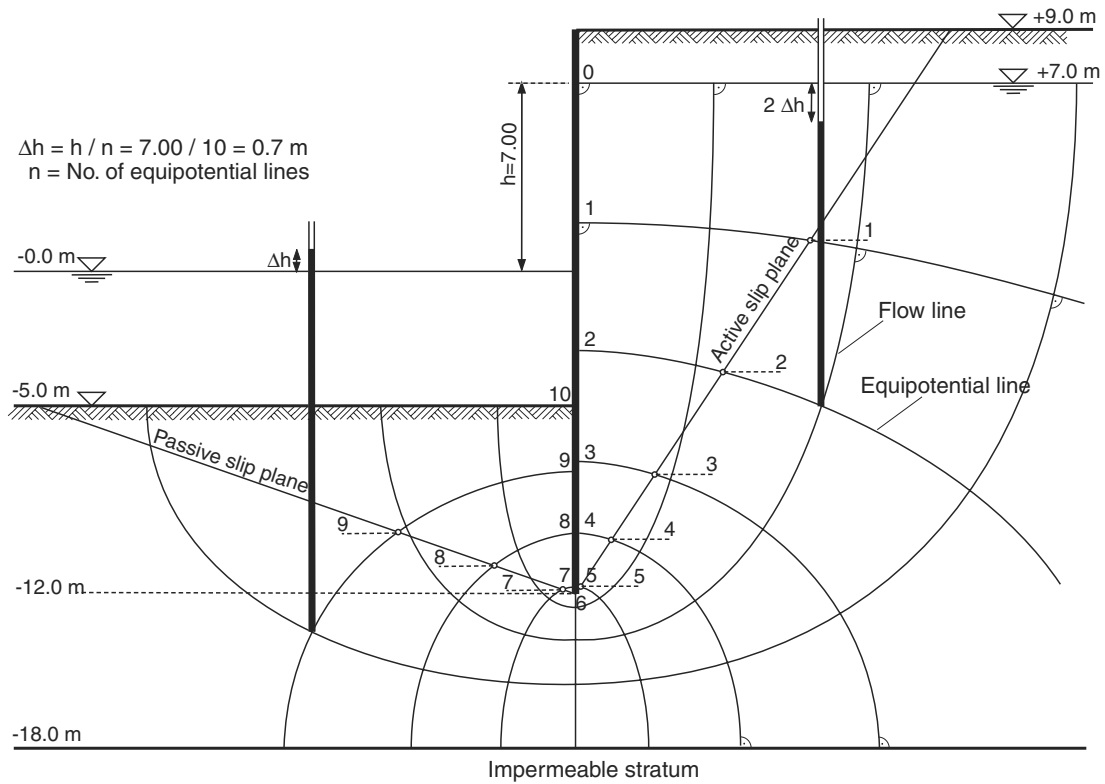


Figure 4.6: Flow net and resultant excess hydrostatic pressure

- The equipotential lines are constructed in such a way that together with the flow lines they form squares with curved borders; the accuracy can be checked by drawing inscribed circles.

Between each pair of equipotential lines there is a potential difference, i.e. a difference in the standpipe levels, which is

$$\Delta h = \frac{h}{n} \quad (4.6)$$

where h is the difference in the water levels and n is the number of equipotential lines (see Fig. 4.6). The pressure drop per equipotential line is equal for each potential field and is calculated from

$$\Delta w_x = \Delta h \cdot \gamma_w \quad (4.7)$$

The hydrostatic pressure w_u acting on the sheet pile wall is obtained by subtracting the sum of the pressure drops Δw from the hydrostatic pressure w_{hydr} :

$$w_u = w_{hydr} - \Sigma \Delta w = z \cdot \gamma_w - n_x \cdot \Delta h \cdot \gamma_w \quad (4.8)$$

where n_x = number of potential fields starting from the boundary equipotential line.

4.3.3 Approximate method assuming modified unit weights

If the flow around the sheet pile wall is essentially vertical, the influence of the flow can be taken into account approximately according to EAU 2004 section 2.9 (R 114) by modifying the unit weights of the water and the soil. The results achieved in this way deviate only marginally from the more accurate values obtained with a flow net.

In this approach, it is first necessary to establish the hydraulic gradient on both sides of the wall:

$$i_a = \frac{0.7 \cdot \Delta h}{h_a + \sqrt{h_a \cdot h_p}} \quad (4.9)$$

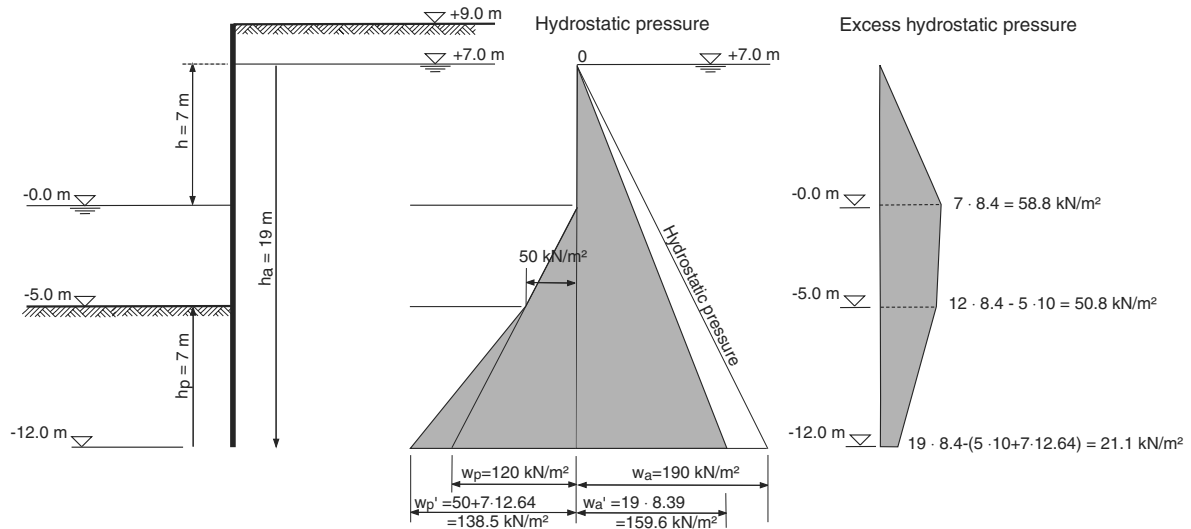
$$i_p = \frac{-0.7 \cdot \Delta h}{h_p + \sqrt{h_a \cdot h_p}} \quad (4.10)$$

where

- i_a = hydraulic gradient on active earth pressure side
- i_p = hydraulic gradient on passive earth pressure side
- Δh = difference in water levels
- h_a = vertical seepage path on active earth pressure side via which a drop in potential takes place
- h_p = vertical seepage path on passive earth pressure side via which a drop in potential takes place

The unit weight of the water on the active earth pressure side influenced by a flow is reduced by the amount $i_a \cdot \gamma_w$, whereas the unit weight of the soil is increased by the same amount. On the passive pressure side, on the other hand, the unit weight of the water influenced by a flow is increased by the amount $i_p \cdot \gamma_w$, whereas the unit weight of the soil is reduced by the same amount.

For the purpose of comparison, the calculation of the hydrostatic pressure distribution with the flow net in section 4.3.2 is repeated here with the approximation method (Fig. 4.7).



$$i_a = \frac{0.7 \cdot h}{h_a + \sqrt{h_a \cdot h_p}} = \frac{0.7 \cdot 7}{19 + \sqrt{19 \cdot 7}} = 0.160$$

$$\gamma_{wa} = (1 - i_a) \cdot \gamma_w = (1 - 0.16) \cdot 10 = 8.4 \text{ kN/m}^3$$

$$i_p = \frac{-0.7 \cdot h}{h_p + \sqrt{h_a \cdot h_p}} = \frac{-0.7 \cdot 7}{7 + \sqrt{19 \cdot 7}} = -0.264$$

$$\gamma_{wp} = (1 - i_p) \cdot \gamma_w = (1 + 0.264) \cdot 10 = 12.6 \text{ kN/m}^3$$

Figure 4.7: Determining the excess hydrostatic pressure with the approximate method

4.3.4 Flow around a sheet pile wall in stratified subsoil

With a permeability ratio of $k_1/k_2 > 5$ between two strata, the pressure drop can be assumed to take place in the stratum of low permeability only. What this means for the flow net is that the equipotential lines are drawn closer together in the stratum of low permeability. In a stratum of low permeability in which the permeability value k is 10 times smaller than the other strata, the ratio of the sides of the flow net mesh is 10:1, in contrast to a side ratio of 1:1 in the other strata. A simpler option for taking into account different permeabilities is to assume an exclusively vertical groundwater flow. In this case the hydraulic gradient i_i for every individual stratum i can be determined in relation to the respective stratum thickness d_i and permeability k_i . To do this, it is first necessary to determine the total permeability k_{sum} of the system in the sense of a series of resistances (Fig. 4.8).

$$k_{sum} = \frac{d}{\sum_1^i (d_i/k_i)} \tag{4.11}$$

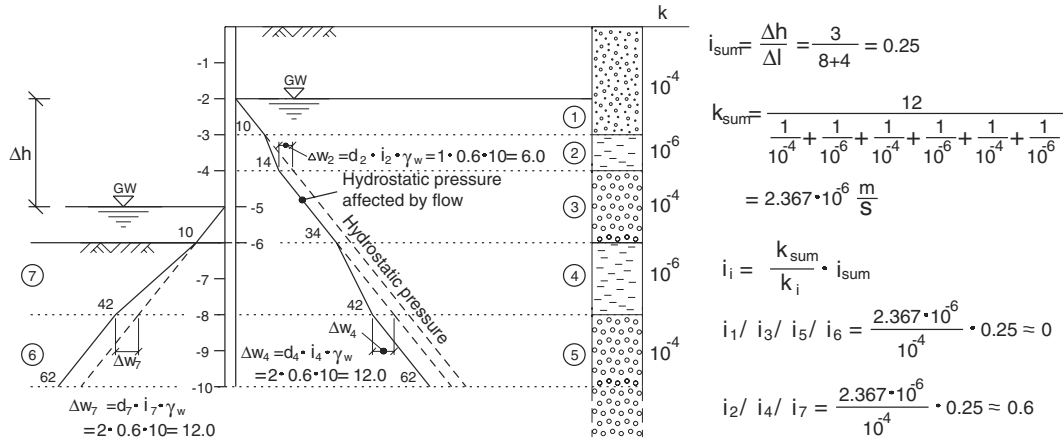


Figure 4.8: Vertical drop in excess hydrostatic pressures in stratified subsoil

The hydraulic gradient for every stratum can be calculated owing to the equal flow velocity in all strata by using

$$i_i = \frac{k_{sum}}{k_i} \cdot i_{sum} \tag{4.12}$$

This approach is only permissible when the vertical groundwater flow through the individual strata prevails over a horizontal flow through the water-bearing strata. Furthermore, the strata of low permeability must exhibit an adequate horizontal spread because otherwise a flow around these strata becomes established instead of a throughflow.

Alternatively, the excess hydrostatic pressure can also be determined with the help of the approximation method given in section 4.3.3. In this case only the impermeable strata, in which a pressure drop takes place, are counted as the seepage paths h_a and h_p .

4.4 Hydraulic ground failure

If there are large differences in the water levels on the two sides of the sheet pile wall, e.g. in a dewatered excavation or a quay structure at low water, a limit state condition can occur due to the flow under the base of the sheet piling. An upward hydrodynamic pressure S' then prevails on the passive earth pressure side. If this hydrodynamic pressure is greater than the effective self-weight G' of the body of soil in front of the base of the sheet pile wall, a **hydraulic ground failure** takes place. In this situation, the soil swells up and a mixture of water and soil infiltrates into the excavation.

Trials have shown that the uplift of the soil for a wall with embedment depth t occurs over a width of approx. $t/2$ from the wall (Fig. 4.9). Therefore, in order to determine the factor of safety against hydraulic ground failure, the vertical force equilibrium in a body of soil with dimensions $t \cdot t/2$ is considered on the passive earth pressure side. Hydraulic ground failure occurs when the weight of this body of soil is less than the vertical component of the hydrodynamic pressure in this area.

$$S'_k \cdot \gamma_H \leq G'_k \cdot \gamma_{G, stb} \tag{4.13}$$

where

- S'_k = characteristic value of hydrodynamic pressure in the body of soil in which the flow occurs
- γ_H = partial safety factor for hydrodynamic pressure (LS 1A, DIN 1054:2005, Tab. 2)
- G'_k = characteristic value of weight of the body of soil in which the flow occurs under buoyancy
- $\gamma_{G,stab}$ = partial safety factor for favourable permanent actions (LS 1A, DIN 1054:2005, Tab. 2)

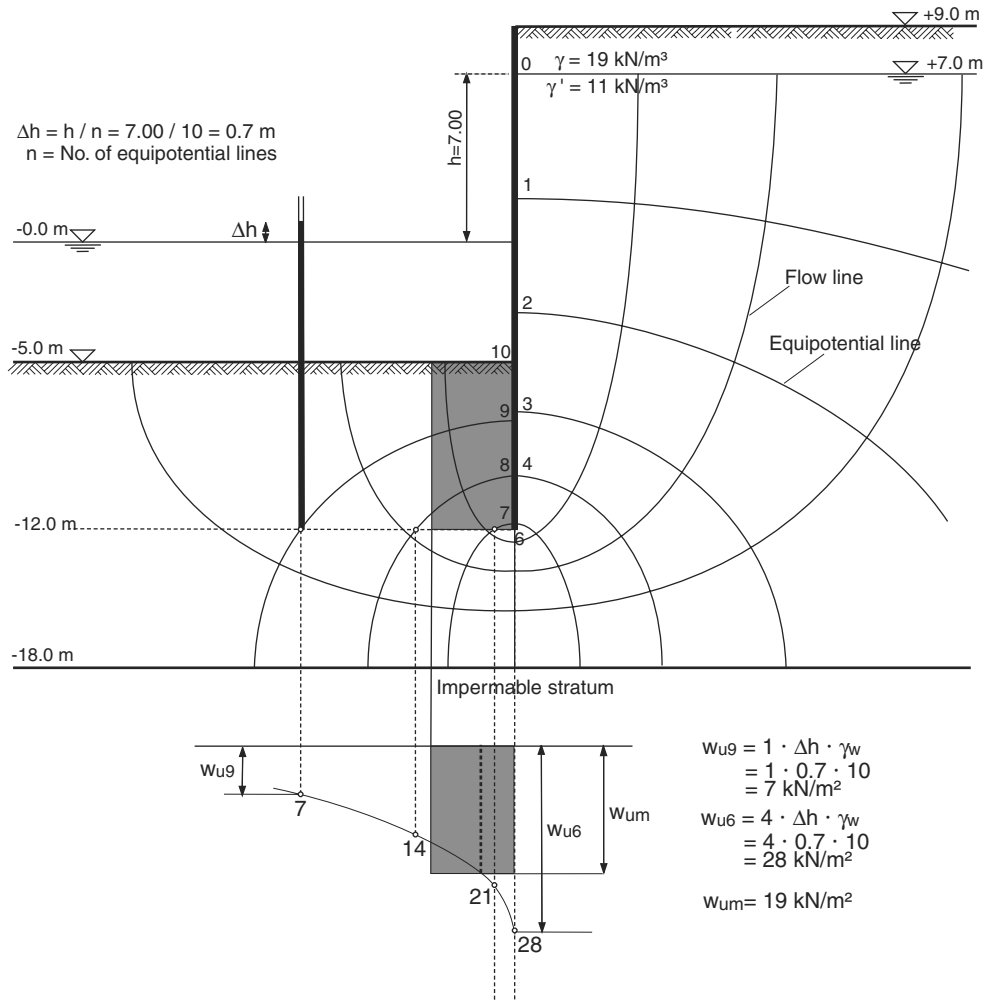
The hydrodynamic pressure can be calculated with the help of a flow net. To do this, the excess hydrostatic pressure prevailing over the underwater level $w_u = n \cdot \Delta h \cdot \gamma_w$ is first applied to the intersections with the equipotential lines at a horizontal joint starting at the base of the sheet pile wall. The average excess hydrostatic pressure w_{um} over the width $t/2$ starting from the wall is now read off at depth t . This excess hydrostatic pressure must decrease within the area of the hydraulic ground failure up to the water level and generate the required hydrodynamic pressure

$$S'_k = t/2 \cdot w_u \quad (4.14)$$

The hydrodynamic pressure can also be approximated using the equation $S'_k = t \cdot t/2 \cdot i_p \cdot \gamma_w$, where i_p is calculated with the approximation equation 4.9.

Special attention has to be given to the corners of excavations because this is where the flow from two sides is concentrated in a small area, and there is a higher risk of hydraulic ground failure. During the driving of sheet pile walls, care should be taken to ensure that declutching of the interlocks is avoided because this shortens the flow path and consequently increases the hydrodynamic pressure locally.

The factor of safety against hydraulic ground failure can be improved by increasing the embedment depth of the sheet pile wall, e.g. by driving it into an impermeable stratum.



Force due to hydrodynamic pressure:

$$S'_k = t/2 \cdot W_{um}$$

$$= 3.5 \cdot 19 = 66.5 \text{ kN/m}$$

Weight under buoyancy:

$$G'_k = t/2 \cdot t \cdot \gamma'$$

$$= 3.5 \cdot 7.0 \cdot 11 = 269.5 \text{ kN/m}$$

Alternative with approximation equation (4.10):

$$S'_k = t/2 \cdot t \cdot i_p \cdot \gamma_w$$

$$= 3.5 \cdot 7.0 \cdot 0.264 \cdot 10 \text{ (} i_p \text{ from Fig. 4.7)}$$

$$= 63.7 \text{ kN/m}$$

Verification:

$$S'_k \cdot \gamma_H < G'_k \cdot \gamma_{G.stb}$$

$$66.5 \cdot 1.80 < 269.5 \cdot 0.9$$

$$119.7 \text{ kN/m} < 242.6 \text{ kN/m}$$

Figure 4.9: Hydraulic ground failure

Chapter 5

Earth pressure

5.1 General

The soil in front of and behind a retaining wall exerts a lateral pressure on the wall known as earth pressure. In contrast to the hydrostatic pressure, the **earth pressure** is not exclusively dependent on the depth below the surface, but instead also to a large extent on the nature and magnitude of the lateral movement of the wall and hence on the yielding and stiffness properties of the wall. Another difference with respect to hydrostatic pressure, which with $p = z \cdot \gamma_w$ is identical in all directions at a depth z below the water level, is that in the soil the lateral earth pressure stresses differ from the vertical stresses.

The vertical stresses due to the self-weight of the soil, for undisturbed flat ground, can be calculated with the simple equation $\sigma_z = z \cdot \gamma$, where z is the depth below the ground surface and γ the unit weight of the soil. Above the water level, the bulk unit weight of the soil is effective, whereas below the water level the submerged unit weight $\gamma' = \gamma_r - \gamma_w$ together with the saturated unit weight γ_r are used (Fig. 5.1). Depending on the wall movement, the earth pressure can be either greater or less than the associated vertical stress.

The earth pressure at a certain point on a wall at a depth z is known as the earth pressure ordinate $e(z)$. The earth pressure acting over the height of a wall produces a force known as the resultant earth pressure force or simply the resultant earth pressure E . The relationship between earth pressure and vertical stresses is described by the earth pressure coefficient K . Consequently, the earth pressure e at depth z due to the self-weight of the soil for a homogeneous soil is

$$e(z) = \sigma_z \cdot K = z \cdot \gamma \cdot K \quad (5.1)$$

and the resultant earth pressure E due to the self-weight of the soil on a wall of height h is

$$E = e(z = h) \frac{1}{2} \cdot h = \frac{1}{2} \cdot \gamma \cdot h^2 \cdot K \quad (5.2)$$

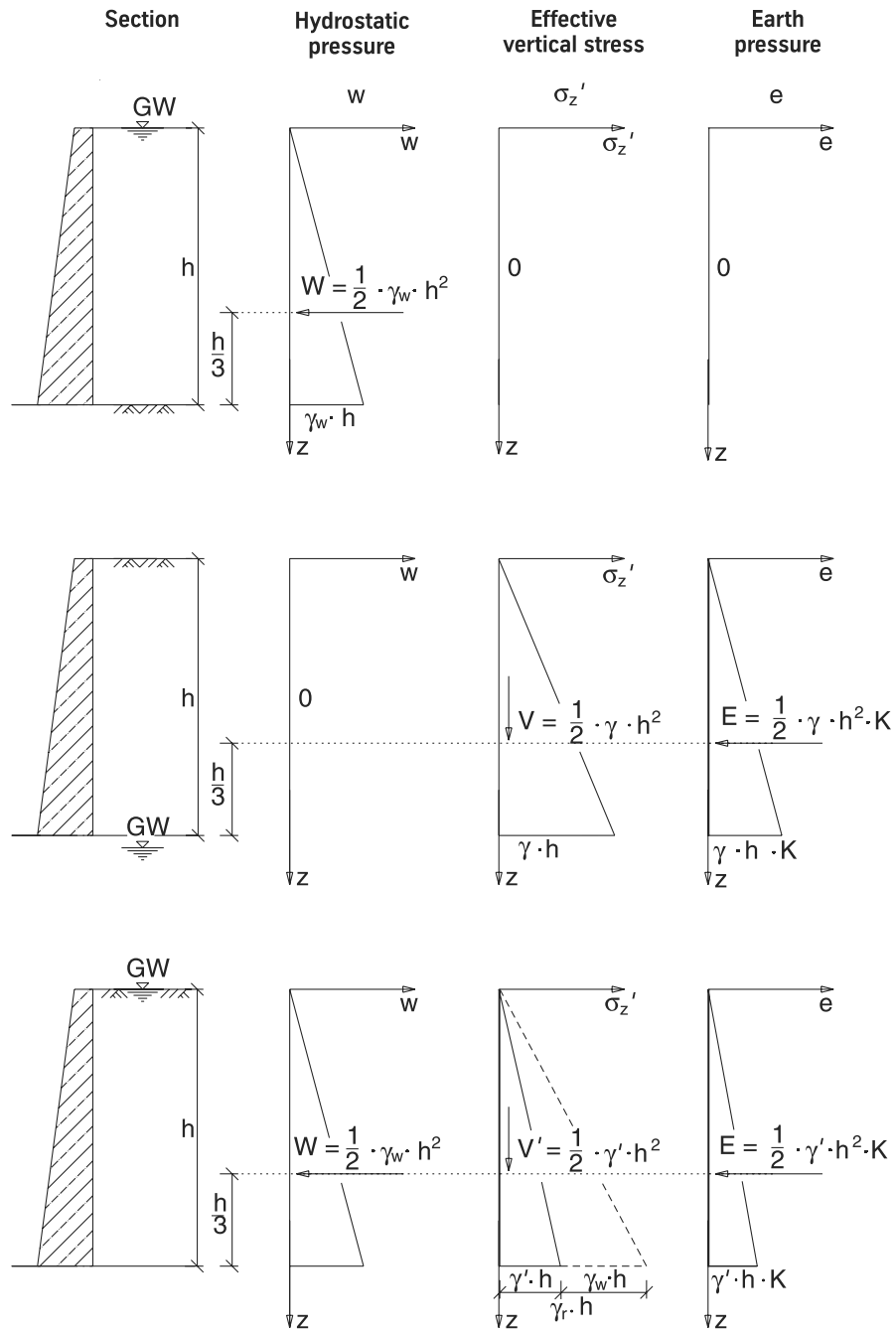


Figure 5.1: Comparison between hydrostatic pressure, vertical stresses in the soil and classic earth pressure distribution

5.2 Limit and intermediate values of earth pressure

If a wall backfilled with soil is rigid and immovable, then the so-called steady-state earth pressure E_0 acts on the wall. This is equivalent to the lateral pressure acting in an undisturbed soil.

If the wall yields and moves away from the soil, then the soil can relax laterally. The earth pressure drops as the movement of the wall increases, until it reaches a minimum. This minimum is known as the **active earth pressure** E_a (Fig. 5.2 a).

If the wall is pressed against the soil, the earth pressure increases. After a sufficient amount of wall movement, which is greater than that required to reach the active earth pressure, the maximum value of the earth pressure is reached, which is known as the **passive earth pressure** E_p (Fig. 5.2 b).

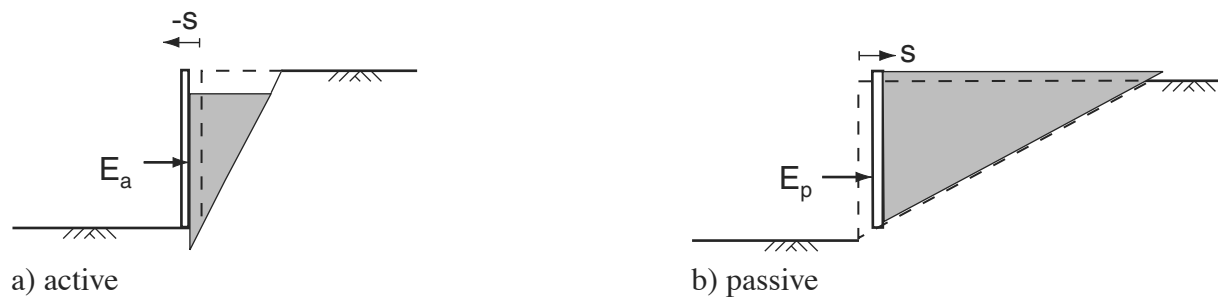


Figure 5.2: Active and passive earth pressures

Different earth pressures become established in the soil because of the internal shear strength of the soil, which is mobilised when the wall moves and opposes the respective movement. The different magnitudes of the earth pressure are described by the different earth pressure coefficients K_a , K_0 and K_p .

The active and passive earth pressure states are known as limit states in which the soil fails along a shear plane (also known as a slip plane) (Fig. 5.2). These states are therefore important for analysing the ultimate limit state.

The active earth pressure becomes established after a wall movement of about 1/1000th of the height of the wall. On the other hand, the passive earth pressure is not reached until a much greater displacement of about 5–10% of the height of the wall is reached (Fig. 5.3).

5.2.1 Active earth pressure after COULOMB

Consider the case of a retaining wall at the **active limit state** with the following conditions (see Fig. 5.4):

- The wall stands in a non-cohesive, homogeneous soil.
- The wall moves away from the body of soil until it forms a straight slip plane rising from

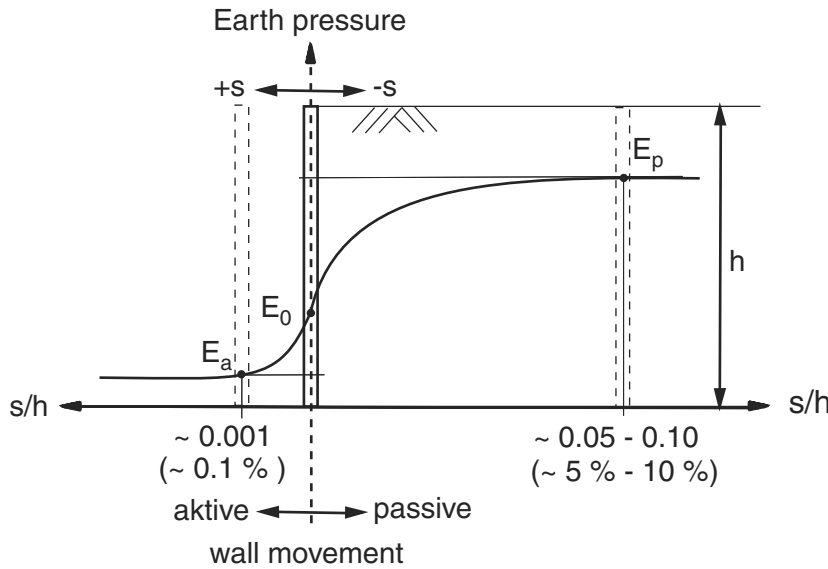


Figure 5.3: Mobilising the active and passive earth pressures

the base of the wall at an angle ϑ to a horizontal line (slip plane angle) on which a rigid wedge of soil slips down.

- The wall is vertical ($\alpha=0$).
- The surface of the ground is horizontal ($\beta=0$).
- The wall is smooth, i.e. the angle of wall friction δ between wall and soil is 0.

The weight of the wedge of soil is $G = \frac{1}{2}\gamma h^2 / \tan \vartheta$. The weight G , the active earth pressure E_a and the internal force Q at the slip plane act on the wedge of soil. The internal force Q is made up of the normal force N acting perpendicular to the slip plane and the shear force T mobilised parallel to the slip plane. The shear force T acts in the opposite direction to the wedge of soil and at the limit state is equal to $T = N \tan \varphi$. Therefore, Q acts at an angle φ with respect to the perpendicular to the slip plane and in the opposite direction to the movement. All three forces are in equilibrium and therefore form a closed polygon of forces.

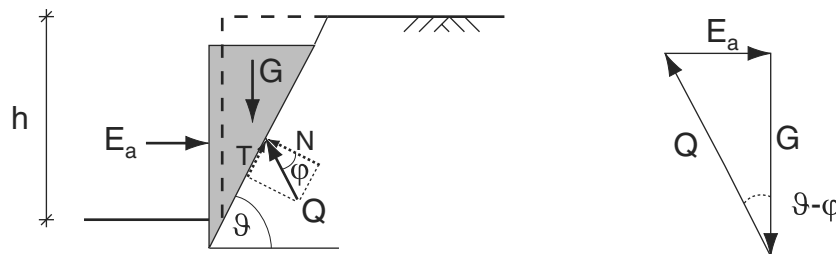


Figure 5.4: Wedge of soil and polygon of forces for active earth pressure after COULOMB

From the polygon of forces it follows that

$$E_a = G \cdot \tan(\vartheta - \varphi) = \frac{1}{2}\gamma h^2 \frac{\tan(\vartheta - \varphi)}{\tan \vartheta} \tag{5.3}$$

According to COULOMB, the slip plane angle that becomes established is the one for which the active earth pressure is a maximum. Therefore, applying the condition $dE_a/d\vartheta = 0$, the critical slip plane angle is

$$\vartheta_a = 45 + \varphi/2 \tag{5.4}$$

and the critical active earth pressure is

$$E_a = \frac{1}{2}\gamma h^2 K_a \tag{5.5}$$

where K_a is the so-called active earth pressure coefficient (for $\alpha = \beta = \delta = 0$), where

$$K_a = \tan^2 \left(45 - \frac{\varphi}{2} \right) = \frac{1 - \sin \varphi}{1 + \sin \varphi} \tag{5.6}$$

If the soil has no shear strength ($\varphi=0$), K_a would be equal to 1. In this case the active earth pressure would be equal to the hydrostatic pressure $\frac{1}{2}\gamma h^2$ of a fluid with unit weight γ .

5.2.2 Passive earth pressure after COULOMB

Similarity to the derivation of the active earth pressure, the passive earth pressure E_p and the associated critical slip plane angle can be determined for the case of the retaining wall being pressed against the body of soil (see Fig. 5.5).

The internal force Q at the slip plane is in this case inclined in the other direction with respect to the perpendicular to the slip plane.

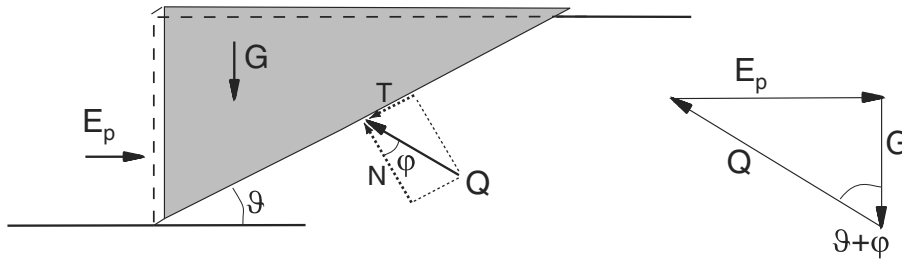


Figure 5.5: Wedge of soil and polygon of forces for passive earth pressure after COULOMB

In this case, it follows from the polygon of forces that

$$E_p = G \cdot \tan(\vartheta + \varphi) = \frac{1}{2}\gamma h^2 \frac{\tan(\vartheta + \varphi)}{\tan \vartheta} \tag{5.7}$$

The slip plane angle ϑ that becomes established in this case is such that the passive earth pressure is a minimum. Using $dE/d\vartheta = 0$, the critical slip plane angle is

$$\vartheta_p = 45^\circ - \varphi/2 \tag{5.8}$$

and the critical passive earth pressure is

$$E_p = \frac{1}{2} \gamma h^2 K_p \quad (5.9)$$

where K_p is the so-called passive earth pressure coefficient (for $\alpha = \beta = \delta = 0$) where

$$K_p = \tan^2 \left(45 + \frac{\varphi}{2} \right) = \frac{1 + \sin \varphi}{1 - \sin \varphi} \quad (5.10)$$

5.2.3 Steady-state earth pressure

The **steady-state earth pressure** is the earth pressure acting on an immovable vertical wall. For a non-preloaded soil, the steady-state earth pressure was calculated approximately by JAKY as

$$E_0 = \frac{1}{2} \gamma h^2 K_0 \quad (5.11)$$

where

$$K_0 \approx 1 - \sin \varphi \quad (5.12)$$

for an angle of friction of $25^\circ < \varphi < 35^\circ$.

For a soil preloaded with $\sigma_{z,v}$, a part of the horizontal stress remains in the soil as a locked-in stress after relieving to σ_z , e.g. also upon compacting the backfilled soil. In this case the earth pressure acting on the wall can be estimated from

$$K_0 \approx (1 - \sin \varphi) \sqrt{\sigma_{z,v} / \sigma_z} \quad (5.13)$$

The steady-state earth pressure should be used instead of the active earth pressure when the wall is rigid and immovable.

A more accurate calculation of the steady-state earth pressure can be found in DIN 4085:2007 section 6.4.

5.2.4 Intermediate earth pressure values

If the yielding of a retaining wall structure is not sufficient to relieve the steady-state earth pressure to the active limit state, an earth pressure approach must be chosen that lies between the steady-state earth pressure and the active earth pressure. This can happen, for example, with a propped excavation enclosure or a retaining structure with prestressed ground anchors.

This approach is known as enhanced active earth pressure. The magnitude of this can be calculated from

$$E'_a = \mu \cdot E_a + (1 - \mu) \cdot E_0 \quad (5.14)$$

The factor μ is chosen between 0 and 1 depending on the yielding of the retaining structure. DIN 4085:2007 tables A.2 and A.3 provide guidance on choosing μ .

Correspondingly, there is a so-called reduced passive earth pressure for the passive case. This lies between the steady-state earth pressure and the passive earth pressure and is used when the movement of the wall towards the soil is not sufficient to mobilise the full passive earth pressure.

5.2.5 Further methods for determining the resultant earth pressure

Straight slip planes

In the case of complex boundary conditions, e.g. local surcharges or inhomogeneous ground, it is not possible to calculate the active and passive earth pressures analytically using COULOMB. Instead, the earth pressure can be determined graphically by varying the angle of the slip plane ϑ .

The commonest graphic methods were developed by CULMANN and ENGESSER. Both methods are based on the assumption of a straight slip plane and varying the angle of the slip plane in steps, with the forces acting in the wedge of soil being calculated for every step and combined in a polygon of forces. The critical slip plane angle is the one that produces the greatest earth pressure.

The CULMANN method is mainly used for non-uniform ground, inconstant surcharges and stratified soils. The ENGESSER method is mainly used in the case of additional forces acting in the area.

Curved and discontinuous slip planes

The assumption of a straight slip plane according to COULOMB represents a simplification which is not entirely free from contradictions. Assuming a straight slip plane means that the moment equilibrium at the wedge of soil cannot be satisfied when considering an angle of wall friction δ . **Curved slip planes** (slip circles) really have been observed in many trials. However, it is also known that assuming a straight slip plane for calculating the active earth pressure results in only a small error and so the use of a straight slip plane is generally adequate.

By contrast, the discrepancy can be considerably greater in the case of the passive earth pressure. For high angles of friction in particular, the assumption of a straight slip plane leads to excessive passive earth pressures that do not become established in practice. The passive earth pressure should therefore be calculated with a curved or discontinuous slip plane. Many different approaches can be used which all lead to different passive earth pressures. The commonest methods of calculation are described below.

KREY (1936) calculated the active and passive earth pressure forces assuming a circular slip plane. In this case the wall together with the body of soil behind rotates about a point at a high level (Fig. 5.6a). The centre and radius of the slip plane must be varied until the passive earth pressure is a minimum.

GUDEHUS (1980) divided the soil behind the wall into several rigid bodies which can be displaced relative to one another along straight slip planes (multiple-body failure mechanisms). A translational movement of the wall is assumed here (Fig. 5.6b). The direction of the shear forces at the slip planes result from the relative displacement of the rigid bodies and the wall.

The passive earth pressure is determined from the force polygons of the individual rigid bodies. Here, too, the coordinates of the nodes must be varied until a minimum passive earth pressure is attained.

CAQUOT & KERISEL (1948) used a failure body in the form of a logarithmic spiral (Fig. 5.6c).

DIN 4085:2007 uses the failure model of SOKOLOVSKY/PREGL for calculating the passive earth pressure. This model is not based on a kinematic failure mechanism, but instead on the method of characteristic curves (Fig. 5.6d). It supplies similar results to the approach of CAQUOT & KERISEL.

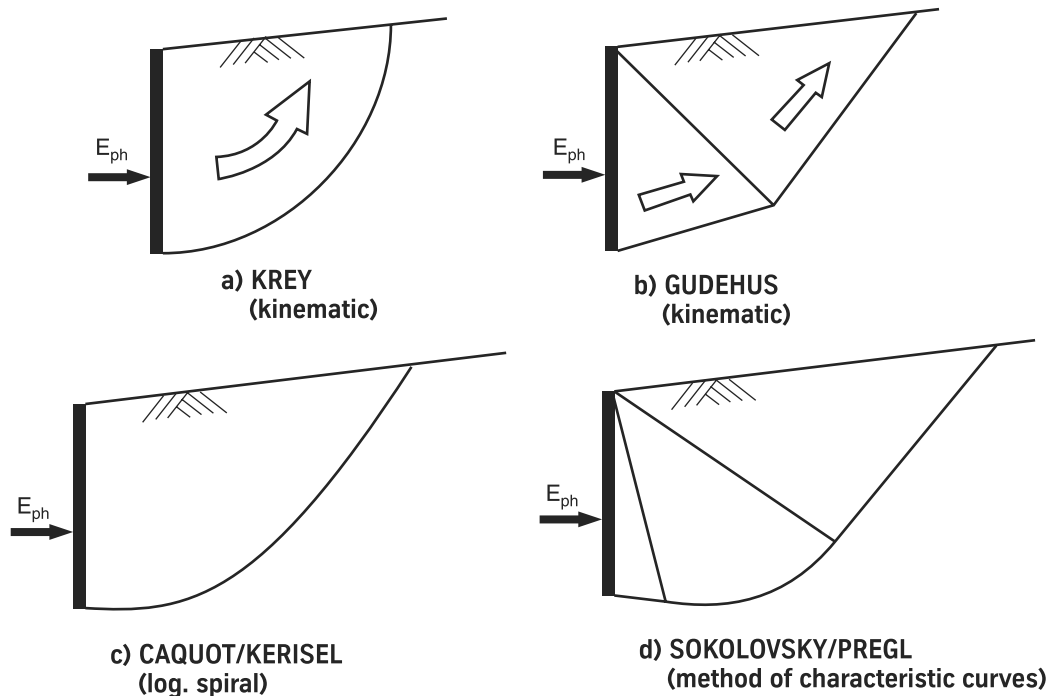


Figure 5.6: Slip planes at the passive limit state after a) KREY, b) GUDEHUS, c) CAQUOT/KERISEL, d) SOKOLOVSKY/PREGL

5.3 Earth pressure distribution

COULOMB's earth pressure theory is based on a kinematic method with rigid failure bodies and says nothing about the distribution of the earth pressure over the height of the wall.

In contrast to this, **RANKINE** assumes a static approach. His approach is not based on a discrete slip plane, but rather on the assumption that the principal stresses satisfy the Mohr-Coulomb limit condition throughout the wedge of soil under investigation (see Fig. 5.7). Here, too, the boundary conditions $\alpha = \beta = \delta = 0$ apply. Such a stress state is known as a failure surface.

From Fig. 5.7 it can be seen that two horizontal limit stresses exist for one vertical stress σ_z .

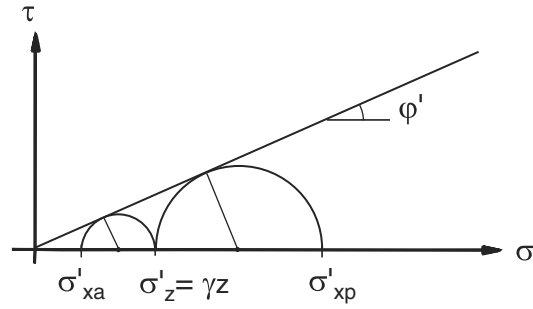


Figure 5.7: MOHR's circles of stress and failure surface after RANKINE

The minimum limit stress σ'_{xa} corresponds to the active earth pressure e_a , and the maximum limit stress σ'_{xp} to the passive pressure e_p .

Using Mohr's circles of stress, the horizontal stresses can be calculated from

$$\sigma_{x,min} = \sigma_z \frac{1 - \sin \varphi}{1 + \sin \varphi} = \gamma z K_a = e_a \quad (5.15)$$

and

$$\sigma_{x,max} = \sigma_z \frac{1 + \sin \varphi}{1 - \sin \varphi} = \gamma z K_p = e_p \quad (5.16)$$

From this it can be seen that according to RANKINE, the earth pressure due to the self-weight of the soil increases linearly with the depth z .

By integrating the horizontal stresses over the height, we get the resultant active earth pressure

$$E_a = \frac{1}{2} \gamma z^2 K_a \quad (5.17)$$

and the resultant passive earth pressure

$$E_p = \frac{1}{2} \gamma z^2 K_p \quad (5.18)$$

Therefore, for the same boundary conditions, the resultant active or passive earth pressures are equal to those of the COULOMB method.

A failure surface like the one assumed here is achieved only for a rotation of the wall about its base for the active case and only with a translation of the wall for the passive case (see Fig. 5.8). Only for these cases do the active or passive earth pressures due to the self-weight of the soil increase linearly with the depth.

Other wall movements do not produce a triangular earth pressure distribution because the deformations required to mobilise the active or passive earth pressure do not occur in certain areas or an arching or bridging effect occurs in the soil. Generally, the earth pressures in these cases are nevertheless initially calculated assuming a triangular distribution and subsequently redistributed while retaining the magnitude of the resultant earth pressure (see section 5.8).

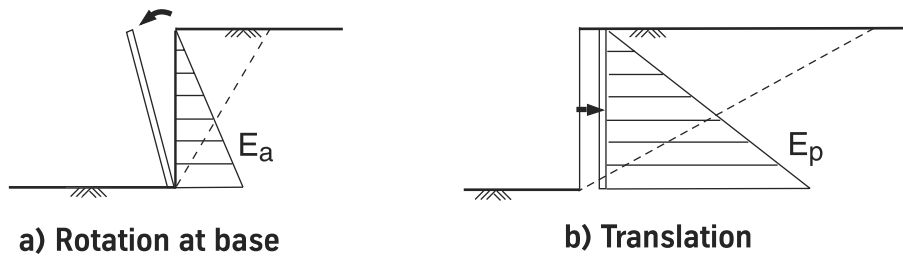


Figure 5.8: Wall movement with a linear earth pressure distribution

5.4 Calculating the earth pressure due to self-weight

5.4.1 Wall friction angle

Generally, the wall is not completely smooth, which means that a **wall friction angle** $\delta \neq 0$ between the wall and the soil is established. This is mobilised when the wall and soil move in relation to each other (Fig. 5.9). Here, δ is the angle between the direction of application of the active or passive earth pressure and a line perpendicular to the surface of the wall.

Assuming a straight slip plane, the wall friction angle in sheet piling structures may be assumed to lie within the limits $\delta_{a/p} = \pm 2/3\varphi$ on the active and passive sides. If a curved slip plane is assumed for the passive earth pressure, the wall friction angle must be increased to $\delta_p = \pm\varphi$ according to EAU 2004 section 8.2.4.2. Normally, $\delta_a \geq 0$ and $\delta_p \leq 0$ because the active wedge of soil moves downwards with respect to the wall and the passive wedge of soil upwards.

It is easy to see that the wall friction angle can change the forces in the polygon of forces (see Figs. 5.4 and 5.5) considerably. In particular, the passive earth pressure increases drastically in the case of a negative wall friction angle $\delta_p \leq 0$.

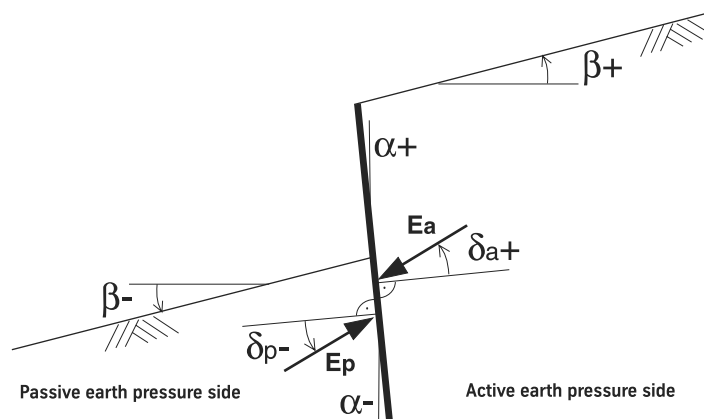


Figure 5.9: Definition of signs for earth pressure

5.4.2 Active and passive earth pressure coefficients for soil self-weight

The coefficients for the active pressure due to self-weight resulting from the COULOMB method are valid only for the special case of $\alpha = \beta = \delta = 0$. Such conditions occur only rarely, as has been shown already by assuming a wall friction angle. Further, a sloping ground surface ($\beta \neq 0$) and an inclined wall ($\alpha \neq 0$) have a considerable influence on the active and passive earth pressures. As an extension of COULOMB's theory, MÜLLER-BRESLAU therefore set up the following for calculating the **active and passive earth pressure coefficients** due to the soil self-weight for $\alpha \neq 0$, $\beta \neq 0$ and $\delta \neq 0$, assuming a straight slip plane:

$$K_{agh} = \frac{\cos^2(\varphi - \alpha)}{\cos^2 \alpha \left[1 + \sqrt{\frac{\sin(\varphi + \delta_a) \sin(\varphi - \beta)}{\cos(\alpha - \beta) \cos(\alpha + \delta_a)}} \right]^2} \quad (5.19)$$

$$K_{pgh} = \frac{\cos^2(\varphi + \alpha)}{\cos^2 \alpha \left[1 - \sqrt{\frac{\sin(\varphi - \delta_p) \sin(\varphi + \beta)}{\cos(\alpha - \beta) \cos(\alpha + \delta_p)}} \right]^2} \quad (5.20)$$

These are the horizontal earth pressure coefficients for calculating the horizontal components (index h) of the resultant active and passive earth pressures (index a and p respectively) due to the soil self-weight (index g)

$$E_{agh/pgh} = \frac{1}{2} \gamma h^2 \cdot K_{agh/pgh} \quad (5.21)$$

and the corresponding horizontal earth pressure ordinates

$$e_{agh/pgh} = \gamma h \cdot K_{agh/pgh} \quad (5.22)$$

The MÜLLER-BRESLAU equation is based on assuming a straight slip plane. However, in the zone of passive earth pressure, curved slip planes are realistic for angles of friction $\varphi > 30^\circ$ (see section 5.2.5). Table 5.1 lists **active and passive earth pressure coefficients** K_{agh} and K_{pgh} according to DIN 4085:2007. The active earth pressure coefficients here are determined with straight slip planes according to MÜLLER-BRESLAU, and the passive earth pressure coefficients with curved slip planes according to SOKOLOWSKY/PREGL.

Due to the wall friction angle δ and a possible wall inclination α , the earth pressure no longer acts horizontally (see Fig. 5.10). It thus gains a vertical component (Fig. 5.10). The vertical earth pressure component E_v can be calculated from

$$E_{av/pv} = E_{ah/ph} \cdot \tan(\delta_{a/p} + \alpha) \quad (5.23)$$

depending on the horizontal component E_h .

Generally, a high wall friction angle has a favourable effect on the loadbearing behaviour because this reduces the active earth pressure coefficient, and the passive earth pressure coefficient increases considerably in the case of a large angle of friction φ . Therefore, the vertical equilibrium $\Sigma V = 0$ of the system should be checked to see whether the wall friction angle assumed really can be mobilised on the passive earth pressure side (see section 6.7.1). If necessary, the wall friction angle should be reduced accordingly.

Table 5.1: Active and passive earth pressure coefficients to DIN 4085:2007

φ	β	K_{agh}		K_{pgh}				K_{ach}		K_{pch}			
		$\delta = 0$	$2/3\varphi$	$\delta = 0$	$-1/3\varphi$	$-1/2\varphi$	$-2/3\varphi$	$\delta = 0$	$2/3\varphi$	$\delta = 0$	$-1/3\varphi$	$-1/2\varphi$	$-2/3\varphi$
20	-20	0.40	0.34	0.87	1.00	1.06	1.11	1.08	0.95	2.52	2.59	2.61	2.62
	-10	0.44	0.37	1.38	1.57	1.67	1.76	1.23	1.07	2.68	3.04	3.19	3.33
	0	0.49	0.43	2.04	2.33	2.47	2.61	1.40	1.18	2.86	3.23	3.40	3.55
	10	0.57	0.51	2.48	2.83	3.00	3.16	1.58	1.29	3.24	3.67	3.86	4.03
	20	0.88	0.88	2.97	3.40	3.60	3.80	1.77	1.40	3.68	4.17	4.38	4.58
22.5	-20	0.37	0.30	0.96	1.13	1.21	1.30	1.04	0.91	2.56	2.98	3.17	3.34
	-10	0.40	0.34	1.51	1.78	1.92	2.05	1.18	1.01	2.77	3.23	3.43	3.62
	0	0.45	0.38	2.24	2.64	2.84	3.03	1.34	1.11	2.99	3.49	3.71	3.91
	10	0.51	0.45	2.78	3.28	3.52	3.76	1.50	1.20	3.46	4.03	4.29	4.52
	20	0.66	0.62	3.40	4.01	4.31	4.60	1.66	1.29	4.00	4.66	4.96	5.22
25	-25	0.32	0.26	0.81	1.00	1.09	1.17	0.93	0.82	2.47	2.98	3.20	3.41
	-20	0.34	0.28	1.05	1.29	1.41	1.52	1.00	0.87	2.59	3.12	3.36	3.57
	-10	0.37	0.31	1.66	2.03	2.22	2.40	1.13	0.96	2.85	3.44	3.70	3.93
	0	0.41	0.35	2.46	3.01	3.29	3.56	1.27	1.04	3.14	3.78	4.07	4.33
	10	0.46	0.40	3.12	3.82	4.16	4.50	1.42	1.12	3.69	4.45	4.79	5.09
27.5	-25	0.29	0.24	0.90	1.14	1.27	1.39	0.90	0.78	2.47	3.08	3.36	3.60
	-20	0.31	0.25	1.16	1.48	1.64	1.80	0.96	0.83	2.61	3.26	3.56	3.82
	-10	0.33	0.28	1.83	2.33	2.59	2.83	1.09	0.91	2.93	3.66	3.99	4.29
	0	0.37	0.31	2.72	3.46	3.83	4.20	1.21	0.98	3.30	4.12	4.49	4.82
	10	0.42	0.36	3.51	4.47	4.96	5.43	1.34	1.05	3.95	4.94	5.38	5.78
30	-30	0.26	0.21	0.75	0.99	1.12	1.24	0.80	0.71	2.29	2.97	3.28	3.56
	-20	0.28	0.23	1.28	1.70	1.92	2.14	0.92	0.79	2.63	3.41	3.76	4.08
	-10	0.30	0.25	2.02	2.69	3.03	3.37	1.04	0.86	3.02	3.91	4.32	4.69
	0	0.33	0.28	3.00	3.98	4.50	5.00	1.15	0.92	3.46	4.49	4.97	5.39
	10	0.37	0.32	3.96	5.26	5.94	6.61	1.27	0.98	4.24	5.50	6.07	6.59
32.5	-30	0.23	0.19	0.83	1.15	1.32	1.49	0.77	0.68	2.23	3.02	3.38	3.70
	-20	0.25	0.21	1.42	1.97	2.27	2.57	0.88	0.75	2.63	3.55	3.98	4.36
	-10	0.28	0.23	2.24	3.12	3.58	4.05	0.99	0.81	3.10	4.18	4.69	5.14
	0	0.30	0.25	3.32	4.62	5.31	6.00	1.10	0.87	3.65	4.93	5.52	6.05
	10	0.34	0.28	4.48	6.23	7.16	8.10	1.20	0.91	4.55	6.16	6.90	7.56
35	-35	0.20	0.16	0.67	0.98	1.15	1.32	0.69	0.62	1.96	2.77	3.15	3.49
	-30	0.21	0.17	0.92	1.34	1.57	1.81	0.74	0.65	2.16	3.05	3.47	3.84
	-20	0.23	0.19	1.58	2.30	2.70	3.10	0.85	0.71	2.62	3.70	4.20	4.66
	-10	0.25	0.20	2.49	3.64	4.26	4.90	0.95	0.77	3.17	4.48	5.09	5.64
	0	0.27	0.22	3.69	5.39	6.32	7.26	1.04	0.81	3.84	5.43	6.17	6.83
37.5	10	0.30	0.25	5.08	7.42	8.70	10.00	1.13	0.85	4.91	6.93	7.88	8.73
	20	0.34	0.30	6.88	10.04	11.77	13.53	1.22	0.87	6.26	8.85	10.06	11.14
	30	0.44	0.39	9.15	13.37	15.67	18.01	1.31	0.88	8.00	11.30	12.84	14.23
	35	0.67	0.67	10.50	15.34	17.99	20.67	1.34	0.88	9.04	12.77	14.51	16.08
	40	-40	0.16	0.13	0.59	0.95	1.17	1.39	0.59	0.54	1.53	2.37	2.78
-30		0.17	0.14	1.14	1.86	2.28	2.71	0.68	0.59	1.98	3.07	3.60	4.07
-20		0.19	0.15	1.97	3.20	3.91	4.66	0.77	0.64	2.56	3.97	4.66	5.27
-10		0.20	0.16	3.10	5.05	6.17	7.35	0.85	0.68	3.31	5.15	6.03	6.83
0		0.22	0.18	4.60	7.48	9.15	10.89	0.93	0.71	4.29	6.66	7.81	8.84
40	10	0.24	0.20	6.61	10.75	13.15	15.65	1.01	0.73	5.75	8.93	10.47	11.85
	20	0.27	0.23	9.30	15.13	18.51	22.03	1.07	0.74	7.70	11.97	14.03	15.88
	30	0.32	0.28	12.86	20.92	25.59	30.45	1.13	0.74	10.33	16.04	18.80	21.29
	40	0.59	0.59	17.49	28.45	34.80	41.42	1.17	0.72	13.84	21.50	25.20	28.53

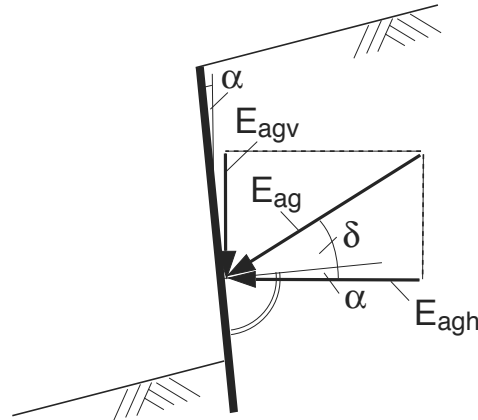


Figure 5.10: Vertical and horizontal components for earth pressure

5.4.3 Slip plane angle

The critical **slip plane angle** ϑ is required for some calculations. Taking the MÜLLER-BRESLAU equation as a basis and assuming a straight slip plane, the critical slip plane angle is calculated from

$$\vartheta_a = \varphi + \operatorname{arccot} \left[\tan(\varphi - \alpha) + \frac{1}{\cos(\varphi - \alpha)} \sqrt{\frac{\sin(\delta_a + \varphi) \cos(\beta - \alpha)}{\sin(\varphi - \beta) \cos(\delta_a + \alpha)}} \right] \quad (5.24)$$

$$\vartheta_p = -\varphi + \operatorname{arccot} \left[\tan(\varphi + \alpha) + \frac{1}{\cos(\varphi + \alpha)} \sqrt{\frac{\sin(\delta_p - \varphi) \cos(\beta - \alpha)}{\sin(-\varphi - \beta) \cos(\delta_p + \alpha)}} \right] \quad (5.25)$$

In the case of more complex boundary conditions caused by additional loads or changes in ground level or an angle of friction $\varphi > 30^\circ$ on the passive earth pressure side, the critical slip plane may need to be determined using a graphical method, or a curved or discontinuous slip plane may have to be assumed.

For the special case of a vertical wall and a flat ground surface, the slip plane angle ϑ can be taken from table 5.2.

5.5 Calculating the earth pressure in cohesive soils

In soils with friction and **cohesion**, the cohesive force

$$C = l \cdot c \quad (5.26)$$

also acts at the slip plane; l designates the length of the slip plane and c the cohesion of the soil.

Table 5.2: Slip plane angle ϑ for $\alpha = \beta = 0$

φ	ϑ_a		ϑ_p	
	$\delta = \pm 0$	$\delta = +\frac{2}{3}\varphi$	$\delta = \pm 0$	$\delta = -\frac{2}{3}\varphi$
15°	52.5°	47.0°	37.5°	28.2°
17.5°	53.8°	48.5°	36.3°	26.6°
20°	55.0°	50.0°	35.0°	24.9°
22.5°	56.3°	51.5°	33.8°	23.2°
25°	57.5°	53.0°	32.5°	21.5°
27.5°	58.8°	54.5°	31.3°	19.8°
30°	60.0°	56.0°	30.0°	18.1°
32.5°	61.3°	57.5°	-	-
35°	62.5°	58.9°	-	-

5.5.1 Cohesion on the active earth pressure side

For the boundary conditions according to COULOMB ($\alpha = \beta = \delta = 0$), the resultant active earth pressure according to Fig. 5.11, also taking into account cohesion, is

$$E_a = \frac{1}{2}\gamma h^2 \frac{\tan(\vartheta - \varphi)}{\tan \vartheta} - c h \left[\tan(\vartheta - \varphi) + \frac{1}{\tan \vartheta} \right] \quad (5.27)$$

The extreme condition $dE/d\vartheta = 0$ supplies the known critical slip plane angle which, irrespective of c , is

$$\vartheta_a = 45 + \varphi/2 \quad (5.28)$$

Therefore, the resultant earth pressure due to self-weight and cohesion is

$$E_a = \frac{1}{2}\gamma h^2 K_a - 2 c h \sqrt{K_a} \quad (5.29)$$

where K_a is calculated using eq. 5.6 after COULOMB. The two earth pressure components due to self-weight and cohesion act as independent sums.

The cohesion reduces the active earth pressure. Cohesion should therefore only be assumed when drying-out or freezing of the soil can be ruled out. The earth pressure component due to cohesion is distributed uniformly over the wall.

For the general case of $\alpha \neq 0, \beta \neq 0$ and $\delta \neq 0$, the critical slip plane angle under the action of cohesion changes only marginally. Therefore, according to DIN 4085:2007, the horizontal component of the earth pressure component due to cohesion is

$$e_{ach} = -c \cdot K_{ach} \quad (5.30)$$

where

$$K_{ach} = \frac{2 \cdot \cos(\alpha - \beta) \cdot \cos \varphi \cdot \cos(\alpha + \delta_a)}{[1 + \sin(\varphi + \alpha + \delta_a - \beta)] \cdot \cos \alpha} \quad (5.31)$$

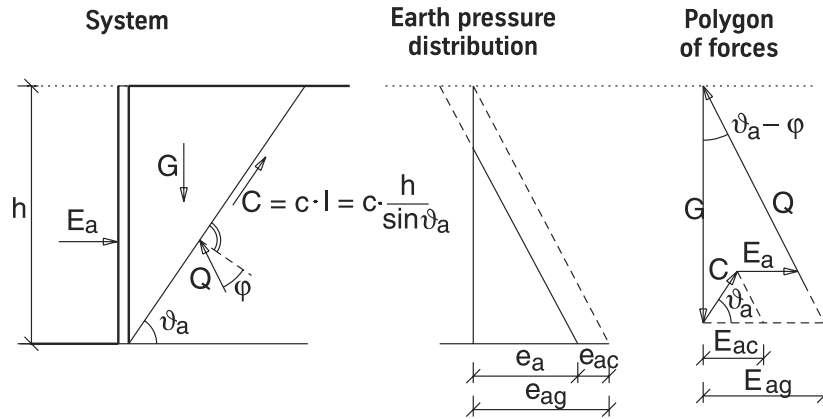


Figure 5.11: Active earth pressure with cohesion

Cohesion therefore reduces the resultant earth pressure for a section of wall of height h by the value

$$E_{ach} = c \cdot h \cdot K_{ach} \tag{5.32}$$

Typical values for K_{ach} are given in table 5.1.

For the boundary conditions according to COULOMB ($\alpha = \beta = \delta = 0$), the earth pressure coefficient is simplified to

$$K_{ach} = 2\sqrt{K_{agh}} \tag{5.33}$$

and is therefore the same approach as with COULOMB (see eq. 5.29).

Near the ground surface, considering the cohesion can lead to very small or negative earth pressures. In this case, a minimum earth pressure should be applied, and the value should not fall below this. The minimum earth pressure corresponds to the earth pressure that results from assuming a shear strength of $\varphi = 40^\circ$ and $c = 0$ due to the self-weight of the soil (Fig. 5.12). The maximum value due to the minimum earth pressure e_{min} and a permanent earth pressure taking into account the cohesion $e_{agh} + e_{ach}$ must be applied at every depth.

5.5.2 Cohesion on the passive earth pressure side

For the boundary conditions according to COULOMB ($\alpha = \beta = \delta = 0$), the resultant passive earth pressure according to Fig. 5.13, also taking into account **cohesion**, is

$$E_p = \frac{1}{2}\gamma h^2 K_p + 2ch\sqrt{K_p} \tag{5.34}$$

where K_p is calculated using eq. 5.10.

By assuming cohesion, the passive earth pressure increases by a component distributed uniformly over the depth.

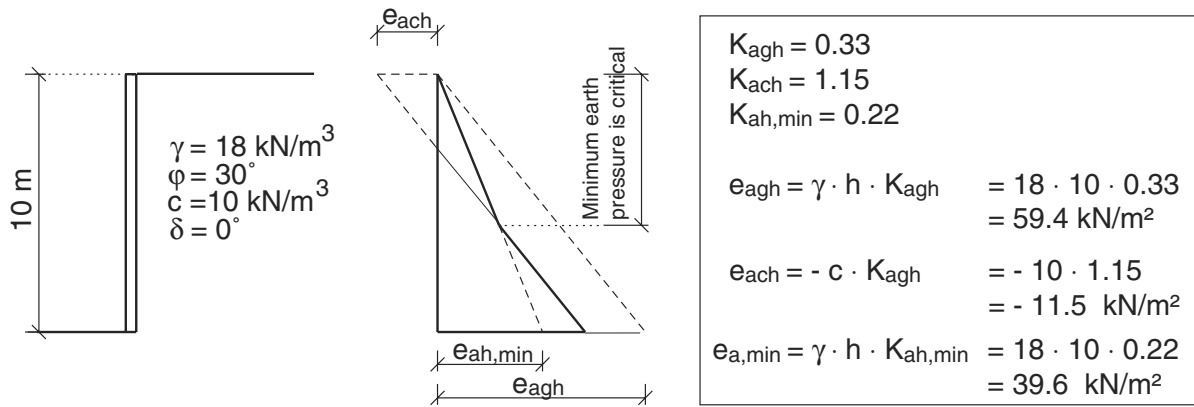


Figure 5.12: Applying a minimum earth pressure

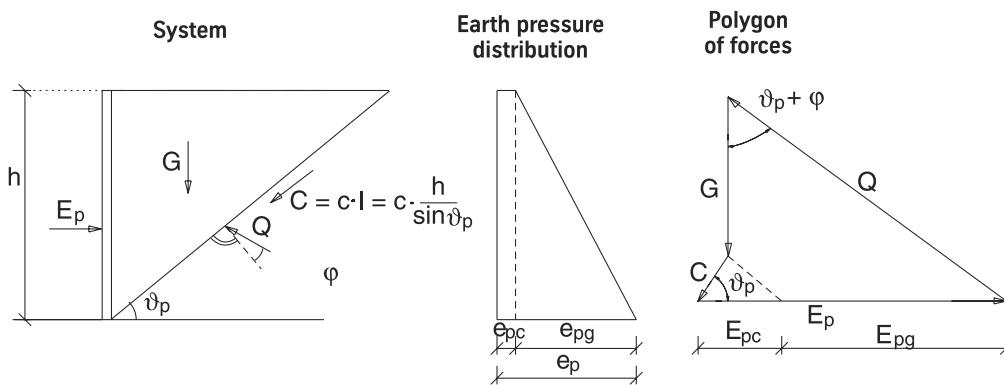


Figure 5.13: Passive earth pressure with cohesion

For the general case of $\alpha \neq 0$, $\beta \neq 0$ and $\delta \neq 0$, the method of SOKOLOVSKY/PREGL with a curved slip plane is used when taking cohesion into account. The horizontal component of the earth pressure component due to cohesion is

$$e_{pch} = c \cdot K_{pch} \quad (5.35)$$

where K_{pch} is taken from DIN 4085:2007 (see table 5.1). Cohesion increases the resultant passive earth pressure over a section of wall of height h by the value

$$E_{pch} = c \cdot h \cdot K_{pch} \quad (5.36)$$

5.6 Earth pressure due to unconfined surcharges

A load per unit area p is regarded as **unconfined** when it extends from the retaining structure to beyond the point where the critical slip plane intersects the ground surface (Fig. 5.14). On the other side of the wedge of soil, the load has no further effect on the wall.

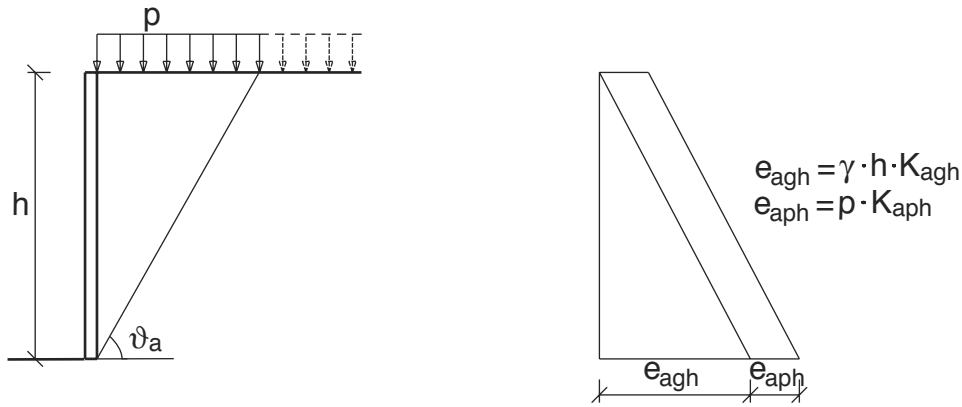


Figure 5.14: Unconfined surcharge

The additional horizontal active earth pressure due to such a surcharge p for $\alpha = \beta = 0$ is

$$e_{aph} = p \cdot K_{aph} = p \cdot K_{agh} \quad (5.37)$$

where K_{agh} is calculated using eq. 5.19.

For the case of $\alpha \neq 0$ and $\beta \neq 0$, the expression is expanded to

$$e_{aph} = p \cdot K_{aph} = p \cdot \frac{\cos \alpha \cdot \cos \beta}{\cos(\alpha - \beta)} \cdot K_{agh} \quad (5.38)$$

The unconfined surcharge therefore generates a uniformly distributed earth pressure on the wall in the case of homogeneous soils. The resultant horizontal earth pressure component is therefore

$$E_{aph} = e_{aph} \cdot h \quad (5.39)$$

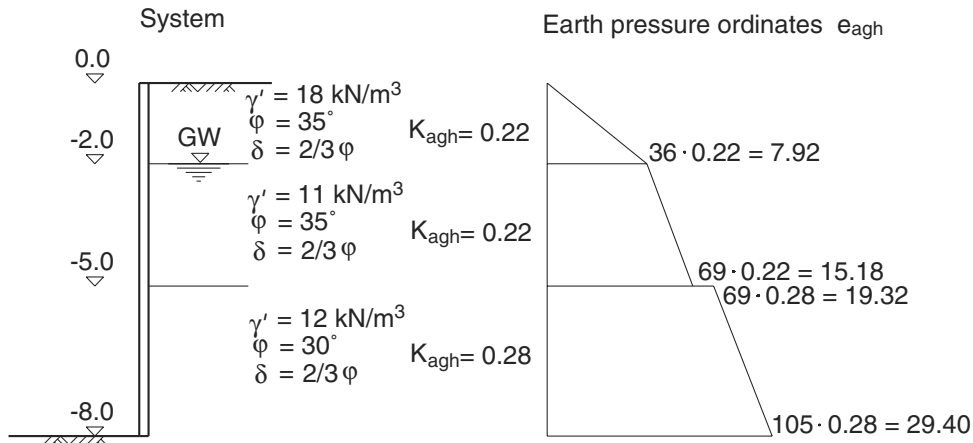


Figure 5.15: Earth pressure with changing soil strata

In the absence of any specific surcharges acting on the ground surface, a general, uniformly distributed load of $p = 10 \text{ kN/m}^2$ is assumed to act on the ground surface behind the retaining wall. This load should be classed as a permanent action.

The corresponding conditions apply to surcharges on the passive earth pressure side. Here, however, the surcharge should be applied only if it can be regarded as permanent.

5.7 Considering special boundary conditions

5.7.1 Stratified soils

It is quite usual to find several soil strata with different soil parameters in front of and behind a retaining wall. For such **stratified soils**, the earth pressure ordinates are calculated as follows

$$e_{ah}(z) = \sigma(z)K_{agh} - c \cdot K_{ach} \quad (5.40)$$

and

$$e_{ph}(z) = \sigma(z)K_{pgh} + c \cdot K_{pch} \quad (5.41)$$

The corresponding vertical stress σ_z at depth z is calculated from the total weight of the soil $\Sigma(\gamma_i \cdot h_i)$ in the overlying strata i plus any permanent, unconfined surcharges p .

From this approach it follows that inconstancies occur in the earth pressure diagram at the boundaries between the strata (Fig. 5.15). If the unit weight γ of the soil changes, the result is a kink in the earth pressure distribution because σ_z increases differently with the depth. This is also the case at the level of the groundwater table because the bulk unit weight γ_f acts above the groundwater table and the effective submerged unit weight γ' below. If the shear parameter c or φ changes at the boundary between strata, the result is a step in the earth pressure distribution. The value of c is entered directly into the cohesion term and φ via the earth pressure coefficient.

5.7.2 Confined surcharges

Confined surcharges on the ground surface or due to foundations behind the sheet pile wall cause local, additional earth pressures on the wall. These additional pressures may be determined independently of the earth pressure due to the self-weight of the soil, provided the load is not larger than the self-weight of the wedge of soil assumed (DIN 4085:2007). If this condition is not satisfied, the slip plane assumed changes substantially. In this case the system should be considered as a whole with all loading influences and the resultant earth pressure calculated via a suitably adapted slip plane. This can be carried out, for example, with CULMANN's graphical method or with the help of multiple-body failure mechanisms (see section 5.2.5).

The following cases are valid for loads less than the self-weight of the wedge of soil assumed. Generally, when describing the extent of a confined vertical load, the angle of friction φ and the slip plane angle ϑ are used as the upper and lower bounds for projecting the load onto the wall.

Strip and line loads

For confined strip or line loads (Fig. 5.16), the additional earth pressure is calculated similarly to eq. 5.3 but also taking into account the angle of wall friction δ :

$$E_{aVh} = V \cdot K_{aVh} = V \cdot \frac{\sin(\vartheta_a - \varphi) \cdot \cos(\alpha + \delta)}{\cos(\vartheta_a - \alpha - \delta - \varphi)} \quad (5.42)$$

where V is either a line load parallel to the sheet pile wall or a strip load $V = b \cdot p$ with width b and magnitude p .

The load spreads out at the angles φ and ϑ to the wall. Various approaches can be used for assessing the distribution of the earth pressure, which are given in EAB 2006 and DIN 4085:2007. The usual approaches are illustrated in Fig. 5.16. In the majority of cases, a constant distribution of the earth pressure over the height of the spread is sufficient. If the spread of the load reaches below the base of the wall, only that part of the earth pressure that actually acts on the wall is used in the calculations.

If, in addition, a horizontal thrust (e.g. from a foundation) is also present, this load can be considered separately from the vertical load. The horizontal earth pressure due to a horizontal force is

$$E_{aHh} = H \cdot K_{aHh} = H \cdot \frac{\cos(\vartheta_a - \varphi) \cdot \cos(\alpha + \delta)}{\cos(\vartheta_a - \alpha - \delta - \varphi)} \quad (5.43)$$

Point loads

In the case of a load confined on all sides V (e.g. pad foundation), a spread of 45° can be assumed on plan (Fig. 5.17). The earth pressure due to such a distributed load V' can then be determined like a strip load.

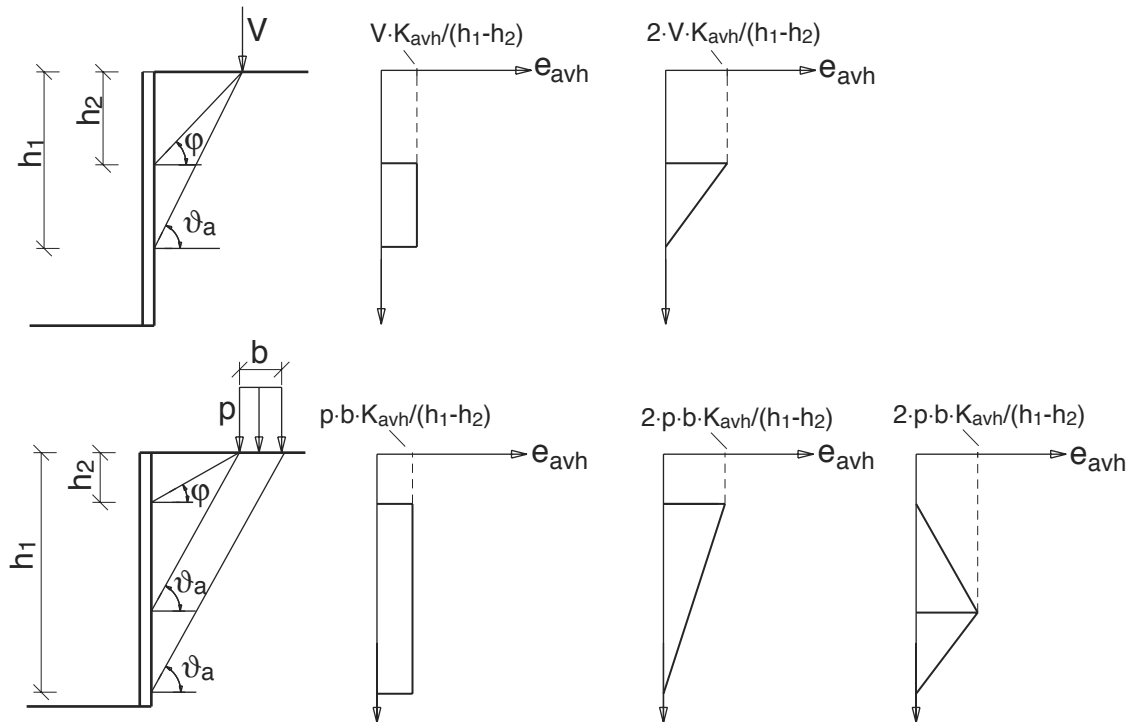


Figure 5.16: Earth pressure for line loads (top) and strip loads (bottom)

5.7.3 Stepped ground surface

If the surcharge on the active earth pressure side increases in steps, e.g. due to a **stepped embankment** or a change in ground level, this change in the load is also reflected in the earth pressure on the wall (Fig. 5.18).

According to an approximation by JENNE, the earth pressure lies within the limits given by the assumptions that, on the one hand, the ground is level at the top of the wall and, on the other, the ground above the embankment extends as far as the wall. The transition between the two earth pressure levels takes place within the upper bound at the angle φ (line of embankment), starting from the base of the embankment, and the lower bound at the angle ϑ (line of rupture), starting from the top of the embankment, or also from the base of the embankment if, for example, cohesion causes the embankment to be steeper than ϑ . The earth pressure between the two bounds may be obtained through linear interpolation.

5.7.4 Earth pressure relief

In quay and waterfront structures, a **relieving platform** can be built to reduce the earth pressure on the sheet pile wall. The earth pressure distribution below such a relieving platform can be calculated similarly to section 5.7.3. Again, the line of the embankment or line of rupture starting from the rear of the platform can be used as the upper and lower bounds respectively of the transition zone.

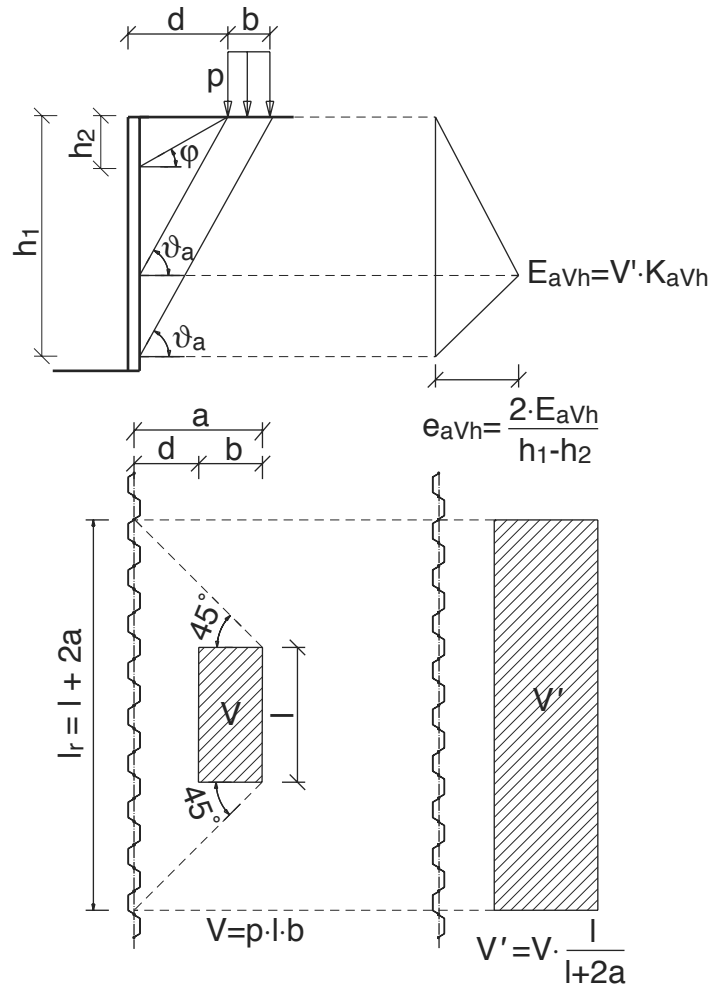


Figure 5.17: Earth pressure due to surcharge confined on all four sides

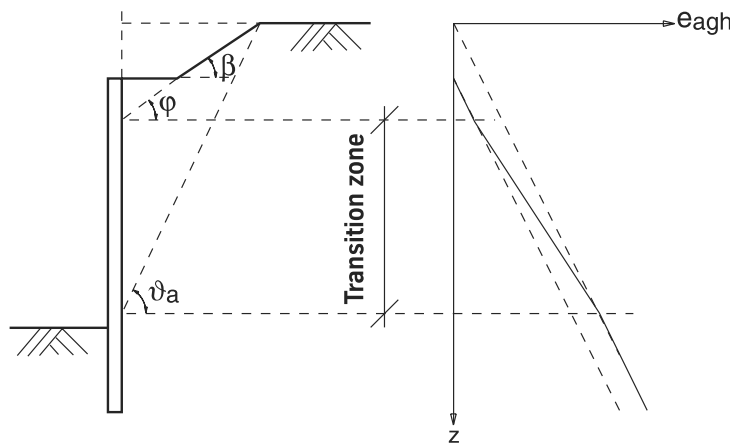


Figure 5.18: Determining the earth pressure approximately for a stepped embankment

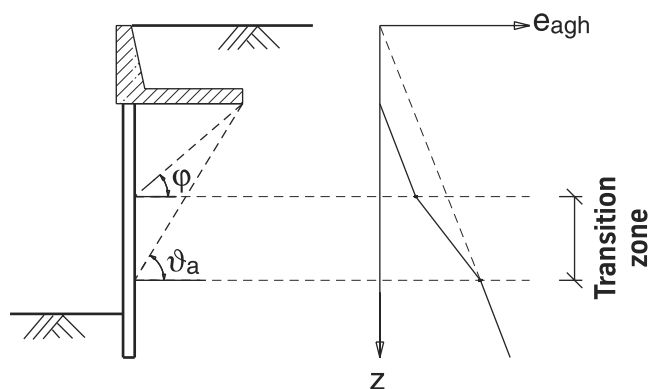


Figure 5.19: The use of a relieving platform

5.7.5 Earth pressure due to compaction

If the soil behind a sheet pile wall is backfilled in layers and subsequently **compacted**, the earth pressure on the wall at a certain depth below the surface of the backfill can exceed the active earth pressure due to self-weight in some circumstances.

DIN 4085:2007 provides design suggestions for applying the compaction pressure depending on the type of compaction (rolling or vibration) and the magnitude of the earth pressure (active earth pressure or steady-state earth pressure).

If the surface is subsequently loaded, e.g. by further layers of fill, the earth pressure due to compaction remains effective only to the extent that it exceeds the earth pressure due to additional loads. From this it follows that in the majority of cases only the earth pressure due to compaction in the upper layers needs to be considered.

5.7.6 Groundwater

The presence of groundwater in front of or behind the sheet pile wall has a direct effect on the earth pressure.

In stationary water, the buoyancy force of the groundwater acting on the granular structure reduces the effective unit weight of the soil such that only its submerged unit weight γ' is effective. The active and passive earth pressures are therefore reduced.

If the groundwater flows around the sheet pile wall, then **hydrodynamic pressures** generate additional forces that act on the granular structure of the soil. The hydrodynamic pressure $f_s = i \cdot \gamma_w$ (see section 4.3) increases the effective stresses on the side where the water flows downwards (normally the active earth pressure side) and reduces the effective stresses on the side where the water flows upwards (normally the passive earth pressure side).

The exact calculation procedure is illustrated with an example in Fig. 5.20. This is the same example as that in section 4.3. There, the intention was to illustrate the effect of the hydrodynamic pressure on the hydrostatic pressure, whereas here it is the effect on the active earth pressure. This can be calculated either with the help of a flow net or the approximation equation 4.9.

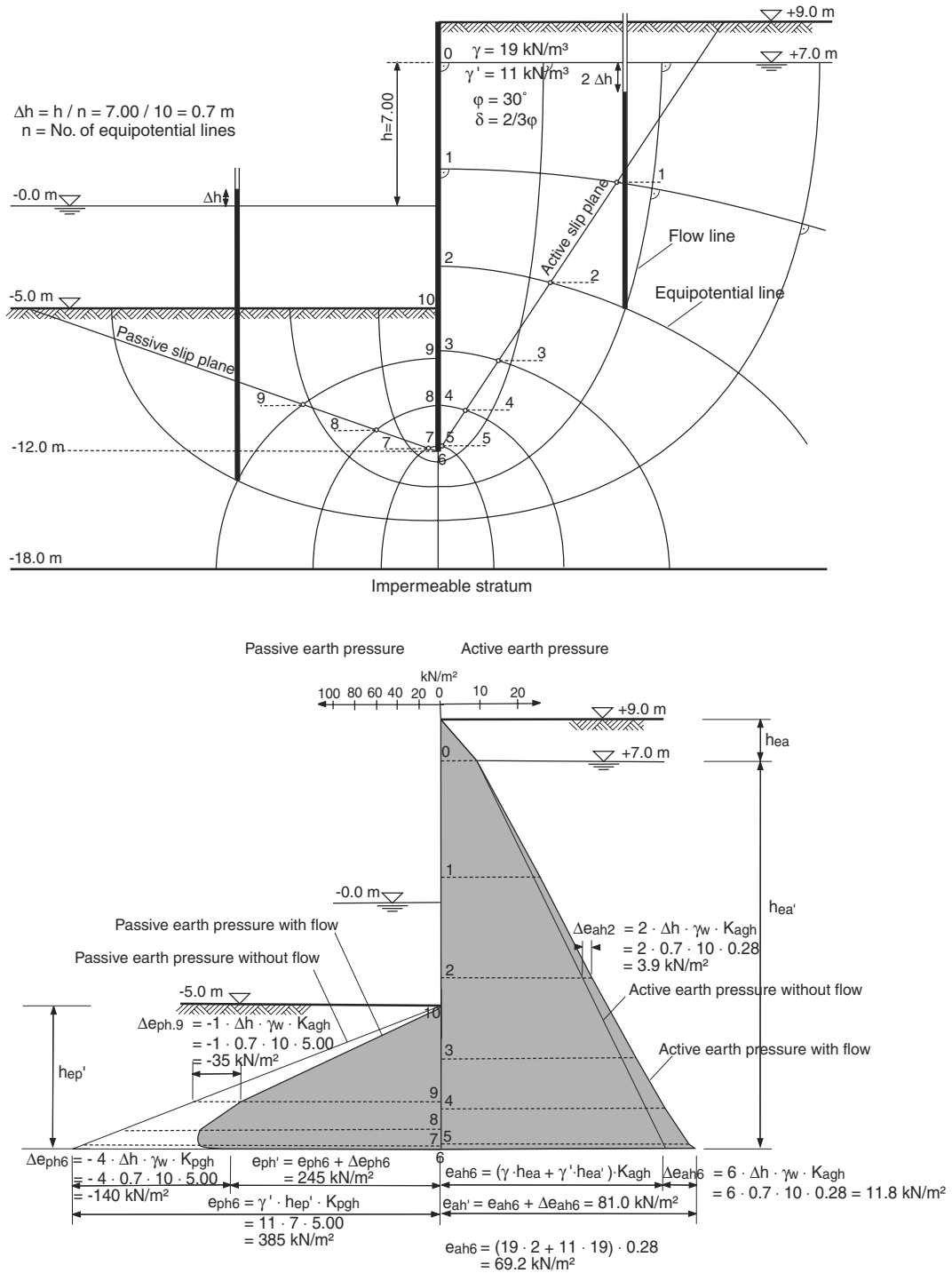


Figure 5.20: Influence of hydrodynamic pressure on active and passive earth pressures

5.7.7 Three-dimensional earth pressure

Quay structures are frequently built as combined sheet pile walls consisting of loadbearing piles and infill piles. In this arrangement, the infill piles are often not driven as deep as the loadbearing piles. The passive earth pressure in the region below the infill piles can only be mobilised by the loadbearing piles. Every one of these generates a **three-dimensional earth pressure figure** which, depending on the spacing of the loadbearing piles, can remain separate or can overlap. In the extreme case, the overlapping is so great that the loadbearing piles can be calculated as a continuous wall. DIN 4085:2007 section 6.5.2 contains further information on calculating the three-dimensional passive earth pressure.

5.8 Earth pressure redistribution

The classic earth pressure distribution only occurs for the active earth pressure with a rotation of the wall about its base. In the case of unpropped cantilever retaining walls fixed in the ground, a classic pressure distribution is to be expected. In the case of stiffened or anchored walls, the stiffening elements and anchors act as supports that prevent free rotation. As a result of this, the earth pressure **redistributes** corresponding to the support points. On the passive earth pressure side, the classic distribution of the earth pressure occurs only in the case of a parallel displacement of the wall. When taking into account a redistribution of the active or passive earth pressure, the active or passive earth pressure determined in the classic way is redistributed according to the movement of the wall to be expected, whereby the total value of the resultant earth pressure normally remains the same.

DIN 4085:2007 provides guidance on the distribution of the active and passive earth pressure for various types of wall movement (Fig. 5.21).

EAB 2006 provides information on the earth pressure redistribution for anchored and stiffened excavation enclosures. In this case, the number and position of the stiffening elements are particularly important. Fig. 5.22 shows the redistribution figures for sheet pile walls with one support.

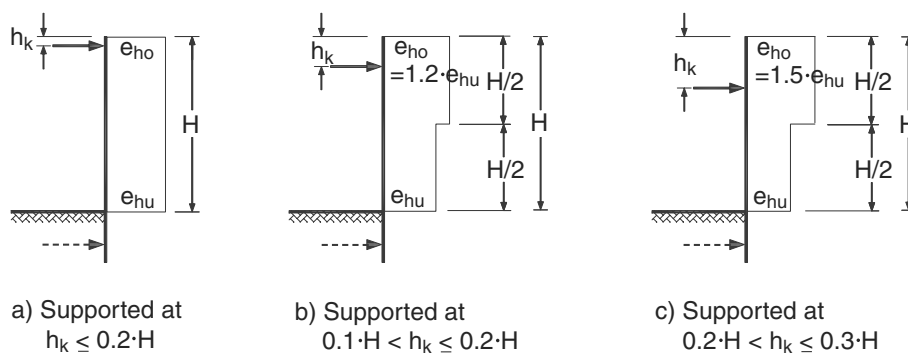


Figure 5.22: Earth pressure redistribution to EAB 2006 for single supports

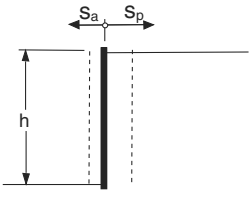
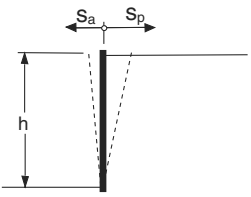
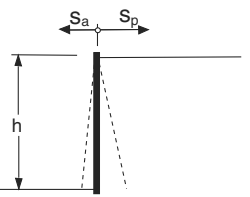
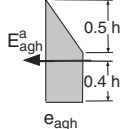
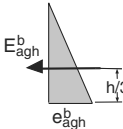
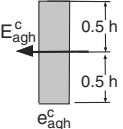
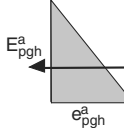
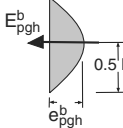
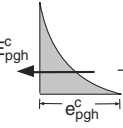
		 Parallel displacement	 Rotation at base	 Rotation at top
Active earth pressure	loose	$0.002 \leq s_a/h \leq 0.003$	$0.004 \leq s_a/h \leq 0.005$	$0.008 \leq s_a/h \leq 0.01$
	dense	$0.0005 \leq s_a/h \leq 0.001$	$0.001 \leq s_a/h \leq 0.002$	$0.002 \leq s_a/h \leq 0.005$
distribution	 E_{agh}^a e_{agh}^a	 E_{agh}^b e_{agh}^b	 E_{agh}^c e_{agh}^c	
	pressure force	$e_{agh}^a = 2/3 e_{agh}^b$ $E_{agh}^a = E_{agh}^b$	$e_{agh}^b = 1/2 \gamma h^2 K_{agh}$ $E_{agh}^b = 1/2 \gamma h^2 K_{agh}$	$e_{agh}^c = 0.5 e_{agh}^b$ $E_{agh}^c = E_{agh}^b$
Passive earth pressure	loose	$0.05 \leq s_p/h \leq 0.10$	$0.07 \leq s_p/h \leq 0.25$	$0.06 \leq s_p/h \leq 0.15$
	dense	$0.03 \leq s_p/h \leq 0.06$	$0.05 \leq s_p/h \leq 0.10$	$0.05 \leq s_p/h \leq 0.06$
distribution	 E_{pgh}^a e_{pgh}^a	 E_{pgh}^b e_{pgh}^b	 E_{pgh}^c e_{pgh}^c	
	pressure force	$e_{pgh}^a = 1/2 \gamma h^2 K_{pgh}$ $E_{pgh}^a = 1/2 \gamma h^2 K_{pgh}$	$e_{pgh}^b = e_{pgh}^a / 2$ $E_{pgh}^b = 2/3 E_{pgh}^a$	$e_{pgh}^c = 0.5 e_{pgh}^a$ $E_{pgh}^c = E_{pgh}^a$

Figure 5.21: Earth pressure redistribution to DIN 4085:2007

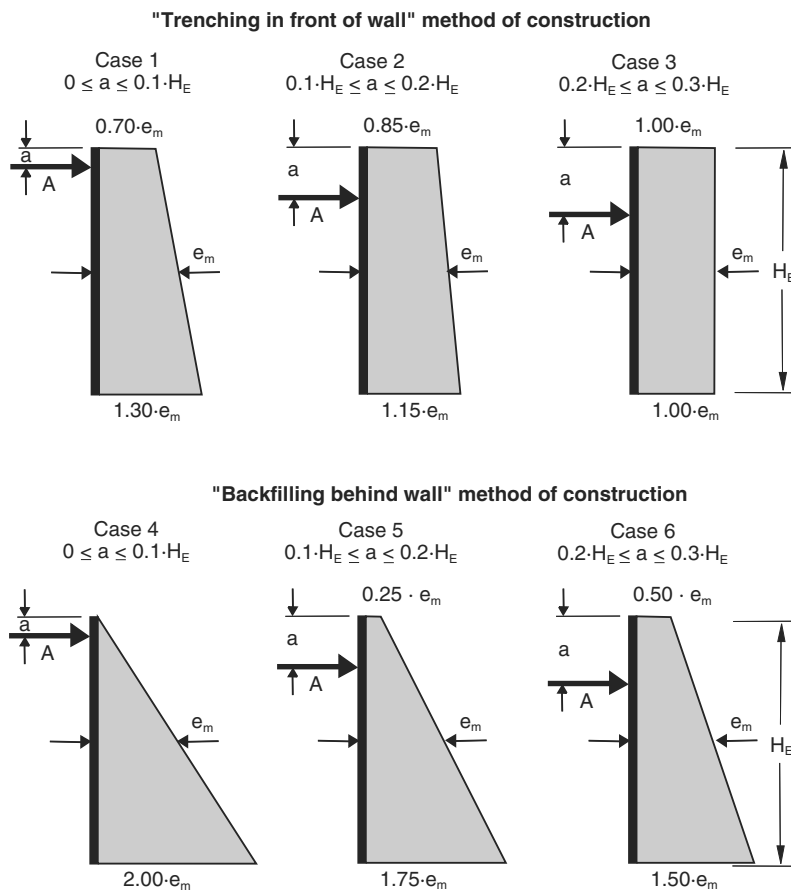


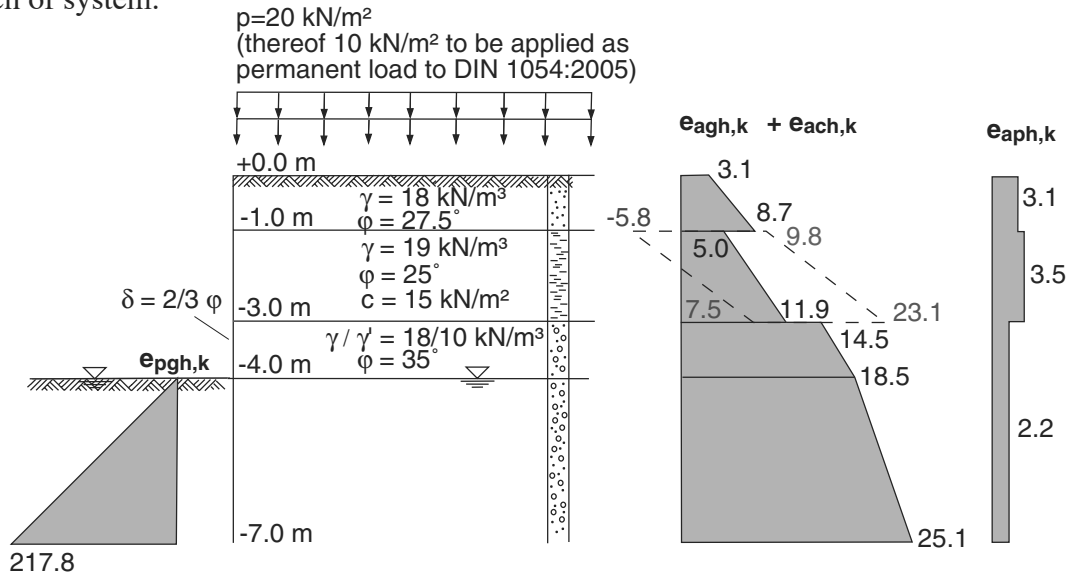
Figure 5.23: Earth pressure redistribution to EAU 2004

EAU 2004 contains earth pressure redistribution figures for anchored waterfront structures which also take into account whether the structure is built on land or in water (Fig. 5.23). On land, the ground in front of the sheet pile wall is excavated so that the earth pressure redistributes towards the anchor position as the excavation proceeds. In water, the ground behind the wall is backfilled in layers so that only a minimal redistribution of earth pressure takes place.

5.9 Examples of earth pressure calculations

Example 5.1 Earth pressure calculation for stratified soil and cohesion

Sketch of system:

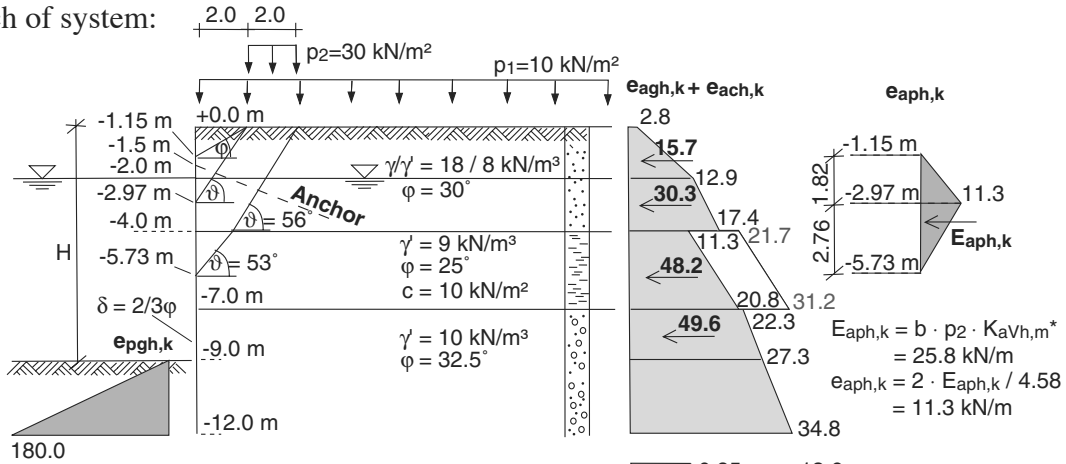


Stratum	Level	h	γ/γ'	$\Delta\sigma'_z$	Act. earth pressure			Pass. earth pressure			Cohesion			Minimum earth pressure		Variable surcharge			
					$\sigma'_{z,a}$	K_{agh}	$e_{agh,k}$	$\sigma'_{z,p}$	K_{pgh}	$e_{pgh,k}$	c	K_{ach}	$e_{ach,k}$	$e_{agch,k}$	$K_{ah,min}$	$e_{ah,min}$	p	K_{aph}	$e_{aph,k}$
1	2	3	4	5	6	7	8	9	10	11	12	13	14	15	16	17	18	19	20
1	0.0 -1.00	1.0	18	18	10 28	0.31	3.1 8.7				-	-	-	3.1 8.7	-	-	10	0.31	3.1
2	-1.0 -3.0	2.0	19	38	28 66	0.35	9.8 23.1	-	-	-	15	1.04	-15.6	-5.8 7.5	0.18	5.0 11.9	10	0.35	3.5
3	-3.0 -4.0 -7.0	1.0 3.0	18 10	18 30	66 84 114	0.22	14.5 18.5 25.1	0 30	7.26	0 217.8	-	-	-	14.5 18.8 25.1	-	-	10	0.22	2.2

Stratum thickness
 Bulk unit weight / effective unit weight
 Change in vertical stress
 Effective vertical stress
 Active earth pressure coefficient for soil self-weight
 Active earth pressure due to soil self-weight
 Effective vertical stress
 Passive earth pressure coefficient for soil self-weight
 Passive earth pressure due to soil self-weight
 Cohesion
 Active earth pressure coefficient for cohesion
 Active earth pressure due to cohesion
 Minimum earth pressure coefficient
 Minimum earth pressure
 Surcharge
 Active earth pressure coefficient for unconfined surcharge
 Active earth pressure due to unconfined surcharge

Example 5.2 Earth pressure calculation with strip load and earth pressure redistribution

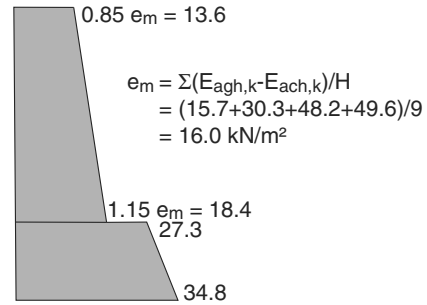
Sketch of system:



Active earth pressure redistribution to EAU:
(built on land)
 $a/H = 1.5/9 = 0.167$: Case 2

* Determination of average active earth pressure coefficient $K_{avh,m}$ for confined surcharges:

$K_{avh,30^\circ} = 0.41$ (Stratum 1)
 $K_{avh,25^\circ} = 0.46$ (Stratum 2)
 $K_{avh,m} = (0.41 \cdot 2.85 + 0.46 \cdot 1.73) / 4.58 = 0.43$

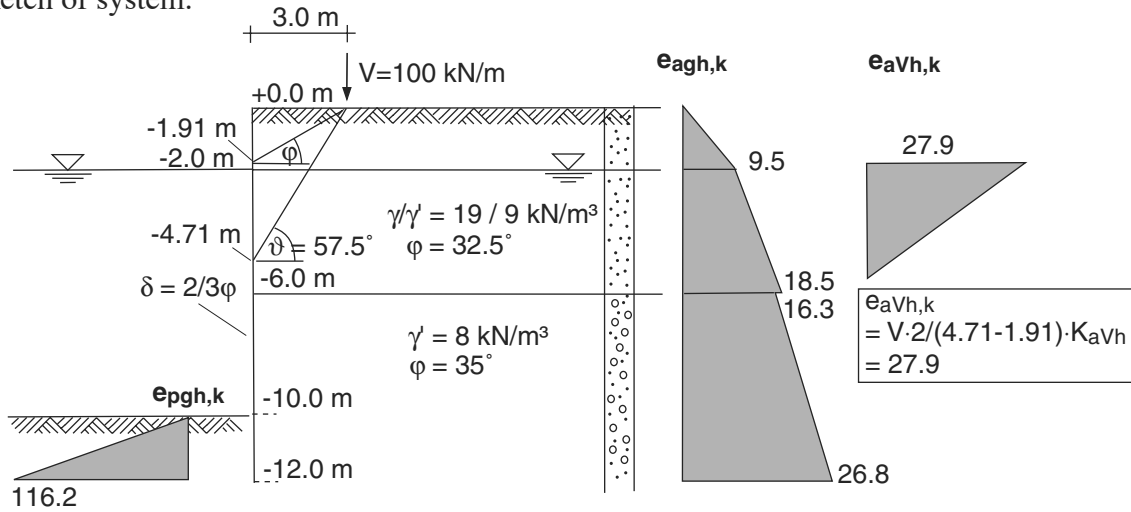


Stratum	Level	h	γ/γ'	$\Delta\sigma'_z$	Active earth pressure			Passive earth pressure			Cohesion			Load p_2				
					$\sigma'_{z,a}$	K_{agh}	$e_{agh,k}$	$\sigma'_{z,p}$	K_{pgh}	$e_{pgh,k}$	c	K_{ach}	$e_{ach,k}$	Level	p_2	K_{avh}	$e_{avh,k}$	
-	m	m	kN/m ³	kN/m ²	kN/m ²	-	kN/m ²	kN/m ²	-	kN/m ²	kN/m ²	-	kN/m ²	-	m	kN/m ²	-	kN/m ²
1	2	3	4	5	6	7	8	9	10	11	12	13	14	15	16	17	18	
1	0.0	2.0	18	36	10	0.28	2.8							-1.15	30	0.43	0	
	-2.0	2.0	8	16	46		12.9				-	-	-	-2.97				11.3
	-4.0				62		17.4							-5.73				0
2	-4.0	3.0	9	27	62	0.35	21.7				10	1.04	-10.4					
	-7.0				89		31.2											
3	-7.0	2.0	10	20	89		22.3											
	-9.0	3.0	10	30	109	0.25	27.3	0	6.00	0								
	-12.0				139		34.8	30		180								

Stratum thickness
 Bulk unit weight / effective unit weight
 Change in vertical stress
 Effective vertical stress
 Active earth pressure coefficient for soil self-weight
 Active earth pressure due to soil self-weight
 Passive earth pressure coefficient for soil self-weight
 Passive earth pressure due to soil self-weight
 Active earth pressure coefficient for cohesion
 Active earth pressure due to cohesion
 Confined surcharge
 Active earth pressure coefficient for confined surcharge
 Active earth pressure due to confined surcharge

Example 5.3 Earth pressure calculation with line load

Sketch of system:

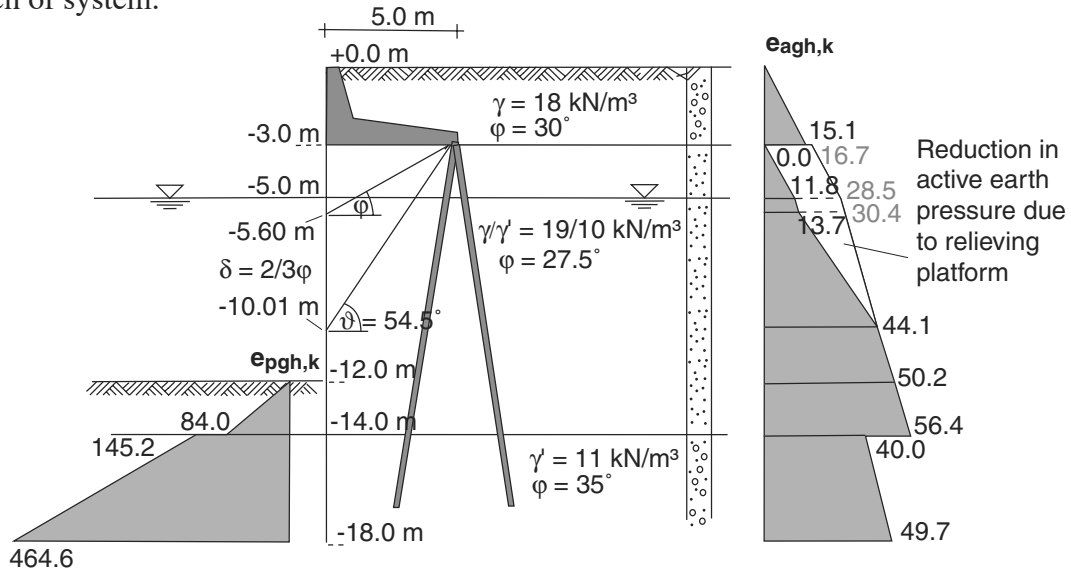


Stratum	Level m	h m	γ/γ' kN/m ³	$\Delta\sigma'_z$ kN/m ²	Active earth pressure			Passive earth pressure			Load V		
					$\sigma'_{z,a}$ kN/m ²	K_{agh} -	$e_{agh,k}$ kN/m ²	$\sigma'_{z,p}$ kN/m ²	K_{pgh} -	$e_{pgh,k}$ kN/m ²	Level m	K_{aVh} -	$e_{aVh,k}$ kN/m ²
1	2	3	4	5	6	7	8	9	10	11	12	13	14
1	0.0	2.0	19	38	0	-	0.0	-	-	-	-1.91	-	27.9
	-2.0	4.0	9	36	38	0.25	9.5	-	-	-	-4.71	0.39	0
	-6.0	-	-	-	74	-	18.5	-	-	-	-	-	-
2	-6.0	4.0	8	32	74	-	16.3	-	-	-	-	-	-
	-10.0	2.0	8	16	106	0.22	23.3	0	7.26	0	-	-	-
	-12.0	-	-	-	122	-	26.8	16	-	116.2	-	-	-

Stratum thickness
 Bulk unit weight / effective unit weight
 Change in vertical stress
 Effective vertical stress
 Active earth pressure coefficient for soil self-weight
 Active earth pressure due to soil self-weight (Tab. 5.1)
 Effective vertical stress
 Passive earth pressure coefficient for soil self-weight
 Passive earth pressure due to soil self-weight (Tab. 5.1)
 Active earth pressure coefficient for confined surcharge
 Active earth pressure due to confined surcharge (eq. 5.42)

Example 5.4 Earth pressure calculation with relieving platform

Sketch of system:



Stratum	Level m	h m	γ/γ' kN/m ³	$\Delta\sigma'_z$ kN/m ²	Active earth pressure			Passive earth pressure			Earth pressure relief		
					$\sigma'_{z,a}$ kN/m ²	K_{agh} -	$e_{agh,k}$ kN/m ²	$\sigma'_{z,p}$ kN/m ²	K_{pgh} -	$e_{pgh,k}$ kN/m ²	$\Delta\sigma'_{z,a}$ kN/m ²	K_{agh} -	$\Delta e_{agh,k}$ kN/m ²
1	2	3	4	5	6	7	8	9	10	11	12	13	14
1	0.00 -3.00	3.00	18	54.0	0.0 54.0	0.28	0.0 15.1	-	-	-	-	-	-
2	-3.00	2.00	19	38.0	54.0	0.31	16.7	-	-	-	-54.0	0.31	-16.7
	-5.00	0.60	10	6.0	92.0		28.5				-54.0		-16.7
	-5.60	4.41	10	44.1	98.0		30.4				-54.0		-16.7
	-10.01	1.99	10	19.9	142.1		44.1				0.0		0.0
	-12.00	2.00	10	20.0	162.0		50.2				0		4.2
-14.00				182.0	56.4		20.0	84.0					
3	-14.00 -18.00	4.00	11	44.0	182.0 226.0	0.22	40.0 49.7	20.0 64.0	7.26	145.2 464.6	-	-	-

Stratum thickness
 Bulk unit weight / effective unit weight
 Change in vertical stress
 Effective vertical stress
 Active earth pressure coefficient for soil self-weight
 Active earth pressure due to soil self-weight (Tab. 5.1)
 Effective vertical stress
 Passive earth pressure coefficient for soil self-weight
 Passive earth pressure due to soil self-weight (Tab. 5.1)
 Vertical stress reduction due to relieving platform
 Active earth pressure reduction due to relieving platform
 Active earth pressure coefficient for soil self-weight (Tab. 5.1)
 Active earth pressure reduction due to relieving platform

Chapter 6

Design of sheet pile walls

6.1 General

Various design methods have proved worthwhile for the **structural analysis** of sheet piling structures. There are methods based on classic active/passive earth pressure theory, idealisation of the subsoil through elastic-plastic spring models, and ultimate load approaches.

Sheet pile walls belong to the class of wall-type retaining structures whose design is covered by section 10 of DIN 1054:2005-01. DIN 1054 is an overriding standard that provides a general format for all analyses. The establishment of actions, resistances, calculation procedures and construction is covered by the specialist standards and recommendations of the German Society for Geotechnics (DGGT).

In accordance with the current state of the art, sheet piling structures are calculated and dimensioned with the help of computers these days. It is nevertheless essential for the design engineer to have a sound knowledge of the various methods of calculation, either for the purpose of checking the computer calculations or for carrying out quick and simple preliminary designs.

6.2 Safety concept

6.2.1 Geotechnical categories

According to DIN 1054:2005-01 and also DIN 4020:2003-09, geotechnical structures are placed in one of the three **geotechnical categories** (GC) (see table 6.1) with respect to requirements concerning the scope and quality of geotechnical investigations, design and supervision.

This classification must be carried out at the start of the planning phase, but can be revised at any time should any of the boundary conditions change. Further gradations of the geotechnical categories into individual subcategories is also possible.

Table 6.1: Geotechnical categories (GC)

Category	Recommendations for inclusion	Assessment of stability
GC 1	<ul style="list-style-type: none"> - simple subsoil conditions - low requirements - up to 2.0 m high in horizontal, unloaded ground - trench sheeting to DIN 4120:2002-10/5. - standard trench sheeting to DIN 4124:2002-10/5.2,7.3 	Assessment based on empirical values, a geotechnical expert is only required in cases of doubt.
GC 2	<ul style="list-style-type: none"> - moderate requirements 	Numerical safety analysis, a report by a geotechnical expert should be available.
GC 3	<ul style="list-style-type: none"> - difficult subsoil conditions - high requirements - close to structures vulnerable to displacement - active earth pressure exceeds steady-state earth pressure - increase in strains/displacements over time - confined groundwater 	Numerous geotechnical findings required for the assessment, the assistance of a geotechnical expert before, during and after construction is necessary.

6.2.2 Limit states

According to DIN 1054:2005-01, the **limit states** are divided into

- Ultimate limit state (LS 1), which means
 - Limit state of loss of support safety (LS 1A)
Failure of the structure due to loss of equilibrium without collapse
 - Limit state of failure of structures and components (LS 1B)
Collapse of the structure due to failure in the structure or in the supporting subsoil
 - Limit state of loss of overall stability (LS 1C)
Collapse of the subsoil due to failure in the subsoil

and

- Serviceability limit state (LS 2)
The state which, if exceeded, means full use of the structure is no longer possible.

6.2.3 Loading cases

The **loading cases** result from the combinations of actions in conjunction with the safety classes.

- Combinations of actions
 - Standard combination CA 1
 - Rare combination CA 2
 - Exceptional combination CA 3

- Safety classes for resistances
 - SC 1: conditions related to the functional life of the structure
 - SC 2: conditions during construction
 - SC 3: conditions occurring just once or probably never during the functional life of the structure
- Loading cases
 - LC 1: permanent design situation (CA 1 in conjunction with SC 1)
 - LC 2: temporary design situation (CA 2 in conjunction with SC 1, or CA 1 in conjunction with SC 2)
 - LC 3: exceptional design situation (CA 3 in conjunction with SC 2, or CA 2 in conjunction with SC 3)

6.2.4 Partial safety factors

The **partial safety factors** for actions, action effects and resistances according to DIN 1054:2005-01 are given in tables 6.2 and 6.3.

Table 6.2: Partial safety factors for actions and action effects to DIN 1054:2005-01

Action	Symbol	Loading case		
		LC 1	LC 2	LC 3
LS 1A: limit state of loss of support safety				
Favourable permanent actions	$\gamma_{G, stb}$	0.90	0.90	0.95
Unfavourable permanent actions	$\gamma_{G, dst}$	1.00	1.00	1.00
Hydrodynamic force in favourable subsoil	γ_H	1.35	1.30	1.20
Hydrodynamic force in unfavourable subsoil	γ_H	1.80	1.60	1.35
Unfavourable variable actions	$\gamma_{Q, dst}$	1.50	1.30	1.00
LS 1B: limit state of failure of structures and components				
General permanent actions ¹	γ_G	1.35	1.20	1.00
Permanent actions due to steady-state earth pressure	γ_{E0g}	1.20	1.10	1.00
Unfavourable variable actions	γ_Q	1.50	1.30	1.00
LS 1C: limit state of loss of overall stability				
Permanent actions	γ_G	1.00	1.00	1.00
Unfavourable variable actions	γ_Q	1.30	1.20	1.00
LS 2: serviceability limit state				
$\gamma_G = 1.00$ for permanent actions				
$\gamma_Q = 1.00$ for variable actions				
¹ including permanent and variable hydrostatic pressure				

Table 6.3: Partial safety factors for resistances to DIN 1054:2005-01

Resistance	Symbol	Loading case		
		LC 1	LC 2	LC 3
LS 1B: limit state of failure of structures and components				
<i>Soil resistances</i>				
Passive earth pressure and ground failure resistance	γ_{Ep}, γ_{Gr}	1.40	1.30	1.20
Sliding resistance	γ_{Gl}	1.10	1.10	1.10
<i>Pile resistances</i>				
Pile compression resistance under test load	γ_{Pc}	1.20	1.20	1.20
Pile tension resistance under test load	γ_{Pt}	1.30	1.30	1.30
Pile resistance in tension and compression based on empirical values	γ_P	1.40	1.40	1.40
<i>Grouted anchor resistances</i>				
Resistance of steel tension member	γ_M	1.15	1.15	1.15
Pull-out resistance of grout	γ_A	1.10	1.10	1.10
<i>Resistances of flexible reinforcing elements</i>				
Material resistance of reinforcement	γ_B	1.40	1.30	1.20
LS 1C: limit state of loss of overall stability				
<i>Shear strength</i>				
Friction angle φ' of drained soil	$\gamma_\varphi, \gamma_{\varphi u}$	1.25	1.15	1.10
Cohesion c' of drained soil and shear strength c_u of undrained soil	γ_c, γ_{cu}	1.25	1.15	1.10
<i>Pull-out resistances</i>				
Ground or rock anchors, tension piles	γ_N, γ_Z	1.40	1.30	1.20
Grout of grouted anchors	γ_A	1.10	1.10	1.10
Flexible reinforcing elements	γ_B	1.40	1.30	1.20

6.2.5 Analysis format

According to DIN 1054:2005-01, the **limit state condition**

$$\sum E_d \leq \sum R_d \quad (6.1)$$

must be satisfied in all analyses for LS 1.

In this equation, E (effect) stands for the actions resulting from the force or deformation variables acting on the structure, and R (resistance) for the internal forces or stresses in or on the structure or in the subsoil as a result of the strength or stiffness of the building materials or the subsoil. The index d (design) indicates that the inequality must be satisfied for the design values.

6.2.6 Further factors

According to EAU 2004, the **stability analyses** should be as simple as possible in structural terms with clearly defined paths for transferring the loads and forces. In the course of the analyses, there should be a clear breakdown with respect to the following points (EAU 2004 section 0.3):

- Details of the use of the structure
- Drawings of the structure with all planned dimensions
- Description of the structure
- Design value of bottom depth
- Characteristic values of all actions
- Soil strata and associated characteristic soil parameters
- Critical unconfined water levels plus associated groundwater levels
- Combinations of actions, or rather loading cases
- Partial safety factors required/applied
- Intended building materials and their strengths or resistance values
- Details of critical building conditions
- Description and reasons for intended verification procedures
- Details of publications referred to and other aids

6.3 Actions and action effects

Sheet piling structures are in the first instance loaded by hydrostatic and earth pressures. The calculation of these variables is dealt with in chapters 4 and 5, and is also addressed in WEISSENBACH (2003).

6.3.1 Earth pressure

The design of sheet pile walls is carried out for limit state LS 1B. As described in section 6.2, the action effects due to characteristic actions are determined and converted into design variables by multiplying with the corresponding partial safety factors from table 6.2, which take into account the nature of the respective action. The characteristic parameters of the soil are used to calculate the earth pressure as a characteristic action specific to earthworks.

6.3.2 Action effects due to earth pressure

The action effects resulting from earth pressure must always be assessed according to the permanent and variable components. According to the concept of partial safety factors, for limit state LS 1B the characteristic action effects are not increased by the partial safety factors for the specific action until they are compared with the respective resistances at the limit state conditions according to DIN 1054:2005-01, whereas the resistances are correspondingly reduced.

6.3.3 Hydrostatic pressure

When defining the hydrostatic pressure critical for the design, it is necessary to perform an accurate assessment of possible water levels during the construction period and lifetime of the structure plus the associated probabilities of occurrence. When determining the characteristic hydrostatic pressure, both maximum and minimum water levels must be defined and investigated.

In contrast to the earth pressure, for which the action effects due to active and passive earth pressures are determined separately, in the case of hydrostatic pressure the component acting on the passive earth pressure side is also considered as an action. The structural calculations can therefore be simplified by considering merely the resultant hydrostatic pressure. According to DIN 1054:2005 section 10.3.2, the hydrostatic pressure should generally be increased by the partial safety factor γ_G for permanent actions.

6.4 Resistances

6.4.1 Passive earth pressure

The passive earth pressure, just like the active earth pressure, is dependent on deformations. Fig. 5.3 clearly shows that a very large wall displacement is required to activate the full passive earth pressure $E_{ph,k}$. So it follows that if the full characteristic passive earth pressure is used in the analysis for LS 1B, large deformations in the passive earth pressure zone must be accepted. This should be assessed with respect to the **serviceability**.

In order to circumvent this problem, DIN 1054:2005-01 section 10.6.3(4) includes the option of reducing the characteristic passive earth pressure by an **adjustment factor** $\eta < 1.0$. However, this reduction factor certainly does not replace the reduction by the partial safety factor γ_{Ep} , which means that

$$E_{ph,d} = \eta \cdot E_{ph,k} / \gamma_{Ep} \quad (6.2)$$

6.4.2 Component resistances

The characteristic **material resistances** $R_{m,k}$ and the partial safety factors γ_M for the individual components of a sheet piling structure, e.g. sheet pile sections, walings, struts, can be found in the respective standards for those constructions.

Merely the design of anchorages using grouted anchors is regulated explicitly in chapter 9 of DIN 1054:2005-01 with respect to pull-out resistance and material failure. The partial safety factors for grouted anchors are also to be found in DIN 1054:2005-01 (see table 6.3).

6.5 Structural systems

The basis of the **structural calculations** is a realistic, idealised representation of the system. Owing to the complex soil-structure interaction, the loading on the sheet pile wall is directly dependent on the deformation behaviour of those two components. The deformation behaviour of the wall depends, on the one hand, on the support conditions at the base of the wall, and, on the other, on possible struts or anchors supporting the wall above the founding level (WEISSENBACH, 1985).

In terms of the **support conditions** at the theoretical base of the wall, we distinguish between simply supported, partially fixed and fully fixed walls.

In terms of possible support, besides unsupported walls, those with single or multiple supports may need to be considered.

Generally, it can be said that for an equal depth of excavation and an identical number of struts or anchors, greater embedment depths are necessary for fully fixed walls when compared with simply supported walls, but that this results in lower internal forces, wall deformations and anchor forces. Walls with partial fixity at the base lie somewhere between the simply supported and fully fixed forms with respect to the stresses and strains. The decision concerning the support condition at the base of the wall is made by the design engineer based on the requirements of the respective construction project.

The **deformation behaviour** of simply supported and fixed walls is fundamentally different. For a fixed wall, a rotation about its theoretical base is assumed, whereas for a simply supported wall, a parallel displacement of the base of the wall is assumed. Fig. 6.1 shows the displacements on which the design is based and their corresponding stress distributions.

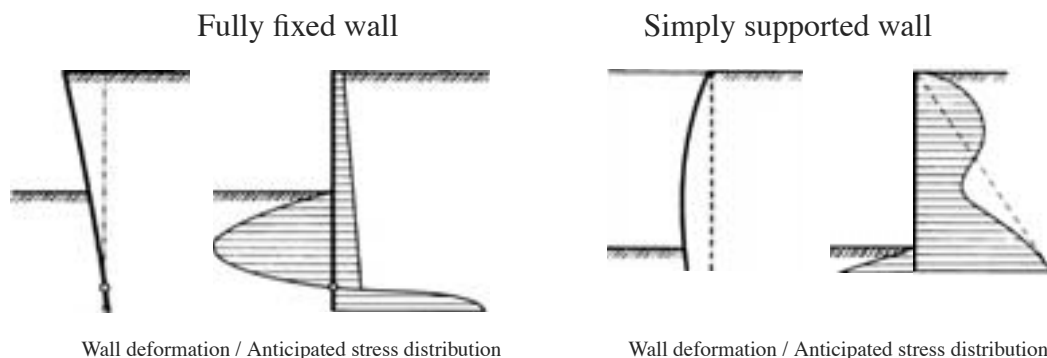


Figure 6.1: Wall movement and stress distribution depending on support conditions, WEISSENBACH (2001)

The method according to BLUM has become established in practice for the analysis of fixity in the soil (BLUM, 1931). In this method, the zone below the base of the excavation is idealised

by a triangular passive earth pressure diagram and an **equivalent force** at the theoretical base of the wall. The true distribution of the passive earth pressure below the theoretical base C is taken into account by adding an allowance to the calculated theoretical embedment depth.

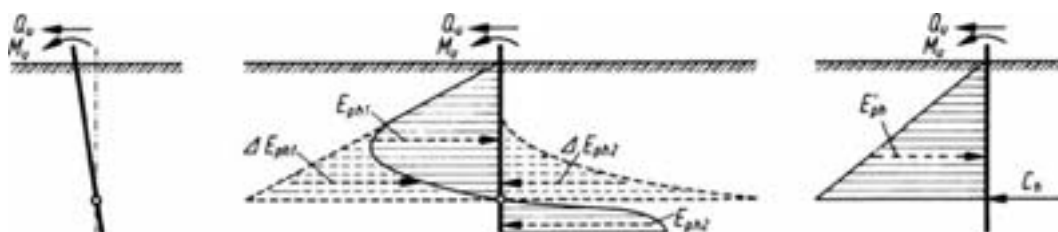


Figure 6.2: System idealisation after BLUM, WEISSENBACH (2001)

By introducing a pinned support C at the theoretical base of the wall F, it is possible to carry out the structural calculations according to the rules of structural analysis for any type of system.

The **support conditions** are guaranteed by way of specific force or deformation boundary conditions at the base of the wall.

The **simple support** in the soil is the minimum embedment length possible at which failure of the sheet pile wall due to horizontal displacement of the base of the wall is prevented. A simply supported condition in the soil is present when the reaction Q_F at the base support is 0, i.e. for the case of equilibrium between the active and passive forces. The associated embedment depth is designated with t_a . From the structural viewpoint, struts or anchors are essential for simply supported walls.

Full fixity is present when a further increase in the embedment depth does not bring about any further change in the loadbearing behaviour of the wall because no wall deformations take place below the theoretical depth necessary for full fixity and the steady-state earth pressure acts on both sides of the wall. Full fixity in the soil is achieved when the inclination of the tangent to the base of the wall is $w'_F = 0$ at the theoretical base of the wall. The associated embedment depth is designated with t_e . Walls fully fixed in the soil do not necessarily require struts or anchors.

If the embedment depth lies between that for simple support in the soil t_a and that for full fixity t_e , then we speak of **partial fixity** of the sheet pile wall in the soil. In the case of partial fixity, neither the end tangent inclination w'_F nor the equivalent transverse force Q_F are equal to 0. Struts or anchors are not essential from the structural viewpoint, but are advisable in order to limit deformations.

According to EAU 2004, a wall with partial fixity is defined by the end tangent angle ε . This lies between 0 for full fixity and ε_{max} for a simple support. The degree of fixity τ_{1-0} is defined in EAU 2004 as

$$\tau_{1-0} := 100 \cdot \left(1 - \frac{\varepsilon}{\varepsilon_{max}} \right) \quad [\%] \quad (6.3)$$

The associated embedment depth is designated with $t_{\tau_{1-0}}$ depending on the **degree of fixity**.

If the degree of fixity is greater than 0, the wall has partial or full fixity, and so the calculated theoretical embedment length of the wall must be increased by the so-called driving allowance, which in reality takes into account the application of the equivalent reaction C at the base of

the wall (see Fig. 6.2). According to EAU 2004 section 8.2.9, for fully fixed walls this can be simplified to

$$\Delta t = \frac{t_{1-0}}{5} \quad (6.4)$$

where

t_{1-0} calculated theoretical embedment depth

A more accurate calculation of the **driving allowance** is given by the further development of the approach after LACKNER according to EAU 2004 section 8.2.9 (LACKNER, 1950):

$$\Delta t \geq \frac{C_{h,d} \cdot \gamma_{Ep}}{e_{phC,k}} \quad (6.5)$$

where

$C_{h,d}$ $\frac{1}{2}$ design value of equivalent force at base of wall after BLUM
 γ_{Ep} partial safety factor for passive earth pressure according to table 6.3
 $e_{phC,k}$ characteristic value of passive earth pressure ordinate at the depth of the point of application of equivalent force C

If the approach after LACKNER is used for calculating the driving allowance, the condition

$$\Delta t > \Delta t_{MIN} = \frac{\tau_{1-0} \cdot t_{1-0}}{10} \quad (6.6)$$

where

τ_{1-0} degree of fixity of sheet pile wall at base support according to eq. 6.3
 t_{1-0} calculated theoretical embedment depth

must be checked and, if necessary, Δt must be adjusted.

Whereas eq. 6.5 takes into account the partial fixity via the equivalent force C after BLUM, partial fixity cannot be taken into account with eq. 6.4.

The driving allowance required increases, just like the equivalent force C , from 0 for a simple support at the base to the maximum value for full fixity at the base, with the intermediate values representing partial fixity. In addition to the aforementioned methods of calculation, the final driving depth can also be determined with

$$t = \alpha \cdot t_{1-0} \quad (6.7)$$

where

α factor according to table 6.4
 t_{1-0} calculated theoretical embedment depth

after BLUM (1931).

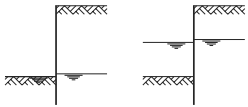
Wall type	 low excess hydrostatic pressure	 higher excess hydrostatic pressure	 very large or purely excess hydrostatic pressure
Not anchored	1.20	1.30	1.40 – 1.60
Anchored, with fixed base	1.10	1.15	1.20 – 1.30
Anchored, with simply supported base	1.05	1.10	1.15 – 1.20

Table 6.4: Factor α for a rough determination of the driving depth taking into account $\delta = \pm \frac{2}{3}\varphi$, Sheet Piling Handbook (1977)

Fig. 6.3 shows the relationships between embedment length, internal forces and wall rotation graphically.

If the aforementioned boundary conditions for the base of the wall are known, it is possible to calculate the embedment length of the wall necessary for the support conditions to be chosen in each situation from the **static equilibrium**. In simple cases, the equilibrium conditions can be solved with the help of **nomograms**. It is also possible to determine the embedment depth by **iteration**, until in the end the desired boundary conditions are created at the base of the wall.

Increasing the embedment length beyond t_e has no effect on the calculation of the wall in terms of statics because at depths below t_e no further actions, or resistances, due to earth pressure can be mobilised. The earth pressure acting on both sides of the wall is mutually exclusive. Figures less than t_a are not possible because such cases do not result in static equilibrium.

The structural calculations and the determination of internal forces are always carried out based on the theoretical embedment depth, and any driving allowance possible is ignored.

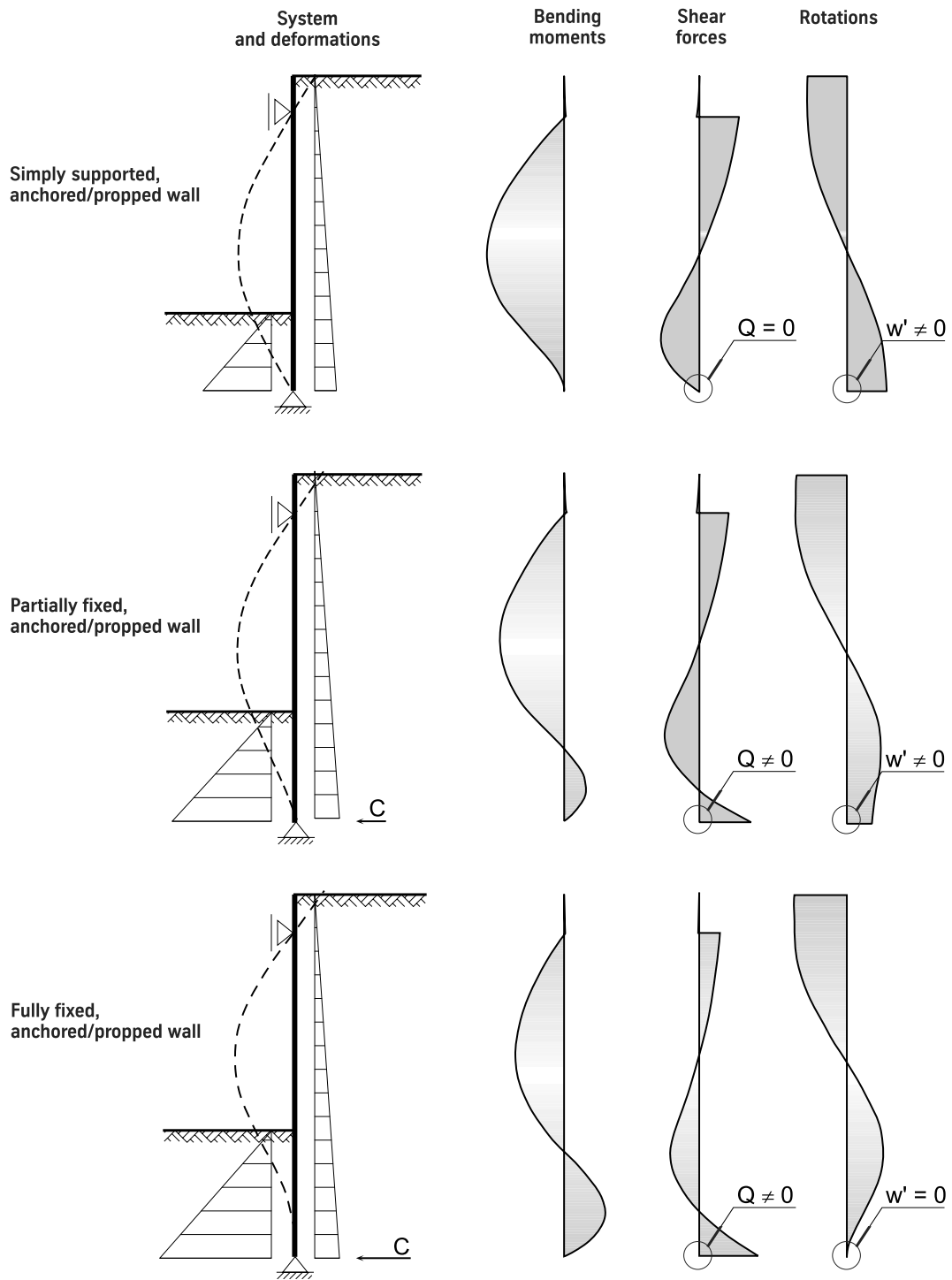


Figure 6.3: Internal forces plus deformation or force boundary condition at base of wall for various support conditions

6.6 Structural calculations

6.6.1 Fully fixed wall without anchors

Contrary to the force or deformation boundary condition for the base of the wall described in section 6.5, when calculating the embedment length of the fully fixed wall without anchors, it is sufficient to consider the static equilibrium. As all active and passive forces result from earth pressure, the embedment length required is exactly that for which moment equilibrium about the base of the wall is achieved. The equilibrium of the horizontal forces which is still necessary is achieved through equivalent force C , which likewise acts at the base of the wall.

In order to achieve equilibrium, the sum of all moments about the base of the wall F due to the actions multiplied by the partial safety factors must be equal to 0:

$$\sum M^F = 0 \quad (6.8)$$

The desired embedment length t_E follows from eq. 6.8.

Equivalent force C is subsequently calculated from

$$\sum H = 0 \quad (6.9)$$

When calculating the system with a **frame program**, it is necessary to assume fixity at the initially unknown base. The embedment depth required is the length for which the fixity moment at the base of the wall is 0.

In structural terms, both approaches for $t = t_E$ are equivalent.

Analytical calculation of embedment depth

By entering the embedment depth t as a variable, the sum of the moments about the base of the wall becomes a function of the embedment depth t . Equilibrium is achieved for

$$\sum M^F(t) = 0 \quad (6.10)$$

From the moment equilibrium for the case illustrated in Fig. 6.4, it follows that

$$\begin{aligned} \sum M^F(t) = & \gamma_G \cdot \sum E_{agh,k,i} \cdot (t + h_{0,i}^*) + \gamma_Q \cdot \sum E_{aqh,k,i} \cdot (t + h_{0,i}^*) \\ & - \frac{1}{\gamma_{Ep}} \sum E_{pgh,k,i} \cdot t_{0,i}^* = 0 \end{aligned} \quad (6.11)$$

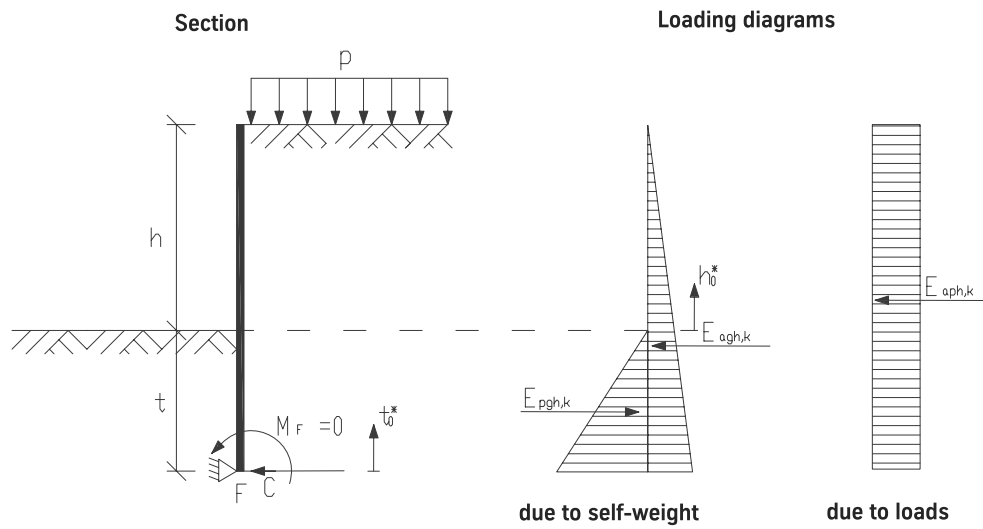
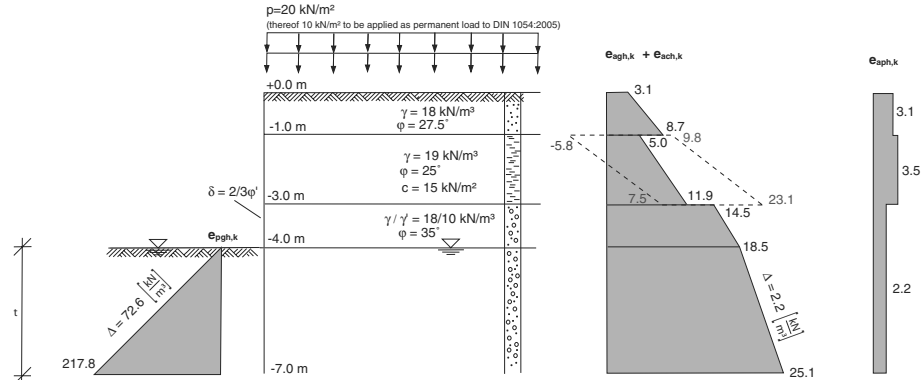


Figure 6.4: Loads and support conditions for a fully fixed sheet pile wall without anchors

The solution of this equation supplies the unknown embedment depth t for a fully fixed wall without anchors, as explained in example 6.1.

Example 6.1 Analytical calculation of embedment depth for a fully fixed wall without anchors

Sketch of system:



The actions due to earth and hydrostatic pressure as a result of permanent and variable loads were already determined in example 5.1.

It follows that

$$\begin{aligned} \sum M^F(t) &= 1.35 \cdot \left[\frac{1}{2} \cdot 3.1 \cdot 1 \cdot \left(t + 3\frac{2}{3}\right) + \frac{1}{2} \cdot 8.7 \cdot 1 \cdot \left(t + 3\frac{1}{3}\right) + \frac{1}{2} \cdot 5.0 \cdot 2 \cdot \left(t + 2\frac{1}{3}\right) \right. \\ &\quad \left. + \frac{1}{2} \cdot 11.9 \cdot 2 \cdot \left(t + 1\frac{2}{3}\right) + \frac{1}{2} \cdot 14.5 \cdot 1 \cdot \left(t + \frac{2}{3}\right) + \frac{1}{2} \cdot 18.5 \cdot 1 \cdot \left(t + \frac{1}{3}\right) \right. \\ &\quad \left. + 18.5 \cdot \frac{t^2}{2} + 2.2 \cdot \frac{t^3}{6} \right] \\ &\quad + 1.50 \cdot \left[3.1 \cdot 1 \cdot (t + 3.5) + 3.5 \cdot 2 \cdot (t + 2) + 2.2 \cdot 1 \cdot (t + 0.5) + 2.2 \cdot \frac{t^2}{2} \right] \\ &\quad - \frac{1}{1.4} \cdot 72.60 \cdot \frac{t^3}{6} = 0 \quad (\text{see eq. 6.10}) \\ &= t^3 - 1.735 t^2 - 8.776 t - 14.652 \end{aligned}$$

The embedment length required is obtained by solving the equations for t .

$$\Rightarrow t_1 = 4.45 \text{ m} \quad (t_2 = -1.36 + 1.21 i \quad t_3 = -1.36 - 1.21 i)$$

The driving allowance Δt required to resist the equivalent force C is calculated (simplified) according to BLUM (see eq. 6.4) as $\Delta t = \frac{4.45}{5} = 0.89 \text{ m}$ or according to LACKNER (see eq. 6.5) as $\Delta t = \frac{143.2 \cdot 1.4}{323.0} = 0.62 \text{ m} > 0.45 \text{ m} = \frac{4.45}{10} = \Delta t_{MIN}$.

The total length of the section is therefore $l = h + t + \Delta t = 4.0 + 4.45 + 0.62 = 9.07 \text{ m}$.

Calculating the embedment depth with the help of nomograms after BLUM

Eq. 6.11 can be considerably simplified if the separation of actions and resistances called for by DIN 1054:2005-01 is abandoned and the design values for the different actions are superimposed to form a resultant load.

If it is also assumed that there is no further stratification of the subsoil below the **point of zero load** u of the superimposed design values for actions and resistances, then the situation is as shown in Fig. 6.5.

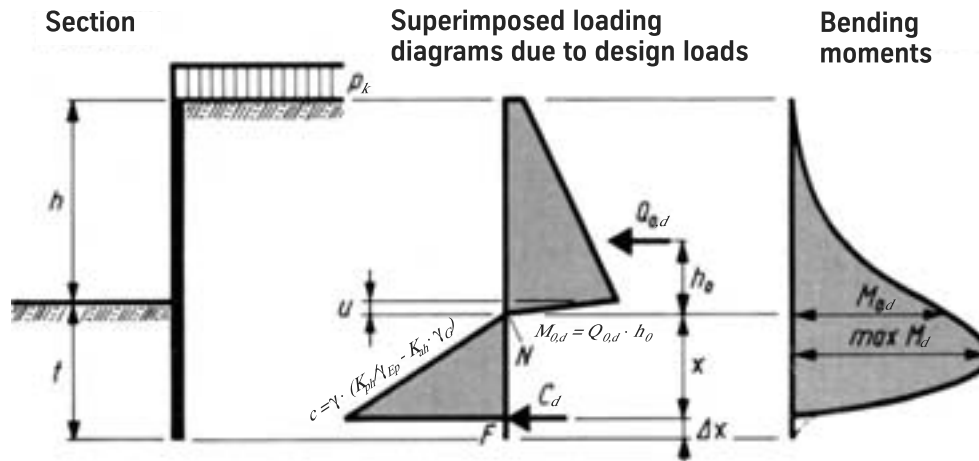


Figure 6.5: Simplified system for the analytical calculation of a sheet pile wall without anchors

Apart from the partial safety factors, this system corresponds to that on which BLUM based his calculations. From the sum of the moments about the base F

$$Q_{0,d} (h_0 + x) - \frac{c}{6} \cdot Q_{0,d} \cdot x^3 = 0 \quad (6.12)$$

where

$$c = \gamma \cdot \left(\frac{1}{\gamma_{Ep}} \cdot K_{ph} - \gamma_G \cdot K_{ah} \right) \quad (6.13)$$

Rewriting eq. 6.12 results in

$$x^3 = \frac{6}{c} \cdot Q_{0,d} \cdot x + \frac{6}{c} \cdot M_{0,d} \quad (6.14)$$

By substituting

$$\frac{6}{c} \cdot Q_{0,d} = m \quad \text{and} \quad \frac{6}{c} \cdot M_{0,d} = n \quad (6.15)$$

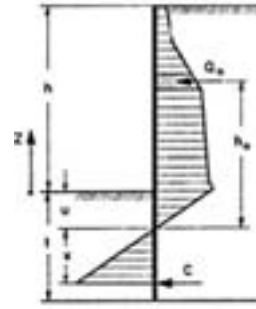
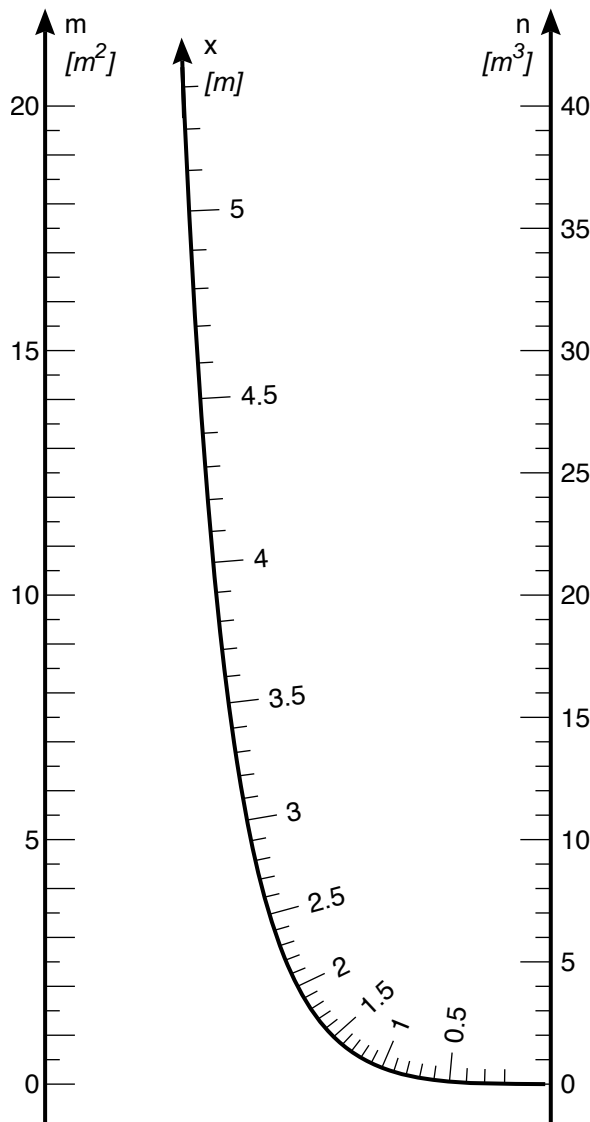
eq. 6.14 can be rewritten as

$$x^3 = mx + n \quad (6.16)$$

The point of zero load u is calculated from

$$u = \frac{e_{ah,d}(z=0)}{c} \quad (6.17)$$

This equation can be solved with the help of the nomogram in table 6.6 (BLUM, 1950).



$$c = \gamma' \cdot \left(\frac{1}{\gamma E_p} \cdot K_{ph} - \gamma_G \cdot K_{ah} \right)$$

$$u = \frac{e_{ah,d}(z=0)}{c}$$

$$m = \frac{6}{c} \cdot \sum_{-u}^h Q_0$$

$$n = \frac{6}{c} \cdot \sum_{-u}^h Q_0 h_0 = \frac{6}{\gamma' \cdot K_r} \cdot \sum_{-u}^h M_0$$

Condition: $x^3 - mx - n = 0$

$$t = u + x$$

$$\max M = M_0 + 0.385 \cdot Q_0 \cdot \sqrt{m}$$

Table 6.6: Nomogram for determining the embedment depth of a fixed wall without anchors (BLUM, 1950)

The point of zero shear is positioned at

$$x_a = \sqrt{\frac{2 \cdot Q_{0,d}}{c}} \tag{6.18}$$

The maximum bending moment is

$$M_{max,d} = Q_{0,d} (h_0 + x_Q) - \frac{c}{6} \cdot x_Q^3 \quad \text{or} \tag{6.19}$$

$$M_{max,d} = M_{0,d} + 0.385 \cdot Q_{0,d} \sqrt{m} \tag{6.20}$$

A condition for the calculation after BLUM is a linear increase in the resultant load below the point of zero load u .

If this condition is not satisfied, the method can still be used by using the weighted mean values $\bar{\gamma}$, \bar{K}_{ph} and \bar{K}_{ah} for the parameters γ , K_{ph} and K_{ah} for an initial estimate of the embedment depth (see Fig. 6.6).

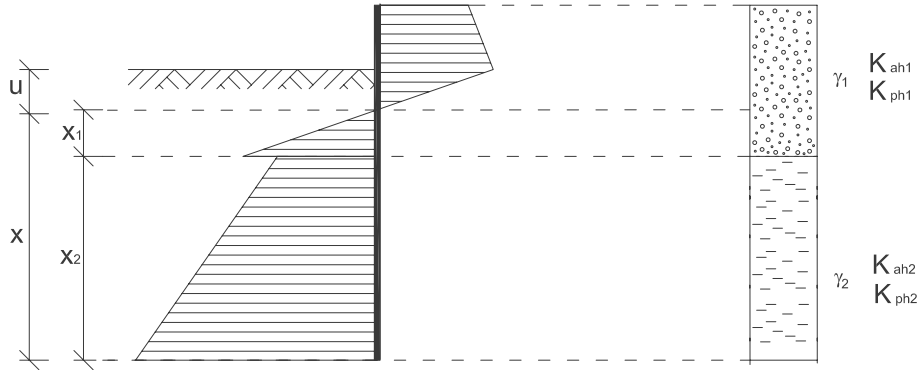


Figure 6.6: Stratification of subsoil below point of zero load u

The following applies:

$$\bar{\gamma} = \frac{\gamma_1 \cdot x_1 + \gamma_2 \cdot x_2}{x_1 + x_2}$$

$$\bar{K}_{ah} = \frac{K_{ah,1} \cdot x_1 + K_{ah,2} \cdot x_2}{x_1 + x_2}$$

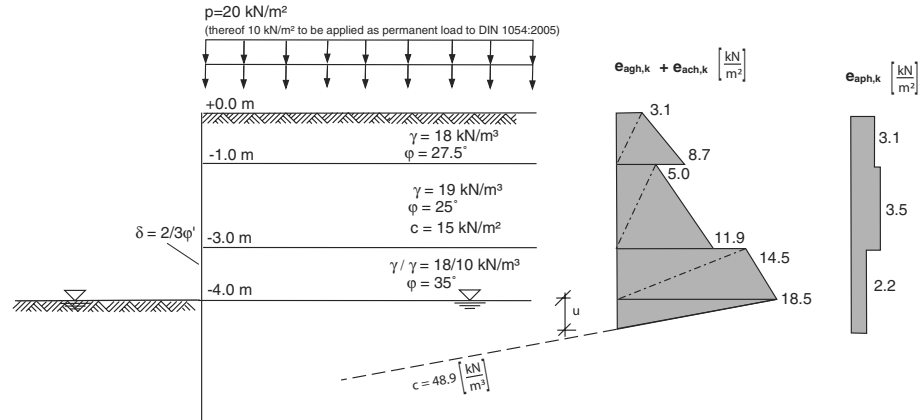
$$\bar{K}_{ph} = \frac{K_{ph,1} \cdot x_1 + K_{ph,2} \cdot x_2}{x_1 + x_2}$$

The assumed embedment depth should be compared with the result of the calculation after BLUM and corrected iteratively if necessary.

The calculation of a fully fixed wall without anchors with the help of the nomograms after BLUM is explained in example 6.2.

Example 6.2 Calculation of embedment depth for a fully fixed wall without anchors with the help of the nomograms after BLUM

Sketch of system:



The actions due to earth and hydrostatic pressure as a result of permanent and variable loads were already determined in example 5.1.

From the ordinates of the resultant loading area it follows that (see eq. 6.13, 6.17)

$$c = 10 \cdot \left(\frac{7.26}{1.4} - 0.22 \cdot 1.35 \right) = 48.9 \frac{\text{kN}}{\text{m}^3} \quad u = \frac{18.5 \cdot 1.35 + 2.2 \cdot 1.5}{48.9} = 0.58 \text{ m}$$

According to table 6.6 it follows that

$$Q_0 = 1.35 \cdot \left(\frac{1}{2} \cdot 1.0 \cdot (3.1 + 8.7) + \frac{1}{2} \cdot 2.0 \cdot (5.0 + 11.9) + \frac{1}{2} \cdot 1.0 \cdot (14.5 + 18.5) + \frac{1}{2} \cdot 0.58 \cdot 18.5 \right) + 1.5 \cdot (3.1 + 2 \cdot 3.5 + 2.2 \cdot (1 + 0.58)) = 80.6 \frac{\text{kN}}{\text{m}}$$

$$M_0 = 1.35 \cdot \left(\frac{3.1}{2} \cdot (0.58 + \frac{11}{3}) + \frac{8.7}{2} \cdot (0.58 + \frac{10}{3}) + 5 \cdot (0.58 + \frac{7}{3}) + 11.9 \cdot (0.58 + \frac{5}{3}) + \frac{14.5}{2} \cdot (0.58 + \frac{2}{3}) + \frac{18.5}{2} \cdot (0.58 + \frac{1}{3}) + \frac{18.5}{3} \cdot 0.58^2 \right) + 1.5 \cdot (3.1 \cdot (0.58 + 3.5) + 3.5 \cdot 2 \cdot (0.58 + 2) + 2.2 \cdot \frac{(0.58+1)^2}{2}) = 164.1 \text{ kN}$$

$$m = \frac{6}{c} \cdot Q_0 = \frac{6}{48.9} \cdot 80.6 = 9.90 \text{ m}^2$$

$$n = \frac{6}{c} \cdot M_0 = \frac{6}{48.9} \cdot 164.1 = 20.14 \text{ m}^3$$

The nomogram in Fig. 6.6 yields $x = 3.88 \text{ m}$ and hence an embedment depth $t = x + u = 3.88 + 0.58 = 4.46 \text{ m}$. The driving allowance Δt required to resist the equivalent force C is calculated (simplified) according to BLUM (see eq. 6.4) as $\Delta t = \frac{4.46}{5} = 0.89 \text{ m}$ and according to LACKNER (see eq. 6.5) as $\Delta t = \frac{143.2 \cdot 1.4}{323.0} = 0.62 \text{ m} > 0.46 \text{ m} = \frac{4.46}{10} = \Delta t_{MIN}$.

The total length of the section is therefore $l = h + t + \Delta t = 4.0 + 4.46 + 0.62 = 9.08 \text{ m}$.

Calculating the embedment depth by way of iteration

The embedment depth required for a wall can also be determined iteratively. In this case the moment equilibrium about the base of the wall, assuming the design values of the actions and resistances, is calculated for a given embedment depth according to eq. 6.8. If the moment in the mathematically positive direction of rotation is greater than 0, the embedment depth must be increased; if the sum is less than 0, the embedment depth must be reduced.

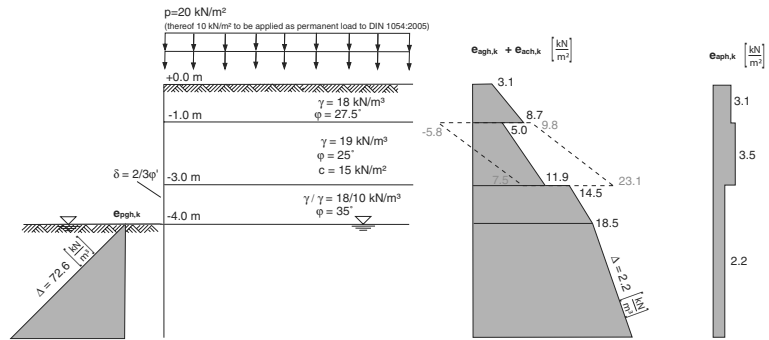
The calculation should be repeated until the desired embedment depth is obtained with sufficient accuracy.

Here, the embedment depth should always be estimated on the safe side with $M^F \leq 0$.

The iterative calculation of a fully fixed wall without anchors is explained in example 6.3.

Example 6.3 Iterative calculation of embedment depth for a fully fixed wall without anchors

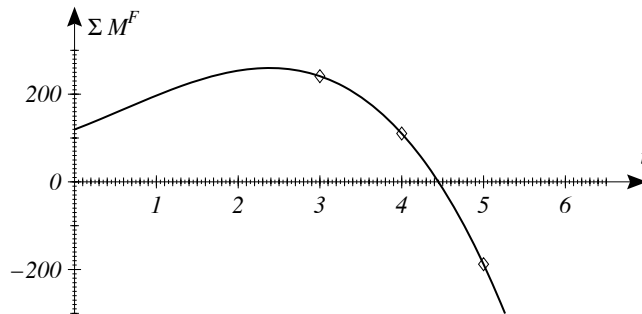
Sketch of system:



The actions due to earth and hydrostatic pressure as a result of permanent and variable loads were already determined in example 5.1.

The embedment depth can now be determined with the help of iteration. The sum of all the moments due to the actions and resistances about the base of the wall multiplied by the partial safety factors $\sum M^F$ (see eq. 6.10) is calculated for a chosen embedment depth and the embedment depth is varied until the sum is equal to 0.

Iteration step	t m	M^F kNm
1	3.00	-240.9
2	4.00	-109.7
3	5.00	189.1
⋮	⋮	⋮
n	4.45	≈ 0



Following a sufficient number of iteration steps, the embedment depth in this example finally amounts to 4.45 m.

The graphic solution also results in $t = 4.45$ m.

The driving allowance Δt required to resist the equivalent force C is calculated (simplified) according to BLUM (see eq. 6.4) as $\Delta t = \frac{4.45}{5} = 0.89$ m and according to LACKNER (see eq. 6.5) as $\Delta t = \frac{143.2 \cdot 1.4}{323.0} = 0.62$ m > 0.45 m = $\frac{4.45}{10} = \Delta t_{MIN}$.

The total length of the section is therefore $l = h + t + \Delta t = 4.0 + 4.45 + 0.62 = 9.07$ m.

6.6.2 Simply supported wall with one row of anchors

The force boundary conditions at the base of the wall shown in Fig. 6.3 are used for the calculation of a simply supported wall with one row of anchors.

The reaction Q^F at the base of the wall must be equal to 0:

$$Q^F = 0 \tag{6.21}$$

Analytical calculation of embedment depth

By entering the embedment depth t as a variable, the reaction at the base of the wall becomes a function of the embedment depth t . The embedment depth required is the one for which

$$Q^F(t) = 0 \quad (6.22)$$

Applying eq. 6.22, the following is true for the moment equilibrium about the point of application of the anchor A

$$\sum M^A(t) = 0 \quad (6.23)$$

For the case as shown in Fig. 6.7, eq. 6.23 is rewritten as

$$\begin{aligned} \sum M^A(t) &= \gamma_G \cdot \sum E_{agh,k,i} \cdot l_i + \gamma_Q \cdot \sum E_{aqh,k,i} \cdot l_i - \frac{1}{\gamma_{Ep}} \sum E_{ph,k} \cdot l \\ &= 0 \end{aligned} \quad (6.24)$$

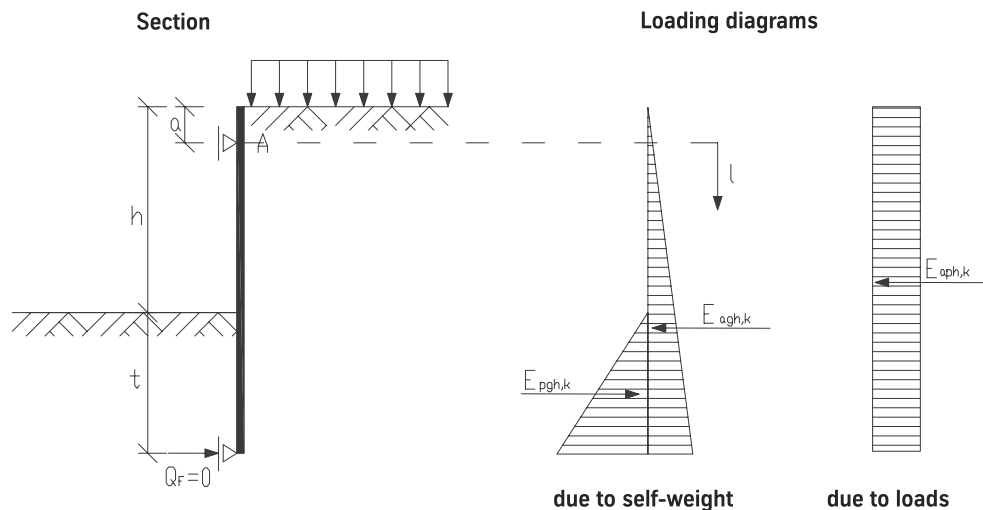


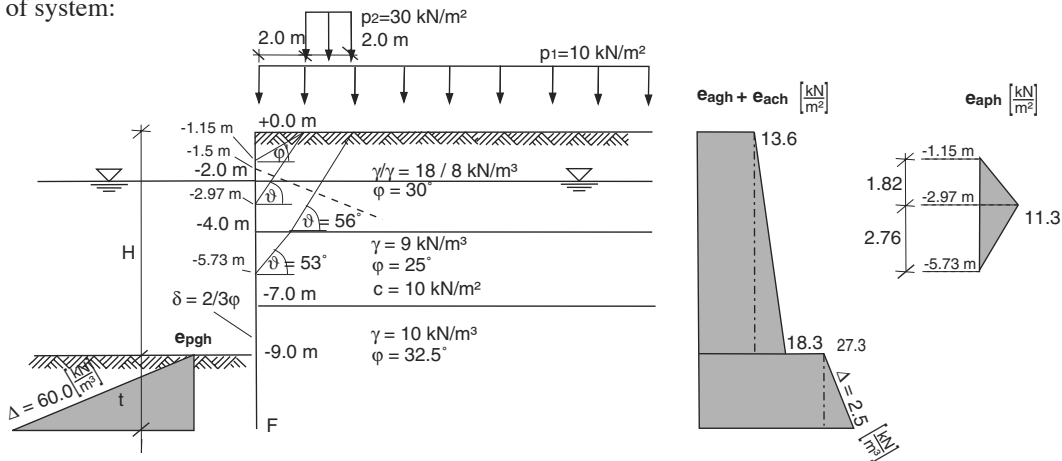
Figure 6.7: Loads and support conditions for a simply supported sheet pile wall with one row of anchors

Solving this equation supplies the unknown embedment depth t for a simply supported wall with one row of anchors.

The following example illustrates the method of calculation:

Example 6.4 Analytical calculation of embedment depth for a simply supported wall with one row of anchors

Sketch of system:



The effects of earth and hydrostatic pressure due to permanent and variable loads were already calculated in example 5.2.

Depending on the embedment length of the wall, the sum of all moments about the point of application of the anchor is

$$\begin{aligned}
 \sum M^A(t) &= 1.35 \cdot \left[13.6 \cdot 9 \cdot \left(\frac{9}{2} - 1.5 \right) + \frac{1}{2} \cdot 4.7 \cdot 9 \cdot \left(\frac{2 \cdot 9}{3} - 1.5 \right) \right. \\
 &\quad \left. + 27.3 \cdot t \cdot \left(9 - 1.5 + \frac{t}{2} \right) + \frac{1}{2} \cdot 2.5 \cdot t^2 \cdot \left(9 - 2.5 + \frac{2t}{3} \right) \right] \\
 &+ 1.5 \cdot \left[\frac{1}{2} \cdot 11.3 \cdot 1.82 \cdot \left(1.15 + \frac{2}{3} \cdot 1.82 - 1.5 \right) \right. \\
 &\quad \left. + \frac{1}{2} \cdot 11.3 \cdot 2.76 \cdot \left(2.97 + \frac{1}{3} \cdot 2.76 - 1.5 \right) \right] \\
 &- \frac{1}{1.4} \cdot \left[\frac{1}{2} \cdot 60.0 \cdot t^2 \cdot \left(9 - 1.5 + \frac{2}{3}t \right) \right] = 0 \quad (\text{see eq. 6.23}) \\
 &= -13.16 t^3 - 129.63 t^2 + 276.41 t + 693.43
 \end{aligned}$$

The embedment length required is obtained by solving the equation for t .

$$\Rightarrow t_1 = 3.00 \text{ m} \quad (t_2 = -11.30 \quad t_3 = -1.55)$$

It is not necessary to add an allowance to the calculated theoretical embedment length.

The total length of the section is therefore $l = h + t = 9.0 + 3.0 = 12.0 \text{ m}$.

Calculating the embedment depth with the help of nomograms after BLUM

Eq. 6.24 can be considerably simplified if the separation of actions and resistances called for by DIN 1054:2005-01 is abandoned and the design values for the different actions are superimposed to form a resultant load.

If it is also assumed that there is no further stratification of the subsoil below the point of zero load u (see eq. 6.17) for the superimposed design values for actions and resistances, then the situation is as shown in Fig. 6.8.

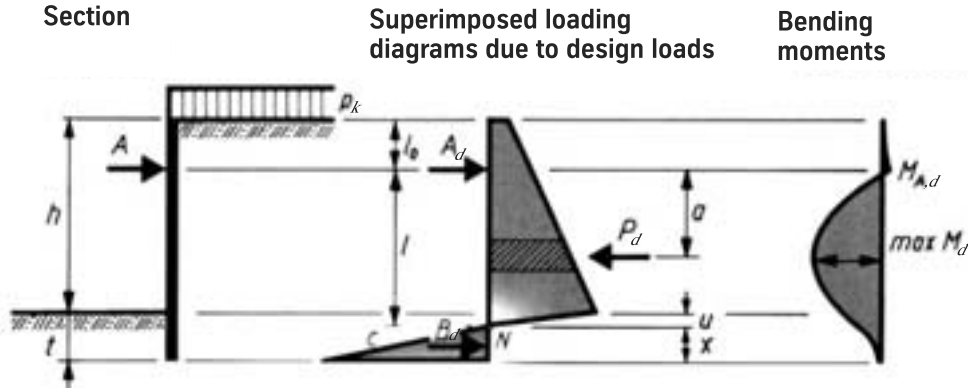


Figure 6.8: Equivalent system after BLUM for the analytical calculation of a simply supported sheet pile wall with one row of anchors

The anchor force is calculated from the sum of all horizontal forces according to

$$A = \sum_{-l_0}^{+l} P - \frac{c}{2} \cdot x^2 \tag{6.25}$$

The sum of the moments about the centre of gravity of the superimposed passive earth pressure triangle is

$$A \left(l + \frac{2}{3} \cdot x \right) = \sum_{-l_0}^{+l} P \left(l - a + \frac{2}{3} \cdot x \right) \tag{6.26}$$

By inserting eq. 6.25 into eq. 6.26, it follows that

$$\frac{c}{2} \cdot x^2 = \frac{\sum_{-l_0}^{+l} P \cdot a}{l + \frac{2}{3} \cdot x} \tag{6.27}$$

If $x = \xi \cdot l$, this means that

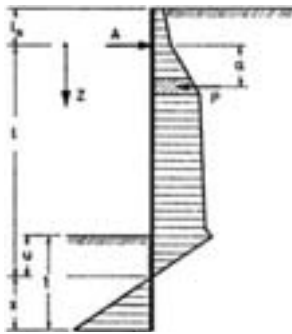
$$\xi^2 (2\xi + 3) = \frac{6}{c \cdot l^3} \sum_{-l_0}^{+l} P \cdot a = m \tag{6.28}$$

Eq. 6.28 is solved with the help of the nomogram shown in table 6.10.

The calculated theoretical embedment depth should be increased according to table 6.4, especially in the case of high loads due to excess hydrostatic pressure. The driving depth required is then given by

$$t = \alpha \cdot (u + x) \tag{6.29}$$

The calculation is explained in example 6.5.



$$K_r = \frac{1}{\gamma E_p} \cdot K_{ph} - \gamma_G \cdot K_{ah}$$

$$m = \frac{6}{\gamma' \cdot K_r \cdot l^3} \cdot \sum_{-l_0}^{+l} P \cdot a$$

Condition: $2\xi^3 + 3\xi^2 - m = 0$

$$t = u + x$$

$$A = \sum_{-l_0}^{+l} P - \frac{K_r \cdot x^2}{2} \cdot \gamma$$

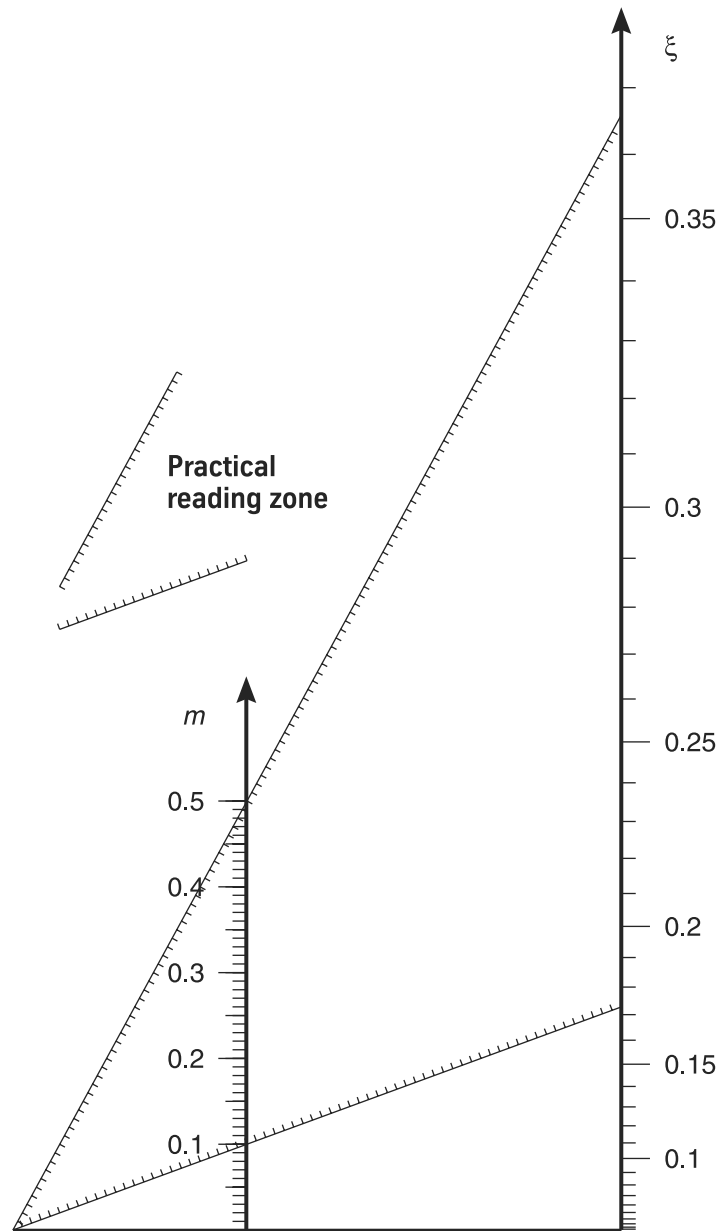
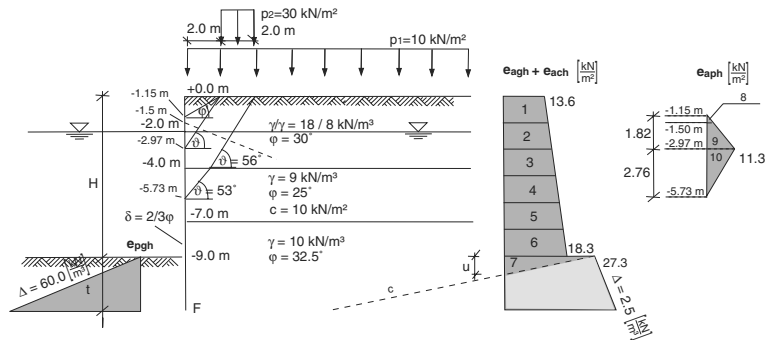


Table 6.10: Nomogram for determining the embedment depth of a simply supported wall with one row of anchors (BLUM, 1950)

Example 6.5 Calculation of embedment depth for a simply supported wall with one row of anchors with the help of the nomograms after BLUM

Sketch of system:



The effects of earth and hydrostatic pressure due to permanent and variable loads were already calculated in example 5.2.

The increase c in the resultant load below the point of zero load plus the position u of the point of zero load, taking into account the partial safety factors, are (see eq. 6.13, 6.17)

$$c = 10 \cdot \left(\frac{6.00}{1.4} - 0.25 \cdot 1.35 \right) = 39.5 \frac{\text{kN}}{\text{m}^3} \quad u = \frac{27.3 \cdot 1.35}{39.5} = 0.933 \text{ m}$$

The values for columns 2 and 5 in the following table are determined from the loaded area shown in the sketch of the system and the resulting loads $P_{n,k}$ are multiplied by the appropriate partial safety factors.

n	$P_{n,k}$ kN/m	γ_G/γ_Q	$P_{n,d}$ kN/m	Δa_n m	a_n m	$P_{n,d} \cdot a_n$ kN	$Q_{n,d}$ kN/m	$Q_{n,d} \cdot \Delta a_n$ kNm/m	$M_{n,d}$ kNm/m	Remarks
1	2	3	4	5	6	7	8	9	10	11
1	20.99	1.35	28.33	0.76	-0.74	-21.05	0.00	0.00	0.00	M_A
8	0.38	1.50	0.57	0.63	-0.12	-0.07	-28.33	-17.75	-17.75	
A	—	—	165.44	0.12	—	—	-28.90	-3.37	-21.12	
2	22.16	1.35	29.92	0.76	0.76	22.64	136.54	103.31	82.19	
2	22.16	1.35	29.92	0.14	0.90	13.38	106.62	15.39	97.58	$M_{S,d}$
9	9.90	1.50	14.85	1.36	2.26	71.09	91.76	124.37	221.95	
3	23.34	1.35	31.51	0.13	2.39	55.90	60.26	8.06	230.01	
10	15.59	1.50	23.39	1.37	3.76	124.29	36.87	50.36	280.37	
4	24.51	1.35	33.09	1.50	5.26	182.26	3.78	5.66	286.03	
5	25.69	1.35	34.68	1.50	6.76	244.98	-30.90	-46.35	239.69	
6	26.86	1.35	36.26	1.06	7.81	134.36	-67.17	-70.91	168.78	
7	12.74	1.35	17.20	0.62	—	—	-84.37	-52.50	116.28	
Σ			249.81			827.79				

The auxiliary value m after BLUM can be determined with the help of the sum of the values in column 7.

$$m = \frac{6}{39.5 \cdot 8.43^3} \cdot 827.8 = 0.21$$

The value $\xi = 0.25$ is obtained with m from the nomogram in table 6.10 or by solving eq. 6.28. This results in $x = \xi \cdot l = 0.25 \cdot 8.43 = 2.07 \text{ m}$ and $t = x + u = 2.07 + 0.93 = 3.00 \text{ m}$. It is not necessary to add an allowance to the calculated theoretical embedment length.

The anchor force A_d is obtained from eq. 6.25 as

$$A_d = \sum_{-l_0}^{+l} P - \frac{c}{2} \cdot x^2 = 249.81 - \frac{39.5}{2} \cdot 2.07^2 = 165.44 \frac{\text{kN}}{\text{m}}$$

Calculating the embedment depth by way of iteration

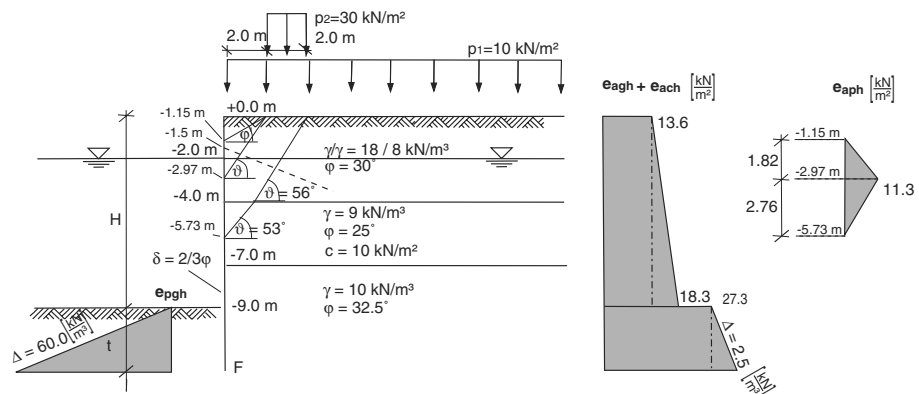
The horizontal reaction at the base of the wall Q^F is determined for a given embedment depth assuming the design values for actions and resistances. If this force is greater than 0 in the direction of the positive axis, the embedment depth must be reduced; if the sum is less than 0, it should be increased.

The calculation should be repeated until the desired embedment depth is obtained with sufficient accuracy.

Here, the embedment depth should always be estimated on the safe side with $Q^F \geq 0$.

Example 6.6 Iterative calculation of the embedment depth for a simply supported wall with one row of anchors

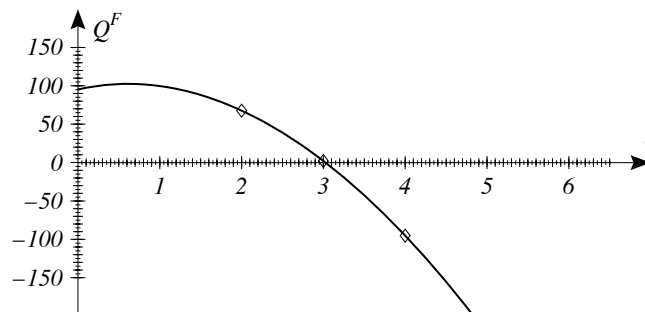
Sketch of system:



The effects of earth and hydrostatic pressure due to permanent and variable loads were already calculated in example 5.2 and are presumed to be known at this point.

The embedment depth can now be determined with the help of iteration. The horizontal reaction at the base of the wall due to the actions and resistances multiplied by the partial safety factors (see eq. 6.22) is calculated for a chosen embedment depth and the embedment depth is varied until the sum is equal to 0.

Iteration step	t m	Q^F kN
1	2.00	-65.5
2	3.00	-0.6
3	3.01	0.8
⋮	⋮	⋮
n	3.00	≈ 0



Following a sufficient number of iteration steps, the embedment depth in this example finally amounts to 3.00 m.

The graphic solution also results in $t = 3.00$ m.

It is not necessary to add an allowance to the calculated theoretical embedment length.

The total length of the section is therefore $l = 9.0 + 3.0 = 12.0$ m.

6.6.3 Fully fixed wall with one row of anchors

Analytical calculation of embedment depth

By entering the embedment depth t as a variable, the rotation of the wall at the base becomes a function of the embedment depth t . The embedment depth required is the one for which

$$w'^F(t) = 0 \quad (6.30)$$

Fig. 6.9 shows possible loading arrangements on the wall for determining the respective resultant rotation at the base for the general case.

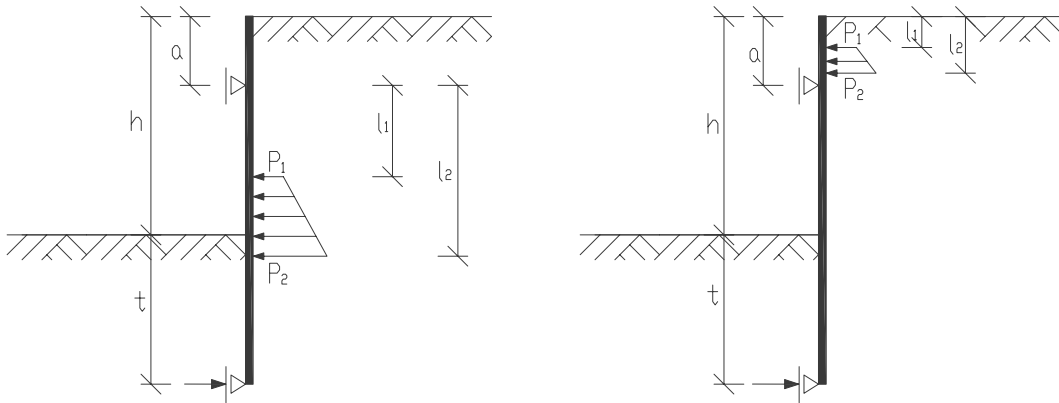


Figure 6.9: Load applied below (left) and above (right) the anchorage

If the trapezoidal load acts in the zone between the point of application of the anchor and the support at the base as shown in Fig. 6.9/left, the theoretical rotation of the theoretical base of the wall is

$$\begin{aligned} EI\delta_{10} = & \frac{l_1 - l_2}{360 \cdot (a - t - h)} \cdot [20p_1 \cdot [l_1 \cdot (t^2 + h^2 + a^2) + l_2 \cdot (h \cdot t - a \cdot t - a \cdot h)] \\ & + 10p_1 \cdot [4l_1 \cdot (t \cdot h - t \cdot a - h \cdot a) + l_2 \cdot (h^2 + a^2 + t^2)] \\ & - 3p_1 \cdot (4 \cdot l_1^3 - 3 \cdot l_1^2 \cdot l_2 + 2 \cdot l_2^2 \cdot l_1 + l_2^3) \\ & + 20p_2 \cdot [l_1 \cdot (t \cdot h - t \cdot a - h \cdot a) + l_2 \cdot (t^2 + h^2 + a^2)] \\ & + 10p_2 \cdot [l_1 \cdot (h^2 + t^2 + a^2) + 4l_2 \cdot (t \cdot h - t \cdot a - h \cdot a)] \\ & - 3p_2 \cdot (4 \cdot l_2^3 + 3 \cdot l_2^2 \cdot l_1 + 2 \cdot l_1^2 \cdot l_2 + l_1^3)] \end{aligned} \quad (6.31)$$

If the trapezoidal load acts above the point of application of the anchor as shown in Fig. 6.9/right, the theoretical rotation of the base of the wall is according to eq. 6.32:

$$EI\delta_{10} = \frac{(l_2 - l_1) \cdot (a - h - t)}{36} \cdot [p_1 (3a - 2l_1 - l_2) + p_2 (3a - l_1 - 2l_2)] \quad (6.32)$$

The embedment depth t required for a fully fixed wall with one row of anchors is obtained by solving for the condition

$$EIw'^F(t) = \sum EI\delta_{10,i} = 0 \quad (6.33)$$

This procedure is illustrated in example 6.7.

Example 6.7 Analytical calculation of embedment depth for a fully fixed wall with one row of anchors

Sketch of system:

The diagram shows a retaining wall of height H with an embedment length t . The soil is divided into three layers:

- Top layer (0.0 m to -1.5 m): $\gamma/\gamma' = 18/8 \text{ kN/m}^3$, $\phi = 30^\circ$
- Middle layer (-1.5 m to -7.0 m): $\gamma = 9 \text{ kN/m}^3$, $\phi = 25^\circ$, $c = 10 \text{ kN/m}^2$
- Bottom layer (-7.0 m to -9.0 m): $\gamma = 10 \text{ kN/m}^3$, $\phi = 32.5^\circ$

Surcharge $p_2 = 30 \text{ kN/m}^2$ is applied over a 2.0 m width, and $p_1 = 10 \text{ kN/m}^2$ is applied over the remaining width. The wall is fixed at the base, and the embedment length is t . The pressure distributions are shown as $e_{agh} + e_{adh}$ and e_{aph} .

The effects of earth and hydrostatic pressure due to permanent and variable loads were already calculated in example 5.2.

The sum of the rotations at the base according to eq. 6.31 and 6.32 supplies the equation required for determining the embedment length t of the wall:

$$w'^F = -1.75 t^5 - 38.06 t^4 - 154.63 t^3 + 922.17 t^2 + 3467.14 t + 6629.73 = 0$$

The embedment length required is obtained by solving the equation for t .

$$\Rightarrow \quad t_1 = 4.93 \text{ m} \quad \left(\begin{array}{l} t_2 = -1.50 + 1.76i \\ t_3 = -1.50 + 1.76i \end{array} \right) \\ \left(\begin{array}{l} t_4 = -11.81 - 1.92i \\ t_5 = -11.81 + 1.92i \end{array} \right)$$

The driving allowance Δt required for resisting the equivalent force C is calculated (simplified) according to BLUM (see eq. 6.4) as $\Delta t = \frac{4.93}{5} = 0.99 \text{ m}$ and according to LACKNER (see eq. 6.5) as $\Delta t = \frac{108.0 \cdot 1.4}{296.3} = 0.51 \text{ m} > 0.49 \text{ m} = \frac{4.93}{10} = \Delta t_{MIN}$.

The total length is therefore $l = h + t + \Delta t = 9.0 + 4.93 + 0.51 = 14.44 \text{ m}$.

Calculating the embedment depth with the help of nomograms after BLUM

The active earth pressure is divided into individual loads. The limitations of this method already mentioned in section 6.6.1 still apply here.

See Fig. 6.10 for system and designations.

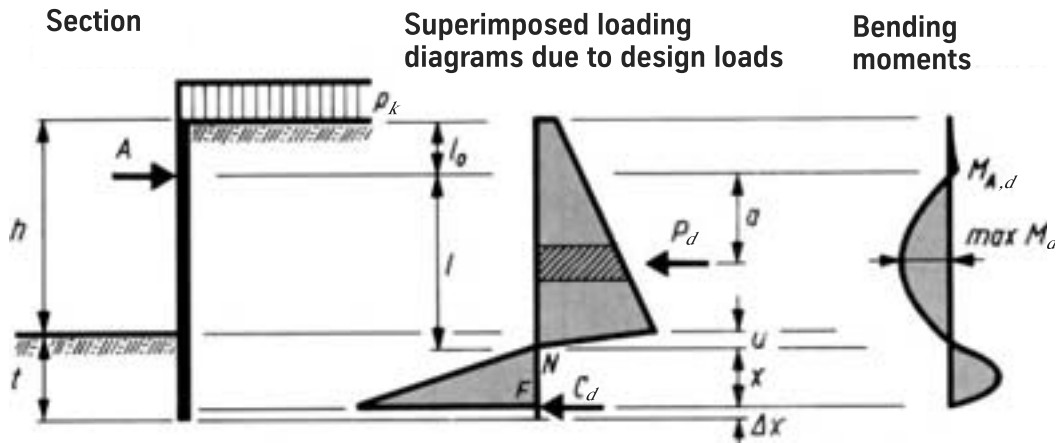


Figure 6.10: Equivalent system after BLUM for the analytical calculation of a fully fixed sheet pile wall with one row of anchors

The sheet pile wall is fixed in the subsoil at depth x below the point of zero load u (see eq. 6.17). From the equilibrium condition $\sum M = 0$ about the base F, it follows that the anchor force is

$$A = \frac{1}{l+x} \left\{ \sum_0^{-l_0} P'_n [(l+x) + a'_n] + \sum_0^{+l} p_n [(l+n) - a_n] - \frac{c}{6} \cdot x^3 \right\} \quad (6.34)$$

Corresponding to Figs. 6.11 and 6.12, the deflection at the point of anchorage is calculated from the partial loads such as anchor force, active earth pressure above and below anchor plus passive earth pressure.

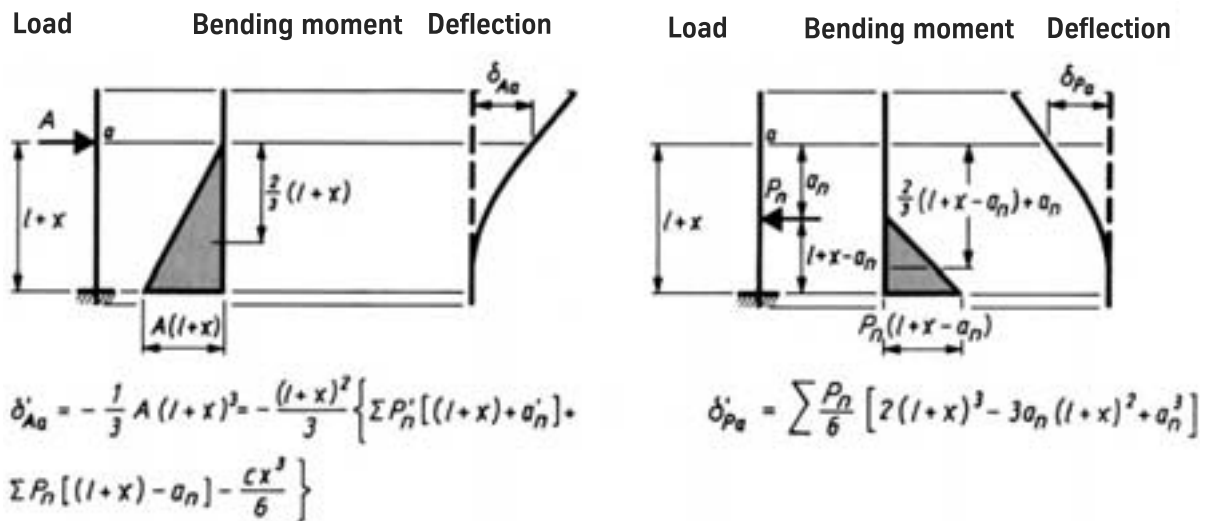


Figure 6.11: Deflection influences part 1, Sheet Piling Handbook (1977)

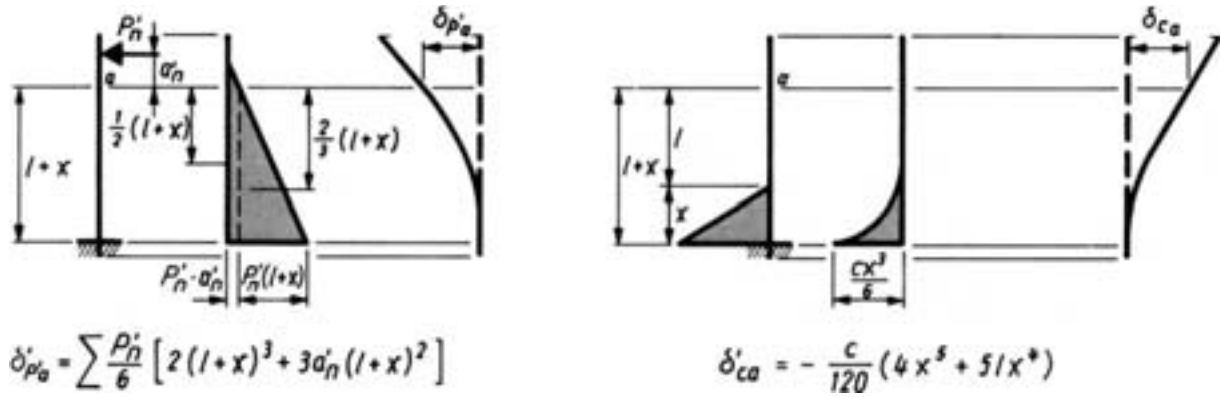


Figure 6.12: Deflection influences part 2, Sheet Piling Handbook (1977)

At the point of anchorage, the sum of all deflections must be equal to 0:

$$\sum \delta_a = 0 = (l+x)^2 \cdot \left(\sum P_n \cdot a_n - \sum P'_n \cdot a'_n \right) - \sum P_n \cdot a_n^3 - \frac{c}{60} \cdot (20l^2x^3 + 25lx^4 + 8x^5) \quad (6.35)$$

By substituting $x = \xi \cdot l$ we obtain

$$\xi^3 (0.8 \cdot \xi^2 + 2.5\xi + 2.0) = (1 + \xi)^2 \cdot m - n \quad (6.36)$$

where

$$m = \frac{6}{c \cdot l^3} \left(\sum P_n \cdot a_n - \sum P'_n \cdot a'_n \right) = \frac{6}{c \cdot l^3} \sum_{-l_0}^{+l} P \cdot a \quad (6.37)$$

$$n = \frac{6}{c \cdot l^5} \cdot \sum P_n \cdot a_n^3 = \frac{6}{c \cdot l^5} \sum_0^{+l} P \cdot a^3 \quad (6.38)$$

Eq. (6.36) is solved with the help of the nomogram shown in table 6.14 (BLUM, 1950).

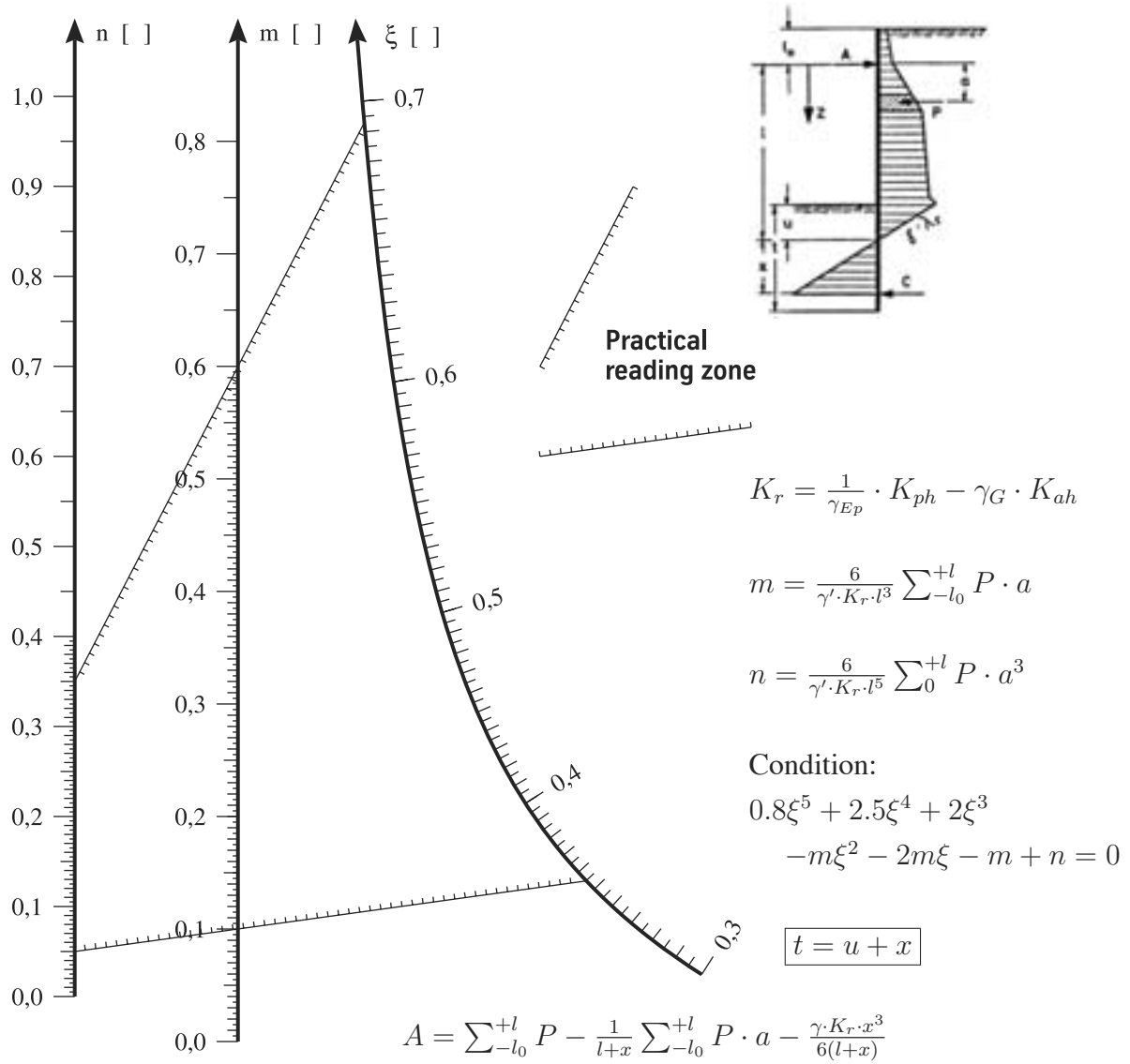


Table 6.14: Nomogram for determining the embedment depth of a fully fixed wall with one row of anchors (BLUM, 1950)

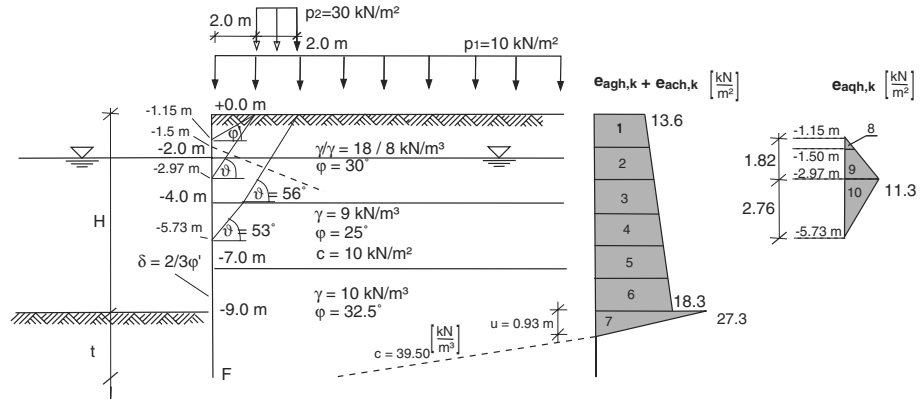
The anchor force is calculated by rewriting eq. 6.34 as follows:

$$A = \sum_{-l_0}^{+l} P - \frac{1}{l+x} \sum_{-l_0}^{+l} P \cdot a - \frac{cx^3}{6(l+x)} \tag{6.39}$$

The calculation is explained in example 6.8.

Example 6.8 Calculation of embedment depth for a fully fixed wall with one row of anchors with the help of the nomograms after BLUM

Sketch of system:



The effects of earth and hydrostatic pressure due to permanent and variable loads were already calculated in example 5.2.

The values for columns 2, 3 and 6 are determined from the loaded area shown in the sketch of the system and the resulting loads $P_{n,k}$ are multiplied by the appropriate partial safety factors. The auxiliary values m and n according to BLUM are calculated with the help of the sums of columns 7 and 8. If the design value of anchor force A_d is known, columns 9 to 11 can be completed.

n	$P_{n,k}$ kN/m	γ_G/γ_Q	$P_{n,d}$ kN/m	Δa_n m	a_n m	$P_{n,d} \cdot a_n$ kN	$P_{n,d} \cdot a_n^3$ kNm ²	$Q_{n,d}$ kN/m	$Q_{n,d} \cdot \Delta a_n$ kNm/m	$M_{n,d}$ kNm/m	Remarks
—	—	—	—	—	—	—	—	—	—	—	—
1	20.99	1.35	28.33	0.76	-0.74	-21.05	-11.62	0.00	0.00	0.00	M_A
8	0.38	1.50	0.57	0.63	-0.12	-0.07	0.00	-28.33	-17.75	-17.75	
A	—	—	149.28	0.12	—	—	—	-28.90	-3.37	-21.12	
2	22.16	1.35	29.92	0.76	0.76	22.64	12.96	120.38	91.08	69.96	$M_{S,d}$
9	9.90	1.50	14.85	0.14	0.90	13.38	10.86	90.46	13.06	83.02	
3	23.34	1.35	31.51	1.36	2.26	71.09	361.89	75.61	102.47	185.49	
10	15.59	1.50	23.39	0.13	2.39	55.90	319.33	44.10	5.90	191.39	
4	24.51	1.35	33.09	1.37	3.76	124.29	1753.46	20.71	28.29	219.68	
5	25.69	1.35	34.68	1.50	5.26	182.26	5034.45	-12.38	-18.57	201.11	
6	26.86	1.35	36.26	1.50	6.76	244.98	11180.12	-47.06	-70.58	130.53	
7	12.74	1.35	17.20	1.06	7.81	134.36	8197.99	-83.32	-87.96	42.56	
				0.62				-100.53	-62.56	-19.99	
Σ			249.81			827.79	26859.44				

According to BLUM, the auxiliary variables m and n are given by eq. 6.37 and 6.38:

$$m = \frac{6}{39.5 \cdot 8.43^3} \cdot 827.79 = 0.21 \quad n = \frac{6}{39.5 \cdot 8.43^5} \cdot 26871.06 = 0.10$$

The value $\xi = 0.47$ is obtained with m and n from the nomogram in table 6.14 or by solving eq. 6.36.

This results in $x = \xi \cdot l = 0.47 \cdot 8.43 = 4.01$ m and $t = x + u = 4.01 + 0.93 = 4.94$ m.

Anchor force A_d is obtained from equation 6.39 as

$$A_d = 249.81 - \frac{827.79}{12.4} - \frac{39.5 \cdot 4.00^2}{6 \cdot 12.4} = 149.28 \text{ kN/m}$$

The driving allowance Δt required to resist the equivalent force C is calculated (simplified) according to BLUM (see eq. 6.4) as $\Delta t = \frac{4.93}{5} = 0.99$ m and according to LACKNER (see eq. 6.5) as $\Delta t = \frac{108.0 \cdot 1.4}{296.3} = 0.51$ m > 0.49 m = $\frac{4.93}{10} = \Delta t_{MIN}$.

The total length is therefore $l = h + t + \Delta t = 9.0 + 4.94 + 0.51 = 14.45$ m.

Calculating the embedment depth by way of iteration

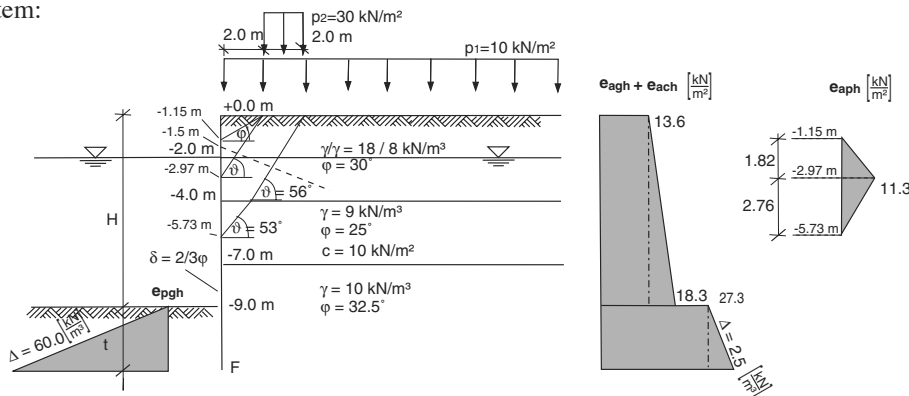
The rotation of the wall at the base $w' F$ is determined according to eq. 6.30 for a given embedment depth assuming the design values for actions and resistances. If the rotation in the mathematically positive direction is greater than 0, the embedment depth must be reduced; if the sum is less than 0, the embedment depth must be increased.

The calculation should be repeated until the desired embedment depth is reached with sufficient accuracy.

Here, the embedment depth should always be estimated on the safe side with $w' F \geq 0$. Please note that the rotation at the base is dependent on the bending stiffness of the section. A bending stiffness of 1 kNm^2 has been chosen for this example.

Example 6.9 Iterative calculation of the embedment depth for a fully fixed wall with one row of anchors

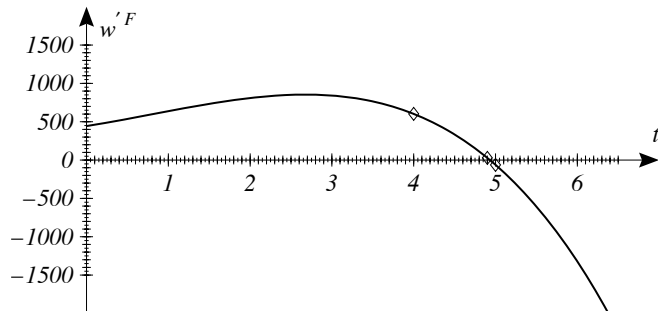
Sketch of system:



The effects of earth and hydrostatic pressure due to permanent and variable loads were already calculated in example 5.2 and are presumed to be known at this point.

The embedment depth can now be determined with the help of iteration. The rotation at the base of the wall due to the actions and resistances multiplied by the partial safety factors is calculated for a chosen embedment depth and the embedment depth is varied until the sum is equal to 0.

Iteration step	t m	$w' F$ mRad
1	4.00	600.8
2	5.00	-63.1
3	4.90	27.1
⋮	⋮	⋮
n	4.93	≈ 0



Following a sufficient number of iteration steps, the embedment depth in this example finally amounts to 4.93 m.

The graphic solution also results in $t = 4.93$ m.

The driving allowance Δt required to resist the equivalent force C is calculated (simplified) according to BLUM (see eq. 6.4) as $\Delta t = \frac{4.93}{5} = 0.99$ m and according to LACKNER (see eq. 6.5) as $\Delta t = \frac{108.0 \cdot 1.4}{296.3} = 0.51$ m $>$ 0.49 m $= \frac{4.93}{10} = \Delta t_{MIN}$.

The total length is therefore $l = h + t + \Delta t = 9.0 + 4.94 + 0.51 = 14.45$ m.

6.6.4 Partially fixed wall with one row of anchors

The embedment depth required for a partially fixed wall depends on the degree of fixity τ_{1-0} chosen. Conversely, the degree of fixity can be calculated for a given length of wall.

The embedment lengths of partially fixed walls should be determined by analytical or iterative means; a BLUM evaluation for different degrees of fixity is not available.

As the maximum **rotation at the base** ε_{max} is required for calculating the degree of fixity according to eq. 6.3, it is first necessary to perform a preliminary calculation for the embedment depth of the wall simply supported in the soil and then determine the rotation at the base for this embedment length. This then corresponds to ε_{max} .

Analytical calculation of embedment depth

By entering the embedment depth t as a variable, the rotation of the wall at the base becomes a function of the embedment depth t . The embedment depth required is the one for which

$$w'^F(t) = w'_{\tau_{1-0}} \quad (6.40)$$

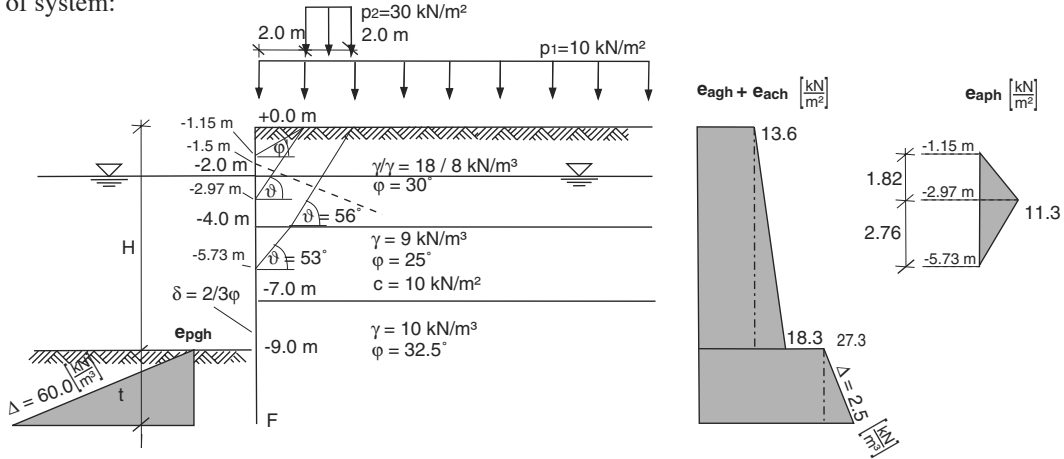
Eq. 6.31 and 6.32 still apply for the different **rotation components**. The embedment length t required for a partially fixed wall with one row of anchors is obtained by solving for the condition

$$w'^F(t) = \sum EI\delta_{10,i} = w'_{\tau_{1-0}} \quad (6.41)$$

This procedure is illustrated in example 6.10 for a wall with 50% fixity.

Example 6.10 Analytical calculation of embedment depth for a partially fixed wall with one row of anchors

Sketch of system:



The effects of earth and hydrostatic pressure due to permanent and variable loads were already calculated in example 5.2.

The rotation at the base of the simply supported wall is 840.34 mRad, the rotation at the base of the wall with 50% fixity to be determined according to eq. 6.3 is 420.17 mRad.

For the sum of all base rotations depending on the embedment length t of the wall, the evaluation of eq. 6.31 and 6.32 results in

$$w'_{50\%} = -1.75 t^5 - 38.06 t^4 - 154.63 t^3 + 922.17 t^2 + 2626.88 t + 327.78 = 0$$

The embedment length required is obtained by solving the equation for t .

$$\Rightarrow \quad t_1 = 4.36 \text{ m} \quad (\quad t_2 = -11.83 + 0.21i \quad t_3 = -11.83 + 0.21i \quad) \\ (\quad t_4 = -0.13 \quad t_5 = -2.26 \quad)$$

The driving allowance Δt required to resist the equivalent force C is calculated (simplified) according to BLUM (see eq. 6.4) as $\Delta t = \frac{4.36}{5} = 0.87 \text{ m}$ and according to LACKNER (see eq. 6.5) as $\Delta t = \frac{69.8 \cdot 1.4}{261.5} = 0.37 \text{ m} > 0.28 \text{ m} = \frac{4.36 \cdot 50\%}{10} = \Delta t_{MIN}$.

The total length is therefore $l = h + t + \Delta t = 9.0 + 4.36 + 0.37 = 13.73 \text{ m}$.

Calculating the embedment depth by way of iteration

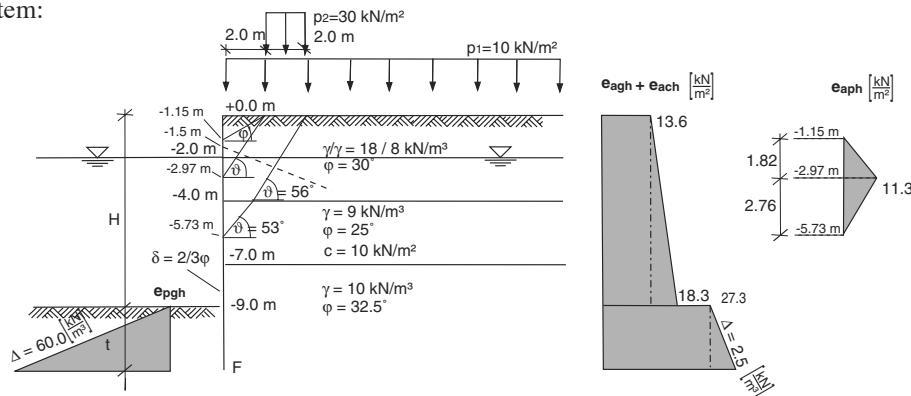
The rotation of the wall at the base $w' F$ is determined for a given embedment depth. If this rotation in the mathematically positive direction is greater than the desired rotation for the chosen degree of fixity, the embedment depth must be reduced; if the sum is less, the embedment depth must be increased.

The calculation should be repeated until the desired embedment depth is reached with sufficient accuracy.

Here, the embedment depth should always be estimated on the safe side with $w' F \geq 0$. Please note that the rotation at the base is dependent on the bending stiffness of the section. A bending stiffness of 1 kNm^2 has been chosen for this example.

Example 6.11 Iterative calculation of the embedment depth for a partially fixed wall with one row of anchors

Sketch of system:

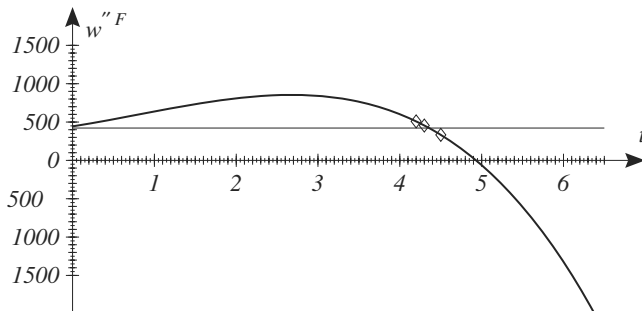


The effects of earth and hydrostatic pressure due to permanent and variable loads were already calculated in example 5.2.

The rotation at the base of the simply supported wall is 840.34 mRad, the rotation at the base of the wall with 50% fixity to be determined according to eq. 6.3 is 420.17 mRad.

The embedment depth can now be determined with the help of iteration. Here, too, the desired value is the base rotation chosen to suit the degree of fixity.

Iteration step	t m	$w' F$ mRad
1	4.20	507.2
2	4.50	332.2
3	4.30	453.6
⋮	⋮	⋮
n	4.36	≈ 420.1



Following a sufficient number of iteration steps, the embedment depth in this example finally amounts to 4.36 m.

The graphic solution also results in $t = 4.36 \text{ m}$.

The driving allowance Δt required to resist the equivalent force C is calculated (simplified) according to BLUM (see eq. 6.4) as $\Delta t = \frac{4.36}{5} = 0.87 \text{ m}$ and according to LACKNER (see eq. 6.5) as $\Delta t = \frac{69.8 \cdot 1.4}{261.5} = 0.37 \text{ m} > 0.28 \text{ m} = \frac{4.36 \cdot 50\%}{10} = \Delta t_{MIN}$.

The total length is therefore $l = h + t + \Delta t = 9.0 + 4.36 + 0.37 = 13.73 \text{ m}$.

6.6.5 Walls with different support conditions at the base and more than one row of anchors

Walls with more than one row of anchors can be calculated as described above by using identical boundary conditions. Establishing the embedment depth is carried out via the force or deformation boundary condition at the base of the wall according to section 6.5.

It should be pointed out that owing to the **static indeterminacy**, the analytical solution involves considerably more work when more than one row of anchors is employed. Nomograms for calculating both simply supported and fully fixed walls with two rows of anchors can be found in the literature (HOFFMANN, 1977) together with accompanying explanations.

It is worthwhile employing a computer for sheet piling structures with more than one row of anchors. Design programs specifically for foundations calculate the required embedment length automatically depending on the chosen support conditions for the section. Any frame program can be used to calculate the embedment length by means of iteration.

For the purposes of **preliminary design**, several rows of anchors can be approximated to one row.

6.7 Analyses for the ultimate limit state

In order to carry out analyses according to DIN 1054:2005-01, it is first necessary to determine the embedment depth of the wall as described above.

6.7.1 Failure of earth resistance

Requirements of DIN 1054:2005-01

According to DIN 1054:2005-01 section 10.6.3, for wall-type retaining structures whose stability is achieved partly or wholly from passive earth pressure forces, it is necessary to prove that the structure is embedded sufficiently deep in the soil in order to rule out **failure by principally horizontal displacement or rotation at the ultimate limit state**.

An adequate margin of safety is assured when the limit state condition

$$B_{h,d} \leq E_{ph,d} \quad (6.42)$$

where

- $B_{h,d}$ design value of horizontal component of resultant reaction
- $E_{ph,d}$ design value of horizontal component of passive earth pressure

is satisfied.

The designations from eq. 6.42 are shown once again in the following figure.

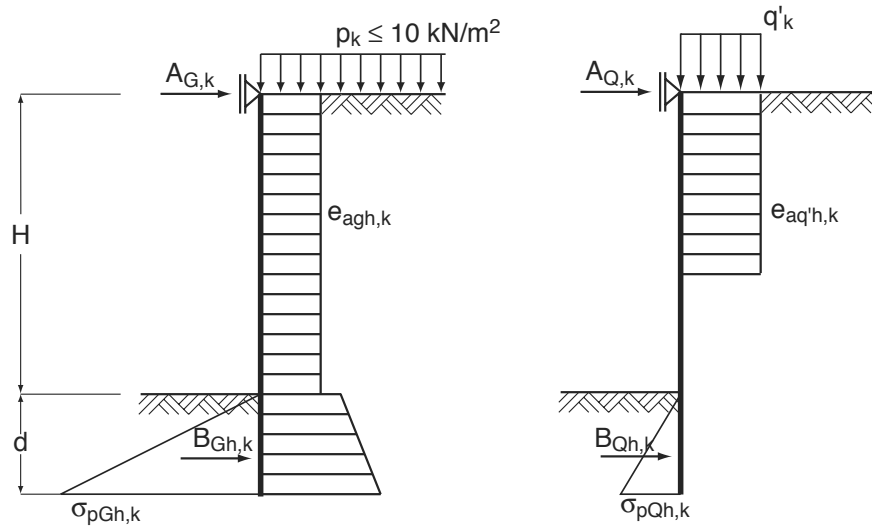


Figure 6.13: Lateral soil reaction for analysing the earth resistance (WEISSENBACH, 2003)

It is also necessary to verify that corresponding to the condition

$$V_k = \sum V_{k,j} \geq B_{v,k} \quad (6.43)$$

where

- V_k vertical component of relevant downward characteristic actions
- $B_{v,k}$ upward vertical force of characteristic reaction

the **negative wall friction angle** δ_p on which the calculation of the passive earth pressure is based agrees with the equilibrium condition $\sum V = 0$.

The verification in practice

Eq. 6.42 requires a breakdown of the **mobilised soil reaction** according to the respective actions as shown schematically in Fig. 6.13. This breakdown is carried out via the proportional **rotation at the base** of the wall due to the individual characteristic loads for the embedment depth corresponding to a simple support in the soil.

Applying the various characteristic actions results in the characteristic rotations at the base of the wall $w'_{G_i,k}$, $w'_{Q_i,k}$, $w'_{H_i,k}$, ... separately for each action. The total rotation at the base of the wall for the design situation corresponds to the sum of all proportional base rotations multiplied by the partial safety factors:

$$w'_{sum,d} = w'_{G_i,k} \cdot \gamma_G + w'_{Q_i,k} \cdot \gamma_Q + w'_{H_i,k} \cdot \gamma_H + \dots \quad (6.44)$$

Assuming that the **soil reaction**, which in this case causes a rotation of the base of the wall in the opposite direction to the actions, is distributed with the same proportions as the rotation, the

proportional mobilised passive earth pressure is

$$B_{h,k,i} = B_{h,k,sum} \cdot \frac{w'_{i,k}}{w'_{sum,d}} = B_{h,k,sum} \cdot \varepsilon_{i,k} \quad (6.45)$$

where

$$B_{h,k,sum} = E_{ph,d} \quad (6.46)$$

for all further loads correspondingly. The distribution of the respective **mobilised passive earth pressure** is related to the distribution of the soil reaction and is designated in the following with $\sigma_{i,h,k}$.

After calculating the individual components $B_{h,k,i}$, the value of $B_{h,d,sum}$ can be determined by adding together the individual components multiplied by the appropriate partial safety factors, and the verification carried out according to equation 6.42.

Example 6.12 Verification of earth resistance according to DIN 1054:2005-01 section 10.6.3

The analysis of failure of the earth resistance is carried out for the system shown in example 6.10 and 6.11. When determining the embedment depth in those examples, 50% partial fixity was called for.

First of all, the rotations of the base of the sheet pile wall are calculated separately according to actions. The rotations in the example resulting from the structural calculations are

$$\begin{aligned} w'_{G,k} &= 15.93 \text{ mRad} \\ w'_{Q,k} &= 1.30 \text{ mRad} \end{aligned}$$

The total rotation for the design is therefore

$$\begin{aligned} w'_{a,sum} &= w'_{G,k} \cdot \gamma_G + w'_{Q,k} \cdot \gamma_Q \\ &= 15.93 \cdot 1.35 + 1.30 \cdot 1.50 \\ &= 23.46 \text{ mRad} \quad (\text{see eq. 6.44}) \end{aligned}$$

The proportional loss of passive earth pressure is calculated via the ε ratios

$$\begin{aligned} \varepsilon_{G,k} &= \frac{w'_{G,k}}{w'_{a,sum}} = \frac{15.93}{23.46} = 67.92\% \\ \varepsilon_{Q,k} &= \frac{w'_{Q,k}}{w'_{a,sum}} = \frac{1.30}{23.46} = 5.54\% \end{aligned}$$

The proportions σ of the mobilised earth resistance can now be calculated according to these ratios and the resultants $B_{h,i,k}$ determined.

$$\begin{aligned} B_{h,G,k} &= E_{ph,d} \cdot \varepsilon_{G,k} = 407.09 \cdot 0.6792 = 276.49 \frac{\text{kN}}{\text{m}} \quad (\text{see eq. 6.45}) \\ B_{h,Q,k} &= E_{ph,d} \cdot \varepsilon_{Q,k} = 407.09 \cdot 0.0554 = 22.55 \frac{\text{kN}}{\text{m}} \quad (\text{see eq. 6.45}) \end{aligned}$$

These forces are entered directly into the verification of the earth resistance, where the following applies

$$\begin{aligned} B_{h,d} &\leq E_{ph,d} \\ B_{h,G,d} + B_{h,Q,d} &= 276.49 \cdot 1.35 + 22.55 \cdot 1.5 \leq E_{ph,d} \\ 407.09 &\leq 407.09 \quad (\text{see eq. 6.42}) \end{aligned}$$

Verifying the vertical component of the reaction

According to DIN 1054:2005-01 section 10.6.5 (5), it is necessary to verify that corresponding to the condition

$$V_k = \sum V_{k,j} \geq B_{v,k} \quad (6.47)$$

where

- V_k vertical component of relevant downward characteristic actions
- $B_{v,k}$ upward vertical component of characteristic reaction

the negative angle of inclination $\delta_{p,k}$ on which the calculation of the passive earth pressure is based agrees with the equilibrium condition $\sum V = 0$. The minimum characteristic total vertical action effect V_k must be at least equal to the upward vertical component $B_{v,k}$ of the characteristic soil reaction B_k to be mobilised.

This analysis uses the same wall friction angles as for the calculation of the active and passive earth pressures. Vertical force components $V_{q,k}$ due to variable effects Q may only be used in equilibrium condition 6.47 if they have an unfavourable effect, i.e. cause significant soil reaction components $B_{v,k}$. The analysis can be simplified by considering the variable loads for the mobilised characteristic soil reaction and ignoring them on the side of the actions; this approach lies on the safe side. If the influence of the variable actions is unclear, the analysis should be carried out for permanent loads and for a combination of permanent and variable loads.

In the course of calculating walls with full or partial fixity in the soil, EAU 2004 permits half the vertical component of equivalent force C_k to be included in the sum of the downward actions $\sum V_{k,i}$. The inclination of this equivalent force should, however, lie within the limits $-\frac{2}{3}\varphi'_k \leq \delta_{C,k} \leq \frac{1}{3}\varphi'_k$ measured from a perpendicular line. As a rule, however, $\delta_{C,k} = 0$ should be used.

Fig. 6.14 shows the forces to be considered.

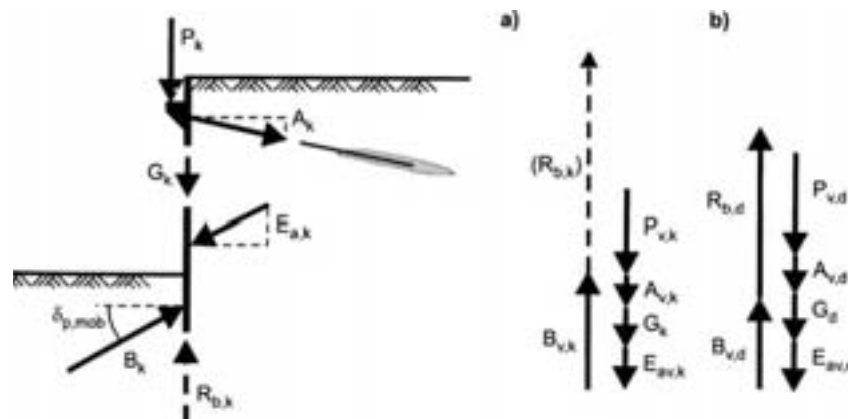


Figure 6.14: Vertical force equilibrium for the wall (ZIEGLER, 2005)

The following characteristic vertical force components occur:

- due to the permanent vertical actions at the top of the wall

$$V_{G,k} = \sum P_{G,k} \quad (6.48)$$

- due to the anchor force $A_{v,k,MIN} = A_{Gv,k} - A_{Qv,k}$

$$V_{Av,k} = A_{v,k,MIN} \quad (6.49)$$

- due to the active earth pressure E_{ah} for n strata down to the theoretical base of the wall F

$$V_{Eav,k} = \sum (E_{ah,k,n} \cdot \tan \delta_{a,k,n}) \quad (6.50)$$

- due to the equivalent force $C_{h,k}$

$$V_{Cv,k} = \frac{1}{2} \cdot C_{h,k} \cdot \tan \delta_{C,k} \quad (6.51)$$

The characteristic upward component $B_{v,k}$ of the soil reaction B_k is calculated

- due to the soil reaction B_k for i strata down to the theoretical base of the wall F

$$B_{v,k} = \left| \sum (B_{h,k,i} \cdot \tan \delta_{p,k,i}) - \frac{1}{2} \cdot C_{h,k} \cdot \tan (\delta_{p,k,F}) \right| \quad (6.52)$$

If the verification of the negative wall friction angle cannot be satisfied, the **negative wall friction angle should be reduced to such an extent** that eq. 6.47 can be satisfied. Please note that altering δ_p also alters the passive earth pressure, and it is usually necessary to recalculate the embedment depth in these cases.

The analysis is explained below by way of an example.

Example 6.13 Verification of passive wall friction angle δ_p to DIN 1054:2005-01 section 10.6.3 (5)

Verification of the mobilisation of the negative angle of friction δ_p is carried out for the system shown in example 6.10 and 6.11. When determining the embedment depth in those examples, 50% partial fixity was called for.

The simplified verification is carried out for the wall friction angle δ_p on which the calculation of the passive earth pressure is based. This means that the variable actions due to Q are considered in the mobilised soil reaction, but neglected on the side of the actions. The individual characteristic vertical force components are calculated below.

$$\begin{aligned} V_{Eg,k} &= 13.7 \cdot 1.05 = 14.44 \frac{\text{kN}}{\text{m}} \\ V_{Av,k} &= 94.7 \cdot \tan 30^\circ = 54.65 \frac{\text{kN}}{\text{m}} \\ V_{Eav,k} &= \left(\frac{13.6+15.7}{2} \right) \cdot 4 \cdot \tan 20^\circ + \left(\frac{15.7+17.3}{2} \right) \cdot 3 \cdot \tan \frac{50^\circ}{3} + \left(\frac{17.3+18.3}{2} \right) \cdot 2 \cdot \tan \frac{65^\circ}{3} \\ &\quad + \left(\frac{27.3+39.5}{2} \right) \cdot 4.36 \cdot \tan \frac{65^\circ}{3} = 108.05 \frac{\text{kN}}{\text{m}} \end{aligned}$$

The characteristic upward component of the soil reaction is

$$B_{v,k} = (276.5 + 22.6) \cdot \tan \frac{65^\circ}{3} = 118.8 \frac{\text{kN}}{\text{m}}$$

Entered into eq. 6.47, this results in

$$V_k = \sum V_{k,j} = 14.44 + 54.65 + 108.05 = 177.14 \geq 118.8 = B_{v,k}$$

i.e. the wall friction angle δ_p selected can be mobilised.

Following the verification of the earth resistance, knowledge of the distribution of the mobilised passive earth pressure enables the final structural calculations to be performed.

Fig. 6.15 shows the results of the structural calculations for the example.

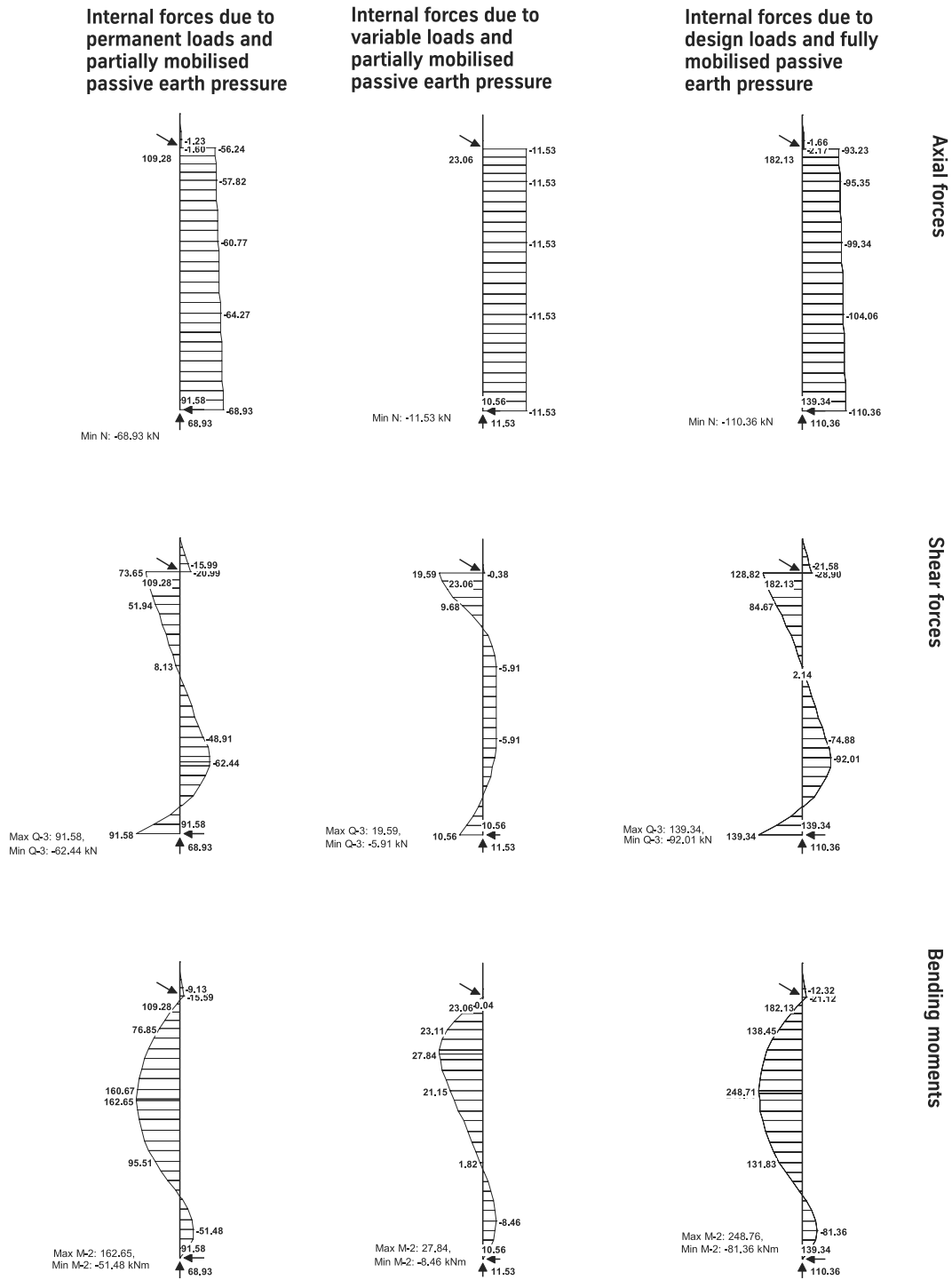


Figure 6.15: Results of structural calculations for sheet pile wall

The internal forces and reactions obtained from the structural calculations are used as the basis for the following examples.

6.7.2 Subsidence of components

DIN 1054:2005-01 section 10.6.6 calls for verification that wall-type retaining structures do not **subside into the ground as a result of action effects parallel to the wall**. An adequate margin of safety against subsidence is assured when the limit state condition

$$V_d = \sum V_{d,i} \leq R_d \quad (6.53)$$

where

- V_d design value of vertical action effects at base of wall
 R_d design value of resistance of wall in axial direction

is satisfied.

The design value of the downward vertical force V_d includes the individual components of the following actions as a result of

- maximum vertical actions P at the top of the wall

$$V_{P,d} = \sum (V_{P,G,k} \cdot \gamma_G + V_{P,Q,k} \cdot \gamma_Q) \quad (6.54)$$

- maximum anchor force components A_v

$$V_{A_v,d} = \sum (V_{A_v,G,k} \cdot \gamma_G + V_{A_v,Q,k} \cdot \gamma_Q) \quad (6.55)$$

- active earth pressure E_a with n strata down to the theoretical base of the wall F

$$V_{E_{a_v},d} = \sum (V_{E_{a_h},G,n,k} \cdot \gamma_G + V_{E_{a_v},Q,n,k} \cdot \gamma_Q) \quad (6.56)$$

- equivalent force C

$$V_{C_v,d} = \sum \left(\frac{1}{2} \cdot V_{C_v,G,k} \cdot \gamma_G + \frac{1}{2} \cdot V_{C_v,Q,k} \cdot \gamma_Q \right) \quad (6.57)$$

The design value of the axial resistance is

$$R_{1,d} = \frac{\sum R_{1k,i}}{\gamma_P} \quad (6.58)$$

The partial safety factor γ_P from table 6.3 is $\gamma_P = 1.4$ for all loading cases, provided the resistance components were determined from empirical values. If test loads are applied to the loadbearing sheet pile wall elements and there is sufficiently accurate information available about the effective resistance $R_{1,k}$, the partial safety factor can be reduced to $\gamma_{P_c} = 1.2$.

The individual partial resistances are calculated based on

- the base resistance due to the end-bearing pressure $q_{b,k}$

$$R_{1b,k} = A_{b,k} \cdot q_{b,k} \quad (6.59)$$

- the mobilised soil reaction B_k with r strata down to the theoretical base of the wall F

$$R_{1Bv,k} = \sum (V_{B,G,r,k} + V_{B,Q,r,k}) \quad (6.60)$$

- the wall friction resistance of equivalent force C_k for negative angles $\delta_{C,k}$

$$R_{1Cv,k} = \sum \left(\frac{1}{2} \cdot V_{Cv,G,k} + \frac{1}{2} \cdot V_{Cv,Q,k} \right) \quad (6.61)$$

- the skin resistance due to skin friction $q_{s,k}$

$$R_{1s,k} = A_{s,k} \cdot q_{s,k} \quad (6.62)$$

According to EAU 2004 section 8.2.11, details about the value of the **end-bearing pressure** $q_{b,k}$ to be assumed and the associated embedment depth required are to be specified by the **geotechnical engineer**. The **bearing area** of a sheet pile wall depends on the **plug formation** around the base of the wall, which can be improved by welding steel flats and/or sections to the base of the wall if required. When using box-type sections, the end-bearing pressure $q_{b,k}$ may be applied to the area enclosed by the wall cross-section. When using trough-type sections with an average web spacing ≥ 400 mm, the bearing area should be reduced. The following equation has proved useful for calculating the effective bearing area for such cases:

$$A_b = n \cdot A_s \quad \text{where} \quad n = 6 - 8 \quad (6.63)$$

More accurate approaches to the calculation of the effective area can be found in WEISSENBACH (2001), which are based on studies by RADOMSKI.

The **skin resistance** $R_{1s,k}$ may only be assumed when lengthening the sheet pile wall beyond the theoretical embedment depth and then only for the additional length of wall. The wall friction resistances $B_{v,k}$ and $C_{v,k}$ and the active earth pressure components $E_{av,k}$ already become effective in the zone above the theoretical embedment depth.

Example 6.14 Analysis of subsidence of components to DIN 1054:2005-01 section 10.6.6

The analysis of subsidence of components is carried out for the system shown in example 6.10 and 6.11. When determining the embedment depth in those examples, 50% partial fixity was called for.

The individual design values of the vertical force components are calculated below.

$$\begin{aligned} V_{Eg,d} &= 13.7 \cdot 1.05 \cdot 1.35 = 19.5 \frac{\text{kN}}{\text{m}} \\ V_{Av,d} &= (95.5 \cdot 1.35 + 19.2 \cdot 1.5) \cdot \tan 30^\circ = 91.1 \frac{\text{kN}}{\text{m}} \\ V_{Eav,d} &= \left[\left(\frac{13.6+15.7}{2} \right) \cdot 4 \cdot \tan 20^\circ + \left(\frac{15.7+17.3}{2} \right) \cdot 3 \cdot \tan \frac{50^\circ}{3} + \left(\frac{17.3+18.3}{2} \right) \cdot 2 \cdot \tan \frac{65^\circ}{3} \right. \\ &\quad \left. + \left(\frac{27.3+39.5}{2} \right) \cdot 4.36 \cdot \tan \frac{65^\circ}{3} \right] \cdot 1.35 = 157.5 \frac{\text{kN}}{\text{m}} \end{aligned}$$

The characteristic values for partial resistances R_{1i} are calculated assuming an end-bearing pressure of $q_{b,k} = 5 \text{ MN/m}^2$.

Calculation of the wall bearing area to be assumed:

Take a HOESCH 1605 section with web spacing $> 400 \text{ mm}$, i.e. assuming the enclosing envelope as the bearing area is not justified. Instead, to be on the safe side, the bearing area is calculated according to eq. 6.63 where $n = 6$:

$$A_b = 6 \cdot 136.3 = 0.08178 \frac{\text{m}^2}{\text{m}}$$

Therefore, the characteristic values for partial resistances R_{1i} are as follows:

$$\begin{aligned} R_{1b,k} &= 0.08178 \cdot 5000 = 408.9 \frac{\text{kN}}{\text{m}} \\ R_{1,Bv,k} &= (276.5 + 22.6) \cdot \tan \frac{2 \cdot 32.5^\circ}{3} = 118.8 \frac{\text{kN}}{\text{m}} \end{aligned}$$

Entering these into eq. 6.53 results in

$$V_d = \sum V_{d,i} = 19.5 + 91.1 + 157.5 = 268.0 \leq 377.0 = \frac{408.9 + 118.8}{1.4} = B_{v,d}$$

Therefore the section has been verified and the embedment depth of 4.75 m is adequate.

6.7.3 Material failure of components

Verification of the **loadbearing capacity of the steel sheet pile section** can be carried out via an **elastic analysis** of the permissible stress. This corresponds to the EAB method for excavations and the EAU method for waterfront structures. However, current research into the determination of the ultimate load capacity $R_{d,i}$ of steel sheet piles at the ultimate limit state enables the advantages of **plastic design** to be exploited for sheet pile walls as well.

Information on the plastic method of analysis can be found in KALLE, (2005) and DIN V ENV 1993-5 (1998).

Example 6.15 shows the design for the elastic-elastic case to DIN 18800 (1990).

Example 6.15 Simplified analysis of material failure of sheet pile wall to DIN 18800-1 (1990)

The analysis of material failure of the sheet pile wall is carried out for the system shown in example 6.10 and 6.11.

From the structural calculations we get the following actions:

		due to permanent loads	due to variable loads	design value
Resultant anchor force A	[kN/m]	109.3	23.1	182.2
Horizontal equivalent force C	[kN/m]	91.6	10.6	139.3
Bending moment M_{max}	[kNm/m]	162.7	27.9	248.7
Normal force N_{max}	[kN/m]	-68.9	-11.5	-110.4

Requirements for the material resistances can be found in the respective standards.

Select: HOESCH 1605 section
steel grade S 240 GP, min. yield strength $f_{y,k} = 240 \text{ N/mm}^2$

Partial safety factor to DIN 18800: $\gamma_M = 1.10$

For simplicity, the comparative stress analysis for the maximum design loads M_{max} and N_{max} is carried out, the shear stress analysis will be neglected.

The limit condition to DIN 1054:2005-01 is rewritten for the limit condition regulated in the standard. In the case of verifying the sheet pile wall section

$$E_d \leq R_{M,d} \quad \text{becomes} \quad \sigma_d \leq f_{y,d}$$

The following applies

$$\sigma_d = \left| \frac{M_{max}}{W_y} \pm \frac{N_{max}}{A_s} \right| = \left| \frac{248.7 \cdot 10^2}{1600} + \frac{110.5}{136.3} \right| = 16.4 \frac{\text{kN}}{\text{m}^2} \leq 21.8 \frac{\text{kN}}{\text{m}^2} = \frac{f_{y,k}}{\gamma_M}$$

The analysis is satisfied; the degree of utilisation of the section amounting to $\mu = 75\%$ may be optimised if required.

6.8 Analysis for the serviceability limit state

According to DIN 1054:2005-01, the **serviceability limit state** is the state of a structure in which the conditions specified for the use of the structure are exceeded. In this context, DIN 1054:2005-01 advises verifying the serviceability of wall-type retaining structures for the case that neighbouring buildings, pipes and cables, other installations or traffic areas could be at risk, e.g.

- due to large displacements with a low stiffness of the supporting soil in front of a wall-type retaining structure,
- due to displacement and overturning of a block of soil held together with ground anchors,
- when an earth pressure higher than the active earth pressure is expected.

DIN 1054:2005-01 section 6.1.3 also states the following: “The interaction of subsoil and structure is to be taken into account if the stiffness of the structure in conjunction with the stiffness of the subsoil causes a considerable redistribution of the forces transferred to the soil.” Furthermore, the DIN standard states that serviceability is to be verified with the characteristic actions and resistances. In doing so, the same structural system shall apply as was used for determining the internal forces or action effects at limit state LS 1B, and variable actions shall only be taken into account if they cause irreversible displacements or deformations. The DIN standard does not mention any particular method of calculation in conjunction with the verification of serviceability.

With respect to the use of methods of calculation for taking into account the soil-structure interaction, EC7 comments: “. . . problems of soil-structure interaction analyses should use stress-strain relationships for ground and structural materials and stress states in the ground that are sufficiently representative, for the limit state considered, to give a safe result”.

Verification of serviceability for wall-type retaining structures can be carried out with the **coefficient of subgrade reaction method** or the **finite element method (FEM)**; see, for example, the excavation recommendations of WEISSENBACH (2003). FEM offers the advantage of a comprehensive modelling of the soil-structure interaction because the material behaviour of structures and soils plus the force transfer to the soil-structure boundary surfaces can be taken into account.

Like in other civil engineering disciplines, FEM has become a standard approach in the verification of serviceability for geotechnical structures. One reason for this is the user-friendly software, another is the progress in the field of material models for soils. However, it should be remembered that in comparison to structural problems, geotechnical problems are based on a much less secure database.

The use of FEM for retaining wall structures is covered in chapter 8.

6.9 Overall stability

The **overall stability** of changes of level in the terrain in the meaning of an embankment or step in the ground is dealt with in DIN 1054:2005-01, with reference to E DIN 4084. An allocation to geotechnical categories is also necessary for this verification.

For a sheet pile structure, an adequate margin of safety against ground failure is assured when the **failure mechanisms** possible with this type of wall and the possible **critical construction conditions** do not exceed the limit state conditions according to E DIN 4084 with the partial safety factors for limit state LS 1C given in table 6.3:

$$E_d \leq R_d \quad (6.64)$$

where

E_d design value of resultant action effect parallel to slip plane, or design value of moment of actions about the centre of the slip circle

R_d design value of resistance parallel to slip plane, or design value of moment of resistances about the centre of the slip circle

The actions and resistances are calculated as follows:

$$E_d = r \cdot \sum_i (G_{d,i} + Q_{d,i}) \cdot \sin \vartheta_i + \sum M_s \quad (6.65)$$

$$R_d = r \cdot \sum_i \frac{(G_{d,i} + Q_{d,i} - u_{d,i} \cdot b_i) \cdot \tan \varphi_{d,i} + c_{i,d} \cdot b_i}{\cos \vartheta_i + \mu \cdot \tan \varphi_{d,i} \cdot \sin \vartheta_i} \quad (6.66)$$

with the design values of the shear parameters

$$\tan \varphi_d = \frac{\tan \varphi_k}{\gamma_\varphi} \quad c_d = \frac{c_k}{\gamma_c} \quad (6.67)$$

The calculation is carried out iteratively by choosing a degree of utilisation for μ and recalculating according to

$$\mu = \frac{E_d}{R_d} \quad (6.68)$$

E DIN 4084 explains how to take account of the **loadbearing effect of tension members, anchors and piles** when checking the overall stability.

See Fig. 6.23 for the general geometrical definition of the aforementioned variables.

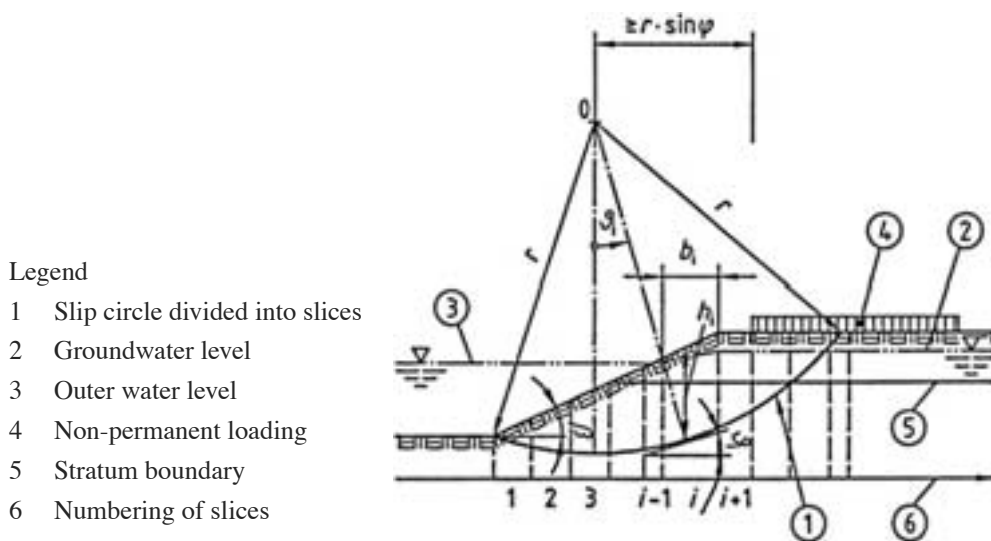
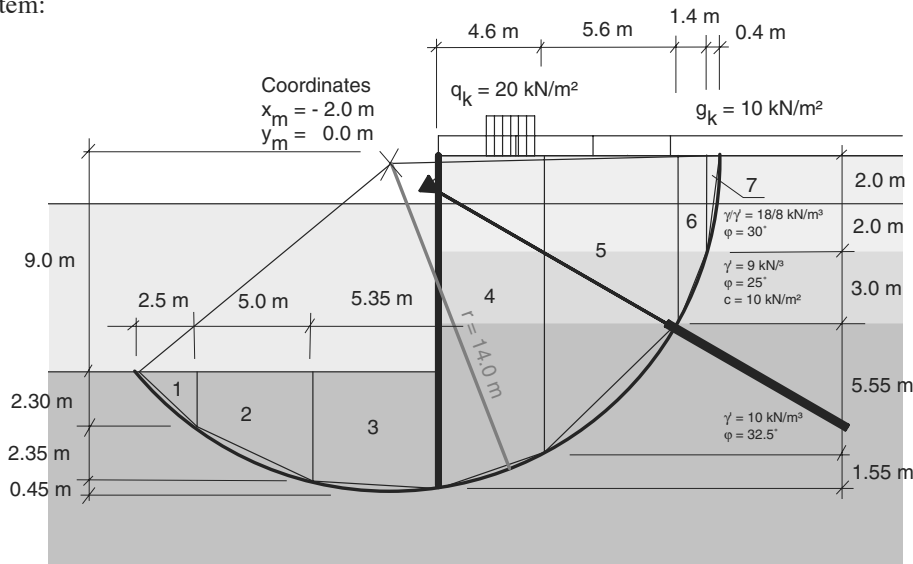


Table 6.23: Example of slip circle and division into slices

Example 6.16 Verification of overall stability of sheet pile wall to DIN 1054:2005-01 / E DIN 4084

Verification of an adequate margin of safety against ground failure is carried out for the system shown in example 6.10 and 6.11. The centre of the slip circle is to be determined iteratively so that the critical slip circle with the smallest margin of safety is considered.

Sketch of system:



According to E DIN 4084, the method of slices after BISHOP should be used for calculating the margin of safety against failure of the ground in stratified soils. In doing so, the slip circle should be formed as accurately as possible by polygonal slices with vertical contact faces. In this example, 7 slices have been chosen.

The vertical loads plus the geometry are then determined for each slice, and with the help of eq. 6.66 and 6.67 the variables E_d and M_d are determined according to eq. 6.64.

i	$G_{k,i}$ kN/m	γ_G	$Q_{k,i}$ kN/m	γ_Q	$G_{d,i} + Q_{d,i}$ kN/m	ϑ °	l m	φ_d °	c_d kN/m ²	E_d kN/m	R_d kN/m
1	2	3	4	5	6	7	8	9	10	11	12
1	28.8	1.0	0.0	1.3	28.8	-42.6	3.4	27.0	0.0	-263	446
2	173.8	1.0	0.0	1.3	173.8	-25.2	5.5	27.0	0.0	-1036	1957
3	260.8	1.0	0.0	1.3	260.8	-4.8	5.4	27.0	0.0	-306	1973
4	700.9	1.0	40.0	1.3	752.9	18.6	4.9	27.0	0.0	3362	4667
5	653.8	1.0	0.0	1.3	653.8	44.7	7.9	27.0	0.0	6438	4025
6	105.7	1.0	0.0	1.3	105.7	65.0	3.3	20.5	8.0	1341	1202
7	16.4	1.0	0.0	1.3	16.4	84.3	4.0	24.8	0.0	228	157
Σ										9766	14427

The anchor force was neglected in the slip circle calculation because its line of action passes approximately through the centre of the slip circle.

The margin of safety against ground failure calculated iteratively results in

$$\mu = 0.68 = \frac{9766}{14427} \leq 1.0$$

and so verification of overall stability is therefore satisfied.

Chapter 7

Ground anchors

7.1 Types of ground anchors

Irrespective of the type of ground anchors, we distinguish between two basic anchor functions: temporary anchors with a maximum service life of two years, and permanent anchors which first and foremost must satisfy higher demands regarding corrosion protection.

Ground anchor types are classified as follows with respect to their form of construction:

- Round steel tie rods (laid in the ground) with anchor wall/plate
- Grouted anchors to DIN EN 1537
- Driven anchor piles
- Driven pile with grouted skin
- Vibratory-driven grouted pile
- Micropiles (diameter \leq 300 mm)
- Jet-grouted piles
- Retractable raking piles

7.1.1 Round steel tie rods

Round steel tie rods consist of tension bars that are laid horizontally in the ground and terminate at an anchor wall or anchor plate. The loadbearing capacity of these anchors may be limited by the passive earth pressure that can be mobilised in front of the anchor wall/plate. Both the threaded and the plain parts of the tie rod must be checked. For practical reasons, the tie rods should not be smaller than 1 1/2 in. Please refer to EAU 2004 sections 8.2.6.3 (R 20) and 9.2.3.3 for further information.

7.1.2 Grouted anchors

Grouted anchors consist of a steel tension bar surrounded by a layer of injected grout. The tensile forces are either transferred continuously from the tie rod to the grout (composite anchor) or they are transferred via a pressure pipe embedded in the injected grout (duplex anchor). Both systems transfer the forces into the soil by way of skin friction. The steel tension bar must be able to deform freely in a sleeve so that the grouted anchor can be prestressed. Threaded bars or wire tendons can be used as the tension members.

Grouted anchors are normally installed by drilling with or without water-jetting. The sleeve is inserted to the right depth and the steel tension member installed. As the sleeve is withdrawn, the cement mortar is injected under pressure. Above the intended layer of grout, the drilled hole is cleared of mortar and filled in order to avoid a force “short-circuit” between the wall and the layer of grout. A special re-injection process can be used to break apart a layer of grout that has already hardened and press it against the soil, which enables much higher skin friction values to be mobilised. Grouted anchors are covered by DIN EN 1537.

7.1.3 Driven anchor piles

Various steel sections and precast concrete piles can be used as anchor piles. Anchor piles carry the tensile forces on their surface by way of skin friction. They are frequently encountered in quay wall structures in which high tensile forces occur (see Fig. 7.1). In such cases, steel piles enable a straightforward welded connection between pile and retaining wall structure.

Driven piles at shallow angles are guided by leaders. Slow-action hammers are preferred to rapid-action devices (EAU 2004 section 9.5.2). In the case of raking anchor piles, settlement due to backfilling, relieving excavations or the installation of further piles behind the sheet pile wall can lead to loads at an angle to the axis of the pile. The additional deformations cause an increase in the stresses in the pile which in some circumstances means that the maximum axial force may not occur at the head of the pile but instead behind the sheet pile wall (see MARD-FELDT, 2006). This must be taken into account when designing the piles and the connection to the wall. For further information regarding the design and driving of piles, please refer to EAU 2004 section 9.5 (R 16).

7.1.4 Driven pile with grouted skin

The driven pile with grouted skin consists of a steel section with a special driving shoe which cuts a prismatic void in the soil during driving. Cement mortar is injected into this at the same time as driving. This creates a bond between pile, cement and soil which enables skin friction values to be achieved that are 3 to 5 times higher than a non-grouted pile (EAU 2004 section 9.2.1.3).

7.1.5 Vibratory-driven grouted pile

The toe of the vibratory-driven grouted pile, a steel H-section, is widened with welded web and flange plates. As the pile is vibrated into the ground, these displacement elements create a void

equal in size to the thickness of the plates, into which a cement suspension is injected in order to increase the skin friction of the pile. Please refer to EAU 2004 section 9.2.1.4 for further information.

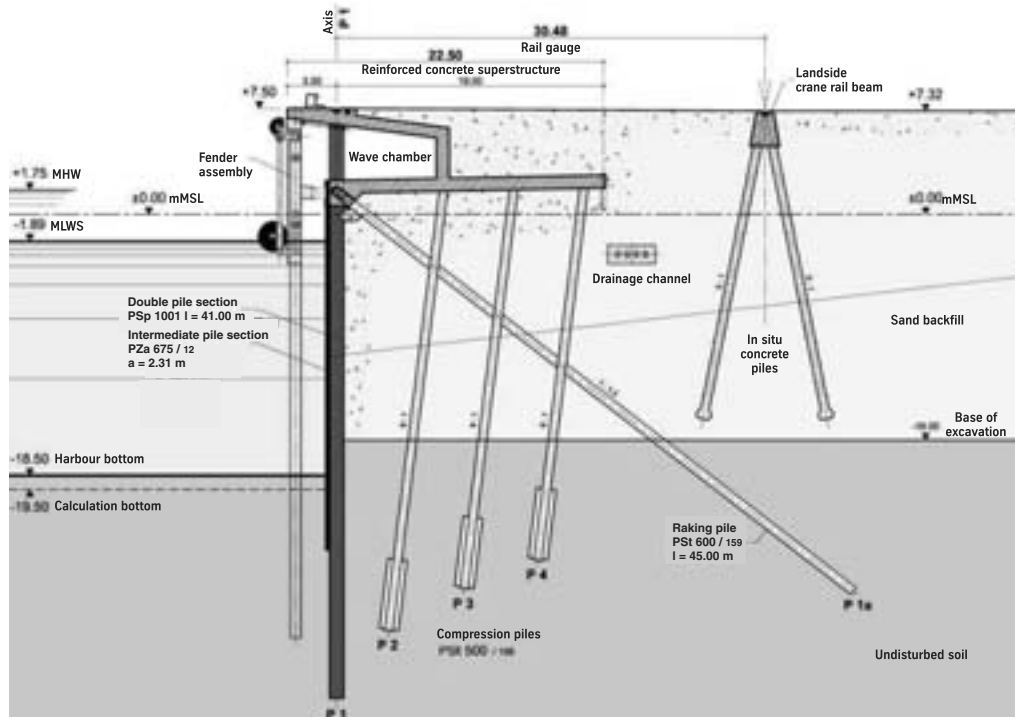


Figure 7.1: Driven anchor piles, CT IV container terminal, Bremerhaven

7.1.6 Micropiles (diameter \leq 300 mm)

The term micropile covers various non-prestressed pile types with a small diameter which transfer the tensile forces into the soil by way of skin friction. These include, for example, self-boring micropiles to DIN 4128 or DIN EN 14199, tubular grouted piles, grouted in situ concrete piles and composite piles. The self-boring micropile is constructed like a ground anchor, with the full length of the pile embedded in mortar, which improves the corrosion protection.

In the case of the TITAN micropile to DIN EN 14199, which belongs to the group of tubular grouted piles, a ribbed steel tube serves as tension member, lost drilling rod and injection pipe. The tip of the rod includes a radial jet with which the soil can be cut away and at the same time filled with mortar. It is not necessary to install the tension member and withdraw the casing with this system. In soft soils, ground with a high water table or weathered rock, where the drilled hole would collapse, a casing is unnecessary because a bentonite slurry can be used to keep the hole open. This increases the efficiency of the installation work by about 2 to 3 times over the method with a casing in the hole.

The dynamic injection of cement slurry directly after drilling results in a mechanical interlock between layer of grout and soil. The good shear bond means that only minor deformations of the pile head ensue under service loads. EAU 2004 section 9.2.2 contains further information.

7.1.7 Jet-grouted piles

Jet-grouted piles are bored piles with an enlarged toe. A steel section acts as the tension member. At the base of the pile, the soil is cut away with a high-pressure water jet and mixed with mortar.

7.1.8 Retractable raking piles

Retractable raking piles are used behind quay walls built in water. A steel section welded to an anchor plate forms the tension element. The connection between the head of the pile and the wall still permits rotation. The pile is fixed to the wall while suspended from a crane and subsequently lowered into place, rotating about its fixing point. The resistance of this construction is first activated upon backfilling the wall and is made up of the horizontal passive earth pressure plus the vertical soil weight acting on the anchor plate. EAU 2004 section 9.2.3.1 contains further information.

7.2 Loadbearing capacity

The loadbearing capacity of a ground anchor is mainly determined by the force transfer between anchor and soil. This is achieved either by enlarging the anchor, e.g. by means of an anchor plate (tie rod, retractable raking pile) or a body of grout (jet-grouted piles) or via skin friction (driven pile, micropile, grouted anchor, pile with grouted skin). The loadbearing capacity of horizontal round steel ties can be calculated from the maximum passive earth pressure that can be mobilised in front of the anchor wall before failure of the anchoring soil occurs. The pull-out resistance is much higher with systems installed at a steeper angle (retractable raking pile, jet-grouted pile). Resistances of 4 to 5 MN can be achieved with jet-grouted piles.

The pull-out resistance of piles that carry their loads via skin friction depends on the effective surface area and the activated skin friction. For displacement piles to EAU 2004 section 9.4 (R 27), the latter can be estimated from the tables in DIN 1054:2005-01 appendix C for preliminary designs where CPT results are available. Empirical values for the skin friction of grouted micropiles are given in appendix D of DIN 1054:2005-01, depending on the type of soil. According to DIN 1054:2005-01, the pull-out resistance should be determined by a suitability test. OSTERMAYER (1997) has compiled empirical values for grouted anchors which can be used for preliminary design purposes. Fig. 7.2 shows these according to type of soil and force transfer length l_0 . Depending on their size, TITAN micropiles can carry service loads of 100 to 1500 kN; they can accommodate tensile or compressive forces.

7.3 Design

When designing ground anchors for sheet pile walls, the following analyses are always required:

- Design against failure of the anchor materials (internal stability)
- Design against pull-out of the anchor from the soil
- Design against uplift (stability of total system)

- Design against failure of the anchoring soil (for horizontal anchors with anchor wall)
- Design for adequate anchorage length (analysis of the lower slip plane)
- Design for serviceability

7.3.1 Design against material failure

The design against material failure is carried out according to the standard for the respective type of anchor or the building authority approval. It is essential to verify that the design value for the actions E_d is less than or equal to the design value of the material resistance $R_{M,d}$. When checking the **internal load-carrying capacity**, in many cases it is not the failure load of the tension member that is critical, but rather the cracking of the layer of grout, which guarantees protection against corrosion. The permissible stress in the tension member is therefore reduced. For grouted anchors, $R_{M,d}$ is calculated, for example, as follows:

$$R_{M,d} = A_S \cdot \frac{f_{t,0.1,k}}{\gamma_M} \quad (7.1)$$

where $f_{t,0.1,k}$: characteristic stress of steel tension member at 0.1% permanent strain

A_S : cross-sectional area of steel tension member

γ_M : partial safety factor to DIN 1054:2005-01 table 3

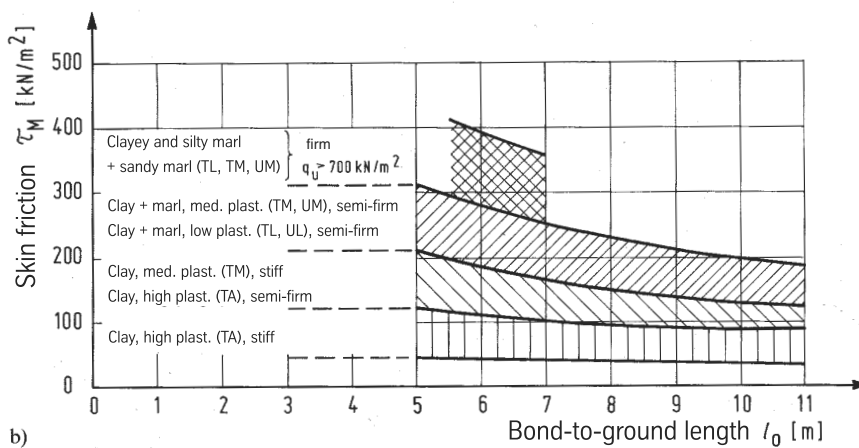
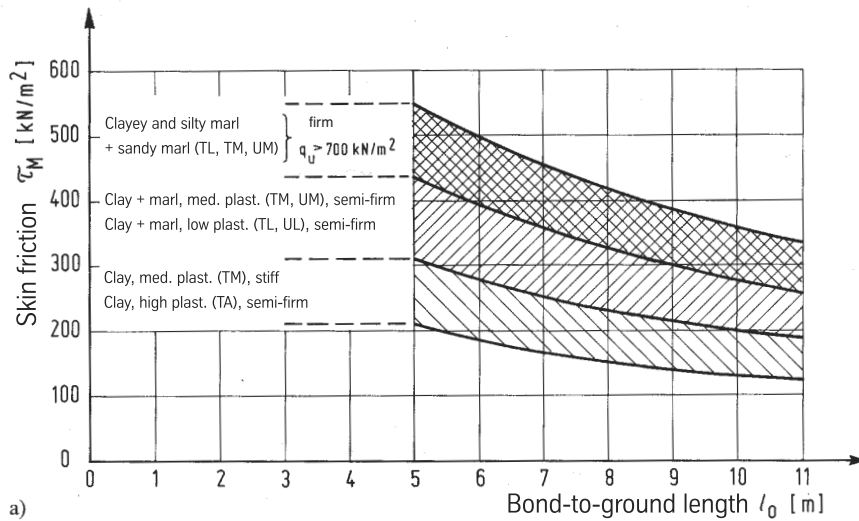
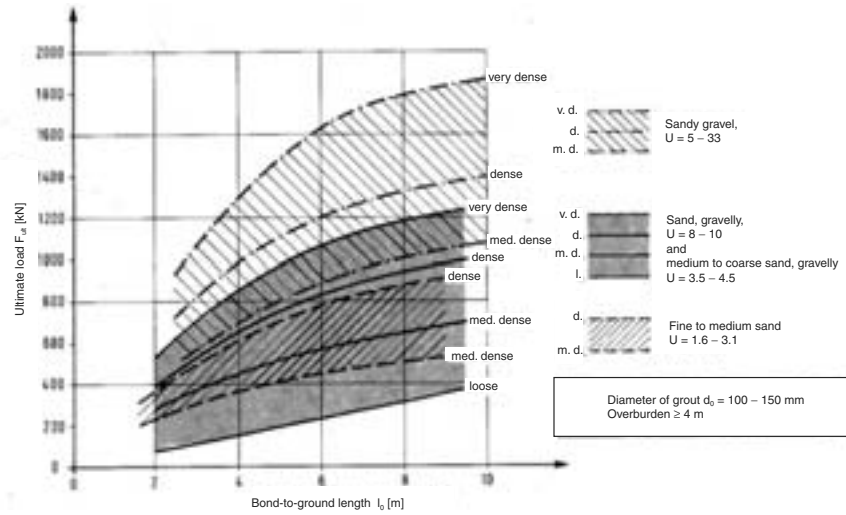


Figure 7.2: Empirical values for the ultimate load of grouted anchors in non-cohesive soils and skin friction values for anchors in cohesive soils, a) with grouted skin, and b) without grouted skin (OSTERMAYER, 1997)

Example 7.1 Design against material failure – grouted anchor

The design against material failure is explained for the anchor of the system shown in example 6.10 or 6.11. The anchor force in the axial direction ($\alpha = 30^\circ$) is

$$A_{G,k} \cdot \gamma_G + A_{Q,k} \cdot \gamma_Q = 109.3 \cdot 1.35 + 23.1 \cdot 1.5 = 182.2 \text{ kN/m} = A_d$$

The chosen anchor spacing a_A is 3 m.

Design value for actions:

$$E_d = A_d \cdot a_A = 182.2 \cdot 3 = 546.6 \text{ kN}$$

A tubular grouted pile is to be used.

Diameter of grout: $d_V = 20$ cm

Tension member: threaded tube d_a/d_i 52/26 mm, $A_{S,min} = 1337 \text{ mm}^2$

Check similar to grouted anchors to DIN 1054:2005-01:

$$f_{t,0.1,k} = 550 \text{ N/mm}^2 \text{ (manufacturer's information)}$$

$$E_d \leq A_S \cdot \frac{f_{t,0.1,k}}{\gamma_M} = R_{M,d} \quad \text{(see eq. 7.1)}$$

$$546.6 \text{ kN} \leq 1337 \cdot \frac{550}{1.15} = 639.4 \text{ kN}$$

The design against material failure of round steel ties and waling bolts can be carried out according to EAU 2004 section 8.2.6.3 (R 20) or DIN EN 1993-5:1998. In this method, the ultimate limit state for material resistance is considered separately for the threaded and plain parts of the bar and a notch factor must be allowed for. The resistance is calculated as follows:

$$R_{M,d} = \min [F_{tg,Rd}; F_{tt,Rd}^*] \quad (7.2)$$

$$F_{tg,Rd} = A_{shaft} \cdot \frac{f_{y,k}}{\gamma_{M0}} = A_{shaft} \cdot \frac{f_{y,k}}{1.10} \quad (7.3)$$

$$F_{tt,Rd}^* = k_t^* \cdot A_{core} \cdot \frac{f_{ua,k}}{\gamma_{Mb}} = 0.55 \cdot A_{core} \cdot \frac{f_{ua,k}}{1.25} \quad (7.4)$$

mit A_{shaft} : cross-sectional area in shaft zone

A_{core} : core cross-sectional area in threaded zone

$f_{y,k}$: yield stress

$f_{ua,k}$: tensile strength

γ_{M0} : partial safety factor to DIN EN 1993-5 for shaft zone

γ_{Mb} : ditto, but for threaded zone

k_t^* : notch factor

The notch factor $k_t = 0.8$ given in DIN EN 1993-5:1998 is reduced to $k_t^* = 0.55$ for the threaded part. This takes into account any additional loads during installation of the anchor. The additional analyses for serviceability required by DIN EN 1993-5:1998 can therefore be omitted.

Example 7.2 Design against material failure – round steel tie rod

The design against material failure is explained for the anchor of the system shown in example 6.10 or 7.6. Design value for actions from example 7.1 ($\alpha = 30^\circ$) for anchor inclination $\alpha = 3.8^\circ$ and anchor spacing $a_A = 3.6$ m:

$$Z_d = E_d = 182.2 \cdot \frac{\cos 30}{\cos 3.8} \cdot 3.6 = 569.3 \text{ kN}$$

A round steel tie rod is to be used as an anchor.

Round steel tie rod with upset ends and rolled thread

Steel grade: S 355 JO

2 3/4 in-52 where $A_{shaft} = 21.2 \text{ cm}^2$ and $A_{core} = 28.8 \text{ cm}^2$

Check according to EAU 2004 section 8.2.6.3 (R 20):

$$F_{tg,Rd} = 21.2 \cdot \frac{35.5}{1.10} = 684.2 \text{ kN} \quad (\text{see eq. 7.3})$$

$$F_{tt,Rd}^* = 0.55 \cdot 28.8 \cdot \frac{48.0}{1.25} = 608.3 \text{ kN} \quad (\text{see eq. 7.4})$$

$$E_d \leq R_{M,d} = \min [F_{tg,Rd}; F_{tt,Rd}^*] \quad (\text{see eq. 7.2})$$

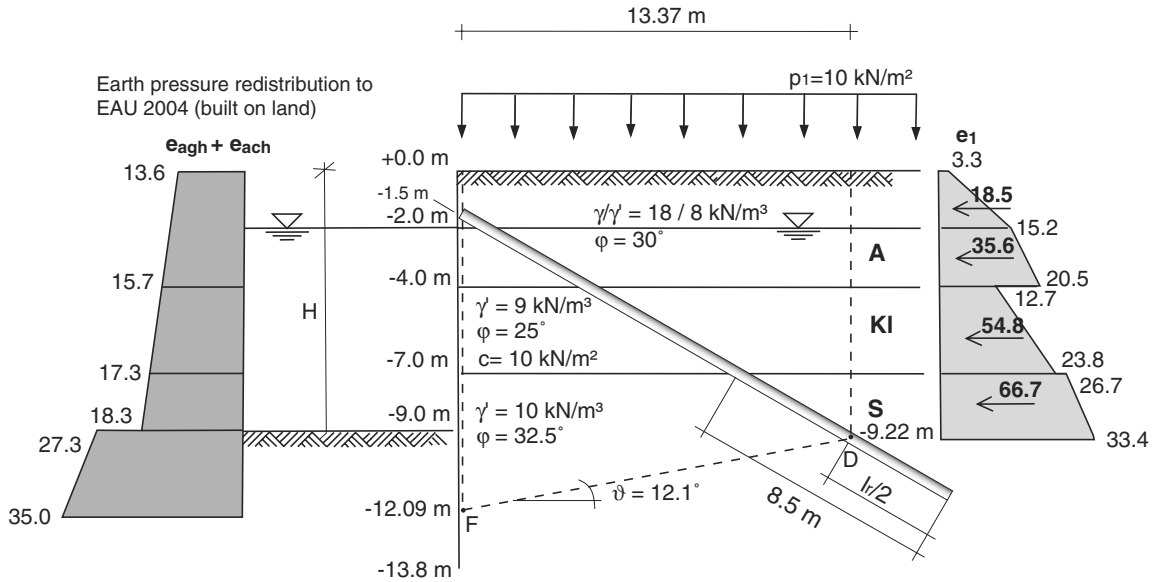
$$569.3 \text{ kN} \leq \min [684.2; 608.3] = 608.3 \text{ kN}$$

7.3.2 Pull-out resistance

Designing against pull-out of the anchor involves checking whether the design value of the actions E_d can be transferred from the anchor to the soil. The pull-out resistance of an anchor is determined by one or more loading tests. DIN EN 1537:2001-01 applies for grouted anchors. The characteristic value for pull-out resistance $R_{U,k}$ is determined from the loading tests in conjunction with a scatter factor. Alternatively, the **pull-out resistance** of anchor piles and micropiles can also be determined via empirical values from comparable loading tests or the general empirical values in DIN 1054:2005-01 appendix D. The anchorage length l_r required for structural purposes is calculated by dividing the design value for the anchor force A_d by the design value for the skin friction T_d .

In the case of grouted anchors, the pull-out resistance should be determined from so-called suitability tests. The maximum test load depends on whether the anchor is to be installed as a temporary or permanent component. The pull-out resistance in a single test is that force causing a creep $k_s = 2$ mm.

Example 7.3 Pull-out resistance



The pull-out resistance given here is for the anchor in example 6.10 or 7.1. The minimum anchorage length l_r is required. In this case only the sand stratum can be used to carry the load.

Design value of resistance:

Skin friction from empirical values in DIN 1054:2005-01 appendix D: $q_{s1,k} = 150 \text{ kN/m}^2$

$$l_r = \frac{A_d}{T_d} = \frac{A_d \cdot \gamma_P}{q_{s1,k} \cdot \pi \cdot d} = \frac{546.6 \cdot 1.4}{150 \cdot \pi \cdot 0.2} = 8.12 \text{ m}$$

An anchorage length of 8.5 m in the sand stratum is selected. The total length of the anchor is 19.5 m.

Note: When calculating the total length of anchor required, the analysis at the lower slip plane (see section 7.3.5) is often critical!

7.3.3 Design against uplift

It must be guaranteed that the anchor is not lifted together with the soil clinging to it. Design against uplift is especially important for groups of anchors at a steep angle. The analysis and the geometry of the body of soil hanging on the anchor is dealt with in DIN 1054:2005-01.

7.3.4 Design against failure of the anchoring soil

The design against failure of the anchoring soil should be carried out in accordance with EAU 2004 section 8.4.9.7 (R 10) for horizontal or slightly inclined anchors with anchor plates. It must be shown that the design value of the resisting horizontal forces from underside of anchor plate to ground level is greater than or equal to the horizontal design forces acting due to anchor force, earth pressure and, possibly, excess hydrostatic pressure. Imposed loads may only be considered in an unfavourable position (i.e. behind the anchor plate). Fig. 7.3 shows the failure body and the forces applied schematically. The passive earth pressure in front of the anchor

plate may only be assumed for an angle of inclination that encloses the sum of all forces acting perpendicular ($\sum V = 0$).

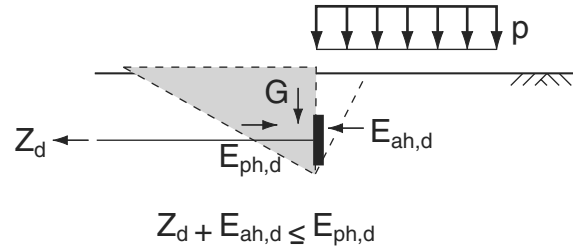


Figure 7.3: Design against failure of the anchoring soil

Example 7.4 Design against failure of the anchoring soil

The design against failure of the anchoring soil is explained for the anchor of the system shown in example 6.10 or 7.2.

Horizontal component of actions related to an anchor inclination $\alpha = 3.8^\circ$:

$$Z_{h,d} = 182.2 \cdot \cos 30 = 157.8 \text{ kN/m}$$

Active earth pressure on anchor plate due to self-weight and imposed loads ($\delta_a = 2/3\varphi$):
See example 7.6 for earth pressure distribution.

$$E_{ah,k} = \frac{1}{2} \cdot 2.0 \cdot (2.8 + 12.9) + \frac{1}{2} \cdot 2.0 \cdot (12.9 + 17.4) = 46.0 \text{ kN/m}$$

Passive earth pressure in front of anchor plate due to self-weight, where $\delta_P = 0$ and $K_{pgh} = 3.0$:

$$\begin{aligned} e_{pgh,k}(0.0) &= 0 \text{ kN/m}^2 \\ e_{pgh,k}(-2.0) &= 2.0 \cdot 18 \cdot 3.0 = 108 \text{ kN/m}^2 \\ e_{pgh,k}(-4.0) &= 108 + 2.0 \cdot 8 \cdot 3.0 = 156 \text{ kN/m}^2 \\ E_{ph,k} &= \frac{1}{2} \cdot 2.0 \cdot 108 + \frac{1}{2} \cdot 2.0 \cdot (108 + 156) = 372.0 \text{ kN/m} \end{aligned}$$

Verification:

$$\begin{aligned} Z_{h,d} + E_{ah,d} &\leq E_{ph,k} \\ 157.8 + 1.35 \cdot 46.0 &\leq \frac{372.0}{1.4} \\ 219.9 &\leq 265.7 \end{aligned}$$

Analysis of vertical forces:

$$\begin{aligned} \sum V = 0 &= Z_{h,d} \cdot \tan \alpha - E_{ah,d} \cdot \tan \left(\frac{2}{3}\varphi \right) \\ &= 157.8 \cdot \tan 3.8 - 1.35 \cdot 46.0 \cdot \tan \left(\frac{2}{3}30 \right) \\ &= 10.5 - 22.6 = -12.1 \text{ kN/m} \end{aligned}$$

The component points downwards and can be carried by the end-bearing pressure.

7.3.5 Verification of stability at the lower slip plane

The **anchorage length** should be chosen such that the body of soil affected by the ground anchor cannot slide down a **lower slip plane**. The analysis is based on the model idealisation that the force transfer from the anchor causes a body of soil to form behind the wall. In the analysis, the maximum possible shear resistance at the lower slip plane is exploited, whereas the base support is not fully activated. The characteristic anchor force $A_{poss,k}$ is the anchor force that can be resisted by this body of soil when exploiting the shear resistance at the lower slip plane to the full. In the method according to KRANZ, the body of soil is bounded by the ground level, a section behind the retaining wall down to point F , from there along the lower slip plane to point D and then back to ground level. Fig. 7.4 shows the body of soil and the internal forces for a system with horizontal anchor plus anchor plate. $A_{poss,k}$ is determined graphically via the polygon of forces shown in the figure. Point F designates the theoretical base of the sheet pile

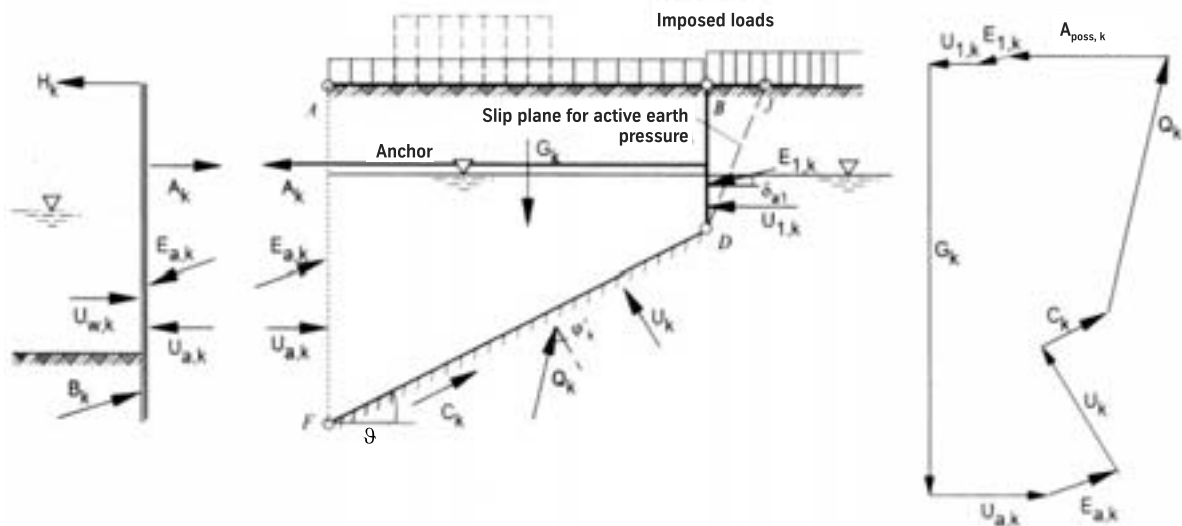


Figure 7.4: Verification of stability at the lower slip plane to EAU 2004, section 8.4.9 (R 10)

wall. In the case of a simply supported wall, this corresponds to the true base of the sheet piling, but in the case of a fixed-base sheet pile wall, it can be assumed to lie at the point of zero shear in the zone of fixity. The position of point F can be taken from the structural calculations for the sheet pile wall. Point D is defined depending on the type of anchor. With an anchor plate, it lies at the lower edge of the plate (see Fig. 7.4). With tension piles and grouted anchors, point D is located in the middle of the theoretical minimum anchorage length l_r required (see section 7.3.2), which starts at the base of the pile (see Fig. 7.5). An equivalent wall is assumed from here up to ground level. Active earth pressures acting on this wall are applied with $\delta_a = 0$. In the case of grouted anchors, the length of the grout is assumed to be equal to l_r . If the anchor spacing a_A is greater than $l_r/2$, the possible anchor force $A_{poss,k}$ must be reduced by the factor $l_r/(2a_A)$. An equivalent wall is also assumed when using individual anchor plates. According

to EAU 2004 section 8.4.9.6 (R 10), this is located at a distance $1/2 \cdot a$ in front of the anchor plates, where a is the clear distance between the plates. In stratified soil, the body of soil is

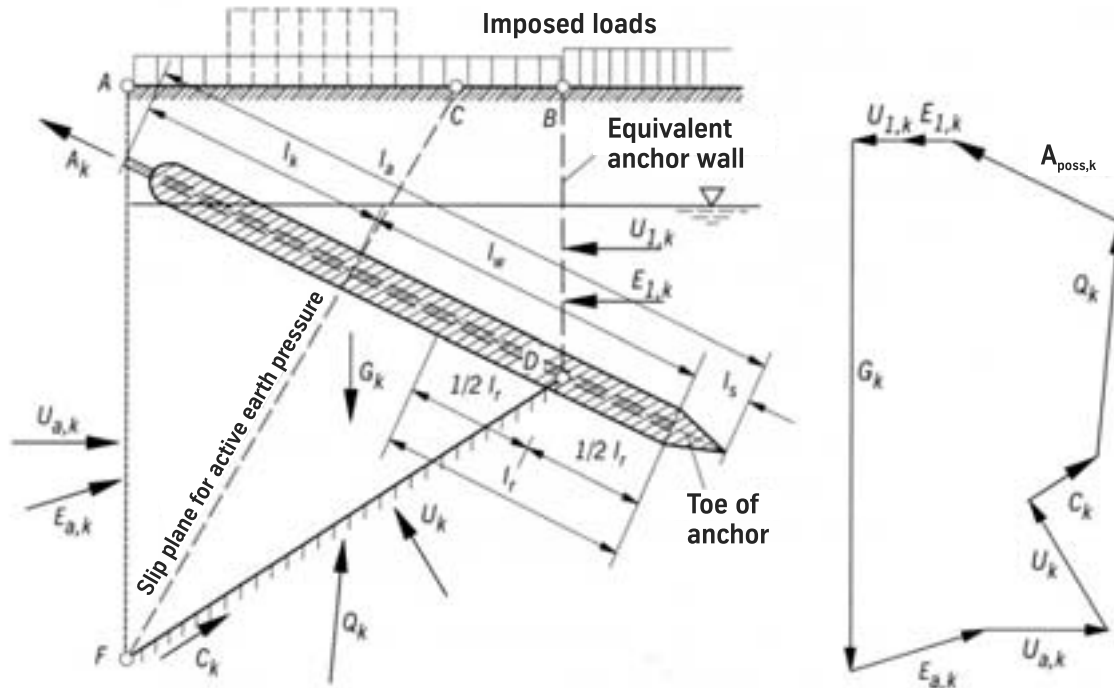


Figure 7.5: Verification of stability at the lower slip plane for piles and grouted anchors to EAU 2004, section 8.4.9 (R 10)

divided into several segments by imaginary perpendicular separating joints that pass through the points where the lower slip plane intersects with the boundaries of the strata. EAU 2004 section 8.4.9 (R 10) contains further information. The following internal forces are required for the analysis:

G_k total characteristic weight of body of soil, plus imposed loads if applicable

E_k characteristic active earth pressure acting on retaining wall $E_{a,k}$, anchor plate or equivalent wall $E_{1,k}$

U_k characteristic hydrostatic pressure acting on retaining wall $U_{a,k}$, lower slip plane U_k , anchor plate or equivalent wall $U_{1,k}$

C_k characteristic shear force at the lower slip plane due to cohesion

Q_k characteristic resultant force at the lower slip plane due to normal force and maximum possible friction (inclined at φ to a line perpendicular to slip plane)

A_k characteristic anchor force due to permanent $A_{G,k}$ and variable actions $A_{Q,k}$

If Q_k is not determined graphically by means of a polygon of forces, the horizontal component $Q_{h,k}$ for the segments i can be calculated as follows ($U_{a,k} = U_k = U_{1,k} = 0$):

$$Q_{h,k,i} = \frac{\sin(\varphi_i - \vartheta)}{\cos(\varphi_i - \vartheta - \alpha)} \cdot [(G_{k,i} - C_{v,k,i} - E_{v,i}) \cos \alpha - (C_{h,k,i} + E_{h,i}) \sin \alpha] \quad (7.5)$$

in the front segment using	$E_{v,i} = +E_{av,k}$
	$E_{h,i} = +E_{ah,k}$
in the middle segment	$E_{v,i} = E_{h,i} = 0$
in the rear segment	$E_{v,i} = -E_{1v,k}$
	$E_{h,i} = -E_{1h,k}$

The possible anchor force $A_{poss,k}$ is then calculated theoretically from the equilibrium of forces in the horizontal direction as follows:

$$A_{poss,k} = \frac{1}{\cos \alpha} \cdot [E_{ah,k} - E_{1h,k} + \sum Q_{h,k,i} + \sum C_{h,k,i}] \quad (7.6)$$

The analysis of stability at the lower slip plane must be carried out for both permanent and variable loads, and in the case of the second analysis the variable actions may be considered only in unfavourable positions. Imposed loads are therefore included in G_k only if the slip plane angle ϑ is greater than φ_k . Stability is assured when

$$A_{G,k} \cdot \gamma_G \leq \frac{A_{poss,k}}{\gamma_{Ep}} \quad (7.7)$$

where $A_{poss,k}$ is calculated from the polygon of forces with permanent loads, and

$$A_{G,k} \cdot \gamma_G + A_{Q,k} \cdot \gamma_Q \leq \frac{A_{poss,k}}{\gamma_{Ep}} \quad (7.8)$$

where $A_{poss,k}$ is calculated from the polygon of forces with permanent and variable loads.

Where more than one row of anchors intersects the lower slip plane, please refer to EAU 2004 section 8.4.9.9 (R 10).

Example 7.5 Verification of stability at the lower slip plane for a sheet pile wall with grouted anchors

Verification of the lower slip plane is carried out for example 6.10 or 7.3.

1. Defining the body of soil:

Point F lies at the point of zero shear, which according to the structural calculations is at level -12.09 m. Point D is located $l_r/2 = 8.12/2 = 4.06$ m from the base of the anchor at a depth of 9.22 m below ground level. A vertical equivalent wall extends from point D up to ground level. The slip plane angle ϑ is calculated to be 12.1° . For further dimensions, see sketch.

2. Active earth pressure behind sheet pile wall:

The earth pressure distribution was determined in example 6.10 or 6.11 (see sketch). In this case only the earth pressure due to permanent loads is required for checking the lower slip plane because the variable loads have a beneficial effect. The missing earth pressure ordinate at level -12.09 m and the resultants from the redistributed earth pressure diagram produce the following:

$$e_{ah}(-12.09) = 27.3 + 3.09 \cdot 10 \cdot 0.25 = 35.0 \text{ kN/m}^2$$

$$E_{a,k}^A = \left(4.0 \cdot \frac{13.6 + 15.7}{2} \right) / \cos \left(\frac{2}{3} \cdot 30 \right) = 62.4 \text{ kN/m}$$

$$E_{a,k}^{Kl} = \left(3.0 \cdot \frac{15.7 + 17.3}{2} \right) / \cos \left(\frac{2}{3} \cdot 25 \right) = 51.8 \text{ kN/m}$$

$$E_{a,k}^S = \left(2 \cdot \frac{17.3 + 18.3}{2} + 3.09 \cdot \frac{27.3 + 35.0}{2} \right) / \cos \left(\frac{2}{3} \cdot 32.5 \right) = 142.0 \text{ kN/m}$$

3. Earth pressure acting on equivalent wall:

The earth pressure acts perpendicular to the equivalent wall ($\delta = 0$).

Backfill: $K_{agh} = 0.33$; clay with sea-silt: $K_{agh} = 0.41$, $K_{ach} = 1.27$; sand: $K_{agh} = 0.30$

That results in the following earth pressure ordinates:

Level	Active earth pressure $e_{agh,k}$ [kN/m ²]	Cohesion $e_{ach,k}$ [kN/m ²]	Permanent load $e_{aph,k}$ [kN/m ²]
0	0	0	3.3
-2	11.9	0	3.3
-4	17.2	0	3.3
-4	21.3	-12.7	4.1
-4.5	23.1	-12.7	4.1
-7	32.4	-12.7	4.1
-7	23.7	0	3.0
-9.22	30.4	0	3.0

Resultant acting on equivalent wall due to permanent actions:

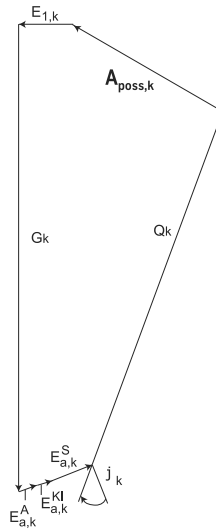
$$E_{1,k} = 2 \cdot \frac{3.3 + 15.2}{2} + 2 \cdot \frac{15.2 + 20.5}{2} + 3 \cdot \frac{12.7 + 23.8}{2} + 2.22 \cdot \frac{26.7 + 33.4}{2}$$

$$= 175.6 \text{ kN/m}$$

4. Weight of body of soil:

$$G'_k = 13.4 \cdot (2 \cdot 18 + 2 \cdot 8 + 3 \cdot 9 + 2.22 \cdot 10 + \frac{12.09 - 9.22}{2} \cdot 10) = 1544.9 \text{ kN/m}$$

5. Draw the polygon of forces and determine $A_{poss,k}$:



permanent loads only:

$$\bar{A}_{poss,k} = 575 \text{ kN/m}$$

$$A_{poss,k} = 575 \cdot 3 = 1725 \text{ kN}$$

$l_r/2 = 4.06 \text{ m} > 3 \text{ m} = a_A \rightarrow$ no need to reduce $A_{poss,k}$

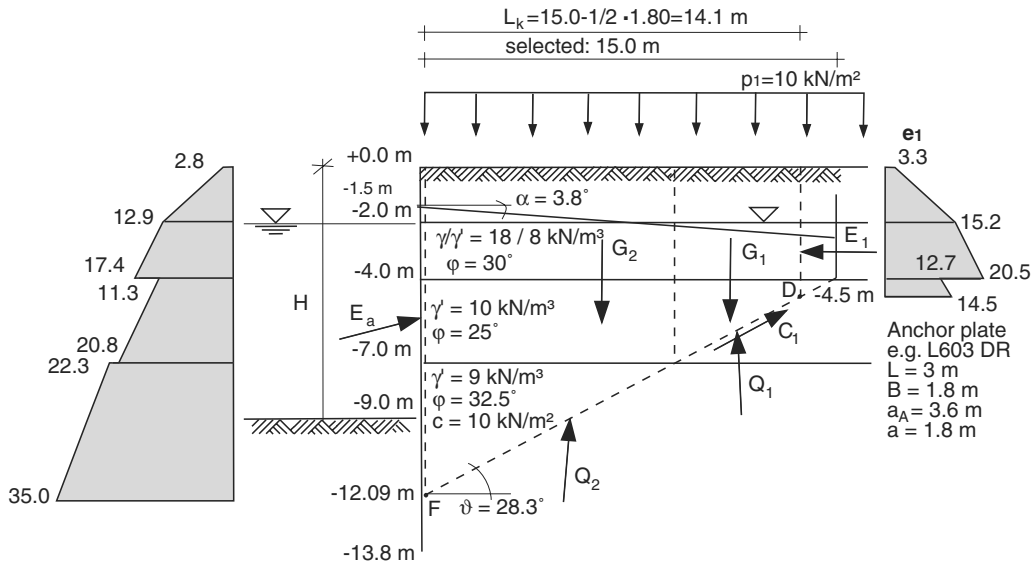
6. Verification:

$$3 \cdot 109.3 \cdot 1.35 \leq \frac{1725}{1.4} \quad (\text{see eq. 7.7})$$

$$442.7 \text{ kN} < 1232.1 \text{ kN}$$

The verification for permanent and variable loads is not required because the variable load acts beneficially on $A_{poss,k}$, and A_d in this case is less than $A_{poss,k}/\gamma_{Ep}$.

Example 7.6 Verification of stability at the lower slip plane for a sheet pile wall with round steel tie rods



Verification of the lower slip plane is carried out for example 6.10 or 7.4.

1. Defining the wedge of soil:

Point *D* is located at the base of the equivalent wall at a depth of 4.5 m. The equivalent wall is located $1/2 \cdot a = 0.9$ m in front of the anchor plates. The slip plane angle ϑ is calculated to be 28.3° . The length selected for the round steel tie rod is 15.0 m. For further dimensions, see sketch.

2. Active earth pressure behind sheet pile wall:

The earth pressure distribution was determined in example 6.10 or 6.11 (see sketch). In this case only the earth pressure due to permanent loads is required for checking the lower slip plane because the variable loads have a beneficial effect. The earth pressure is determined without excess hydrostatic pressure.

$$\begin{aligned}
 E_{ah,k} &= 2.0 \cdot \frac{2.8 + 12.9}{2} + 2.0 \cdot \frac{12.9 + 17.4}{2} + 3.0 \cdot \frac{11.3 + 20.8}{2} + 5.09 \cdot \frac{22.3 + 35.0}{2} \\
 &= 15.7 + 30.3 + 48.2 + 145.8 \\
 &= 240.0 \text{ kN/m} \\
 E_{av,k} &= 15.7 \cdot \tan\left(\frac{2}{3}30\right) + 30.3 \cdot \tan\left(\frac{2}{3}30\right) + 48.2 \cdot \tan\left(\frac{2}{3}25\right) + 145.8 \cdot \tan\left(\frac{2}{3}32.5\right) \\
 &= 5.7 + 11.0 + 14.4 + 57.9 \\
 &= 90.0 \text{ kN/m}
 \end{aligned}$$

3. Earth pressure acting on equivalent wall:

The earth pressure acts perpendicular to the equivalent wall ($\delta = 0$).

Backfill: $K_{agh} = 0.33$; clay with sea-silt: $K_{agh} = 0.41$, $K_{ach} = 1.27$

See example 7.5 for earth pressure ordinates.

$$E_{1h,k} = 2 \cdot \frac{3.3 + 15.2}{2} + 2 \cdot \frac{15.2 + 20.5}{2} + 0.5 \cdot \frac{12.7 + 14.5}{2} = 61.0 \text{ kN/m}$$

4. Weight of body of soil:

The body of soil is divided into 2 segments to match the soil strata; p_1 must be considered if $\varphi < \vartheta$.

$$G_{k,1} = \frac{7.0 - 4.5}{\tan 28.3} \cdot \left(2.0 \cdot 18 + 2.0 \cdot 8 + 0.5 \cdot 9 + \frac{7.0 - 4.5}{2} \cdot 9 + 10 \right) = 361.2 \text{ kN/m}$$

$$G_{k,2} = \frac{12.09 - 7.0}{\tan 28.3} \cdot \left(2.0 \cdot 18 + 2.0 \cdot 8 + 3.0 \cdot 9 + \frac{12.09 - 7.0}{2} \cdot 10 \right) = 987.4 \text{ kN/m}$$

5. Cohesion at the lower slip plane:

$$C_{v,k,1} = 10 \cdot (7.0 - 4.5) = 25.0 \text{ kN/m}$$

$$C_{h,k,1} = \frac{25.0}{\tan 28.3} = 46.4 \text{ kN/m}$$

$$C_{k,2} = 0 \text{ kN/m}$$

6. Friction forces at the lower slip plane according to eq. 7.5:

$$Q_{h,k,1} = \frac{\sin(25 - 28.3)}{\cos(25 - 28.3 - 3.8)} \cdot [(361.2 - 25) \cdot \cos 3.8 - (46.4 + 61.0) \sin 3.8] = -19.5 \text{ kN/m}$$

$$Q_{h,k,2} = \frac{\sin(32.5 - 28.3)}{\cos(32.5 - 28.3 - 3.8)} \cdot [(987.4 - 90.0) \cdot \cos 3.8 - (240.0) \sin 3.8] = 64.4 \text{ kN/m}$$

7. Verification:

$$A_{poss,k} = \frac{1}{\cos 3.8} \cdot (240.0 - 61.0 - 19.5 + 64.4 + 46.4) = 270.9 \text{ kN/m} \quad (\text{see eq. 7.6})$$

$$A_d = A_{G,k} \cdot \frac{\cos 30}{\cos 3.8} \cdot \gamma_G$$

$$= 109.3 \cdot \frac{\cos 30}{\cos 3.8} \cdot 1.35 = 128.1 \text{ kN/m}$$

$$128.1 \text{ kN/m} < \frac{270.9}{1.4} = 193.5 \text{ kN/m} \quad (\text{see eq. 7.7})$$

The verification for permanent and variable loads is not required because the variable load acts beneficially on $A_{poss,k}$ and A_d in this case is also less than $A_{poss,k}/\gamma_{Ep}$.

$$A_d = (A_{G,k} \cdot \gamma_G + A_{Q,k} \cdot \gamma_Q) \cdot \frac{\cos 30}{\cos 3.8} = 158.1 \text{ kN/m} < 193.5 \text{ kN/m}$$

7.3.6 Design for serviceability

When designing for **serviceability** it is important to show that an anchor under load is not subjected to excessive deformations. This is carried out on the basis of a test loading. It is especially important to make sure that individual anchors are not subjected to significantly more severe deformations than other anchors. Verification calls for the characteristic resistance $R_{2,k}$ associated with a characteristic deformation $s_{2,k}$ to be determined from the load-deformation curve of the anchor. The characteristic resistance must be greater than or equal to the characteristic loads $E_{2,k}$.

In the case of grouted anchors, the serviceability of an individual anchor is validated by means of an acceptance test to DIN EN 1537:2001-01.

7.4 Testing

The suitability of anchors should always be checked in a loading test. Grouted anchors must satisfy special requirements, which means proving their suitability by testing at least three anchors. In addition, every anchor undergoes an acceptance test. After the test, the grouted anchors are generally defined with respect to their prestressing force. DIN EN 1537:2001-01 describes the execution of loading tests.

7.5 Construction details

The hinged connection of an anchor to a trough-type sheet pile wall is carried out on the centre-of-gravity axis in the trough, especially on walls with interlocks. In the case of combined sheet pile walls, the web of the loadbearing pile offers the best connection options. The connection via a capping beam at the top of the sheet pile wall is another option primarily suited to smaller tension piles and lightweight sheet pile walls. With threaded anchors there is the additional option of a connection with a washer plate, hinged splice plate and nut. In order to avoid having to install an anchor at every trough, a horizontal **waling** of steel or reinforced concrete can be provided to spread the load. This should be positioned on the land side in the case of quay structures, and on the excavation side in the case of excavation enclosures in order to guarantee easy removal.

Anchors can be installed before or after erecting the sheet pile wall. Maintaining the intended position of the anchor, which is necessary to achieve an accurate connection, is easier to establish when installing the anchors afterwards. Anchor piles can be driven through an opening cut in the sheet pile wall, for instance. Figs. 7.6 to 7.8 show possible anchor-sheet pile connection details.

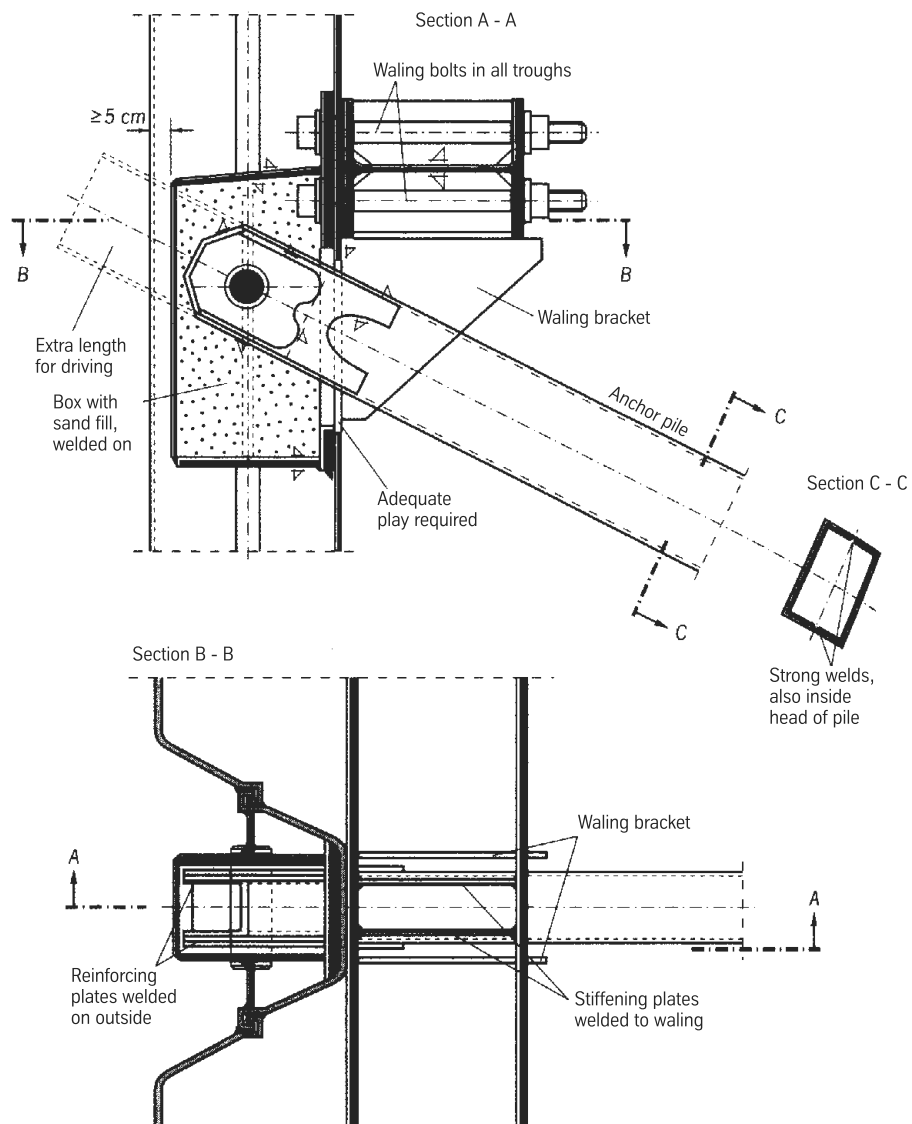


Figure 7.6: Hinged connection of a steel anchor pile to heavy sheet piling by means of a hinge pin to EAU 2004 section 8.4.14.4

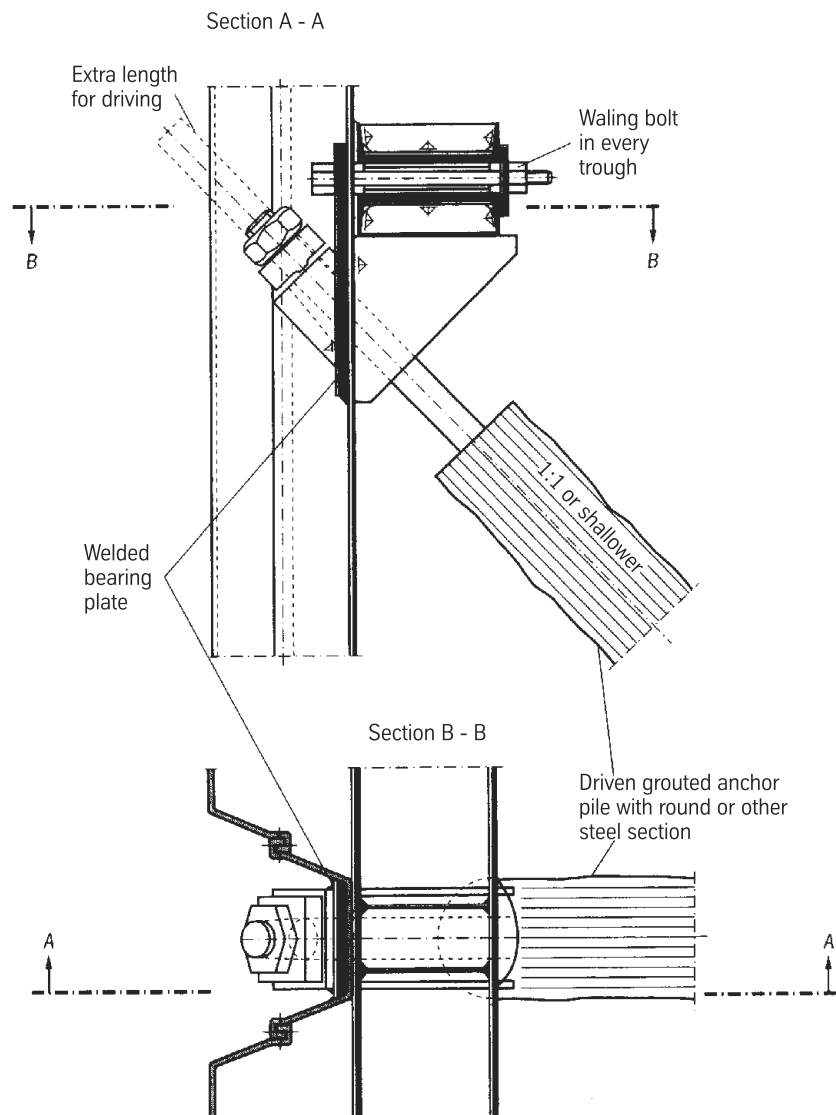


Figure 7.7: Hinged connection of a driven grouted anchor pile to heavy sheet piling to EAU 2004 section 8.4.14.4

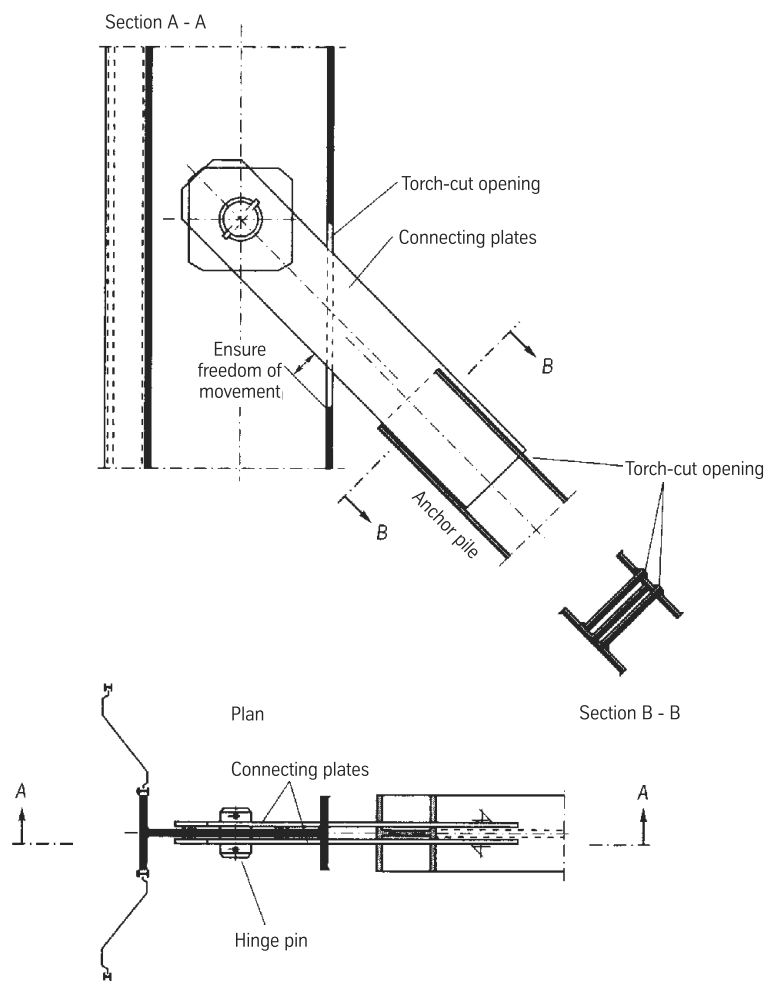


Figure 7.8: Hinged connection of a steel anchor pile to combined steel sheet piling with single bearing piles by means of a hinge pin to EAU 2004 section 8.4.14.4

Chapter 8

Using FEM for the design of sheet piling structures

8.1 Possibilities and limitations

Like analytical methods of computation, FEM involves **modelling errors** due to deviations of the physical-mathematical equivalent problem from the initial problem plus **data errors** due to deviations in the chosen values of the initial parameters of the finite element model from the real values. And like other discretisation methods, FEM also involves **procedural errors** (numerical errors) due to the deviation of the solution of the discretised problem from the solution of the continuum problem plus **rounding errors** due to the deviation of the solution with exact numerical values from the solution with approximated numerical values (computer arithmetic).

8.2 Recommendations regarding the use of FEM in geotechnics

Since 1991 the “Numerics in Geotechnics” working group has published four sets of recommendations (in German only) for the use of FEM in geotechnics:

- Set 1 – General recommendations for modelling (Meißner, 1991)
- Set 2 – Modelling recommendations for underground tunnels (Meißner, 1996)
- Set 3 – Modelling recommendations for excavations (Meißner, 2002)
- Set 4 – Recommendations for material models for soils, modelling for serviceability analyses, stability and groundwater (Schanz, 2006)

In EAB recommendation R 103, WEISSENBACH (2003) speaks about the use of FEM within the scope of the new DIN 1054. Further recommendations regarding modelling can also be

found in POTTS ET AL. (2002). A description of various sources of errors and corresponding error effects when using FEM in geotechnics is given, for example, in (HÜGEL 2004/2005).

Recommendations for reducing procedural errors can be obtained from general textbooks on FEM, especially for non-linear problems, e.g. in (WRIGGERS, 2001) or (BATHE, 2002).

8.2.1 Advice on the use of FEM for retaining walls

2D/3D problem

Retaining wall structures are generally simulated with 2D equivalent models for FEM purposes (which is, of course, not possible with distinctly 3D problems such as the corners of excavations). Resolved structures such as struts, anchors, staggered sheet pile walls or bearing pile walls can be taken into account approximately in the 2D equivalent model but assuming equivalent stiffnesses related to a 1 m length of wall. Every individual case must be checked to ensure that the equivalent structure does not exhibit any unrealistic properties. Examples of this are: 2D equivalent anchors may not relieve the earth pressure acting on the retaining wall, 2D equivalent walls for staggered sheet pile walls may not be impermeable at the level of the staggered pile ends, 2D equivalent walls for bearing pile walls may not mobilise any unrealistically large passive earth pressures. It is not always clear whether all the deformations and stresses calculated with the 2D equivalent model are on the safe side; see (HÜGEL, 2004), for example. Examples of complex 3D analyses of sheet piling structures can be found in (BOLEY ET AL., 2004) and (MARDFELDT, 2006).

Generalisation of the subsoil

Soil strata and groundwater conditions should be generalised in the finite element model depending on the database. However, when doing so, it must be ensured that the mechanical and hydraulic behaviour of the finite element model is comparable with the initial problem.

Subsoil segment and boundary conditions

The size of the subsoil segment should be specified such that the boundaries do not have any significant effect on the deformations at the point of load transfer or such that the boundary conditions are known. Estimates of the dimensions necessary can be found in (MEISSNER, 2002) for the case of excavations.

Geometric non-linearity

Retaining wall structures are generally designed to be so stiff that finite element analyses may be based on geometric linearity. In the case of a yielding earth resistance and/or yielding anchorage, comparative analyses can be used to check whether geometric non-linearity needs to be taken into consideration.

Modelling of sheet pile walls

Sheet pile walls are usually discretised with structural elements (beam or shell elements). This type of discretisation can lead to problems if under vertical loading a significant part of the load is carried via the base of the wall. In the case of individual sections, an extension of interface elements can be taken into consideration at the base of the wall so that the sheet piling section can penetrate into the ground and no unrealistic stress peaks can occur in the body of soil below the base of the wall – see recommendation E4-15 in (SCHANZ, 2006). In the case of combined sheet pile walls under vertical loading where significant bearing pressures are mobilised, a bearing pressure can be modelled with the help of a stiff transverse beam at the base of the wall (MEISSNER, 2002).

In the case of a staggered sheet pile wall, the 2D equivalent model must take into account the fact that the base of the equivalent wall is permeable.

Where possible, the force transfer between sheet pile wall and soil should be modelled with interface elements or by way of kinematic contact formulation. This guarantees that no tensile stresses are transferred along the sheet pile/soil boundary surfaces and that, with corresponding action effects, irreversible sliding between sheet pile wall and soil can take place. Bilinear contact and friction principles are used for this in the simplest case.

Modelling of struts and anchors

Struts and anchors are usually discretised with structural elements (bar or beam elements). In 2D equivalent models, the strain stiffness EA is related to 1 m of sheet pile wall. The bending stiffness EI of stiffeners should be dealt with similarly. On the other hand, the bending stiffness of equivalent anchors should be neglected so that the earth pressure acting on the sheet pile wall is not relieved in the 2D equivalent model.

The anchor/soil boundary surfaces are not normally discretised with contact elements. If this method is used, however, a lower wall friction angle δ must be guaranteed so that a comparable anchor pull-out resistance is established in the 3D problem and in the 2D equivalent model (the surface area of the 2D equivalent anchor is considerably larger than that of an individual anchor).

Material models for soils

The choice of the **material models** for soils is limited in some finite element programs. The material models of the “linear elastic, ideal plastic” category can lead to incorrect predictions in the case of retaining wall structures – see, for example, (HÜGEL, 2005), (VERMEER & WEHNERT, 2005) and recommendation E3-4 in (SCHANZ, 2006). The use of high-quality elastoplastic or hypoplastic material models is called for which can at least describe the main phenomena of the mechanical behaviour of soils:

- stiffnesses not dependent on pressure,
- different stiffnesses for unloading and reloading,
- shear behaviour for drained and undrained conditions,

- dilatancy behaviour.

For a detailed explanation of the main phenomena of the mechanical behaviour of soils, see, for example, (HERLE & MAŠÍN, 2005) or (SCHANZ, 2006). High-quality material models may even be necessary during the feasibility studies for sheet piling structures.

Initial state of soil

A steady-state earth pressure (K_0 -state) is normally assumed. This is, however, linked to various conditions (HÜGEL, 2004). It should not be forgotten that the steady-state earth pressure coefficient K_0 depends on the loading history of the soil. Initial values for pore water pressures and excess pore water pressures can be determined from in situ measurements. Initial values for the in situ density of the soil can be specified by penetrometer tests or, in the case of high-quality material models, in conformity with their compression law.

Simulating construction processes

The majority of published finite element projects do not include any simulation of the installation of the sheet pile wall, but instead the corresponding elements are activated in their final position in the finite element model. This technique is often referred to as **wished-in-place**. The changes to state variables and stresses and strains in structures due to the construction process are therefore ignored. However, these may be relevant, especially where problems with small deformations occur (HÜGEL, 1996; VON WOLFFERSDORFF, 1997).

Currently, the simulation of the construction process is restricted to university facilities because only they have the necessary hardware and software. In practice the construction processes are usually not simulated.

8.3 Example of application

8.3.1 Initial problem

The quay structure already considered in examples 6.10 and 6.11 (sheet pile wall plus tubular grouted anchors) will be used for this example (see Fig. 8.1). The quay structure is to be constructed from the land side.

The system dimensions are as for the structural calculations given in examples 6.10 and 6.11 for a partially fixed sheet pile wall. A deformation forecast for the structure is to be generated with the help of a 2D finite element model. To do this, the commercially available finite element program PLAXIS Professional, version 8.2-8 in this example, will be used.

There are no neighbouring structures in this case. With the help of the finite element analysis, the serviceability of the ground surface on the land side for traffic is to be checked and the displacement of the sheet pile wall assessed in this context.

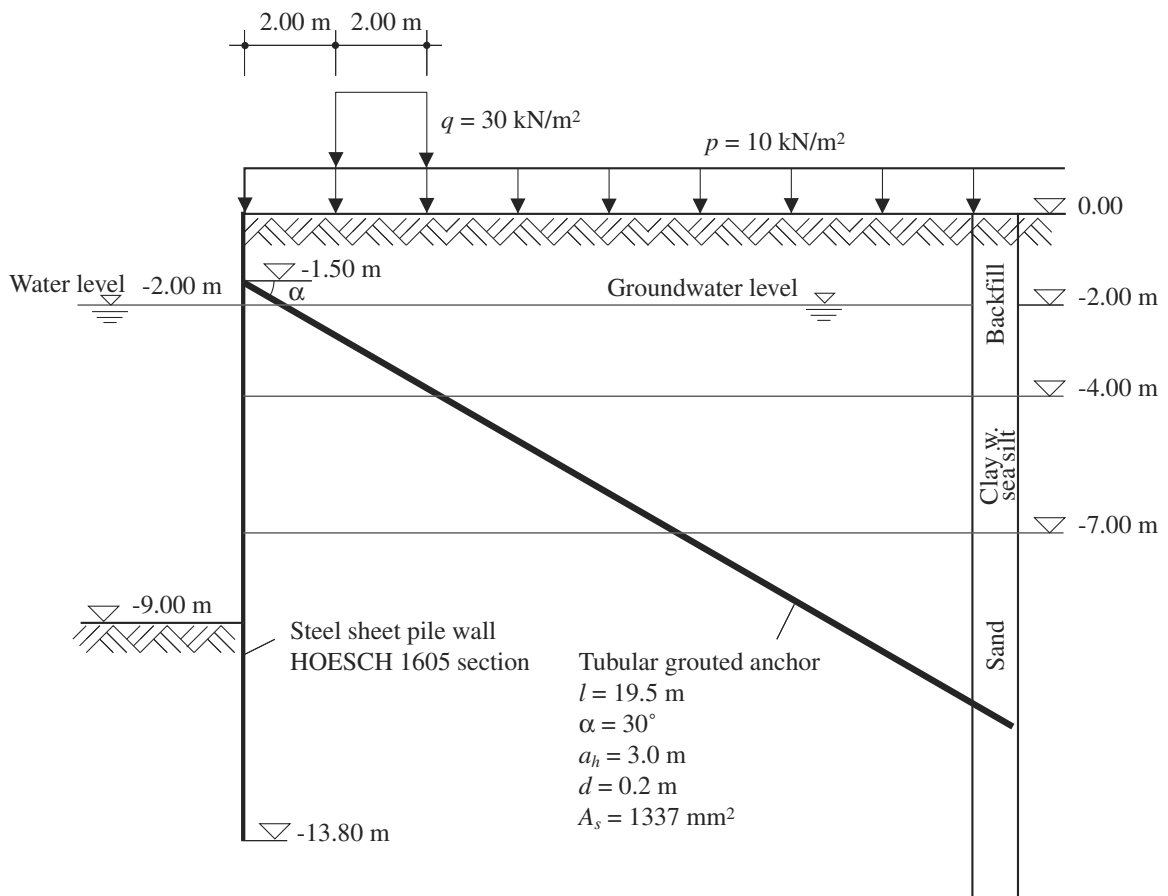


Figure 8.1: Initial problem – quay structure

8.3.2 Modelling

Subsoil segment and boundary conditions

The subsoil segment is specified according to the recommendations of (MEISSNER, 2002) as 71×41 m (see Fig. 8.2). The following boundary conditions are specified for the granular structure and the groundwater (see Fig. 8.2):

- Displacements are specified for the bottom and lateral boundaries (Dirichlet boundary condition), the ground surface is unstressed (Neumann boundary condition).
- The pore water pressure $u = 0$ at the level of the water table (Dirichlet boundary condition), the hydraulic head $h = \text{const.}$ at the bottom and lateral boundaries (Dirichlet boundary condition).

Modelling the body of soil

The body of soil is discretised using 6-node continuum elements with quadratic displacement assumption and a linear assumption for the pore water pressure. The mechanical behaviour of the soil is modelled with the “Hardening Soil Model” implemented in PLAXIS.

It should be mentioned at this point that the “Hardening Soil Model” does not describe how the stiffnesses and strengths are dependent on the void ratio and hence does not describe the deconsolidation exhibited by dense, non-cohesive soils and preloaded cohesive soils. The following limitations of the model are pointed out here even though they are not critical for this particular boundary value problem:

- When using the “Hardening Soil Model” for undrained analyses, like with other material models it should be remembered that the cohesion of the undrained soil c_u is not a material parameter, but instead is calculated from the material model. This can lead to discrepancies with c_u values obtained from soil investigations. In order to carry out finite element analyses with given c_u values, various procedures are possible, see, for example, (MEISSNER, 1991) or (VERMEER & WEHNERT, 2005). The choice of a particular method should be made in consultation with the geotechnical engineer.
- The inherent anisotropy of soils is not modelled.
- The viscosity of cohesive soils is not taken into account.
- As the model only models the isotropic solidification, it cannot be used for problems with cyclic actions.

Please refer to the PLAXIS manual and (SCHANZ, 1998) in order to identify the parameters for the “Hardening Soil Model”. The sets of parameters chosen with characteristic soil parameters are listed in table 8.1. The unit weights and shear parameters have been taken from examples 6.10 and 6.11, missing parameters have been estimated. In practice, the material model and corresponding soil parameters should be specified in consultation with the geotechnical engineer so that no discrepancies ensue between his model of the soil and the finite element model.

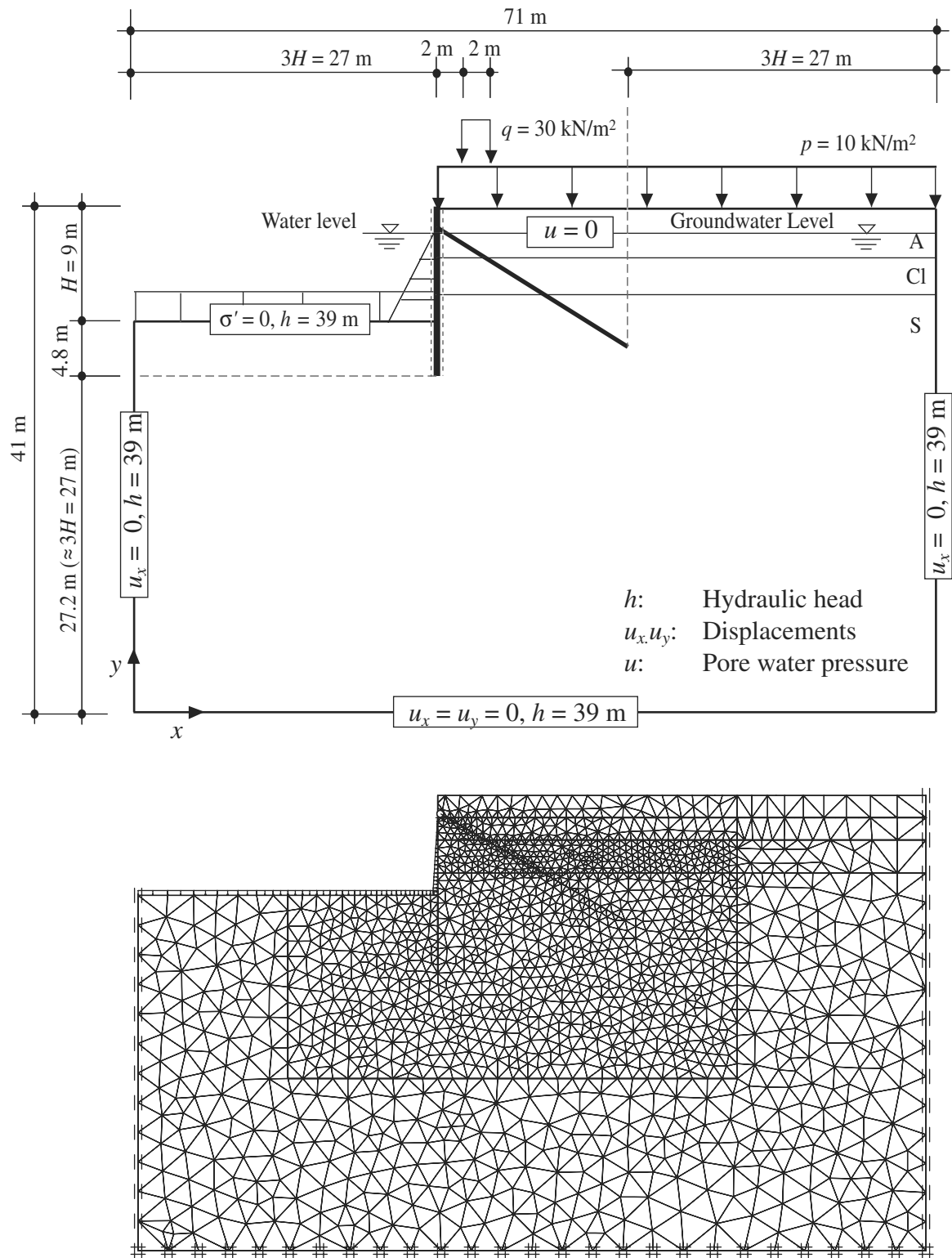


Figure 8.2: FE model with dimensions and boundary conditions for the final state

Parameter	Unit	Fill	Clay w. sea-silt	Sand
γ	[kN/m ³]	18	19	20
γ'	[kN/m ³]	8	9	10
p^{ref}	[kN/m ²]	100	100	100
E_{oed}^{ref}	[kN/m ²]	7000	2000	30 000
m	[-]	0.5	1.0	0.5
E_{50}^{ref}	[kN/m ²]	7000	2000	30 000
E_{ur}^{ref}	[kN/m ²]	21 000	6000	90 000
ν_{ur}	[-]	0.2	0.2	0.2
φ	[°]	30.0	25.0	32.5
c	[kN/m ²]	0	10.0	0
ψ	[°]	0	0	2.5

Table 8.1: Set of parameters chosen for the “Hardening Soil Model” in PLAXIS

Modelling the sheet pile wall

The HOESCH 1605 sheet pile wall section is discretised with 3-node beam elements assuming a quadratic displacement. A linear elastic behaviour is assumed for the sheet pile wall. Using the section properties from appendix A, we get the following system parameters:

$$\left. \begin{aligned} E &= 2.1 \cdot 10^8 \text{ kN/m}^2 \\ A &= 1.363 \cdot 10^{-2} \text{ m}^2/\text{m} \\ I &= 2.8 \cdot 10^{-4} \text{ m}^4/\text{m} \\ G &= 1.05 \text{ kN/m/m} \end{aligned} \right\} \begin{aligned} EA &= 2\,862\,300 \text{ kN/m} \\ EI &= 58\,800 \text{ kNm}^2/\text{m} \end{aligned}$$

The sheet pile/soil boundary surface is discretised with interface elements. The wall friction angle for the steel/soil boundary surface is given as $\delta = 2\varphi/3$. In order to achieve a realistic bond between base of wall and body of soil, the interface elements are extended 2 m into the body of soil. However, $\delta = \varphi$ applies for these interface elements.

Modelling the anchors

The tubular grouted anchors (19.5 m long, $d = 20$ cm OD, cross-sectional area of steel tendon $A_s = 1337 \text{ mm}^2$) positioned at a horizontal spacing of 3.0 m are discretised approximately in the 2D equivalent model by means of beam elements. In order to prevent the equivalent anchor plate relieving the active earth pressure, its bending stiffness is given as $EI = 1 \text{ kNm}^2/\text{m}$. Using $A_s = 1.337 \cdot 10^{-3} \text{ m}^2$ and $E_s = 2.1 \cdot 10^8 \text{ kN/m}^2$, the strain stiffness of an individual anchor is calculated approximately as:

$$EA \approx E_s A_s = 2.1 \cdot 10^8 \cdot 1.337 \cdot 10^{-3} = 280\,770 \text{ kN}$$

A strain stiffness related to 1 m should be assumed for the 2D equivalent model:

$$\frac{EA}{a_h} = \frac{280\,770}{3.0} = 93\,590 \text{ kN/m}$$

Interface elements are omitted along the anchor/soil boundary surface because the 2D equivalent model contains an unrealistically large surface area, which can lead to an overestimate of the anchor's pull-out resistance. If interface elements are taken into account, the corresponding wall friction angle must be adjusted so that the individual anchors and the 2D equivalent anchor plate provide a pull-out resistance of similar magnitude.

Degree of discretisation

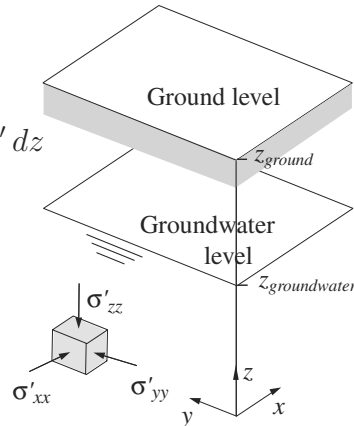
The degree of discretisation should be specified in combination with the cut-off tolerance for the equilibrium iteration such that the global total error in the finite element analysis does not exceed a given error tolerance. (HÜGEL, 2004) includes a corresponding sample analysis for a comparable retaining wall structure. Based on this, a sufficiently accurate combination of degree of discretisation (see Fig. 8.2) and cut-off tolerance for the equilibrium iteration amounting to $F_u/F_e = 0.01$ (F_u : out-of-balance force, F_e : external force) is assumed for this system.

Loading history

The following states are considered (see Fig. 8.3):

- 0 Initial state: As the stratum boundaries, the ground surface and the water table are horizontal, a steady-state earth pressure situation (K_0 -state) can be assumed. The effective stresses and the pore water pressure are then calculated:

$$\begin{aligned}\sigma'_{zz} &= \int_{z_{\text{ground}}}^{z_{\text{groundwater}}} \gamma \, dz + \int_{z_{\text{groundwater}}}^z \gamma' \, dz \\ \sigma'_{xx} &= \sigma'_{yy} = K_0 \sigma'_{zz} \\ u &= \int_{z_{\text{groundwater}}}^z \gamma_w \, dz\end{aligned}$$



In this case the steady-state earth pressure coefficient K_0 for initial loading is given:

$$K_0 = 1 - \sin \varphi$$

In the initial state, all structures in and on the ground plus all surcharges are deactivated in the finite element model.

- 1 Steel sheet pile wall installed (wished-in-place).

- 2 Excavation on water side down to -1.5 m.
- 3 Tubular grouted anchors installed (wished-in-place).
- 4 Excavation on water side down to -9.00 m (corresponds to serviceability state for LC 1 with $p = 0$).
- 5 Permanent surcharge p activated (corresponds to serviceability state for LC 1 with $p = 10$ kN/m²).
- 6 Additional variable surcharge q activated (corresponds to serviceability state for LC 2 with $p = 10$ kN/m² and $q = 30$ kN/m²).
- 7 Variable surcharge q deactivated (check whether q causes irreversible deformations).

8.3.3 Results

Selected results from the finite element analyses are given in table 8.2 and in Figs. 8.4 to 8.7. These can be summarised as follows:

- **Loading:** In state 7 the finite element analysis indicates irreversible deformations due to the variable load q . According to DIN 1054:2005-01, the variable load should therefore be taken into account when checking the serviceability of the structure in the finite element model.
- **Earth pressure distribution:** As expected, at the serviceability limit state the passive earth pressure is lower than that given by the calculations in example 5.2 owing to the flexibility of the retaining wall. The active earth pressure is greater in the finite element analysis (see Fig. 8.6).
- **Support at base of wall:** The moment distributions calculated confirm that with an embedment depth of 4.8 m in the soil, the base of the sheet pile wall is partially fixed (see Figs. 8.5 and 8.6).
- **Deformations:** As expected, the deformations of the sheet pile wall correspond to a flexible installation, the anchors yield. The large wall displacement causes corresponding settlement of the ground surface on the land side, a maximum inclination of approx. 1:80 occurs (see Fig. 8.7). During the construction phase, the deformations do not represent a problem for quay structures. When in service, the depression caused by the settlement can be compensated for by backfilling so that the area is trafficable, e.g. for stacking containers.

Other possible issues for this boundary value problem might be the long-term behaviour of the quay structure due to other actions, the change in the water table over time and viscous processes in the stratum of clay with sea-silt. To do this, the finite element model described here would need to be adjusted with respect to the material model and the identification of parameters.

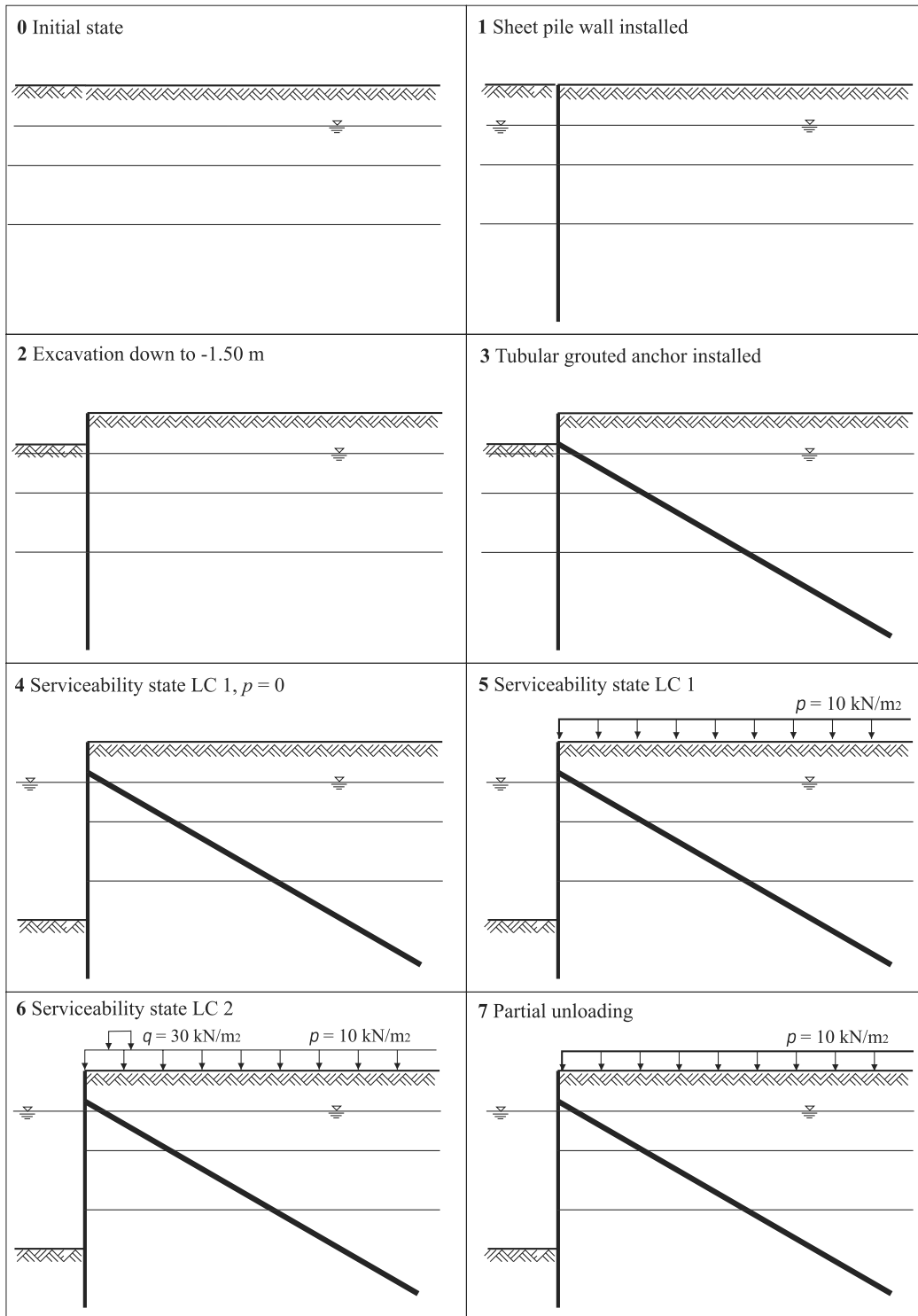


Figure 8.3: Construction situations when simulating the loading history in PLAXIS

Loading step	Loading case	Sheet pile wall		Anchor
		N_{\max} [kN/m]	M_{\max} [kNm/m]	N_{\max} [kN/m]
2		25.8	19.6	–
4	LC 1, $p = 0 \text{ kN/m}^2$, $q = 0 \text{ kN/m}^2$	135.8	187.9	119.5
5	LC 1, $p = 10 \text{ kN/m}^2$, $q = 0 \text{ kN/m}^2$	179.7	239.7	162.4
6	LC 2, $p = 10 \text{ kN/m}^2$, $q = 30 \text{ kN/m}^2$	216.6	274.3	201.0

Table 8.2: Calculated maximum internal forces in sheet pile wall and anchor

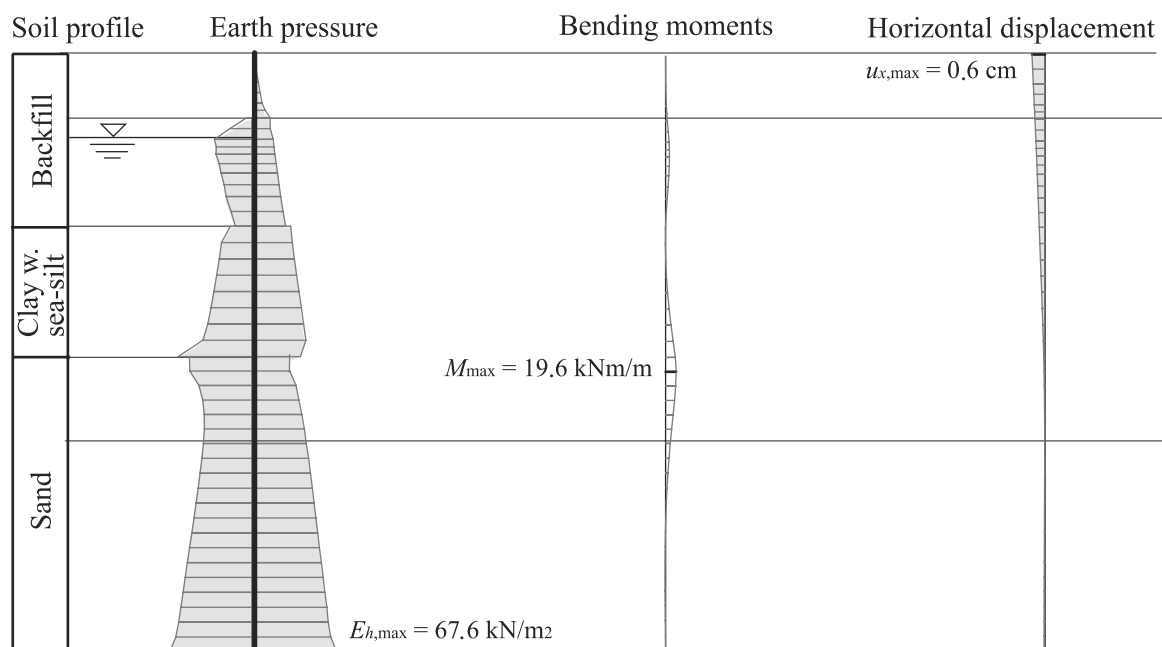


Figure 8.4: Calculated earth pressure, bending moment and horizontal displacement diagrams for state 2

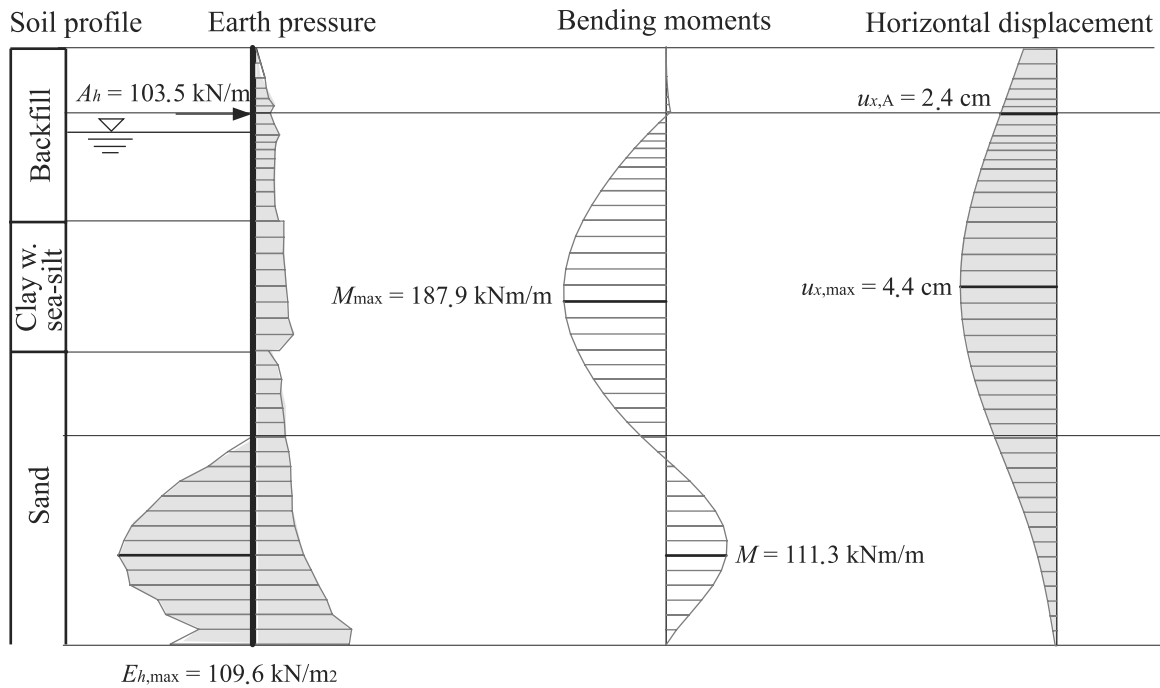


Figure 8.5: Calculated earth pressure, bending moment and horizontal displacement diagrams for state 4 (LC 1, $p = 0, q = 0$)

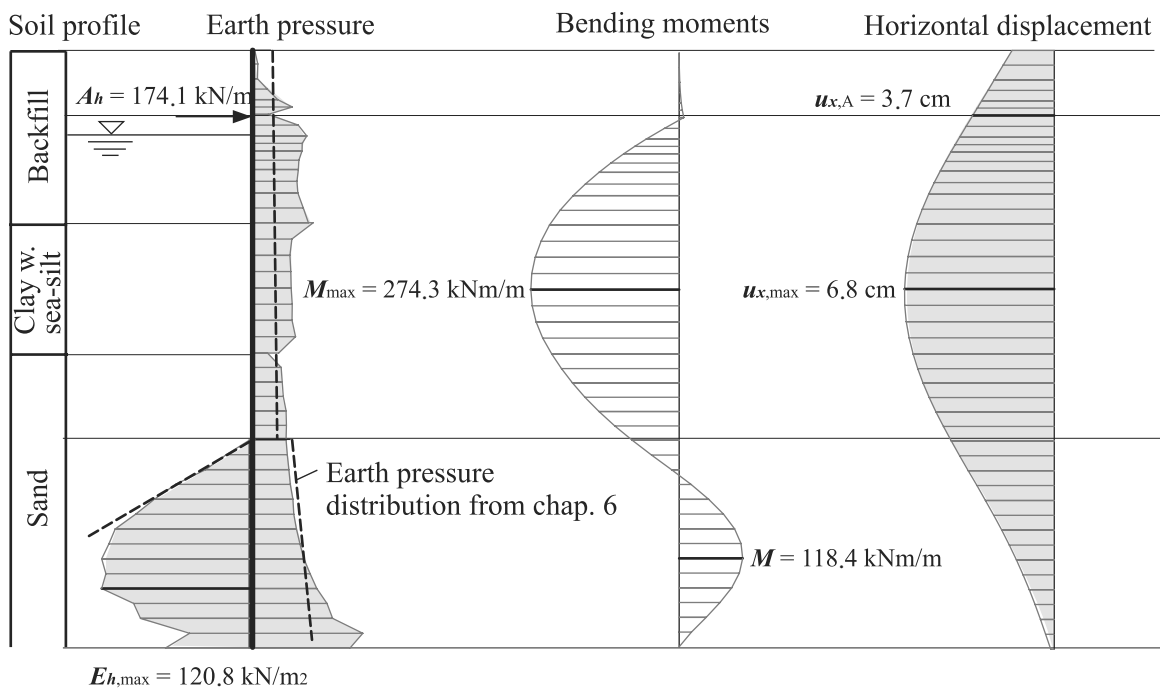


Figure 8.6: Calculated earth pressure, bending moment and horizontal displacement diagrams for state 6 (LC 2, $p = 10, q = 30$)

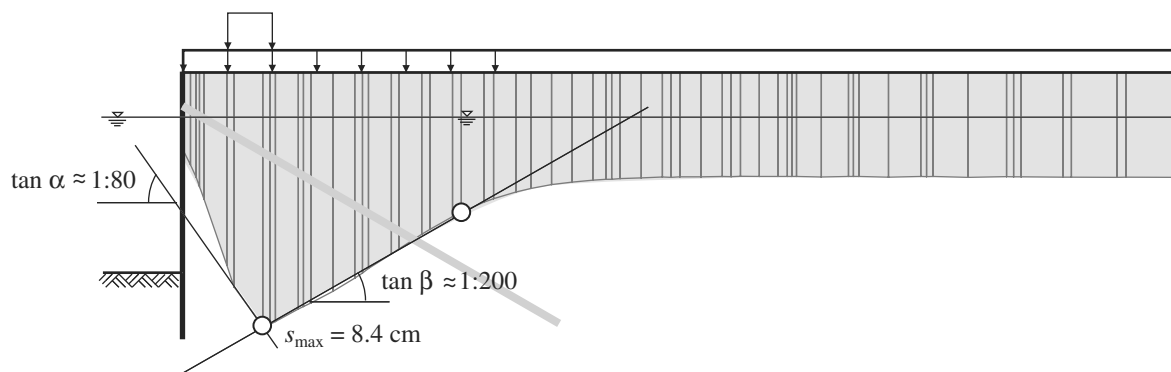


Figure 8.7: Calculated settlement of ground surface on land side for partially fixed sheet pile wall for LC 2

Chapter 9

Dolphins

9.1 General

Dolphins are required in waterways and ports for various tasks: as berthing or mooring dolphins. Their various functions require an analysis of different actions. Berthing dolphins must be designed for the impact of ships, mooring dolphins are subjected to the pull of mooring lines, wind loads and hydrodynamic pressures.

Dolphins can consist of single piles or groups of piles, the latter usually being met with in the form of lightweight timber piles in old structures. In the form of single piles, steel tubes or compound sections assembled from sheet piles, e.g. LARSSEN steel sheet piles, are to be recommended.

9.2 Loads

The critical design loads for dolphins result from the impact of ships during berthing manoeuvres or the pull on the mooring lines of ships. The latter effect is made up of ship movements due to currents, wind, waves or ice. Berthing dolphins are designed for the ship impact loading case with a force $F_{S,k}$ such that the berthing energy can be converted into deformation work in the dolphin. The **energy absorption capacity** $A_{k,exist}$ of a dolphin is calculated from the ship impact force F_S and the horizontal deflection f of the dolphin at the level of application of the force:

$$A_{k,exist} = 1/2 \cdot F_{S,k} \cdot f \quad (9.1)$$

The available energy absorption capacity $A_{k,exist}$ of a dolphin should be selected such that it is greater than or equal to the required energy absorption capacity A . The required energy absorption capacity A describes the component of the kinetic energy of the ship that must be absorbed by the dolphin. This is calculated using the mass, length, speed, turning speed and displacement of the ship, the spacing of the dolphins and the clearance under the keel. An exact description of how to calculate the required energy absorption capacity can be found in EAU 2004 section 13.3 (R 128).

Subjected to the critical impact action F_S , the design value of the steel stresses may not exceed

the yield strength f_y in the case of berthing dolphins. For mooring dolphins, the design value of the steel stresses due to line pull, wind loads and water pressure may be equal to the maximum steel stress f_u .

9.3 Determining the passive earth pressure

The passive earth pressure is calculated as a three-dimensional passive earth pressure E_{ph}^r from the components due to the self-weight of the soil, cohesion and a possible bottom surcharge according to DIN 4085:2007.

$$E_{ph,k}^r = E_{pgh,k}^r + E_{pch,k}^r + E_{pph,k}^r \tag{9.2}$$

The three-dimensional stress state is calculated assuming dolphin equivalent widths depending on the depth and the nature of the loading. In doing so, we distinguish between “near the surface” and “low position”. Fig. 9.1 illustrates the approach using the three-dimensional passive earth pressure variables. In cohesive soils, the undrained shear parameters φ_u and c_u must be used owing to the rapid loading. The BLUM equivalent force C is calculated from

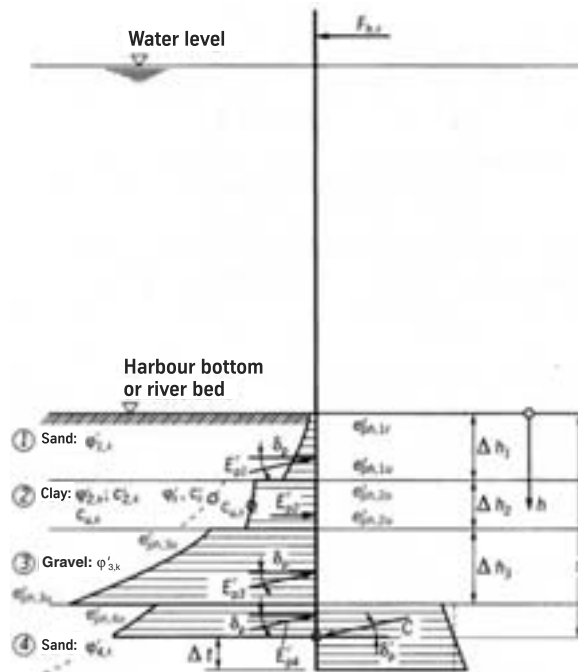


Figure 9.1: Applying the three-dimensional passive earth pressure and equivalent force C in stratified soil (EAU 2004)

the difference between the mobilised three-dimensional passive earth pressure and the forces applied while neglecting the effect of the active earth pressure. This force may be inclined at an angle of up to $\delta'_p = +2/3\varphi$ to a line perpendicular to the dolphin, whereby the condition

$\sum V = 0$ must always be satisfied.

$$C_{h,k} = E_{ph,mob}^r - \sum F_{h,k,i} \tag{9.3}$$

$\sum F_{h,k,i}$: sum of actions
 $E_{ph,mob}^r$: mobilised three-dimensional passive earth pressure
 $= E_{ph,k}^r / (\gamma_Q \cdot \gamma_{Ep})$
 γ_Q, γ_{Ep} : partial safety factors for actions and passive earth pressure

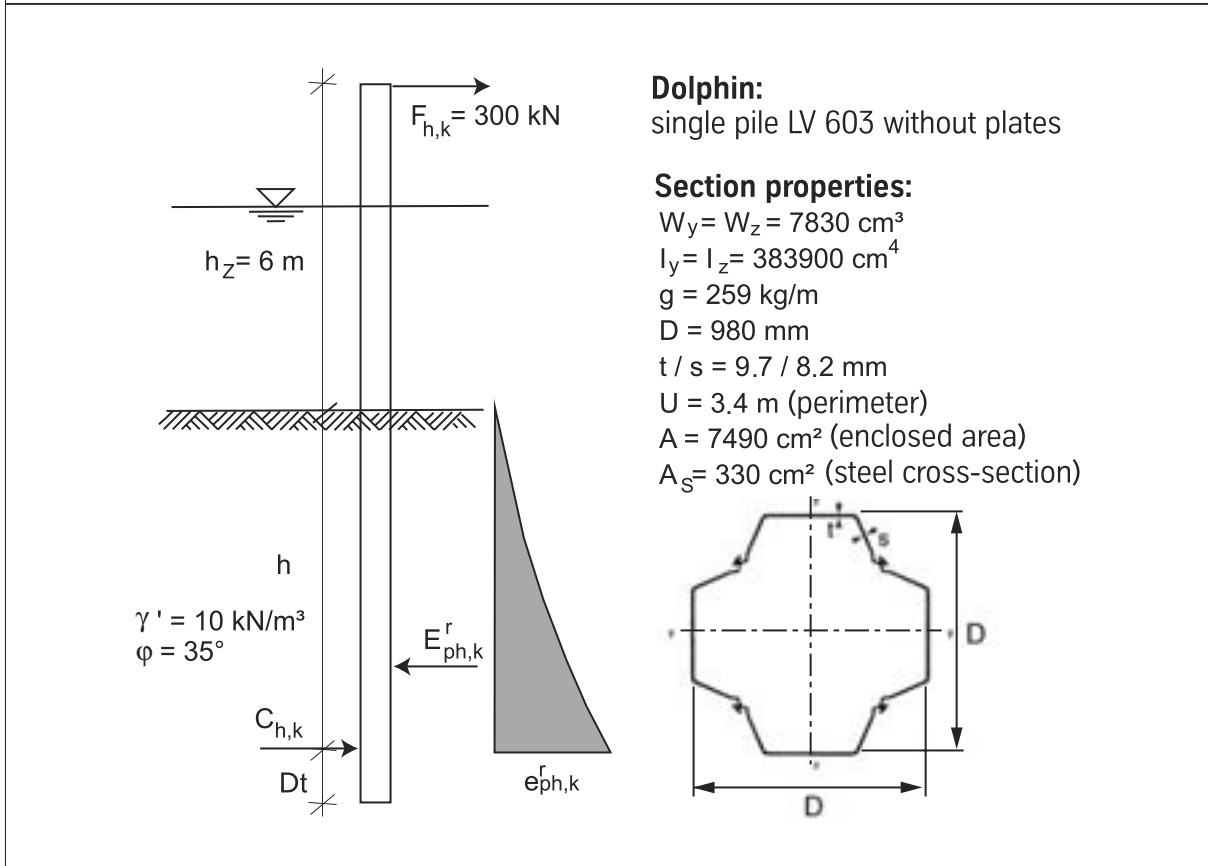
The additional embedment depth Δt is calculated as follows:

$$\Delta t = \frac{1}{2} \cdot C_{h,k} \cdot \gamma_Q \cdot \frac{\gamma_{Ep}}{e_{ph,k}^{r'}} \tag{9.4}$$

$e_{ph,k}^{r'}$: ordinate of characteristic three-dimensional active earth pressure at the level of equivalent force C (see Fig. 9.1)

DIN 4085:2007 and EAU 2004 section 13.1 (R 69) contain further information for calculating the passive earth pressure.

Example 9.1 Verification of load-carrying capacity at limit state LS 1B



Passive three-dimensional active earth pressure for non-cohesive soils:

$$E_{ph}^r = \gamma' \cdot \frac{h^2}{2} \cdot K_{pgh} \cdot D_{pg}^{Er}$$

where $K_{pgh} = 7.3$ to DIN 4085:2007 for $\varphi = 35^\circ$, $\delta = -\frac{2}{3}\varphi$

$$D_{pg}^{Er} = 0.55(1 + 2 \cdot \tan\varphi)\sqrt{D \cdot h} \text{ for } D < 0.3 \cdot h$$

Iterative determination of h from moment equilibrium about the point of application of C . Point of application of $E_{ph,mob}^r = E_{ph}^r/(\gamma_Q \cdot \gamma_{Ep})$ at $h/4$.

$$\begin{aligned} \sum M = 0 &= \gamma' \cdot \frac{h^2}{2} \cdot K_{pgh} \cdot 0.55(1 + 2 \cdot \tan\varphi)\sqrt{D \cdot h}/(\gamma_Q \cdot \gamma_{Ep}) \cdot \frac{h}{4} - F_{h,k} \cdot (h + h_Z) \\ \rightarrow h &= 5.54 \text{ m} \\ E_{ph}^r &= 3449.2 \text{ kN} \end{aligned}$$

Partial safety factors γ_Q and γ_{Ep} to EAU 2004 section 13.1.1 (R 69). Characteristic equivalent force $C_{h,k}$ to EAU 2004 section 13.1.2 (R 69):

$$\begin{aligned} C_{h,k} &= E_{ph,mob}^r - F_{h,k} = E_{ph}^r/(\gamma_Q \cdot \gamma_{Ep}) - F_{h,k} \\ &= \frac{3449.2}{1.2 \cdot 1.15} - 300 = 2199.4 \text{ kN} \quad (\text{see eq. 9.3}) \end{aligned}$$

Determining the driving allowance:

$$\begin{aligned} e_{ph,k}^{r'} &= \gamma \cdot K_{pgh} \cdot h \cdot 0.55(1 + 2 \cdot \tan\varphi)\sqrt{D \cdot h} = 1244.8 \text{ kN/m} \\ \Delta t &= \frac{1}{2} \cdot 2199.4 \cdot 1.2 \cdot \frac{1.15}{1244.8} = 1.22 \text{ m} \quad (\text{see eq. 9.4}) \\ h_{sum} &= h + \Delta t = 5.54 + 1.22 = 6.76 \text{ m, select: 7 m} \end{aligned}$$

Check $\sum V$ ($\tau = 150 \text{ kN/m}^2$ is used for skin friction):

$$\begin{aligned} \downarrow \sum V &= \underbrace{g \cdot (h_{sum} + h_Z) + (A - A_S) \cdot h_{sum} \cdot \gamma'}_{\text{self-weight of dolphin + soil}} + \underbrace{C_{h,k} \cdot \tan(2/3 \cdot \varphi)}_{C_{v,k}} \\ &\quad + \underbrace{U \cdot h_{sum} \cdot \tau}_{\text{skin friction}} - \underbrace{E_{ph}^r \cdot \tan(2/3 \cdot \varphi)}_{E_{pv}^r} \\ &= 2.59 \cdot (7.0 + 6.0) + (7490 - 330)/100^2 \cdot 7.0 \cdot 10 + 2199.4 \cdot \tan(2/3 \cdot 35^\circ) \\ &\quad + 3.4 \cdot 7.0 \cdot 150 - 3449.2 \cdot \tan(2/3 \cdot 35^\circ) = 3114.7 > 0 \end{aligned}$$

→ Verification satisfied!

9.4 Spring constants

When designing and calculating elastic berthing dolphins and heavy-duty fenders for the berths of large vessels, specifying the **spring constant** is especially important. The spring constant c describes the ratio of the applied load F to the resulting deformation f in the line of action of the force.

$$c = \frac{F}{f} \tag{9.5}$$

The dolphin converts the berthing energy of the ship into deformation work. The spring constant specifies the maximum impact forces or deflections of the energy absorption capacity necessary for accommodating the loads. The spring constant should be adapted to the requirements for each dolphin design case. Stiff mooring lines, for example, call for stiff fenders, soft mooring lines and soft fenders. With a given maximum dolphin deformation $\max f$ and given energy absorption capacity A , the minimum spring stiffness is

$$c_{min} = \frac{2 \cdot A}{\max f^2} \tag{9.6}$$

The maximum spring stiffness is limited by the maximum impact force F_S that can be accommodated:

$$c_{max} = \frac{F_S^2}{2 \cdot A} \tag{9.7}$$

Fig. 9.2 shows the magnitude of the spring constant in relation to the energy absorption capacity and the impact force. In the normal case, c should be selected such that it lies in the shaded area and as close as possible to the curve for $c = 1000$ kN/m. EAU 2004 section 13.2 (R 111) contains further information.

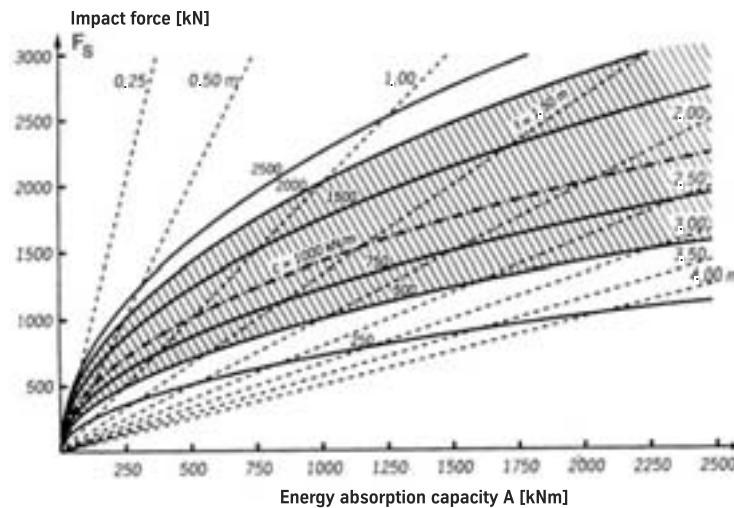


Figure 9.2: Spring constant c and deflection f for berthing dolphins in relation to energy absorption capacity A and impact force F_S (EAU 2004)

Chapter 10

Choosing pile sections

The following criteria are generally relevant when choosing pile sections:

1. Dimensions required according to DIN 1054:2005-01 for ultimate limit state (LS 1) and serviceability limit state (LS 2)

Chapters 6 and 7 show how to determine the relevant dimensions and moments of resistance of sheet piling structures and anchors. Verification of serviceability limit state requirements is dealt with in chapter 8.

2. Adequate moment of resistance for transport and installation of sheet pile wall

Proper support is important during handling on the building site, e.g. attachment of crane slings, because otherwise inadmissible deformation of the sheet pile prior to driving can occur which is not the fault of the fabricator. Furthermore, driving by means of pressing, impact hammer and vibration places severe loads on the pile in some situations. These loads depend on:

- the length of the pile,
- the flexibility and position of the pile guides,
- the method of driving plus the chosen driving parameters (mass and drop height of impact hammer), vibration parameters (amplitude of eccentric weights, frequency, static preload), pressing force in comparison to weight of section,
- prior deformation of the sheet pile caused by transport,
- the subsoil, especially type of soil, density in the case of non-plastic soils, consistency in the case of cohesive soils, natural obstacles such as rocks plus inclined, hard bearing strata, man-made obstacles such as existing works, and
- deviations of the adjacent sections and piles (and their interlocks) already driven.

Owing to the multitude of aforementioned influencing factors, the section is mainly specified based on experience. Reference manuals for the driving of sheet piles offer help and advice in this respect.

3. Adequate material thicknesses taking account of intended service life and expected rate of corrosion

Section 2.2.4 includes empirical values for average corrosion rates which enable an adequate section thickness to be selected depending on the intended service life. It should be remembered that the zone with the highest corrosion rate does not necessarily coincide with the point of maximum structural loading. If conditions are unfavourable or additional protection is required, active or passive corrosion protection measures can be specified instead of a heavier section.

4. If applicable, planned multiple use of the sheet pile walls taking into account the aforementioned aspects

The choice of steel grade (see section 2.2) essentially depends on the desired steel properties, e.g. with respect to suitability for welding.

For driving and economic reasons, sheet piles are sometimes driven to different depths within the same wall according to R 41 of EAU 2004. A value of 1 m is customary for the so-called stagger dimension, and experience shows that a structural analysis of the longer sheet piles is then unnecessary. Please refer to EAU 2004 for further details.

The commonest sections are listed in the appendix. Detailed information can be found in the Sheet Piling Handbook published by ThyssenKrupp GfT Bautechnik. And the staff at ThyssenKrupp GfT Bautechnik will be pleased to help you should you require any further information.

Bibliography

- [1] Bathe, K.-J.: Finite-Elemente-Methoden. Springer, Berlin, 2002
- [2] Blum, H.: Einspannungsverhältnisse bei Bohlwerken. Ernst & Sohn, Berlin, 1931
- [3] Blum, H.: Beitrag zur Berechnung von Bohlwerken. *Bautechnik*, 27(2), 1950, pp. 45-52
- [4] Boley, C., Morgen, K., Piepenbreier, O., Stahlmann, J.: Numerische Untersuchungen zum Einfluss der Erddruckabschirmung durch Pfähle bei Kaimauern. HTG/TUHH Joint Conference on Quay Walls, Hamburg, Institute of Geotechnics & Construction, Hamburg-Harburg TU, No. 7, 2004, pp. 131-49
- [5] Buja, H.O.: Handbuch des Spezialtiefbaus. Werner Verlag, Düsseldorf, 2001
- [6] Caquot, A., Kerisel, J.: Tables for the calculation of passive pressure, active pressure and bearing capacity of foundations. Paris, Gauthier-Villars, 1948
- [7] DIN 1054: Subsoil – Verification of the safety of earthworks and foundations. Deutsches Institut für Normung, 2005
- [8] DIN 4020: Geotechnical investigations for civil engineering purposes, Deutsches Institut für Normung, 2003
- [9] DIN 4021: Subsoil – Ground exploration by excavation, boring and sampling, Deutsches Institut für Normung, 1990
- [10] DIN 4084: Subsoil – Calculation of embankment failure and overall stability of retaining structures, Deutsches Institut für Normung, 2002
- [11] E DIN 4085: Subsoil – Calculation of earth pressure, Deutsches Institut für Normung, 2002
- [12] DIN 4094: Subsoil – Field testing, Deutsches Institut für Normung, 2003
- [13] DIN 18125: Soil, investigation and testing – Determination of density of soil, Deutsches Institut für Normung, 2006
- [14] DIN 18126: Soil, investigation and testing – Determination of density of non-cohesive soils for maximum and minimum compactness, Deutsches Institut für Normung, 1996

- [15] DIN 18136: Soil, investigation and testing – Unconfined compression test, Deutsches Institut für Normung, 2003
- [16] DIN 18137: Soil, testing procedures and testing equipment; determination of shear strength; concepts and general testing conditions, Deutsches Institut für Normung, 1990
- [17] DIN 18125: Soil, investigation and testing – Determination of density of soil, Deutsches Institut für Normung, 2006
- [18] DIN 18800-1 (1990): Steel structures, design and construction, Deutsches Institut für Normung, 1990
- [19] DIN EN 440: Welding consumables; wire electrodes and deposits for gas-shielded metal-arc welding of non-alloy and fine-grain steels; classification, Deutsches Institut für Normung
- [20] DIN EN 499: Welding consumables; covered electrodes for manual metal-arc welding of non-alloy and fine-grain steels; classification, Deutsches Institut für Normung
- [21] DIN EN 756: Welding consumables; wire electrodes and wire-flux combinations for submerged arc welding of non-alloy and fine-grain steels; classification, Deutsches Institut für Normung
- [22] DIN EN 1537: Execution of special geotechnical works – Ground anchors, Deutsches Institut für Normung, 2001
- [23] DIN EN 1997-1: Eurocode 7: Geotechnical design – Part 1: General rules, Deutsches Institut für Normung, 2005
- [24] DIN EN 10025: Hot-rolled products of non-alloy structural steels; technical delivery conditions, Deutsches Institut für Normung
- [25] DIN EN 10248: Hot-rolled sheet piling of non-alloy steels, Deutsches Institut für Normung, 1995
- [26] DIN EN 10249: Cold-formed sheet piling of non-alloy steels, Deutsches Institut für Normung, 1995
- [27] DIN EN 12063: Execution of special geotechnical work – Sheet pile walls, Deutsches Institut für Normung
- [28] DIN ENV 1993: Eurocode 3: Design of steel structures, Deutsches Institut für Normung
- [29] DIN ENV 1997: Eurocode 7: Design of geotechnical structures, Deutsches Institut für Normung
- [30] DIN 4150: Vibrations in buildings , Deutsches Institut für Normung, 2001
- [31] Recommendations of the Committee for Waterfront Structures, Harbours and Waterways, 8th ed., EAU 2004, Ernst & Sohn, 2006

- [32] Recommendations of the Committee for Excavations, EAB 2006
- [33] Grabe, J., Mahutka, K.-P.: Finite Elemente Analyse zur Vibrationsrammung von Pfählen. *Bautechnik*, 82(9):, 2005, pp. 632-40
- [34] Herle, I., Mašín, D. (2005): Einfluss von bodenmechanischen Aspekten auf numerische Ergebnisse. Workshop Proceedings, “FEM in der Geotechnik – Qualität, Prüfung, Fallbeispiele”, Hamburg, 2005, Institute of Geotechnics & Construction, Hamburg-Harburg TU, No. 10, 2005, pp. 53-66
- [35] Hoffmann H. (1958): Nomographische Berechnung doppelt verankerter Bohlwerke, *Bautechnik*, 35(2): pp. 59-63
- [36] HSP HOESCH Spundwand und Profil GmbH: Rammfibel für Stahlspundbohlen
- [37] Hügel, H.M.: Prognose von Bodenverformungen, doctorate thesis, Institut für Bodenmechanik und Felsmechanik, Karlsruhe University, No. 136, 1996
- [38] Hügel, H.M.: Qualitätssicherung bei der Anwendung der Finite-Elemente-Methode in der Geotechnik. HTG/TUHH Joint Conference on Quay Walls, Hamburg, Institute of Geotechnics & Construction, Hamburg-Harburg TU, No. 7, , 2004, pp. 51–96
- [39] Hügel, H.M.: FEM – Fehlerquellen, Fehlereffekte – Qualitätssicherung. Workshop Proceedings, “FEM in der Geotechnik – Qualität, Prüfung, Fallbeispiele”, Hamburg, 2005, Institute of Geotechnics & Construction, Hamburg-Harburg TU, No. 10, 2005, pp. 3-52
- [40] Jenne, G.: Praktische Ermittlung des Erddruckbildes, *Bautechnik*, No. 6, 1960, p. 233
- [41] Kalle, H.-U.: Bemessung von Stahlspundwänden gemäß EN 1993-5. *HANSA International Maritime Journal*, 06/2005
- [42] Kranz, E.: Über die Verankerung von Spundwänden. Ernst & Sohn, Berlin, 1953
- [43] Lackner, E.: Berechnung mehrfach gestützter Spundwände. Ernst & Sohn, Berlin, 1950
- [44] Mardfeldt, B.: Zum Tragverhalten von Kaimauerkonstruktionen im Gebrauchszustand. Institute of Geotechnics & Construction, Hamburg-Harburg TU, No. 11, 2006
- [45] Meißner, H.: Recommendations of DGGT study group “Numerik in der Geotechnik” – Part 1: Modellbildung, *Geotechnik*, 14:1-10, 1991
- [46] Meißner, H.: Recommendations of DGGT study group “Numerik in der Geotechnik” – Part 2: Tunnelbau unter Tage, *Geotechnik*, 19:99-108, 1996
- [47] Meißner, H.: Recommendations of DGGT study group “Numerik in der Geotechnik” – Part 3: Baugruben, *Geotechnik*, 25(1):44-56, 2002
- [48] Müller-Breslau, H.: Erddruck auf Stützmauern, Stuttgart, Verlag Kröner, 1906
- [49] Ostermayer, H.: Verpreßanker, in: GBT, vol. 2, 1997, p. 137

- [50] Potts, D., Axelsson, K., Grande, L., Schweiger, H., Long, M.: Guidelines for the use of advanced numerical analysis, Thomas Telford, London, 2002
- [51] Schanz, T.: Die numerische Behandlung von Stützwänden: der Einfluss des Modellsansatzes, in *Stahlpundwände (3) – Planung und Anwendung*, Stahl-Informations-Zentrum, 2000, pp. 11-21
- [52] Schanz, T.: Recommendations of DGGT study group “Numerik in der Geotechnik” – Part 4: Aktuelle Entwicklungen bei Standsicherheits- und Verformungsberechnungen in der Geotechnik, *Geotechnik*, 29(1):13-27, 2006
- [53] Vermeer, P.A., Wehnert, M.: Beispiele von FE-Anwendungen – Man lernt nie aus. Workshop Proceedings, “FEM in der Geotechnik – Qualität, Prüfung, Fallbeispiele”, Hamburg, 2005, Institute of Geotechnics & Construction, Hamburg-Harburg TU, No. 10, 2005, pp. 101-19
- [54] Weißenbach, A.: *Baugruben Teil 2 – Berechnungsgrundlagen*. Ernst & Sohn, Berlin, 1985
- [55] Weißenbach, A.: *Baugruben Teil 3 – Berechnungsverfahren*. Ernst & Sohn, Berlin, 2001
- [56] Weißenbach, A., Hettler, A.: Berechnungen von Baugrubenwänden nach der neuen DIN 1054. *Bautechnik*, 80(12), 2003, pp. 857-74
- [57] Weißenbach, A.: Recommendations of study group ‘Baugruben’ on the use of modulus of subgrade reaction and FEM, *Bautechnik*, 80(2), 2003, pp. 75-80
- [58] Woods, P.: Screening of surface waves in soils. *J. Soil Mech. Found. Div. ASCE*, 94, 1968, pp. 951-79
- [59] Wolffersdorff, P.-A. von, Mayer, P.-M.: Gebrauchstauglichkeitsnachweise für Stützkonstruktionen, *Geotechnik*, 19(4):291-300, 1996
- [60] Wolffersdorff, P.-A. von: *Verformungsprognosen für Stützkonstruktionen*. Habilitation thesis, Institute of Soil Mechanics & Rock Mechanics, Karlsruhe University, No. 141, 1997
- [61] Ziegler, M.: *Geotechnische Nachweise nach DIN 1054*. Ernst & Sohn, Berlin, 2005

Appendix A

Section tables for preliminary design

LARSSEN sections

	Section modulus		Weight		Second moment of inertia	Back thickness	Web thickness	Wall height	Section width
	W_y ¹⁾				I_y	t	s	h	b
	cm ³ /m	cm ³ / Single pile	kg/m ²	kg/m	cm ⁴ /m	mm	mm	mm	mm
	Wall	Single pile	Wall	Single pile	Wall	mm	mm	mm	mm
LARSSEN sections									
LARSSEN 755	2000	580	127.5	95.6	45000	11.7	10.0	450	750
LARSSEN 703	1210	414	96.4	67.5	24200	9.5	8.0	400	700
LARSSEN 703 K	1300	426	103.0	72.1	25950	10.0	9.0	400	700
LARSSEN 703 10/10 ³⁾	1340	437	108.0	75.6	26800	10.0	10.0	400	700
LARSSEN 704	1600	529	115.0	80.5	35200	10.2	9.5	440	700
LARSSEN 600	510	130	94.0	56.4	3825	9.5	9.5	150	600
LARSSEN 600 K	540	133	99.0	59.4	4050	10.0	10.0	150	600
LARSSEN 601	745	251	78.0	46.8	11520	7.5	6.4	310	600
LARSSEN 602	830	265	89.0	53.4	12870	8.2	8.0	310	600
LARSSEN 603	1200	330	108.0	64.8	18600	9.7	8.2	310	600
LARSSEN 603 K	1240	340	113.5	68.1	19220	10.0	9.0	310	600
LARSSEN 603 10/10 ³⁾	1260	350	116.0	69.6	19530	10.0	10.0	310	600
LARSSEN 604 n	1600	415	123.0	73.8	30400	10.0	9.0	380	600
LARSSEN 605	2020	520	139.2	83.5	42420	12.5	9.0	420	600
LARSSEN 605 K	2030	537	144.5	86.7	42630	12.2	10.0	420	600
LARSSEN 606 n	2500	605	157.0	94.2	54375	14.4	9.2	435	600
LARSSEN 607 n	3200	649	190.0	114.0	72320	19.0	10.6	452	600
LARSSEN 22 10/10 ³⁾	1300	369	130.0	65.0	22100	10.0	10.0	340	500
LARSSEN 23	2000	527	155.0	77.5	42000	11.5	10.0	420	500
LARSSEN 24	2500	547	175.0	87.5	52500	15.6	10.0	420	500
LARSSEN 24/12	2550	560	185.4	92.7	53610	15.6	12.0	420	500
LARSSEN 25	3040	562	206.0	103.0	63840	20.0	11.5	420	500
LARSSEN 43	1660	483	166.0	83.0	34900	12.0	12.0	420	500
LARSSEN 430	6450	–	234.5⁴⁾	83.0	241800	12.0	12.0	750	708 ⁴⁾

1) The section modulus values of the LARSSEN sections may only be used in structural calculations if at least every second interlock in the wall is crimped to absorb shear forces.

2) Wall assembly fabricated from LARSSEN 43 sections. Where quad pile assemblies are supplied, allowance must be made for the weight of the weld seams and reinforcements.

3) Rolling/delivery on request only.

4) With the use of quadruple piles b = 1416 mm

LARSSEN sections, HOESCH sections and UNION straight web sections available in lengths from 30 m to 36 m on request.

The basis for billing is the weight of the single pile (kg/m).

LARSSEN rolled-up and rolled-down sections

		Section modulus		Weight		Second moment of inertia	Back thickness	Web thickness	Wall height	Section width
		W_y ³⁾				I_y	t	s	h	b
		cm ³ /m	cm ³ /	kg/m ²	kg/m	cm ⁴ /m	mm	mm	mm	mm
		Wall	Single pile	Wall	Single pile	Wall				
LARSSEN sections		Rolled-down sections -								
LARSSEN 755	- 0.5	1920	573	124	93.0	43200	11.2	9.7	450	750
LARSSEN 703	- 0.5	1150	408	93	65.1	23000	9.0	7.7	400	700
LARSSEN 703 K		---								
LARSSEN 703 10/10 ³⁾		---								
LARSSEN 704	- 0.5	1530	523	111.4	78.0	33660	9.7	9.2	440	700
LARSSEN 600	- 0.5	480	124	90.0	53.4	3600	9.0	9.1	150	600
LARSSEN 600 K		---								
LARSSEN 601		---								
LARSSEN 602	- 0.5	790	254	85.5	51.3	12245	7.7	7.6	310	600
LARSSEN 603	- 0.5	1150	320	104.5	62.7	17825	9.2	7.9	310	600
LARSSEN 603 K	- 0.5	1190	335	109.5	65.7	18445	9.5	8.7	310	600
LARSSEN 603 10/10 ³⁾		---								
LARSSEN 604 n	- 0.5	1540	415	119.5	71.7	29260	9.5	8.8	380	600
LARSSEN 605	- 0.5	1950	515	135.5	81.3	40950	12.0	8.8	420	600
LARSSEN 605 K		---								
LARSSEN 606 n	- 0.5	2410	585	153.7	92.2	52420	13.9	9.0	435	600
LARSSEN 607 n	- 0.5	3130	671	186.5	111.9	70740	18.5	10.4	452	600
LARSSEN 22 10/10 ³⁾		---								
LARSSEN 23	- 0.5	1930	539	151.6	75.8	40530	11.0	9.8	420	500
LARSSEN 24	- 0.5	2440	542	171.6	85.8	51240	15.1	9.8	420	500
LARSSEN 24/12		---								
LARSSEN 25	- 0.5	2980	625	202.6	101.3	62580	19.5	11.3	420	500
LARSSEN 43		---								
LARSSEN 430		---								
Rolled-up sections +										
LARSSEN 755	+ 0.5	2060	586	131.5	98.6	46350	12.2	10.3	450	750
LARSSEN 703	+ 0.5	1270	433	100.0	70.0	25400	10.0	8.3	400	700
LARSSEN 703 K		---								
LARSSEN 703 10/10 ³⁾		---								
LARSSEN 704	+ 0.5	1670	548	118.6	83.0	36740	10.7	9.8	440	700
LARSSEN 600	+ 0.5	540	132	99.0	59.4	4050	10.0	9.9	150	600
LARSSEN 600 K		---								
LARSSEN 601	+ 0.5	790	246	81.8	49.1	12245	8.0	6.8	310	600
LARSSEN 602	+ 0.5	880	264	92.5	55.5	13640	8.7	8.4	310	600
LARSSEN 603	+ 0.5	1250	340	111.5	66.9	19375	10.2	8.5	310	600
LARSSEN 603 K	+ 0.5	1290	343	116.5	69.9	19995	10.5	9.3	310	600
LARSSEN 603 10/10 ³⁾		---								
LARSSEN 604 n	+ 0.5	1667	421	126.5	75.9	31675	10.5	9.2	380	600
LARSSEN 605	+ 0.5	2090	525	142.5	85.5	43890	13.0	9.2	420	600
LARSSEN 605 K		---								
LARSSEN 606 n	+ 0.5	2570	610	160.5	96.3	55900	14.9	9.4	435	600
LARSSEN 607 n	+ 0.5	3270	681	193.5	116.1	73900	19.5	10.8	452	600
LARSSEN 22 10/10 ³⁾		---								
LARSSEN 23	+ 0.5	2070	551	158.6	79.3	43470	12.0	10.2	420	500
LARSSEN 24	+ 0.5	2560	581	178.6	89.3	53760	16.1	10.2	420	500
LARSSEN 24/12		---								
LARSSEN 25	+ 0.5	3100	626	209.6	104.8	65100	20.5	11.7	420	500
LARSSEN 43		---								
LARSSEN 430		---								

Footnotes as for LARSSEN sections.

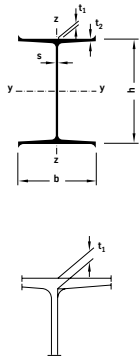
HOESCH sections, UNION straight-web sections

	Section modulus		Weight		Second moment of inertia	Back thickness	Web thickness	Wall height	Section width
	$W_y^{(1)}$ cm ³ /m Wall	cm ³ / Single pile	kg/m ² Wall	kg/m Single pile	I_y cm ⁴ /m Wall	t mm	s mm	h mm	b mm
HOESCH sections (LARSEN interlock)									
HOESCH 1706	1700	1148	110.8	74.8	32300	8.7	8.4	380	675
HOESCH 1806	1800	1215	117.5	79.3	34200	9.5	9.3	380	675
HOESCH 1856 K	1860	1256	123.7	83.5	35340	10.1	10.0	380	675
HOESCH 1906	1900	1283	126.3	85.3	36200	10.4	10.3	380	675
HOESCH 2506	2500	1687	142.9	96.5	53750	12.0	10.9	430	675
HOESCH 2606	2600	1755	149.9	101.2	55900	12.7	11.7	430	675
HOESCH 2706	2700	1823	157.2	106.1	58050	13.4	12.5	430	675
HOESCH sections (finger-and-socket interlock)									
HOESCH 1105	1100	628	101.0	58.1	14300	8.8	8.8	260	575
HOESCH 1205	1140	655	107.0	61.5	14820	9.5	9.5	260	575
HOESCH 1205 K	1200	690	112.5	64.7	15600	10.2	10.2	260	575
HOESCH 1255	1250	719	118.0	67.9	16250	10.8	10.8	260	575
HOESCH 1605	1600	920	107.0	61.5	28000	9.2	8.1	350	575
HOESCH 1655	1650	949	111.9	64.3	28870	9.6	8.5	350	575
HOESCH 1705	1720	989	116.0	66.7	30100	10.0	9.0	350	575
HOESCH 1705 K	1700	978	117.0	67.3	29750	9.5	9.5	350	575
HOESCH 1755	1750	1006	120.8	69.5	30625	10.4	9.5	350	575
HOESCH 1805	1800	1035	125.0	71.9	31500	10.8	9.9	350	575
HOESCH 2305	2320	1334	142.3	81.8	40600	11.5	8.4	350	575
HOESCH 2405	2400	1380	148.0	85.1	42000	12.1	9.0	350	575
HOESCH 2505	2480	1426	152.0	87.4	43400	12.5	9.5	350	575
HOESCH 2555 K	2540	1460	155.0	89.1	44450	12.8	10.0	350	575
HOESCH 2555	2550	1466	158.1	90.9	44625	13.0	10.0	350	575
HOESCH 2605	2600	1495	162.3	93.3	45500	13.3	10.3	350	575
HOESCH 3406	3420	2308	166.1	112.1	82940	13.5	10.8	485	675
HOESCH 3506	3500	2363	171.7	115.9	84880	14.0	11.4	485	675
HOESCH 3606	3600	2430	177.0	119.5	87300	14.5	12.0	485	675
HOESCH 3706	3700	2497	183.9	124.1	89730	15.1	12.7	485	675
HOESCH 3806	3780	2552	188.4	127.2	91665	15.5	13.2	485	675
UNION straight-web sections									
FL 511	90	45	136.0	68.0	350	11.0	–	88	500
FL 512	90	45	142.0	71.0	360	12.0	–	88	500
FL 512.7 ⁽³⁾	92	46	146.8	73.4	360	12.7	–	88	500

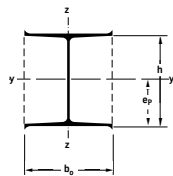
Footnotes as for LARSEN sections.

PEINE steel piles, PEINE sheet pile walls

PEINE steel piles	Section PSt	Weight kg/m	Dimensions						Perimeter		Cross-section		Axis y-y			Axis z-z		
			Section depth h	Flange width b	Web thickness s	Flange thickness t ₁	Flange thickness t ₂	Total	Out-line	Steel	Out-line	I _y	W _y	i _y	I _z	W _z	i _z	
			mm	mm	mm	mm	mm	cm	cm	cm ²	cm ²	cm ⁴	cm ³	cm	cm ⁴	cm ³	cm	
	300/ 80	80.3	305.0	305.0	9.0	13.9	9.2	181	128	102	938	18440	1209	13.4	6050	397	7.69	
	300/ 85	85.4	306.0	306.0	10.0	14.4	9.7	182	129	109	944	19492	1274	13.4	6416	419	7.68	
	300/ 95	95.4	308.0	308.0	12.0	15.4	10.7	183	129	122	957	21575	1401	13.3	7122	462	7.66	
	300/106	106.0	310.0	310.0	14.0	16.4	11.8	184	131	135	970	23767	1533	13.3	7906	510	7.66	
	370/107	107.0	366.0	379.0	9.0	15.2	12.0	225	157	136	1402	36489	1994	16.4	13176	695	9.84	
	370/116	116.0	366.0	382.0	12.0	15.2	12.0	226	158	148	1415	38148	2085	16.0	13827	724	9.66	
	370/122	122.0	370.0	380.0	10.0	17.2	14.0	225	158	155	1422	42274	2285	16.5	15192	800	9.89	
	370/132	132.0	369.4	383.7	13.7	16.9	13.8	227	159	168	1434	43594	2360	16.1	15790	823	9.69	
	370/153	153.0	374.0	386.0	16.0	19.2	16.1	229	161	195	1462	51212	2739	16.2	18555	961	9.75	
	400/100	100.0	392.0	379.0	10.0	13.2	10.0	230	162	127	1501	37668	1922	17.2	11380	601	9.45	
	400/119	119.0	396.0	381.0	12.0	15.2	12.0	231	163	151	1525	44969	2271	17.3	13568	712	9.48	
	400/127	127.0	400.0	380.0	11.0	17.2	14.0	231	164	162	1536	50469	2523	17.6	15210	801	9.69	
	400/175	176.0	408.0	387.0	18.0	21.2	18.2	235	168	224	1597	68363	3351	17.5	20748	1072	9.63	
	500/108	108.0	492.0	379.0	10.0	13.2	10.0	250	182	137	1880	61745	2510	21.2	11381	601	9.10	
	500/136	136.0	500.0	380.0	11.0	17.2	14.0	251	184	173	1916	81947	3278	21.8	15211	801	9.38	
	500/158	158.0	506.0	381.0	12.0	20.2	17.0	253	185	201	1944	97895	3869	22.1	18179	954	9.50	
	500/177	177.0	511.0	382.0	13.0	22.7	19.6	254	186	226	1968	111837	4377	22.3	20774	1088	9.59	
	600S/159	159.0	592.0	460.0	12.5	17.3	12.0	300	218	203	2737	130820	4420	25.4	23174	1008	10.70	
	600/188	188.0	600.0	460.0	14.0	21.2	14.0	301	220	239	2774	158226	5274	25.7	26886	1169	10.60	



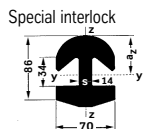
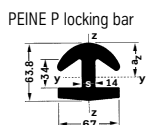
PEINE sheet piling	Section PSp ¹⁾	Section modulus		Weight kg/m	Width b mm	Depth h mm	Perimeter		Coating surface on one side inclusive of locking bars m ² /m	Cross-section		Second moment of inertia		Radius of gyration		Distance from edge e _p cm
		W _y	W _z				Total	Outline		Steel	Outline	I _y	I _z	i _y	i _z	
		cm ³	cm ³				cm	cm		cm ²	cm ²	cm ⁴	cm ⁴	cm	cm	
	370	2285	800	122	380	370	225	158	0.39	155	1422	42274	15192	16.5	9.9	18.5
	400	2523	801	127	380	400	231	164	0.39	162	1536	50469	15210	17.6	9.7	20.0
	500	3278	801	136	380	500	251	184	0.39	173	1916	81947	15211	21.8	9.4	25.0
	600	5274	1169	188	460	600	301	220	0.47	239	2774	158226	26886	25.7	10.6	30.0
	606	5847	1262	204	460	606	301	220	0.47	260	2795	177170	29035	26.1	10.6	30.3
	700	6353	1169	199	460	700	321	240	0.47	253	3234	222343	26889	29.6	10.3	35.0
	706	7028	1262	215	460	706	321	240	0.47	274	3255	248090	29037	30.1	10.3	35.3
	800	7980	1216	221	460	800	339	260	0.47	281	3694	319198	27973	33.7	10.0	40.0
	806	8754	1310	237	460	806	339	260	0.47	302	3715	352788	30122	34.2	10.0	40.3
	900	9221	1216	232	460	900	359	280	0.47	295	4154	414958	27975	37.5	9.7	45.0
	906	10098	1310	248	460	906	359	280	0.47	316	4175	457433	30124	38.1	9.8	45.3
	1000	10509	1216	243	460	1000	379	300	0.47	309	4614	525471	27978	41.2	9.5	50.0
	1006	11489	1310	259	460	1006	379	300	0.47	330	4635	577873	30126	41.9	9.6	50.3
	1001	11912	1317	267	460	1000	377	300	0.47	340	4614	595586	30302	41.9	9.4	50.0
	1013	12521	1369	277	460	1004	377	300	0.47	353	4627	628532	31495	42.2	9.4	50.2
	1016	12882	1411	283	460	1006	377	300	0.47	361	4635	647988	32450	42.4	9.5	50.3
	1016 S	13872	1509	300	460	1012	377	300	0.47	382	4656	701909	34711	42.9	9.5	50.6
	1017	14705	1593	314	460	1017	377	300	0.47	400	4674	747730	36630	43.2	9.6	50.9
	1030	15815	1596	351	460	1030	378	303	0.47	447	4739	814488	36712	42.7	9.1	51.5
	1035 S	16656	1680	365	460	1035	378	303	0.47	464	4757	861951	38632	43.1	9.1	51.8



$$W_{yP} = \frac{I_y}{e_p}$$

1) In steel grades up to S 355 GP, all PSp sections can be assigned to Class 2 in accordance with the ENV 1993-5 classification.

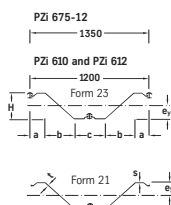
PEINE interlocks, PEINE intermediate sections



Locking bar P	Section modulus		Weight	Dimensions			Perimeter total	Cross-section	Second moment of inertia		Distance from edge
	W_y cm ³	W_z cm ³		h mm	b mm	s mm			I_y cm ⁴	I_z cm ⁴	
	28	19.3	18.4	63.8	67	14	35.4	23.5	91.7	65.2	32.8

For driving in heavy soils, a special interlock for foot reinforcement can be used. This is attached to the foot of the PZ intermediate sections over a length of 300 to 500 mm. Dead weight 30.1 kg/m, cross-sectional area 38.3 cm².

PEINE PZ intermediate sections



Section PZ	Form	Weight	Dimensions					Perimeter total	Cross-section	Coating area ²⁾	Section moment of inertia	Distance from edge
			a mm	b mm	c mm	t / s mm	H mm					
610 ¹⁾	23	175	152	296	304	10	270	3.35	223	3.19	23400	15.0
612 ¹⁾	23	195	152	296	304	12	272	3.35	249	3.19	25820	14.9
675-12	23	209	142	410	246	12	312	3.7	266	3.53	34640	16.8
610 ¹⁾	21	138	152	296	304	10	270	2.95	176	2.95	16740	14.8
612 ¹⁾	21	158	152	296	304	12	272	2.95	202	2.95	19030	14.9
675-12	21	172	142	410	246	12	312	3.27	219	3.29	27360	16.8

1) Rolling/delivery on request only.

2) Excl. internal surface of free interlock. Coating on both sides.

Weights and section moduli of composite PEINE sheet pile walls.

Weights

When calculating the m² weight of composite sheet piling, the ratio of the different lengths has to be taken into account. The true m² weight of the wall, related to the structurally required length of the PSp bearing piles, can be read from the tables for the lengths given in %. Intermediate values can be interpolated.

Section moduli

When calculating the static values for composite sheet piling, the loadbearing capacity of the individual piling elements is taken into account in accordance with their moment of inertia:

$$I_y = \frac{I_p + I_{ZW}}{a}$$

$$W_y = \frac{I_p + I_{ZW}}{a \cdot e_p}$$

$$W_{y'} = \frac{I_p + I_{ZW}}{a \cdot e_p'}$$

I_p = Moment of inertia of PSp piles in cm⁴

I_{ZW} = Moment of inertia of PZ piles in cm⁴

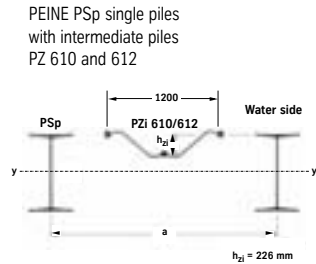
a = Spacing of PSp piles in m

e_p/e_p' = Edge spacing of neutral axis in cm (related to pile / interlock steel outer edge)

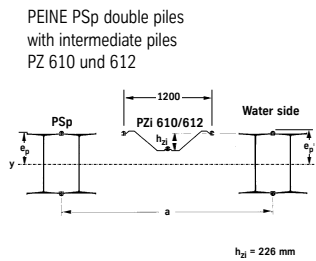
The section moduli W_y , $W_{y'}$ and the moment of inertia J_G are stated in the following tables.

Combined PEINE sheet pile walls

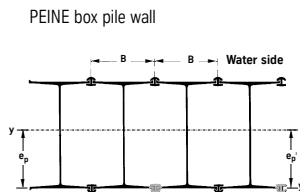
Selection from the complete range Combination 10/23	Section PSP	System width a m	Second moment of inertia I_y cm ⁴ /m	Section modulus		Dead weight in relation to PSp length PZ length as % of PSp length				Coating area Water side m ² /m
				W_y cm ³ /m	W_y^j cm ³ /m	PZ 610 60 % kg/m ²	PZ 612 100 % kg/m ²	PZ 610 60 % kg/m ²	PZ 612 100 % kg/m ²	
	370	1.60	41100	2230	-	142	186	149	198	1.24
	400	1.60	46230	2320	-	145	189	153	202	1.24
	500	1.60	65930	2640	-	151	195	158	207	1.24
	600	1.68	108240	3610	-	174	216	182	228	1.23
	606	1.68	119530	3950	-	184	226	191	238	1.23
	700	1.68	146450	4190	-	181	223	188	235	1.23
	706	1.68	161800	4590	-	191	232	198	244	1.23
	800	1.68	204180	5110	-	194	236	201	248	1.23
	806	1.68	224190	5570	-	204	246	211	257	1.23
	900	1.68	261240	5810	-	201	242	208	254	1.23
	906	1.68	286560	6330	-	210	252	218	264	1.23
	1000	1.68	327100	6550	-	207	249	214	261	1.23
	1006	1.68	358330	7130	-	217	259	224	271	1.23
	1001	1.68	368890	7380	-	222	263	229	275	1.23
	1013	1.68	388520	7740	-	228	269	235	281	1.23
	1016	1.68	400120	7960	-	231	273	238	285	1.23
	1016 S	1.68	432250	8550	-	241	283	248	295	1.23
	1017	1.68	459560	9040	-	250	291	257	303	1.23
	1030	1.68	499340	9700	-	272	313	279	325	1.23
	1035 S	1.68	527630	10200	-	280	322	287	333	1.23



Selection from the complete range Combination 22/23	Section PSP	System width a m	Second moment of inertia I_y cm ⁴ /m	Section modulus		Dead weight in relation to PSp length PZ length as % of PSp length				Coating area Water side m ² /m
				W_y cm ³ /m	W_y^j cm ³ /m	PZ 610 60 % kg/m ²	PZ 612 100 % kg/m ²	PZ 610 60 % kg/m ²	PZ 612 100 % kg/m ²	
	370	2.00	62590	3390	2820	193	228	199	238	1.22
	400	2.00	72190	3610	3040	199	234	205	244	1.22
	500	2.00	109110	4370	3800	207	242	213	252	1.22
	600	2.16	177830	5930	5270	240	272	246	282	1.20
	606	2.16	195410	6450	5790	255	288	261	297	1.20
	700	2.16	244460	6990	6310	250	283	256	292	1.20
	706	2.16	268350	7610	6930	265	298	271	307	1.20
	800	2.16	342540	8570	7830	270	303	276	312	1.20
	806	2.16	373700	9280	8550	286	318	291	327	1.20
	900	2.16	440700	9800	9040	281	313	286	322	1.20
	906	2.16	480100	10600	9850	296	328	301	338	1.20
	1000	2.16	553620	11080	10300	291	323	296	333	1.20
	1006	2.16	602230	11980	11210	306	338	312	348	1.20
	1001	2.16	618660	12380	11510	313	346	319	355	1.20
	1013	2.16	649220	12940	12080	323	355	328	365	1.20
	1016	2.16	667270	13270	12420	328	361	334	370	1.20
	1016 S	2.16	717290	14180	13350	344	376	349	386	1.20
	1017	2.16	760460	14960	14070	357	389	362	399	1.20
	1030	2.16	824380	16010	15010	391	423	397	433	1.20
	1035 S	2.16	867410	16770	15920	404	436	410	446	1.20



Selection from the complete range Combination C 23	Section PSP	Width B m	Weight kg/m ²	Cross section cm ² /m	Second moment of inertia I_y cm ⁴ /m	Section modulus		Coating area Water side m ² /m
						W_y cm ³ /m	W_y^j cm ³ /m	
	370	0.398	376	478	137550	7000	5880	1.11
	400	0.398	389	495	163270	7700	6550	1.11
	500	0.398	411	523	262250	9930	8690	1.11
	600	0.478	451	574	398380	12730	11370	1.11
	606	0.478	485	617	438080	13910	12540	1.11
	700	0.478	474	603	556420	15280	13850	1.11
	706	0.478	508	647	610370	16660	15230	1.11
	800	0.478	519	661	786680	18960	17390	1.11
	806	0.478	554	705	857040	20550	18990	1.11
	900	0.478	542	691	1018230	21850	20220	1.11
	906	0.478	577	734	1107200	23650	22030	1.11

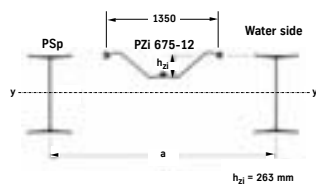


The grey coloured interlocks serve as guide interlocks and are not fitted over the entire length.

Combined PEINE sheet pile walls

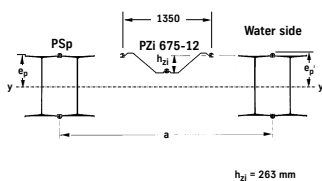
Selection from the complete range	Section	System width	Second moment of inertia	Section modulus		Dead weight in relation to PSp length		Coating area							
				I_y cm ⁴ /m	W_y cm ³ /m	W_y^j cm ³ /m	PZ length as % of PSp length		PZ length as % of PSp length						
Combination 10/23	PSp	a m					60 %	100 %	Water side m ² /m						
							kg/m ²	kg/m ²							
							370	1.75		44010	2380	-	141	189	1.23
							400	1.75		48700	2440	-	145	192	1.23
							500	1.75		66700	2670	-	149	197	1.23
							600	1.83		105510	3520	-	171	217	1.22
							606	1.83		115880	3830	-	180	226	1.22
							700	1.83		140590	4020	-	177	223	1.22
							706	1.83		154670	4390	-	186	232	1.22
							800	1.83		193570	4840	-	189	235	1.22
							806	1.83		211950	5260	-	198	244	1.22
							900	1.83		245960	5470	-	195	241	1.22
							906	1.83		269190	5950	-	204	250	1.22
							1000	1.83		306410	6130	-	201	247	1.22
							1006	1.83		335080	6670	-	210	256	1.22
							1001	1.83		344770	6900	-	215	260	1.22
							1013	1.83		362790	7230	-	220	266	1.22
							1016	1.83		373430	7430	-	224	269	1.22
							1016 S	1.83		402930	7970	-	233	278	1.22
							1017	1.83		428000	8420	-	240	286	1.22
1030	1.83	464520	9020	-	260	306	1.22								
1035 S	1.83	490480	9480	-	268	314	1.22								

PEINE PSp single piles
with intermediate piles
PZ 675 - 12



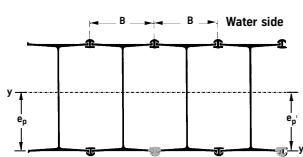
Selection from the complete range	Section	System width	Second moment of inertia	Section modulus		Dead weight in relation to PSp length		Coating area							
				I_y cm ⁴ /m	W_y cm ³ /m	W_y^j cm ³ /m	PZ length as % of PSp length		PZ length as % of PSp length						
Combination 22/23	PSp	a m					60 %	100 %	Water side m ² /m						
							kg/m ²	kg/m ²							
							370	2.15		63450	3430	2860	189	228	1.21
							400	2.15		72380	3620	3050	194	233	1.21
							500	2.15		106720	4270	3720	202	241	1.21
							600	2.31		171140	5710	5080	233	269	1.19
							606	2.31		187570	6200	5560	247	284	1.19
							700	2.31		233440	6670	6030	243	279	1.19
							706	2.31		255770	7250	6610	257	293	1.19
							800	2.31		325140	8130	7440	262	298	1.19
							806	2.31		354270	8800	8100	276	312	1.19
							900	2.31		416910	9270	8560	271	307	1.19
							906	2.31		453740	10020	9310	285	322	1.19
							1000	2.31		522480	10450	9730	281	317	1.19
							1006	2.31		567930	11300	10570	295	331	1.19
							1001	2.31		583290	11670	10860	302	338	1.19
							1013	2.31		611870	12190	11390	311	347	1.19
							1016	2.31		628740	12500	11700	316	352	1.19
							1016 S	2.31		675510	13350	12570	330	367	1.19
							1017	2.31		715870	14080	13250	343	379	1.19
1030	2.31	775630	15070	14120	374	411	1.19								
1035 S	2.31	815860	15770	14970	387	423	1.19								

PEINE PSp double piles
with intermediate piles
PZ 675 - 12



Selection from the complete range	Section	Width	Weight	Cross section	Second moment of inertia	Section modulus		Coating area								
						I_y cm ⁴ /m	W_y cm ³ /m		W_y^j cm ³ /m							
Combination C 23	PSp	B m	kg/m ²	cm ² /m				Water side m ² /m								
									1000	0.478	565	720	1284310	24840	23160	1.11
									1006	0.478	599	764	1394060	26860	25180	1.11
									1001	0.478	616	785	1431170	27750	25870	1.11
									1013	0.478	638	812	1918570	37100	34720	1.11
									1016	0.478	650	828	1500180	27150	27900	1.11
									1016 S	0.478	685	872	1653800	31800	29980	1.11
									1017	0.478	714	910	1751940	33560	31620	1.19
									1030	0.478	791	1008	1898470	35990	33780	1.19
									1035 S	0.478	820	1045	1994450	37670	35810	1.19

PEINE box pile wall



The grey coloured interlocks serve as guide interlocks and are not fitted over the entire length.

Appendix B

Round steel tie rods

Round steel tie rods to EAU 2004

Tie Rods - with rolled threads											
nominal diameter D	inch	1 ½	1 ¾	2	2 ¼	2 ½	2 ¾	3	3 ¼	3 ½	3 ¾
	mm	38	45	50	57	63	70	75	83	90	95
with upset ends											
R_d¹⁾ kN	ASF 600	361	486	598	812	1025	1120	1393	1750	2029	2329
	S 460	220	297	392	496	626	752	911	1071	1259	1442
	S 355	196	265	349	442	558	670	812	954	1122	1285
d_{shaft} (mm)		35	41	38	45	50	52	58	65	70	75
d_{core} (mm)		32.7	37.9	43.6	49.1	55.4	60.6	66.9	72.5	78.9	84.4
d_{flank} (mm)		35.4	41.2	47.2	53.1	59.4	65.2	71.6	77.6	83.9	89.8
l (mm)		190	190	220	220	250	250	270	270	270	270
kg/m		7.6	10.4	8.9	12.5	15.4	16.7	20.7	24.5	30.2	34.7
without upset ends											
R_d¹⁾ kN	ASF 600	361	486	641	812	1025	1231	1492	1752	2061	2360
	S 355 / S 460	see above (thread governs)									
d (mm)		35	41	47	53	59	65	71	77	83	89
kg/m		7.6	10.4	13.6	17.3	21.5	26.1	31.1	36.6	42.5	48.8
eye tie rod											
a (mm)		72	85	105	110	125	135	155	165	180	190
B_{hole} (mm)		34	40	50	53	60	66	73	78	83	88
B_{bolt} (mm)		32	38	48	50	57	63	70	75	80	85
c (mm)		25	30	33	39	42	47	50	55	60	63
k (mm)		50	60	70	75	85	90	105	110	120	130
T-head tie rod											
a (mm)		100	100	110	115	125	135	145	160	180	
b (mm)		38	40	50	55	60	60	70	70	75	
head (kg)			1.9	2.9	3.6	4.5	5.7	6.7	8.8	10.8	12.0

d = D for length under 4.00 m

¹⁾ permissible design resistance R_d

- A_{shaft}: cross-sectional area at shaft
- A_{tension}: tensile stress area calculated with (d_{core} + d_{flank})/2
- f_{y,k}: yield stress: S 355 = 355 N/mm² / S 460 = 460 N/mm² / ASF 600 = 580 N/mm²
- f_{u,a,k}: tensile stress: S 355 = 490 N/mm² / S 460 = 550 N/mm² / ASF 600 = 900 N/mm²
- γ_{Mo}: partial safety factor to DIN EN 1993-5 for anchor shaft with 1.10
- γ_{Mb}: ditto, but for threaded segment with 1.25
- k_t: notch factor to EAU 2004 R20 with 0.55

Round steel tie rods to EAU 2004

Tie rods - with rolled threads											
nominal diameter D	inch	4	4 ¼	4 ½	4 ¾	5	5 ¼	5 ½	5 ¾	6	
	mm	100	110	115	120	125	130	140	145	150	
with upset ends											
R_d¹⁾ kN	ASF 600	2650	2853	3354	3737	4141	4566	5011	5477	5963	
	S 460	1662	1882	2130	2376	2651	2927	3229	3531	3873	
	S 355	1480	1676	1897	2117	2362	2608	2877	3146	3451	
d (mm)		80	83	90	95	100	105	110	115	120	
d_{core} (mm)		90.8	96.7	103.0	108.8	115.1	121.0	127.2	133.0	139.6	
d_{flank} (mm)		96.2	102.3	108.7	114.8	121.1	127.2	133.5	139.6	145.9	
l (mm)		270	270	270	270	270	270	270	270	270	
kg/m		39.5	42.5	49.9	55.6	61.7	68.0	74.6	81.5	88.8	
without upset ends											
R_d¹⁾ kN	ASF 600	2719	3079	3485	3887	4338	4790	5285	5778	6338	
	S 355 / S 460	see above (thread governs)									
d (mm)		96	102	108	114	121	127	133	139	145	
kg/m		56.8	64.1	71.9	80.1	90.3	99.4	109.1	119.1	129.6	
eye tie rod											
a (mm)		210	230	240	255	280	275	290	300	310	
B_{hole} (mm)		93	98	103	113	118	123	128	133	143	
B_{bolt} (mm)		90	95	100	110	115	120	125	130	140	
c (mm)		66	72	75	80	85	90	95	100	105	
k (mm)		135	165	175	180	190	195	205	205	230	
T-head tie rod											
a (mm)		185	190	205	220	235	235	245	260	270	
b (mm)		75	80	90	90	95	100	130	135	140	
head (kg)		14.4	17.8	19.7	23.8	26.1	29.0	30.0	35.0	40.0	

d = D for length under 4.00 m ¹⁾ permissible design resistance R_d

Analysis format $Z_d < R_d$ for the limit state condition of loadbearing capacity to DIN EN 1993-5

- Z_d: design value for anchor force $Z_d = Z_{G,k} \times \gamma_G + Z_{Q,k} \times \gamma_Q$
- R_d: design resistance of anchor $R_d = \text{Min} [F_{tg,Rd}; F_{tt,Rd}]$
- $F_{tg,Rd} = A_{shaft} \times f_{y,k} / \gamma_{M0}$
- $F_{tt,Rd} = k_t \times A_{tension} \times f_{ua,k} / \gamma_{Mb}$

Index

- K₀-state, 158
- active and passive earth pressure coefficients
 - after MÜLLER-BRESLAU, 63
- active and passive earth pressure coefficients to DIN 4085, 63
- active earth pressure, 55
- adjustment factor for passive earth pressure, 88
- analysis of wall friction angle, 119
- anchorage length, 143
- backward lean, 13
- bearing area, 126
- body waves, 18
- borehole, 24
- coefficient of subgrade reaction method, 129
- cold-worked steel sheet piles, 9
- compression test, unconfined, 29
- cone penetration test, 24
- consistency, 28
- corrosion, 10
- corrosion zones, 11
- critical construction condition, 129
- data errors, 155
- declutching, 6
- deformation behaviour of wall, 89
- degree of fixity, 90
- direct shear test, 30
- dolphin, 169
- driving allowance, 91
- dynamic penetration test, 26
- earth pressure, 53
- earth pressure calculation after COULOMB, 55
- earth pressure calculation after RANKINE, 60
- earth pressure due to compaction, 74
- earth pressure due to confined surcharge, 71
- earth pressure due to stepped ground surface, 72
- earth pressure due to unconfined surcharge, 69
- earth pressure in cohesive soil, 65
- earth pressure in flowing groundwater, 74
- earth pressure in stratified soil, 70
- earth pressure redistribution, 76
- elastic-elastic, 127
- end-bearing pressure, 126
- energy absorption capacity, 169
- equipotential lines, 45
- equivalent force, 90
- excess hydrostatic pressure, 41
- failure mechanism, 129
- failure of passive earth pressure, 118
- finite element method, 129
- flow around sheet pile wall, 42
- flow net, 45
- forward lean, 13
- frame program, 94
- full fixity, 90
- geotechnical category, 83
- geotechnical engineer, 126
- granulometric composition, 27
- ground anchor types, 133
- ground vibrations, 17
- hot-rolled steel sheet piles, 8
- hydraulic gradient, 40
- hydraulic ground failure, 49
- hydraulic head, 39
- hydrostatic pressure, 39
- impact driving, 15
- in situ density, 27
- interlock seal, 6
- interlocks, 5
- internal load-carrying capacity, anchor, 137
- iteration, 92
- limit state, 84
- limit state condition, 86

- loadbearing effect of tension members, 130
- loading case, 84
- lower slip plane, 143
- material failure of components, 127
- material models, 157
- material resistance, 88
- mobilised passive earth pressure, 120
- mobilised soil reaction, 119
- modelling errors, 155
- modulus of compressibility, 29
- nomogram, 92
- overall stability, 129
- partial fixity, 90
- partial safety factor, 85
- passive earth pressure, 55
- passive earth pressure in cohesive soil, 67
- passive earth pressure with curved slip plane, 59
- penetrometer test, 24
- plastic-plastic, 127
- plug formation, 126
- point of zero load, 96
- pore water pressure, 39
- preliminary design, 118
- pressing, 14
- procedural errors, 155
- properties of steel, 8
- pull-out resistance, 140
- reduction in wall friction angle, 122
- relieving platform, 72
- rotation at the base, 115, 119
- rotation components, 115
- rounding errors, 155
- serviceability, 88
- serviceability limit state, 128
- serviceability, anchor, 149
- settlement, 17
- shear parameters, 30
- simple support, 90
- skin resistance, 126
- slip plane angle, 65
- soil investigations, 23
- soil parameters, 33
- soil reaction, 119
- spring constant, 172
- stability analysis, 87
- static equilibrium, 92
- static indeterminacy, 118
- steady-state earth pressure, 58
- steel grades, 8
- structural analysis, 83
- structural calculations, 89
- subsidence of components, 125
- support conditions, 90
- support conditions at base of wall, 89
- surface waves, 18
- tensile strength, 8
- three-dimensional earth pressure, 76
- triaxial compression test, 30
- vane shear test, 26
- vibrations, 17
- vibratory driving, 16
- waling, 150
- wall friction angle, 62
- welding, 9
- wished-in-place, 158
- yield strength, 8

ThyssenKrupp GfT Bautechnik GmbH

P.O. Box 10 22 53, 45022 Essen, Germany
Altendorfer Strasse 120, 45143 Essen, Germany
Phone: +49 201 188-2313
Fax: +49 201 188-2333
bautechnik@thyssenkrupp.com
www.tkgftbautechnik.com

Export

Altendorfer Strasse 120, 45143 Essen, Germany
Phone: +49 201 188-3991
Fax: +49 201 188-3974
export-bautechnik@thyssenkrupp.com

Eastern Europe

Altendorfer Strasse 120, 45143 Essen, Germany
Phone: +49 201 188-2703
Fax: +49 201 188-3730
osteuropa-bautechnik@thyssenkrupp.com